BERICHTE

aus dem MARUM und dem Fachbereich Geowissenschaften der Universität Bremen

No. 306

Bohrmann, G.
R. Alvarez, T. Biller, S. Buchheister, H. Büttner, O. Canoni, K. Dehning, C. Ferreira, P. Geprägs, S. Heinken, D. Hüttich, C. Johansen, S. Klar, S. Klüber, T. Leymann, H.A. Mai, Y. Marcon, F. Mary, G. Meinecke, W. Menapace, N. Nowald, T. Pape, D. Praeg, A. Raeke, R. Rehage, J. Renken, C. Reuter, C. Rohleder, M. Römer, H. Sahling, C. Sans i Coll, T. Schade, C. Seiter, P. Spalek, U. Spiesecke, L. Tamborrino, M. Torres, T. von Wahl, M. Wiebe, P. Wintersteller, M. Zarrouk

REPORT AND PRELIMINARY RESULTS OF R/V METEOR CRUISE M112

DYNAMIC OF MUD VOLCANOES AND SEEPS IN THE CALABRIAN ACCRETIONARY PRISM, IONIAN SEA

CATANIA (ITALY) – CATANIA (ITALY)
NOVEMBER 6 – DECEMBER 15, 2014

Berichte, MARUM – Zentrum für Marine Umweltwissenschaften, Fachbereich Geowissenschaften, Universität Bremen, No. 306, 217 pages, Bremen 2015

ISSN 2195-9633

Berichte aus dem MARUM und dem Fachbereich Geowissenschaften der Universität Bremen

published by

MARUM – Center for Marine Environmental Sciences
Leobener Strasse, 28359 Bremen, Germany
www.marum.de

and

Fachbereich Geowissenschaften der Universität Bremen
Klagenfurter Strasse, 28359 Bremen, Germany
www.geo.uni-bremen.de

The "Berichte aus dem MARUM und dem Fachbereich Geowissenschaften der Universität Bremen" appear at irregular intervals and serve for the publication of cruise, project and technical reports arising from the scientific work by members of the publishing institutions.

Citation:

Bohrmann, G., Alvarez, R., Biller, T., Buchheister, S., Büttner, H., Canoni, O., Dehning, K., Ferreira, C., Geprägs, P., Heinken, S., Hüttich, D., Johansen, C., Klar, S., Klüber, S., Leymann, T., Mai, H.A., Marcon, Y., Mary, F., Meinecke, G., Menapace, W., Nowald, N., Pape, T., Praeg, D., Raeke, A., Rehage, R., Renken, J., Reuter, C., Rohleder, C., Römer, M., Sahling, H., Sans i Coll, C., Schade, T., Seiter, C., Spalek, P., Spiesecke, U., Tamborrino, L., Torres, M., von Wahl, T., Wiebe, M., Wintersteller, P., Zarrouk, M.: Report and preliminary results of R/V METEOR cruise M112, Dynamic of Mud Volcanoes and Seeps in the Calabrian Accretionary Prism, Ionian Sea, Catania (Italy) – Catania (Italy), November 6 – December 15, 2014. Berichte, MARUM – Zentrum für Marine Umweltwissenschaften, Fachbereich Geowissenschaften, Universität Bremen, No. 306, 217 pages. Bremen, 2015. ISSN 2195-9633.

An electronic version of this report can be downloaded from:
http://nbn-resolving.de/urn:nbn:de:gbv:46-MARUM9

Please place requests for printed copies as well as editorial concerns with reports@marum.de

R/V METEOR
Cruise Report M112

Dynamic of Mud Volcanoes and Seeps in the Calabrian Accretionary Prism, Ionian Sea

M112
Catania – Catania
06 November – 15 December, 2014

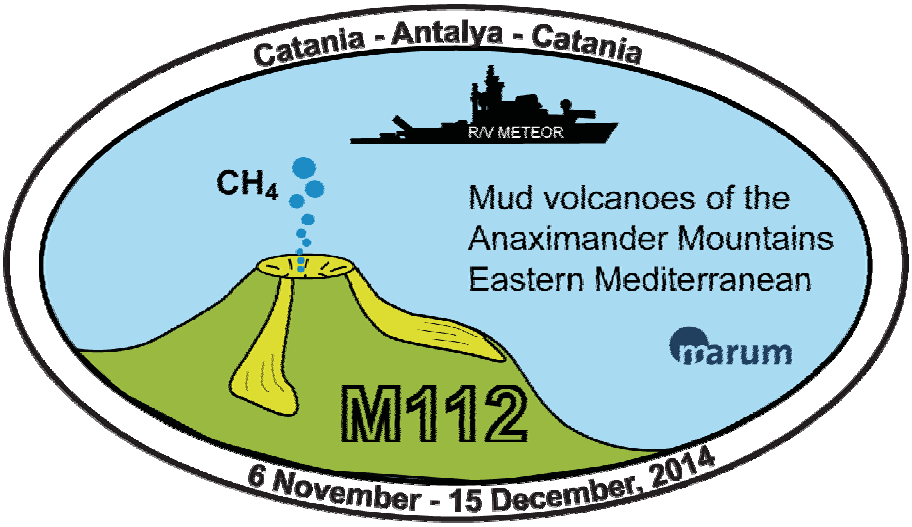

Cruise sponsored by Deutsche Forschungsgemeinschaft (DFG)

Edited by
Gerhard Bohrmann and Greta Ohling
With contributions of cruise participants

The cruise was performed by
MARUM – Center for Marine Environmental Sciences

marum

Universität Bremen

R/V METEOR Cruise Report M112

Table of Contents

1 Preface

R/V METEOR cruise M112 was planned to investigate mud volcanoes of the Anaximander Mountains between Cyprus and Crete. Due to problems in getting the research permission in Turkish waters the program to investigate mud volcanoes was shifted to mud volcanoes of the Calabrian Arc in Italian Waters. The research permission from the Italian foreign ministry was performed on a very fast track. We are thankful to all authorities who helped to reach this permission, like the German embassy in Rome, the foreign ministry in Berlin and the Control Station German Research Vessels in Hamburg.

The cruise was coordinated and carried out by MARUM Center for Marine Environmental Sciences at the University of Bremen. The research program is part of the DFG Research Center and Cluster of Excellence "The Ocean in the Earth System" in Research Area "Geosphere Biosphere Interactions", project GB3 "Contribution of Cold Seeps to Geological Processes, Carbon Fluxes, and Ecosystem Diversity". The cruise was financed by MARUM, the German Research Foundation (DFG) within GB3 and by an incentive fund proposal "Anaximander Mud volcanoes". The shipping operator Reederei Briese Schiffahrts GmbH & Co KG provided technical support on the vessel. We would like to specially acknowledge the master of the vessel Rainer Hammacher, and his crew for their continued contribution to a pleasant and professional atmosphere aboard R/V METEOR.

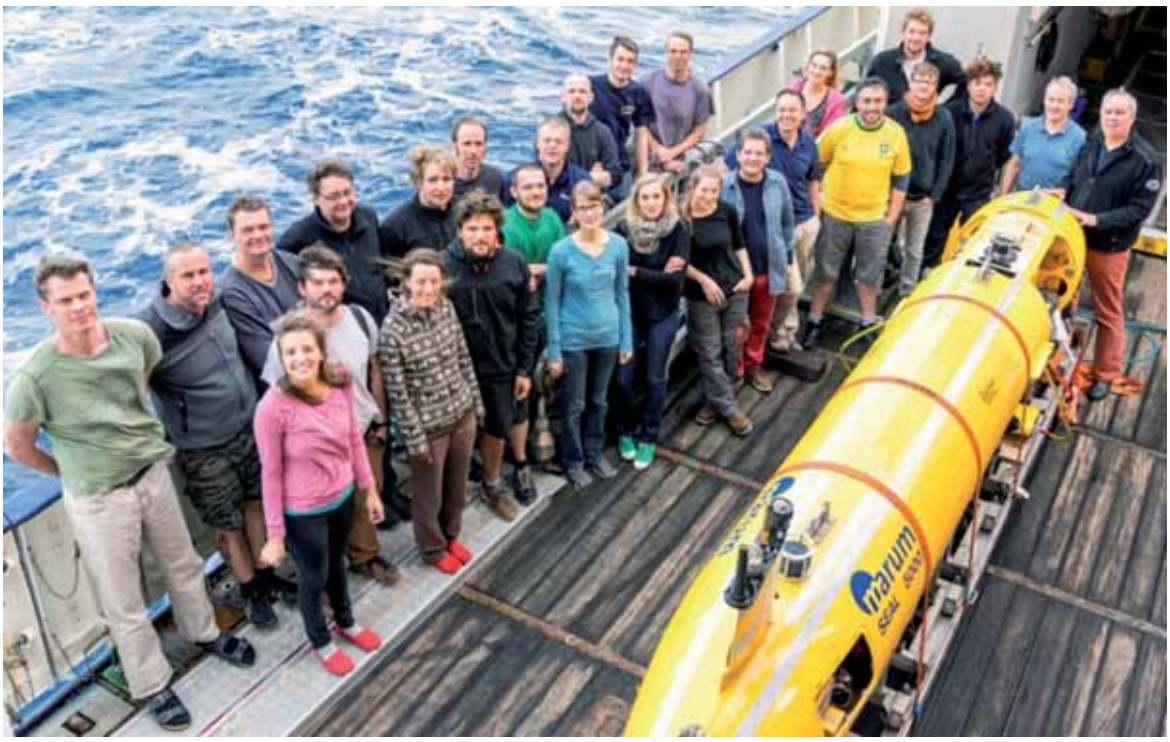

Fig. 1: Scientific crew aboard R/V METEOR M112, Leg 1

Personel aboard R/V METEOR

Table 1: Scientific crew

Name	Discipline	Affiliation	Leg
Alvarez, Ruben	Pore water	MARUM	2
Biller, Tiago	Multibeam/Parasound	MARUM	2
Bohrmann, Gerhard	Chief Scientist	GeoB	1 & 2
Buchheister, Stefanie	Pore water and gases	GeoB	1 & 2
Büttner, Hauke	ROV	MARUM	1 & 2
Canoni, Oliviero	Observer	OGS	2

Dehning, Klaus	DAPC, gravity cores	MARUM	2
Ferreira, Christian	Multibeam/Parasound	MARUM	1 & 2
Geprägs, Patrizia	OA-ICOS	MARUM	1 & 2
Heinken, Siebo	Web log	NG	1
Hüttich, Daniel	ROV	MARUM	1
Johansen, Caroline	ROV mapping	MARUM	1
Klar, Steffen	ROV	MARUM	1 & 2
Klüber, Sven	ROV tools	MARUM	1 & 2
Leymann, Tom	ROV	MARUM	1 & 2
Mai, Hoang Anh	ROV	MARUM	1 & 2
Marcon, Yann	Mosaicking/ROV	AWI	1
Mary, Flore	Sediments	OGS	1
Meinecke, Gerrit	AUV	MARUM	1
Menapace, Walter	T-lance	MARUM	2
Nowald, Nicolas	ROV	MARUM	1
Pape, Thomas	DAPC	MARUM	2
Präg, Daniel	Observer	OGS	1 & 2
Raeke, Andreas	Weather technician	DWD	1 & 2
Rehage, Ralf	ROV	MARUM	2
Renken, Jens	AUV	MARUM	1
Reuter, Christian	ROV	MARUM	1 & 2
Rohleder, Christian	Weather technician	DWD	1 & 2
Römer, Miriam	Flares/data handling	MARUM	1 & 2
Sahling, Heiko	ROV dives	GeoB	1
Sans i Coll, Cristina	T-lance, observatory	GeoB	2
Schade, Tobias	DAPC, gravity cores	MARUM	2
Seiter, Christian	ROV	MARUM	2
Spalek, Philipp	Photography	NG	1
Spiesecke, Ulli	AUV	MARUM	1
Tamborrino, Leonardo	Sediment cores	DCGS	2
Torres, Marta	Pore water	OSU	2
von Wahl, Till	AUV	MARUM	1
Wiebe, Monika	Multibeam/Parasound	MARUM	1 & 2
Wintersteller, Paul	Multibeam/Parasound	MARUM	1 & 2
Zarrouk, Marcel	ROV	MARUM	1 & 2

MARUM Center for Marine and Environmental Sciences, DFG Research Center and Cluster of Excellence, University of Bremen, Postfach 330440, 28334 Bremen, **Germany**

GeoB Department of Geosciences, University of Bremen, Klagenfurter Str., 28359 Bremen, **Germany**

OGS Istituto Nazionale di Oceanografia e di Geofisica Sperimentale - OGS Borgo Grotta Gigante 42/c, 34010 Sgonico, Trieste**, Italy**

NG National Geographic Deutschland, G+J/RBA GmbH & Co KG; Am Baumwall 11; D-20459 Hamburg, **Germany**

OSU Oregon State University, Corvallis OR, **USA**

DCGS Department of Chemical and Geological Sciences of the University of Modena and Reggio Emilia, Modena**, Italy**

AWI Alfred-Wegener-Institut, Helmholtz Zentrum für Meeres- und Polarforschung, Bremerhaven, **Germany**

DWD Deutscher Wetterdienst, Bernhard-Nocht-Str. 76, 20359 Hamburg**, Germany**

Fig. 2: Scientific crew aboard R/V METEOR M112, Leg 2

Table 2: Crew members onboard

Name	Discipline	Leg
Hammacher, Rainer Karl	Master	1 & 2
Birnbaum-Fekete, Tilo	Chief Mate	1 & 2
Stegmaier, Eberhard	1st Mate	1 & 2
Reinstädter, Marco	2nd Mate	1 & 2
Rathnow, Klaus	Doctor	1
Hinz, Michael	Doctor	2
Neumann, Peter	Ch/Eng	1
Hartig, Volker Joachim	Ch/Eng	2
Heitzer, Ralf	2nd Eng	1 & 2
Dölling, Paul	2nd Eng	1 & 2
Starke, Wolfgang	Electrician	1 & 2
Willms, Olaf	1st Electronic	1 & 2
Hebold, Catharina	Electronic	1 & 2
Reize, Emmerich Luk	Sys Op	1
Seidel, Stefan	Trainee	2
Sebastian, Frank	Fitter	1 & 2
Hadamek, Peter	Boatswain	1 & 2
Bussmann, Piotr Marek	AB	1
Zimmermann, Dirk	AB	2
Ledwig, Christian	AB	1 & 2
Zeigert, Michael	AB	1 & 2
Kruszona, Torsten	AB	1 & 2

Behlke, Hans-Joachim	AB	1 & 2
Weiß, Eberhard	AB	1 & 2
Drakopoulos, Evgenios	AB	1 & 2
Kudraß, Werner	Motorman	1 & 2
Krüger, Frank	Motorman	1 & 2
Schröder, Manfred	Motorman	1 & 2
Götze, Rainer	Chief Cook	1 & 2
Wernitz, Peter	Cook	1 & 2
Wege, Andreas	1st Steward	1 & 2
Zimmermann, Petra Edith	2nd Steward	1
Hinz, Nina Irene	2nd Steward	2
Montevirgen, Mario	2nd Steward	1 & 2
Durst, Alexander	Apprentice	1 & 2
Seidel, Stefan	Trainee	1
Schulte, Toni Clemens	Trainee	1
Zhang, Guomin	Laundryman	1 & 2

Shipping operator: Briese Schiffahrts GmbH & Co KG, Abteilung Forschungsschifffahrt, Hafenstr. 12, 26789 Leer, **Germany**

2 Introduction

2.1 Objectives, Background and Research Program

(G. Bohrmann)

Mud volcanoes are geological structures that morphologically and dynamically remember magmatic volcanoes. Besides the morphology the erupting fine-grained sediments like mud containing very often clasts from deeper strata are further characteristics of mud volcanism.

Mud volcanoes are often associated to petroleum reservoirs in deeper sediment sequences and are therefore interesting for hydrocarbon exploration. The structures are highly dynamic systems and are responsible for greenhouse gas emissions which may influence global climate regimes and several attempts to estimate their contribution have been made. Besides gases mud volcanoes are also important interfaces for the transfer of water and other dissolved elements including hydrocarbons and oil. Due to violent release of large amounts of mud and mud breccia the submarine mud volcanoes pose a geohazard for drilling and platform constructions. For chemosynthetic animals the dynamic of mud extrusion is sometimes too high, so that faunal populations are less developed on mud volcanoes. On the other side mud volcanoes represent in certain areas the dominant seeps generating the environment for seep communities.

Mud volcanoes have been found in various geological settings on passive and active margins, but are mostly known from collision zones on earth like along the southern rim of the Eurasian plate. Mud volcanoes are well known on land like Azerbaijan, where at least 1,000 mud volcanoes have been counted. The amount of submarine mud volcanoes is much larger and recent improvements in seafloor mapping and imagery as well as numerous seismic surveys led to the discovery of many mud volcanoes in all oceans. The number of such mud extrusions in the ocean seems gradually increasing with proceeding marine research activities. Specifically in the Eastern Mediterranean Sea approximately more than 500 mud volcanoes are known from several regions like the Mediterranean Ridge, the Anaximander Mountains and Florence Rise, the Nile deep-sea fan area and the Calabrian arc (Mascle et al. 2014). Within the framework of several European projects scientists from Italy and other countries collected over the last 10 years numerous multibeam echosounder data from the inner and outer Calabrian arc. By combining multibeam bathymetry and backscatter imagery, integrated with sub-bottom profiles and locally proven from geological sampling a total of 54 mud volcanoes have been identified in a sector of 35,600 km^2 (Ceramicola et al. 2014). Detailed sampling and seafloor investigations have been performed from only two mud volcanoes: the Madonna dello Ionio and Pythagoras Mud Volcano (Praeg et al. 2009).

The main goal of our expedition was to investigate active mud volcanoes which are characterized by recent mud flows and emissions of fluids and gases, which we can image by hydro-acoustic recording of the water columns. Of particular interest was the presence of methane hydrates, which form within sediments of the mud volcanoes under certain conditions of pressure and temperature, and may play a sealing role during eruptions. At the same time, methane hydrates are a concentrated source of methane that is used by chemosynthetic organisms living at and below the seabed.

Fig. 3: Research tools used during R/V METEOR cruise M112. R/V METEOR at sea (above left); MARUM ROV QUEST 4000 m launched from the A-frame of the vessel (above right); AUV SEAL 5000 m is launched from the starboard side of the working deck (below left) and the dynamic autoclave piston corer (DAPC) deployed from the vessel.

The working program varied between the two legs: During the first two weeks (Leg 1) we planned to use the hull-mounted multibeam EM122 and the PARASOUND system to explore which of the mud volcanoes have gas emission sites. Those gas flares are ideal indicators for mud flow activities and are also very good indicators for active seafloor seepage. MARUM AUV SEAL 5000 (Fig. 3) was used to map single structure of mud volcanoes mostly during night time. During day time used the MARUM ROV QUEST 4000 (Fig. 3) which is also the main program during Leg 2. Another focus during the three weeks of Leg 2 was coring distinct mud flows in order to investigate the minimum age of the mud flows revealed from the pelagic sediments overlying the mud flow breccia. Furthermore deployments of the dynamic autoclave piston corer (DAPC; Fig. 3) were planned to quantify the gas and gas hydrate saturation in sediments of mud volcanoes. Heat flow measurements and water column work were planned to complete the work program.

The following scientific questions were addressed during the cruise:

- How different are the mud volcanoes in their construction?
- Are there relative fresh mud flows which can be identified and how are the shallow gas hydrates associated to those recent flows?
- Are the hydrates in older or younger sediments?
- Are there differences in hydrate concentrations for different lithologies e.g. pure mud, or mud breccia?

- Which conditions control the escape of fluids (liquid, gas) and mud and how does this shape the appearance of the seeps?
- How much methane is escaping as gas bubbles from the sea floor to the water column?
- What is the advective fluid flow and what is the source of the fluids?
- How much gas and gas hydrates exist in the sediments?
- Which organisms live at the seeps?

2.2 Geological Setting of the Calabrian Arc

(D. Praeg)

The eastern Mediterranean Sea contains the convergent plate boundary where the African plate is being subducted beneath Europe, along which accretionary complexes extend over 1500 km from Calabria to Cyprus (Fig. 4). The Calabrian accretionary prism lies at the SE tip of the arcuate Apennine-Maghrebide subduction system, a product of rapid roll-back of a NW dipping oceanic slab over the last ca. 30 Ma (Neogene) to open back-arc basins in the western Mediterranean Sea (Malinverno and Ryan 1986; Gueguen et al. 1998).

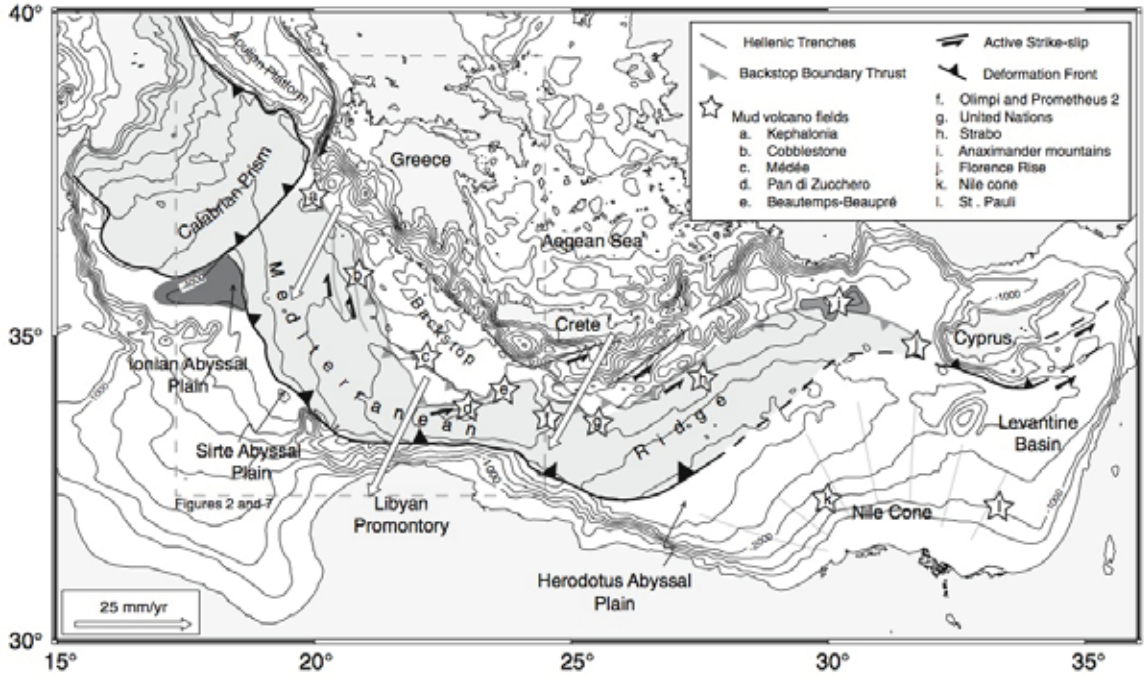

Fig. 4: Geological setting of the eastern Mediterranean (from Rabaute and Chamot-Rooke 2007), showing the Calabrian accretionary prism against the larger accretionary complex of the Mediterranean Ridge. White arrows indicate motion of the Aegean backstop with respect to Africa.

Since ca. 10 Ma (late Miocene), slab retreat has driven the pulsed opening of back-arc basins in the Tyrrhenian Sea during migration of the accretionary system up to 380 km towards the Ionian domain (Faccenna et al. 2001, 2004; Sartori 2003). Consumption of the slab, and its fragmentation during episodes of tearing beneath bordering continental margins, has narrowed the subduction zone to a tongue of Ionian lithosphere confined between the Maltese and Apulian escarpments (Fig. 5), descending NW into the mantle beneath the Aeolian volcanic arc (Faccenna et al. 2004; Guillaume et al. 2010). Roll-back of the subducting slab has slowed or ceased following a regional plate tectonic

reorganization at ca. 0.8-0.5 Ma (Goes et al. 2004; Mattei et al. 2007). Over the same time period, Calabria has undergone a rapid km-scale uplift (Westaway 1993; Zecchin et al. 2012), argued to be a response to mantle circulation around a slab window beneath the southern Apennines (Faccenna et al. 2011).

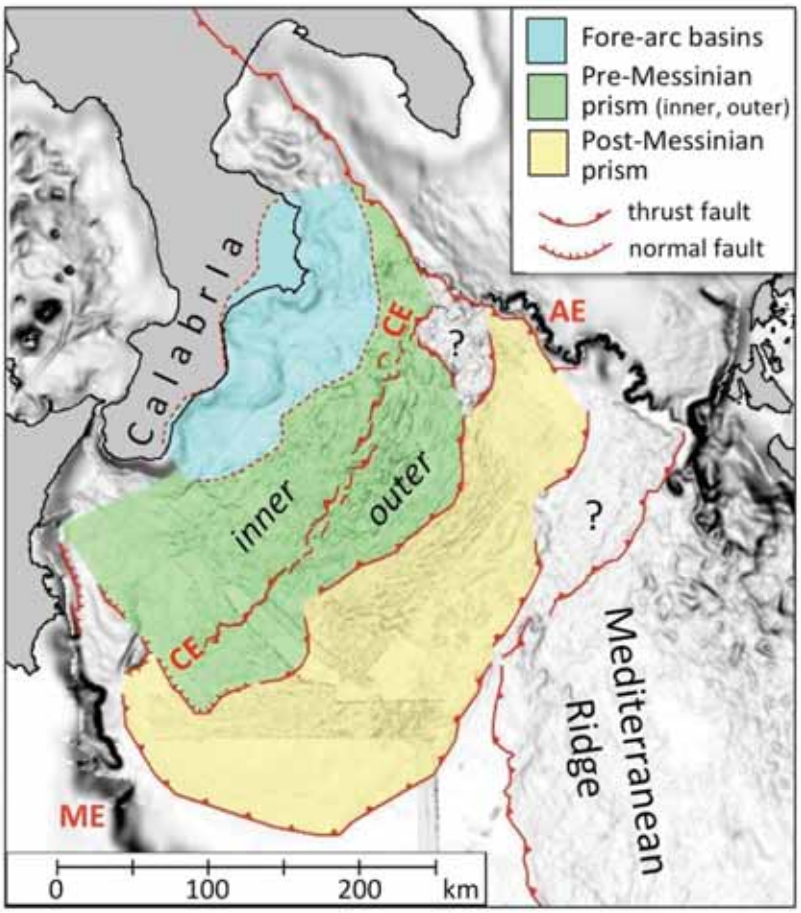

Fig. 5: Main morpho-tectonic zones of the Calabrian accretionary prism (Ceramicola et al. 2014). The inner parts of the fore-arc basins have been raised above sea level by on-going uplift of Calabria (Sartori 2003). The pre-Messinian prism to seaward is divided into inner and outer parts by the Calabrian Escarpment, up to 200 km long and 750 m high. The post-Messinian prism incorporates thick evaporites, also present in the outer Mediterranean Ridge (drawn from Chamot-Rooke et al. 2005). AE Apulian Escarpment, CE Calabrian Escarpment, ME Malta Escarpment.

Above the subduction zone, the Calabrian accretionary prism is 300 km wide and extends almost 300 km from elevations of up to 1928 m in Calabria, to a frontal thrust in water depths of c. 4000 m that intersects that of the Mediterranean Ridge (Fig. 5; Chamot-Rooke et al. 2005). The onshore Calabro-Peloritano 'Arc' - so-called due to its shape - is a thrust stack of metamorphic and sedimentary units, onlapped on both its Tyrrhenian and Ionian sides by fore-arc sedimentary basins (Barone et al. 2008). In the Ionian Sea, Rossi and Sartori (1981) showed the seaward-thinning accretionary prism, referred to as the 'External Calabrian Arc', to contain three main morpho-structural zones (Fig. 5), recognized in all subsequent work and corresponding to fore-arc basins and pre- and post-Messinian wedges (Finetti 1982, 2005; Praeg et al. 2009; Cernobori et al. 1996; Minelli and Faccenna 2010; Polonia et al. 2011). The inner fore-arc basins, up to 80 km wide, are underlain by strata up to 2 km thick that is inferred to include thin (<500 m) Messinian evaporites (Rossi and Sartori 1981; Minelli and Faccenna 2010). The pre-Messinian wedge to seaward, up to 100 km wide, is an area of irregular relief that corresponds to thrusts and back-thrusts; it is divided by the up to 750 m high Calabrian Escarpment (Fig. 5) into an inner plateau and an outer area of higher gradient

and relief (Rossi and Sartori 1981; Minelli and Faccenna 2010; Polonia et al. 2011; Ceramicola et al. 2014). The post-Messinian wedge is up to 100 km wide and includes two main lobes (Fig. 5), the western with a décollement at the base of Messinian evaporites and the eastern cutting down into older strata (Polonia et al. 2011). Seismic reflection and refraction data across the outer wedge and its foreland indicate the down-going slab to comprise oceanic or highly-extended crust overlain by up to 4 km of pre-Messinian sedimentary strata, in turn overlain by thick Messinian evaporites (Finetti 1982, 2005; De Voogd et al. 1992; Polonia et al. 2011).

Seismic reflection profiles across the pre-Messinian wedge and fore-arc basins show that many seabed thrust structures record post-Messinian tectonic movements, expressed as offsets of the reflector marking the base of the Plio-Quaternary succession, the largest example being the Calabrian Escarpment (Minelli and Faccenna 2010; Polonia et al. 2011). With reference to critical wedge theory, these movements are argued to record a response to the rapid frontal incorporation of Messinian evaporites, resulting in a reduction in taper that was corrected by out-of-sequence thrusting (OOSTs) and sedimentary underplating throughout the Plio-Quaternary advance of the prism (Minelli and Faccenna 2010). Within the fore-arc basins, seabed thrusts and normal faults could also reflect on-going gravity-driven sliding above thin evaporites (Minelli and Faccenna 2010; Minelli et al. 2013). It has subsequently been suggested that the Calabrian Escarpment and other large OOSTs to seaward could have acted as pathways for post-Messinian fluid flow and mud volcanism, although no structurally-controlled pathways were identified (Polonia et al. 2011; Panieri et al. 2013). Fluid migration within the prism has also been invoked in reference to seismically-imaged diapiric structures within the Plio-Quaternary succession of the fore-arc basins, originally suggested to be of halokinetic origin (Rossi and Sartori 1981), but recently argued to be shale diapirs recording upward fluid migration from Messinian or older successions (Polonia et al. 2011; Capozzi et al. 2012; see also Ceramicola et al. 2014).

Mud volcanoes (MVs) are abundant within the eastern Mediterranean accretionary systems, and were first identified in the eastern Ionian Sea from cores of mud breccia from a structure on the western Mediterranean Ridge (Cita et al. 1978). The Mediterranean Ridge and its eastern extensions have since become one of the most intensively studied MV populations on Earth, through seabed studies that have identified hundreds of mud volcanoes (Kopf 2002; Mascle et al. 2014), and scientific drilling of two examples that has provided evidence of extrusive activity over at least the last 1.2 Ma (Robertson et al. 1996). In contrast, until recently little was known about mud volcanism on the Calabrian accretionary prism. In 1981, two cores containing ‘pebbly mudstones’ were recovered from a seismically unstratified body on the inner prism (subsequently identified as Sartori MV, Fig. 6), but mud diapirism as proposed by Cita et al. (1981) was rejected in favour of tectonic chaoticisation along thrusts (Rossi and Sartori 1981; Morlotti et al. 1982). The presence of mud volcanoes on the Calabrian accretionary prism was tentatively suggested from a few high backscatter patches observed on partial GLORIA sidescan coverage (Fusi and Kenyon 1996). However, mud volcanoes were not proven until 2005, during a campaign of the R/V OGS Explora that acquired the first regional multibeam coverage of Italian waters SE of Calabria, along with cores of mud breccia from two distinctive morphological features (Ceramicola et al. 2006), referred to as the Madonna dello Ionio MVs in the Spartivento fore-arc basin, and Pythagoras MV on the pre-Messinian wedge to seaward (Fig. 6; Praeg et al. 2009). Targeted seismic investigations of these two sites showed both to be the tops of buried extrusive edifices that interfinger with Plio-Quaternary sediments above a regional unconformity (Praeg et al. 2009), inferred to be of mid-Pliocene age (3-3.5 Ma) by

correlation to tectono-stratigraphic records exposed onshore in the Crotone fore-arc basin (see Zecchin et al. 2012). These findings supported a model in which mud breccia extrusion was triggered by a tectonic reorganization of the accretionary prism c. 3 Ma and has remained episodically active since, making these among the longest-lived mud volcanoes on record (Praeg et al. 2009; cf. Somoza et al. 2012).

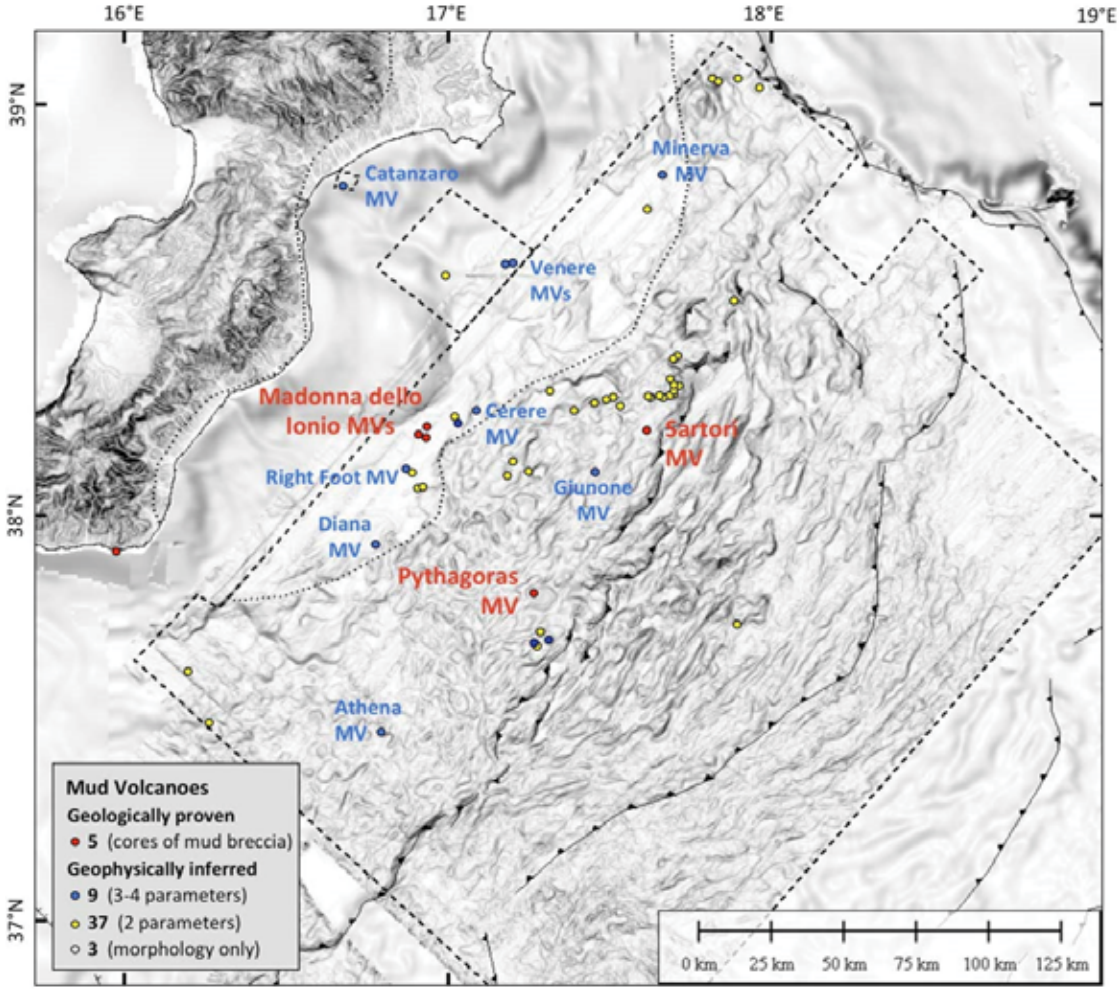

Fig. 6: Shaded relief map of the Calabrian accretionary prism showing locations of mud volcanoes geologically proven by coring and geophysically inferred from up to 4 parameters (morphology, backscatter, subbottom acoustic facies and, in the case of Catanzaro MV, a possible hydroacoustic flare). Dashed lines show extent of multibeam bathymetric and backscatter data coverage (100 m DEM). After Ceramicola et al. 2014.

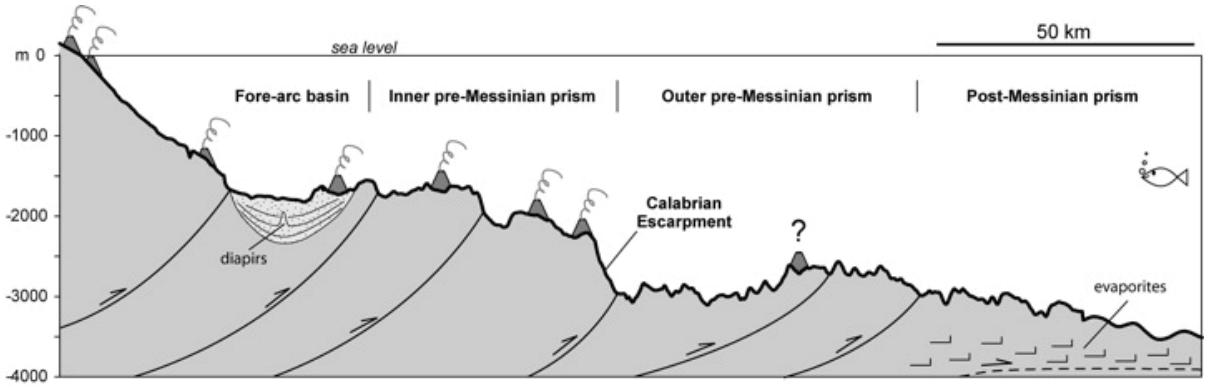

Fig. 7: NW-SE bathymetric profile 250 km long across the central part of the Calabrian accretionary prism, schematically summarizing the distribution of mud volcanoes in relation to the main morpho-tectonic zones (from Ceramicola et al. 2014).

More recently, integration of multibeam morpho-bathymetry with backscatter data across the Calabrian accretionary prism has revealed at least 54 mud volcanoes across the fore-arc basins and pre-Messinian prism (Fig. 6; Ceramicola et al. 2014). Five of the MVs were proven by coring, while the remainder were identified based on up to four geophysical parameters, the vast majority (40/54) from morphology and/or backscatter from on a 100 m multibeam grid. Nine of the geophysically inferrred MVs were identified with sufficient confidence to be given names (Fig.6). With one possible exception, all of the MVs are restricted to the inner plateau of the Calabrian prism, landward of the Calabrian Escarpment (Figs 6 and 7). The majority (50/54 MVs) have high backscatter signatures that, based on hemipelagic sedimentation rates and assumed sonar penetration, imply extrusion of mud breccias within the last 56 ka, i.e. during the last glacial-interglacial cycle, consistent with the depths of cored mud breccias at the Madonna dello Ionio, Pythagoras and Sartori MVs (Fig. 6; Ceramicola et al. 2014). The Madonna dello Ionio and Pythagoras MVs were further investigated during two HERMES campaigns equipped with ROVs, which found geological and biological evidence of ongoing mud and/or gas seepage (Foucher et al. 2009; Praeg et al. 2012).

3 Cruise Narrative

(G. Bohrmann)

On Thursday, 6 November 2014, at 9 a.m. local time R/V METEOR left berth No. 12 of road Sporgente Central in the port of Catania, heading for research work on the Calabrian Arc. Before sailing, R/V METEOR had spent time at dock in Catania while the scientists and research tools of cruises M111 and M112 were exchanged. New research tools on board for M112 are the deep-sea remotely operated vehicle ROV MARUM QUEST 4000 and the autonomous underwater vehicle AUV SEAL 5000, as well as a number of geologic sampling devices. In total seven 20' containers from Bremen had to be stored on deck – partly in double layers - and the entire contents of a 40' container were distributed to the labs by the vessel's boatswain and seamen.

The scientists from Germany, Italy, Switzerland, Austria, Netherlands, France and Brazil embarked between 3 – 5 November and used the time to do necessary deck work together with the vessel's crew, as well as to set up the labs. We faced quite stormy weather, and were surprised by some heavy blasts while still in the port and upon sailing. Consequently the first days at sea, Thursday and Friday (6 and 7 Nov), were quite bumpy, and despite medical precautions resulted in some seasick persons. In particular, the first two nights were characterized by wind speeds on Beaufort-Scale of up to 7-8, peaking up to 9. Nonetheless, we were able to undertake the planned measurements using our hull-mounted hydro-acoustic systems, following the acquisition on Thursday, 6 November of a first underwater sound profile in water depths of up to 1,500 m using the SVP-Sonde.

Until Saturday night (8 November), under improving weather conditions, further potential locations were surveyed using the hull-mounted PARASOUND and Multibeam systems, including the „Madonna dello Ionio" which shows a complex structure comprising several individual mud volcanoes (Fig. 8). During the night from Saturday to Sunday we sailed back to Catania where, off the entrance to the port, we could gather a very important spare part for the ROV, which had not been delivered before our official time of departure last Thursday. This was also an opportunity to bring on board the luggage of our French colleague, which had been lost during her flight to Catania. On Sunday, 9 November R/V METEOR sailed back to Venere Mud Volcano under ideal weather conditions.

After a preliminary mapping of our target area at the foot of Venere Mud Volcano (Fig. 9) on 9 November we deployed ROV QUEST 4000 for the first time during the cruise on Monday 10 November, in the darkness of night until sunrise at 06:00 a.m. When the ROV reached the seafloor we saw numerous, dark stained patches of different sizes, their centers mostly covered by white bacterial mats, characteristic of cold seeps. The recognition of direct indicators of fluid seepage right at the beginning of the dive was only possible due to our preliminary investigations based on thorough analyses of hydro-acoustic data. Most scientists of this cruise watched the dive on the large projection screen in the lab which showed the most important camera images from the ROV. The dive is controlled by two scientists together with the two pilots in the ROV's control container, and communication with them was considerably facilitated by the new intercom facility.

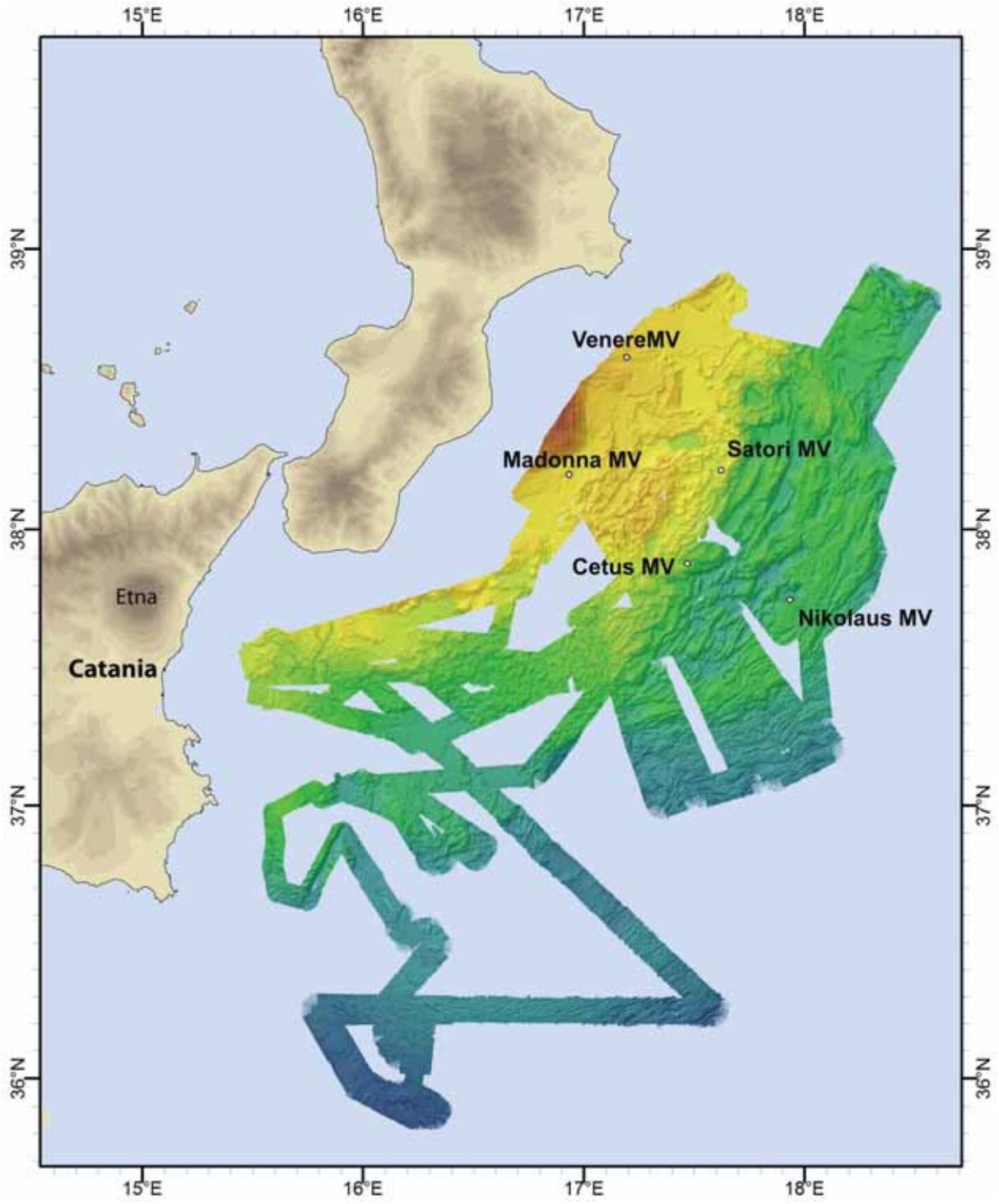

Fig. 8: Bathymetric tracks acquired during R/V METEOR cruise M112 of the Ionian Sea, covering parts of the inner and outer Calabrian arc and 5 mud volcanoes where detailed investigations were performed.

For the first time, more scientists could be actively involved in the dive, leading to a dynamic exchange between lab and container. When gas bubble emissions from the seafloor were observed, at several locations, there was great enthusiasm. Based on the broad signal of the ship's echo-sounder we had already concluded that there should be more than one location of gas emission. Unfortunately we could not take samples of the gas, of organisms or of other seafloor manifestations of seepage because the ROV's manipulator arm developed a technical fault after a short period of operation. Therefore we used the dive time for careful documentation of the seep area, and in the

second half we traversed upslope towards the western peak of Venere MV. This peak is characterized by high values in the backscatter intensity in our maps which made us suspect a near-surface exposure of clast-rich mud breccia. The entire seafloor upslope was observed to be characterized by fine-grained pelagic sediments highly bioturbated by benthic organisms such as crabs, sea urchins and shrimp. Clast-rich mud breccia was not directly exposed on the seafloor, but the occurrence of mud breccia only a few centimeters below the surface was proven by sediments we took on Monday 11 November using our gravity corer. Downslope in the seep area, the sediments contained a high proportion of vesicomyid clams whose chemosynthetic lifestyle is linked to environments of methane escape.

During the following ROV dive (ROV-338) we were able to make use of the high-resolution micro-bathymetry map acquired during the first dive using the AUV SEAL 500 (AUV-62). In particular, the AUV map showed an area of about 100 x 100 m with high seafloor backscatter intensities, characteristic of fluid and/or gas emissions. By observations along four profiles across the area we could prove that backscatter intensity correlated to the appearance at seabed of carbonate crusts. The seep carbonates were further associated with bacterial mats and chemosynthetic organisms such as clams and sporadic tubeworms. During that past week we had two days of bad weather, which were used for mapping the very interesting morphology of the seafloor of the over 5 million year old pre-Messinian accretionary wedge of the Calabrian Arc. Backscatter intensity maps showed, in addition to the numerous mud volcanoes with their impressive mud flows, a number of tectonic elements, including strike-slip faults, thrust-fold ridges and intervening basins. Additionally PARASOUND sub-bottom profiles show the third dimension, and we could trace mud flows from the volcanic structures into the basins.

On Thursday 13 November we received news saying that, unfortunately, we will not obtain the research permit for the Turkish Anaximander Mountains, where we had originally planned to do our work during METEOR cruise M112. Despite the strong efforts during the past weeks of the German Federal Foreign Office (AA), the German Embassy in Ankara, the Control Station German Research Vessels in Hamburg and many others, trying to obtain the research permit for our work in Turkish waters, this could not be achieved. A kind of paralyzing shock soon disappeared, and we started to adapt to the new situation. After long discussions among the scientific team we were sure that we will be able to successfully continue our expedition using the available equipment on the Calabrian Arc until 15 December.

Following last week's decision to refocus the expedition M112 on the Calabrian Arc in Italy, we developed several new ideas for planning the scientific program for the next days. First priority was given to deployment of the AUV, as the autonomous underwater vehicle and its crew were only available until our stopover in Catania on 20-21 November. Several AUV dives were therefore planned, and professionally and perfectly undertaken by the AUV team, but some problems were experienced with the recording of data by the new multi-beam system on the vehicle. Although we tried several times to get in touch with the producer of the system via their hotline and email, the problems could not be solved satisfactorily. A severe intervention into the electronic part of the pressure chamber and a change of hard disks finally brought a workaround, so that – after a short processing – on 17 November we could admire a fantastically detailed micro-bathymetry map of Venere MV. A striking difference between the two summits of the mud volcano was immediately apparent: whereas the western summit showed fresh mud flows northwards, but especially to the

south, the eastern summit does not show any recent mud flows, but includes fractures along its northeastern flank, which cut both structures. The map backscatter intensity from our AUV dives indicates a clear distinction between the different mud flows, which probably is connected to difference in their ages.

We do not yet know the ages of mud flows at Venere MV, but by means of micro-bathymetry it becomes clear that there has been recent activity at the western peak. On Monday, 17 Nov and Tuesday, 18 Nov we sampled the water column with the CTD/rosette, with interest in samples near seabed and at high resolution above the northern flank of the mud volcano, where the ship's PARASOUND echo-sounder show gas bubbles emissions to occur. With the CTD we simultaneously measured the flow of different water bodies by means of a lowered acoustic Doppler-Sonar current profiler (LADPC). This was crucial for understanding the three-dimensional drift of methane plumes from the emission point.

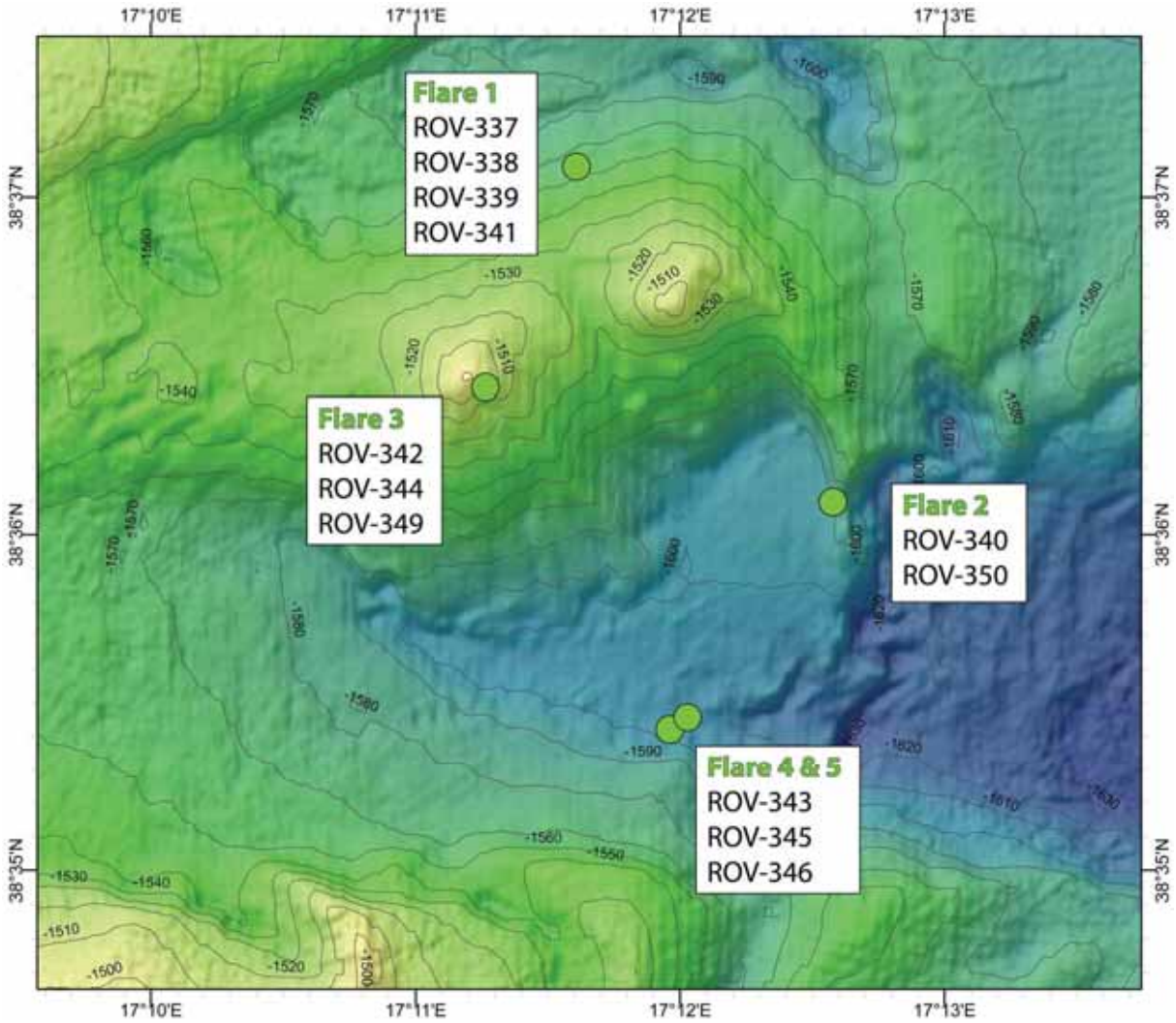

Fig. 9: Flare numbers 1-5 explored at the two summits and surrounding Venere Mud Volcano, and distribution of ROV dives using QUEST 4000 m for detailed surveys on the seafloor.

On Monday 17 November, we also performed a 10-hour dive with the ROV QUEST 4000 (ROV-339) in the area of the most prominent gas emission (Flare 1; Fig. 9). All experiments and samplings at the seafloor were performed without technical problems and to the participating scientists' great

satisfaction. The ROV successfully acquired several short sediment cores from various habitats and pore-water environments, as well as samples of gas bubbles, and sediment temperature measurements using the T-stick. Furthermore we measured two profiles with our new downward-looking Prosilica camera, which will be combined in a mosaic to allow high-resolution mapping and quantification of the details of this seep area. A preliminary comparison of the dive observations with the high-resolution backscatter map of the AUV suggests the seep area to correspond with an area of particularly high backscatter. This map information was used in planning further dives in the area.

The 340th dive of the ROV QUEST was performed on Tuesday 18 November, at the foot of the southern flank of Venere MV, where acoustic data indicate a relatively weak gas emission (Flare 2 Fig. 9). By sampling and targeted observation we documented a heterogeneous seep area similar to that north of the mud volcano, also including thick carbonate crusts and occurrences of tube worms. The final AUV dive (AUV-66) of this cruise was performed during the night, in the area of the central caldera of Cetus MV. Its mapped micro-bathymetry was astonishing because of the high details. On Wednesday 19 Nov, after acquiring two gravity cores and a water column profile measurement at Cetus MV, we headed for Catania and arrived punctually in the port under best possible weather conditions on Thursday 20 November.

The two days in harbor with Mount Etna the highest active volcano of Europe in the back, were used for an exchange of expedition equipment, scientists and crew members, and divided our cruise into two legs. After leaving the port of Catania last Saturday 22 November we focused on mapping the seafloor in the southern part of our working area using the hull-mounted multi-beam sonar (Fig. 8). In addition to looking for new mud volcanoes, we simultaneously prospected for gas emission sites on the seafloor. The Spartiviento and Crotone fore-arc basin, as well as part of the inner pre-Messinian accretionary wedge were in our focus, but now we concentrated on further tectonic segments from the outer part of the Calabrian Arc. From a long mapping profile across a major part of the tectonic sections of the Calabrian Arc, we got a very good impression of the complexity of this part of the collision zone between Africa and Europe. An extremely high quantity of closely folded ridge segments alternate with intercalated sediment basins that document the higher complexity of this accretionary wedge relative to others. A further complication of this system is the presence of Messinian salt deposits in the underground, which are partly involved in the tectonic folding and may serve as a thrust plane in the younger, outer part of the accretionary wedge. Most sub-seafloor structures are manifested in a complex seafloor morphology, from which we also tried to identify the presence of mud volcanoes. The first station work of Leg 2 occurred on Tuesday, 25 November, and included a sediment core and a CTD-deployment in the 3,100 m deep basin. The rest of that day and throughout the night we conducted mapping on several crooked profile lines north of Venere MV. During the following day, 26 November, we performed a dive at the northern Flare 1, which is the same location where we had observed the strongest gas emissions at the seafloor the previous week.

During our acoustic surveys, we found up to five gas emission locations at Venere Mud Volcano, which were chronologically named Flare 1 to 5 according to their discovery date (Fig. 9). The ROV QUEST dive (Dive ROV- 341) on Wednesday morning, 26 November, started with a surprise. At the seafloor in 1,570 m water depth, we could not see any gas bubbles at the emission location that always showed strongest gas emission at the PARASOUND records. Such a change in gas bubble activity after only a few days revealed the high variability of the active gas emissions, both in time and space. From now on we focused on studying the variability patterns of these 5 flares in more

detail by crossing the locations almost daily and checking them with PARASOUND several times in a 1.5-hours transit. Nevertheless the dive, which was accompanied intensively in the all-purpose lab of the ship, brought very valuable information even without bubbles. Water samples were taken above an active seep field from which the methane concentration will complement samples taken from the water column with rosette/CTD. Combining both data sets will allow us to better characterize the seepage area and the methane transport in the water column. In addition we obtained several temperature measurements in the sediment using our T-stick, as well as a targeted sediment sampling from hydrogen sulfide rich seeps by push coring.

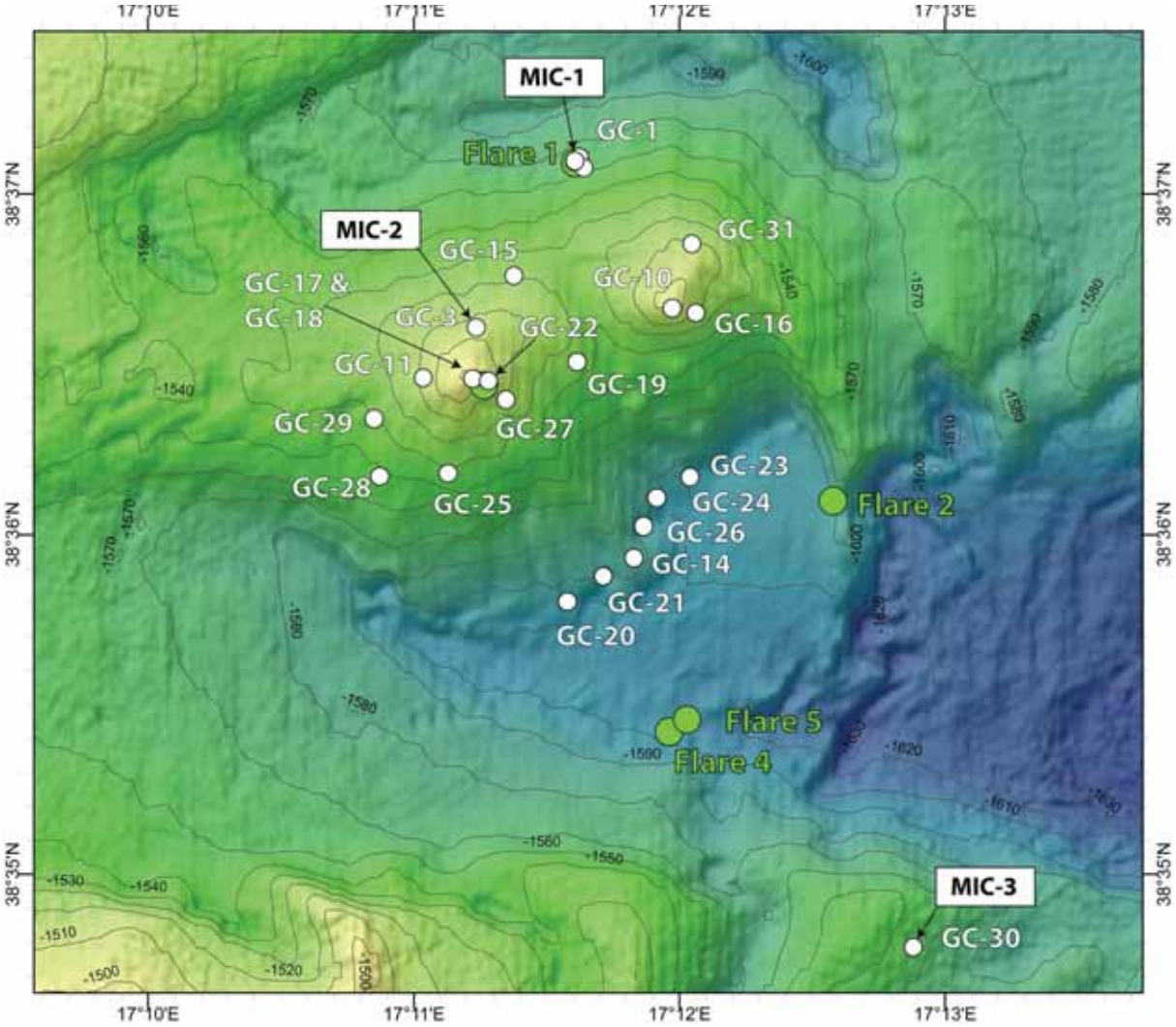

Fig. 10: Stations of gravity corer and mini corer sampling at Venere Mud Volcano.

During the night to 27 November, we steamed for Catania in order to obtain a late parcel from the USA and some luggage lost during the flight from Germany. The parcel contained spare parts for the ROV QUEST, and the luggage contained a number of cables and spare parts for our ROV. The handing over went well and again gave us an opportunity to gaze at the surmounting volcano Mount Etna. Back in the northern work area off Calabria we successfully conducted ROV Dive 342 at the western summit of Venere MV on 28 November. This investigation visualized for the first time fresh mud flows 'live' at the seafloor. These flows are moving downhill from the summit area in well-defined channels via more than 100 m altitude difference along the slope at the southern flank. The

following Saturday, 29 November, became a day of gravity coring, which we continuously deployed at six different locations within the mud volcano area (Fig. 10). Selection of the stations was supported by the AUV backscatter map. On Sunday, 30 November, we had an early CTD-station for studying the methane plume in the water column. Afterwards we conducted the extremely fascinating ROV dive 343 at Flares 4 and 5, at the southern edge of the mud volcano structure.

R/V METEOR's fifth week of the 112nd expedition was dominated by dives using the MARUM remotely operated vehicle QUEST 4000 m. We conducted dives almost daily, during which the scientific payload that included push cores, a temperature probe, gas bubble samplers, bubble catcher, nets and a shovel was routinely utilized on the seafloor, representing the main program of this cruise. On Monday, Wednesday, and Thursday we performed dives at Venere MV, which was well-known to us from the AUV-map, while on Friday, 05 December, and Saturday, 06 December, dives ROV-347 and 348 were conducted at Cetus (Fig. 11) and Nikolaus MVs (Fig. 8). On Wednesday, 03 December we placed our autonomous Sonar called ASSMO together with a temperature lance at the gas emission site Flare 5 on the seafloor. It detected the bubble escape from the seafloor every 10 minutes for 24 hours. After recovery of the device during the following ROV Dive 346, the ASSMO recordings showed the variety of bubble release emissions on the seafloor during an entire day.

ROV QUEST Dive 344 on Monday, 01 December, guided us to quite fresh looking mud flows coming down from the summit of Venere MV. Under optical control of ROV-video cameras we picked the freshest looking one and followed it upslope to the summit. It is hard to describe our fascination when we discovered flows at the emission location right from the chimney. Although there was no visible movement of the flow, we could see from its fractures, furrows and other fabrics that it must have been flowing lately. This was confirmed by the temperature lance measurements, which recorded 22° C in 50 cm depth at the emission location, corresponding to an increase of 8° C from bottom water temperature. This very high heat flow is caused by the ascent of mud within the conduit of the mud volcano from greater depth, and certainly made the ROV-based sampling of sediments and bottom water direct from the chimney very exciting. After that dive, and during a further processing of the sediments, we found that the pore water of the mud has a drastically reduced salinity, which reach values of 10 ‰. Such fluids are quite rare in the Mediterranean because of the omnipresent Messinian salts. Furthermore the gas composition of the mud clearly showed a thermogenic source. This finding was surprising to us because the gas composition of Flares 1-5 in the surrounding regions of the mud volcano revealed of a mixture of biogenic and thermogenic sources. We could successfully sample and quantify the gas in the sediments by means of our autoclave piston corer, because this device encases the sediment with its pore water and gas content in an autoclave under *in situ*-pressure, and therefore the sample comes to the surface without any loss of gas. The quantification under atmospheric pressure documented a more than threefold volume of gas to sediment, and explained why the mud deposits in the cores have a bubble-like appearance throughout. This phenomenon reminding us of „Mousse au Chocolat" is well known to sedimentologists describing its appearance as "moussy texture". This is an unmistakable indicator for strong degasing of the sediments.

In contrast to Venere Mud Volcano Cetus and Nikolaus MVs show only little evidence of any recent activity. In the central caldera of Cetus MV, we measured a slight increased heat flow, however, a bottom water sample collected near the seafloor in the volcanic cone of Nikolaus MV showed a clear increase in methane concentration (Fig. 11). Both facts are very typical for mud

volcanoes; however, the low values indicate a calmer phase in mud volcanism currently. Nikolaus mud volcano was discovered just two days ago, during a night geophysical survey and we named it Nikolaus because the ROV-dive at this newly discovered mud volcano was conducted on St. Nicolas' day, 6 December. Besides all the diving activities also numerous gravity cores from single mud flows (Fig. 10) had been taken, as well as CTD-stations with sampling of water column in order to follow more in detail the near-bottom methane spreading and the methane plume formation of seeps.

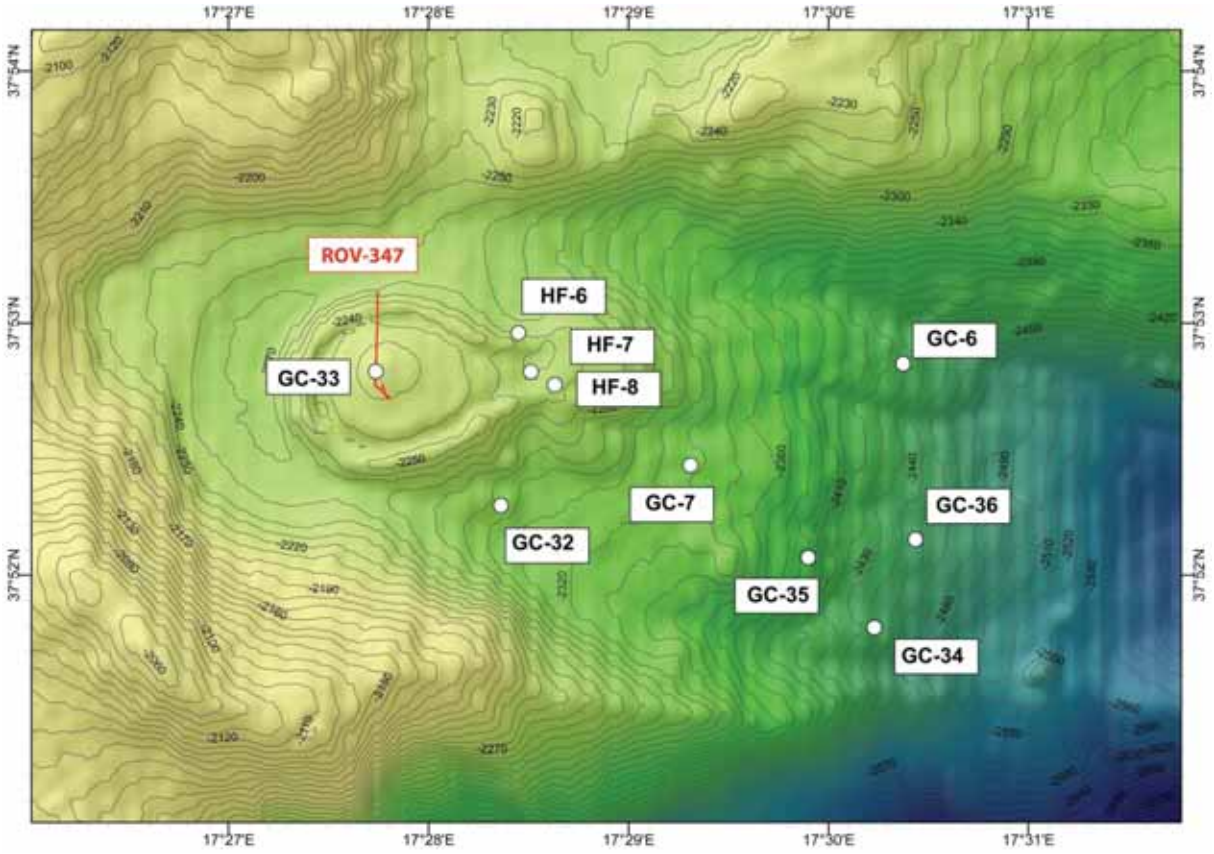

Fig. 11: Bathymetry of Cetus Mud Volcano and gravity corer, heat flow and ROV dive stations performed in the area of the mud volcano.

The weather forecast for the 6th working week showed considerably worse weather so that we used the week and the weekend before for more dives than originally planned. Wind and waves, however, were a bit milder and we could perform a last dive on this cruise with ROV QUEST 4000 m – it was dive number 350 since the ROV was installed in 2003. ROV QUEST dived at gas emission site Flare 2 which was already visited during the first leg of the cruise. Dive 350 was mainly used for exploration and mapping and left behind a bit the geological and geochemical sampling. During several flare mapping surveys using METEOR's sonar systems Flare 2 became stronger especially during the past few days, while Flare 1 decreased considerably in the water column records of the hydro-acoustic measurement. Our multiple surveys of the 5 flare locations clearly show that the seep activities around Venere MV are highly variable and we can hardly describe this variability by rules. Nevertheless the gas seepage is connected with the activity of the mud volcano. After exploration of more than ~50 mud volcanoes at the Calabrian Arc, Venere MV seems to be the only active one right now in the surveyed part of the Calabrian accretionary wedge. During the dive we intensively sampled seeps, characterized by chemo-synthetic organisms like tubeworms and clams, as well as by authigenic carbonate precipitates, by means of push cores, gas bubble sampler and T-sticks. The

sampling location was labeled on the seafloor by a very special marker. Normally our markers are composed of lifting bodies showing a number and bound with a weight as anchor, this time for the 350th dive the ROV-crew constructed a special marker whose appearance was a great surprise for all of us. According to the wintery time, they had constructed a snow-woman with a hat showing the M112 logo.

Monday, Tuesday and Thursday of the last week were characterized by gravity core sampling at Venere and Cetus MVs and sediment cores had been taken from different mud flows. Cetus Mud Volcano showed a further highlight as we could precisely determine the chimney of the mud volcano after temperature measurements during ROV dive 347 and sample it with a so-called plastic bag gravity corer. The difference to a normal gravity corer is that we do not use a plastic liner inside the corer for sampling but a big plastic bag. Sampling of pore water and sediment gas after taking cores could be executed faster and easier this way in our Geo-lab. A pore water analysis of the mud breccia core showed that like in Venere MV the salinity of seawater concentration of 38.2 ‰ is decreasing by increasing depth and reaches a constant salinity value of 10 ‰ in a depth of 50 cm. By means of that curve we can clearly prove the freshwater signal from the underground but also – by the curve progression – we can model the time of the latest mud volcano eruption via the rate of diffusion of the overlying seawater.

On Friday, 12 December, last station work of this cruise was performed by sampling some mud flows of Satori MV (Fig. 8) and since Friday night some mapping with PARASOUND and Multibeam in the deeper part of the Calabrian accretionary wedge was performed. We continued with this program until Sunday night, 14 December, and on Monday morning, 15 December, we arrived in Catania port as planned. Despite the short-term change of the research area the cruise M112 ends as a very successful cruise of METEOR.

4 Hydroacoustic Work

(M. Römer, P. Wintersteller, M. Wiebe, C. de Ferreira, D. Praeg, C. Johansen, H. Sahling, O. Candoni, T. Biller, W. Menapace)

4.1 Overview Surveys

In total, 36 surveys for hydroacoustic mapping have been performed during M112. The surveys were consecutively numbered but do not correspond to individual days. A new survey number was given when interrupted by station work and/or a different purpose for mapping was followed. Surveys 1 to 10 were conducted during Leg 1 and surveys 11 to 36 during the second leg (Table 3). The main purposes of most of the surveys were mapping for bathymetry and searching for gas flares in the water column, often both in combination. Therefore, both hydroacoustic systems available on R/V METEOR a) the multibeam KONGSBERG EM 122 and b) the parametric sub-bottom profiler ATLAS PARASOUND P70 were operating almost continuously. The shallow water multibeam system was not operating as the water depth was generally deeper than the system is capable to (>1000 m). Bathymetric surveys were usually conducted with a vessel speed of maximum 10kn, depending on the weather conditions. For the search of flares a reduced speed of 5-6kn is needed in order not to miss a flare due to the ping rate. During the seven dedicated flare surveys over the five flares at Venere MV a speed of only 3-4kn was chosen to image the known flares as precise as possible.

Table 3: Short description of the hydroacoustic surveys conducted during M112.

Survey	Purpose
1	Mapping known mud volcanoes and search for flares. Detection of Flare 1 at Venere MV
2	Bathymetric mapping
3	Flare mapping
4	Bathymetry mapping and flare search
5	Bathymetric mapping. Detection of Flare 2 at Venere MV
6	Bathymetry on transit to Cetus MV and flare survey at Cetus MV
7	Bathymetry on transit to Madonna MV and Venere MV and flare search over BS-patches
8	Narrow spaced lines over Venere MV (southern part) for flare search
9	Bathymetry on transit from Venere MV to Cetus MV
10	Bathymetry on transit from Cetus MV to Catania
11	Bathymetry survey in the south of the working area and flare search at particular structures
12	Bathymetry on transit to Venere MV and two lines for subbottom imaging over Venere MV. Detection of Flares 3,4 and 5 at Venere MV
13	Bathymetry on transit to Catania
14	Bathymetry on transit to Venere MV and three lines over Flare 3
15	**Flare survey over all 5 flares at Venere MV**
16	Bathymetry survey
17	**Flare survey over all 5 flares at Venere MV**
18	Bathymetry survey
19	**Flare survey over all 5 flares at Venere MV**
20	Bathymetry survey
21	Bathymetry survey
22	**Flare survey over all 5 flares at Venere MV**
23	Bathymetry survey and two lines over Madonna MVs
24	Backscatter survey of three lines over Venere MV
25	Bathymetry survey
26	Bathymetry on transit to Cetus MV
27	Flare survey over Calypso MV, Pythagoras MV and Nikolaus MV
28	Bathymetry on transit to Venere MV

29	Bathymetry survey
30	**Flare survey over all 5 flares at Venere MV**
31	Bathymetry survey
32	**Flare survey over all 5 flares at Venere MV**
33	**Flare survey over all 5 flares at Venere MV** And two lines for subbottom profiles east and west of Venere MV
34	Bathymetry survey
35	Bathymetry survey
36	Bathymetry survey filling gaps and transit to Catania

4.2 Bathymetry

During Cruise M112 (Leg 1 and 2) in total 36 multibeam surveys (Table 3) were performed using the multibeam echosounders (aka, MBES) installed onboard R/V METEOR, EM122 and EM710 both from KONGSBERG Maritime. Since the depths of the research area were more than 1500 meters the shallow & midwater MBES EM710 was not used. Therefore the EM122 was our main tool. This MBES is a deep sea system operating with 12 kHz, a configuration of 1 by 2 degrees, swath angle of up 150 degrees and a maximum coverage of 6 times the water depth.

During surveys the ping mode was manually set by the operators according the depth range to improve the water column resolution. When possible the orientation of the survey lines was designed to avoid waves and creating aeration under the vessel. The maximum swath angle was set between 120 and 130 degrees to improve data quality, reduce the amounts of noisy data at the outer beams and increase the ping rate. Nevertheless, the weather was quite bad during some days of this cruise, and the many artifacts created by the weather were only removed during post-processing.

All data from M122 was post-processed during this cruise using the free and open source software MB-System version 5.4.2213 (Caress and Chayes, 1995). Most of the time spent during the processing was because of the days with bad weather. Sound velocity profiles (SVPs) were periodically measured and inserted into the acquisition software (SIS from KONGSBERG), and only in one occasion it was necessary to re-apply a modified SVP to correct the raytraycing of the multibeam data. Amplitude (aka, backscatter) and sidescan (time series) values were corrected based on a function of grazing angle with respect to the seafloor (slope). The resulting maps are presented by Fig. 12 (bathymetry), Fig. 13 (amplitude).

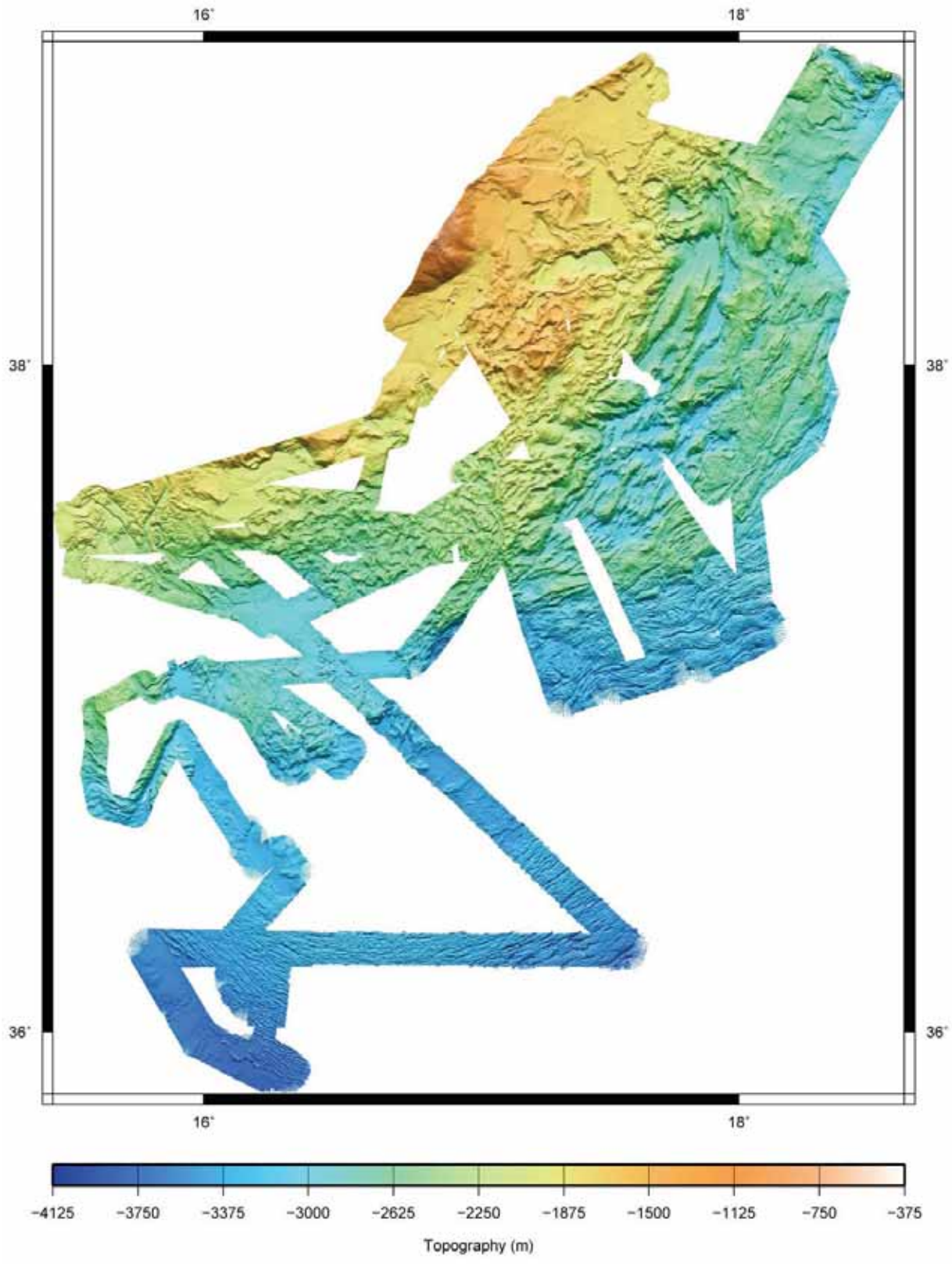

Fig. 12: Bathymetry of the MBES surveys of M112.

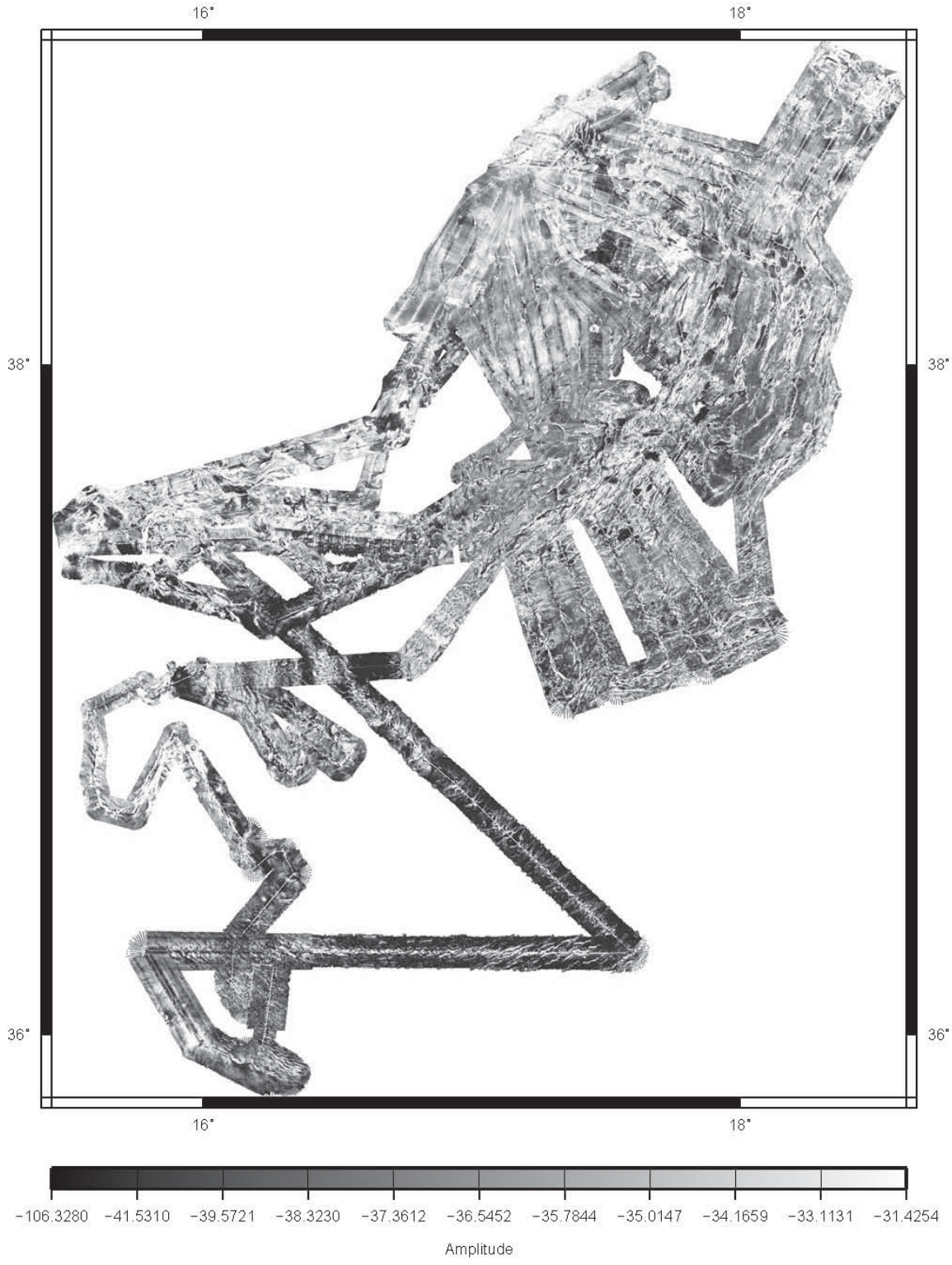

Fig. 13: Backscatter amplitude of the surveys of M112.

Since one of our objectives was a comprehensive and high resolution map of the research area, we requested MBES data from the previous cruise (M111, Chief scientist Heidrun Kropp (GEOMAR)), also mapping within this area and final-post-processed this data during M112 cruise. The result is a state-of-the-art map of the Calabrian Arc made with a resolution of 50 meters (Fig. 14).

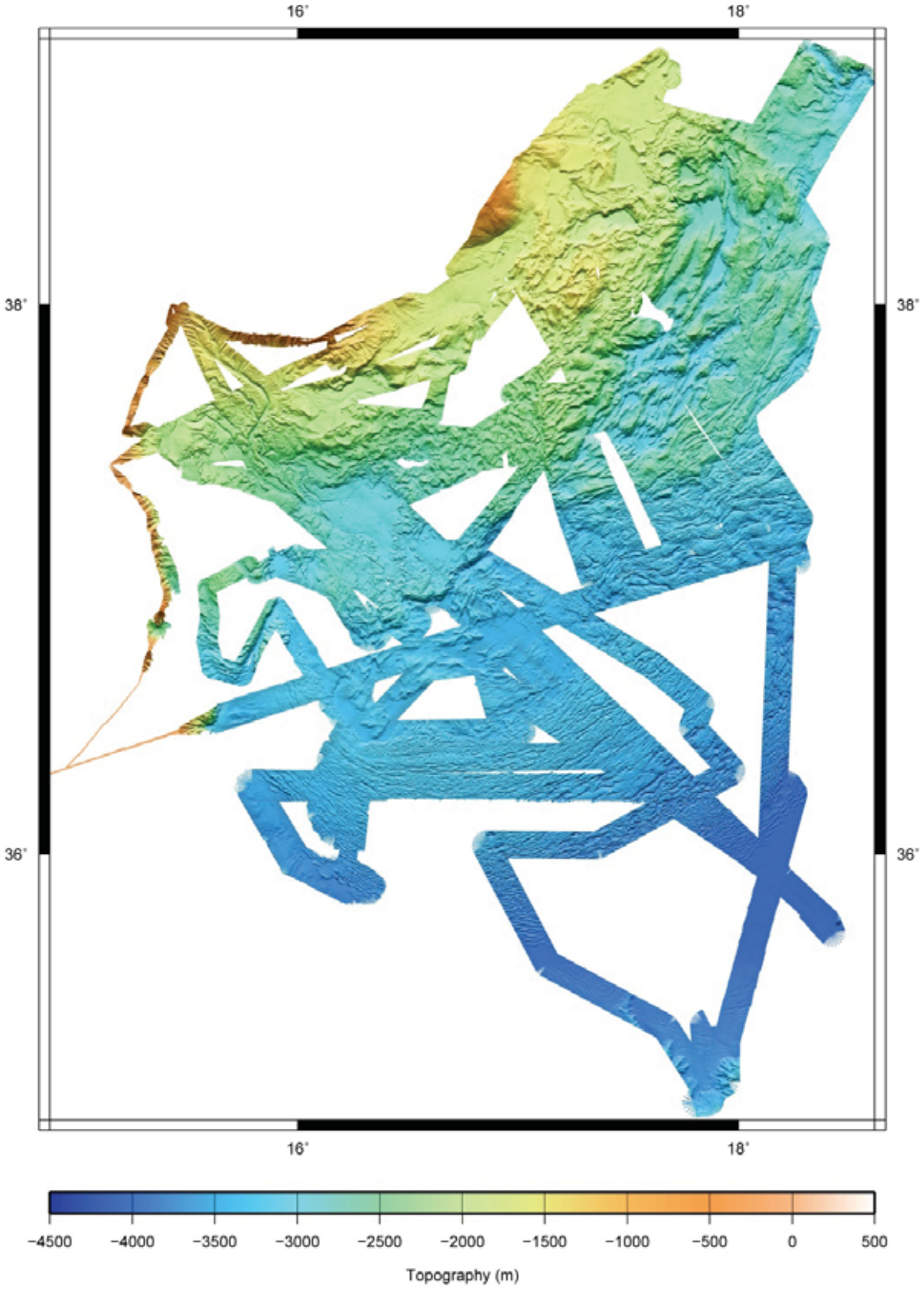

Fig. 14: Bathymetry of the combinded data of M111 and M112

Not least, the data acquired by surveys on the first leg of M112 were as the basement for planning the AUV dives, performed during this leg of the cruise.

4.3 PARASOUND

The PARASOUND echosounder utilizes the parametric effect based on the non-linear relation of pressure and density during sonar propagation. Two high intensity waves with frequencies of about 18-20 kHz (primary high frequency, PHF) and 22-24 kHz were used to create a so called secondary high (about 40-42 kHz) and a secondary low (about 4 kHz) frequency (SLF). While the SLF is used for the sub-bottom profiling, the PHF can be used and recorded to image gas bubbles, plankton and fishes in the water column. The opening angle of the transducer is 4 by 5°, which corresponds to a footprint size of about 7 % of the water depth.

The program ATLAS PARASTORE is used for storing and displaying echograms whereas the program ATLAS Hydromap Control (AHC) is used to set proper hydroacoustic settings during aquisition. The settings applied in PARASTORE for PHF and SLF displaying are variable and dependent on the actual performance influenced by, e.g., water depth, water and weather conditions. Three file formats are recorded during PARASOUND operations: Original *.asd files, which can be replayed in PARASOUND containing data of the entire water column as well as the sub-seafloor. PARASTORE also produces *.ps3 and *.sgy-files recorded along with the auxiliary data. The depth range of the *.ps3 files was set identical to those of the online display window. While *.sgy-files were not further used during the cruise, *.ps3-files were plotted in the program SENT for interpretation. *.ps3 and *.sgy-files can also be produced by replaying the *.asd files in PARASTORE.

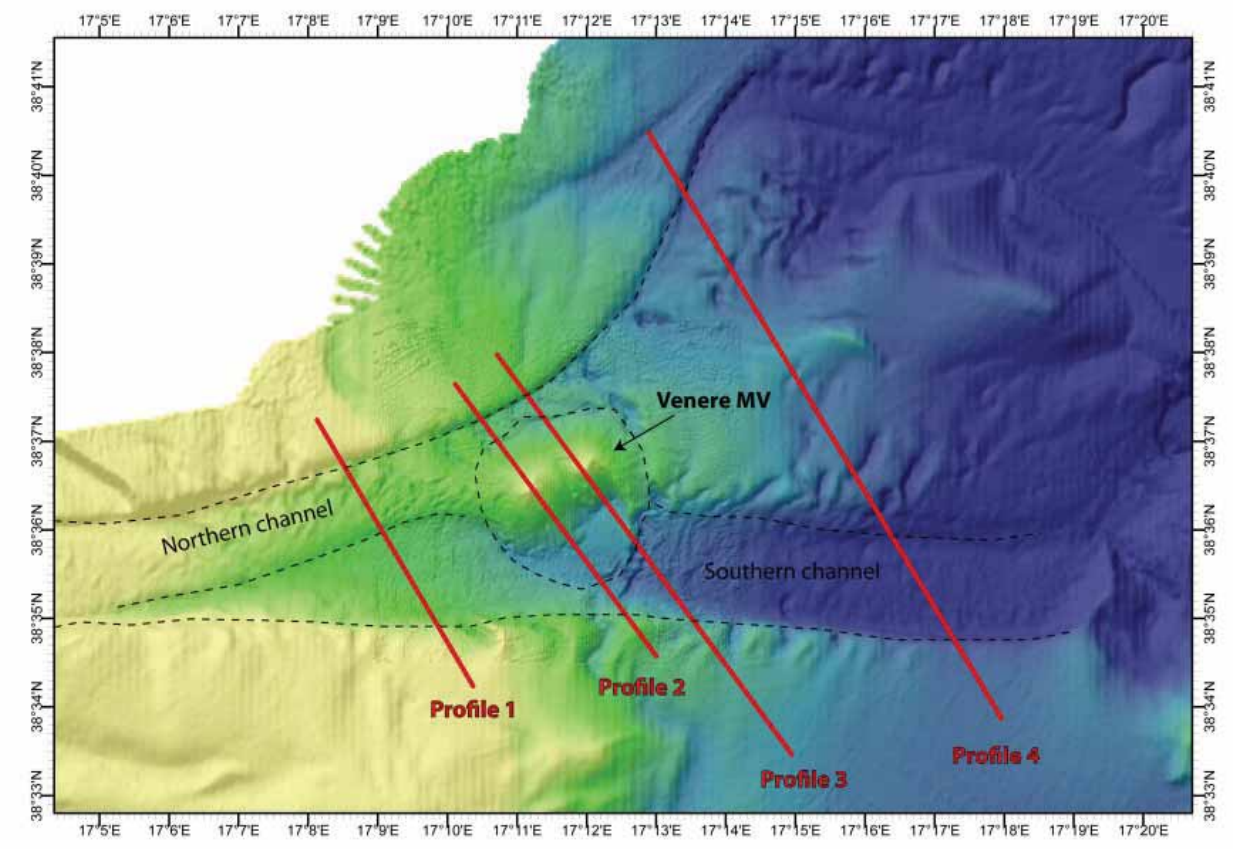

Fig. 15: Bathymetric map of Venere MV with the locations of subbottom profiles acquired during M112.

Venere MV:

Four profiles were acquired in order to investigate and understand the subbottom structures at the Venere MV (Fig. 15). They are all NW-SE directed and covering the channel structure in which the mud volcanos are situated (Fig. 16). Profile 2 and 3 cross the peaks of the Venere MV whereas Profile 1 is located west and Profile 4 was acquired east of the mud volcano.

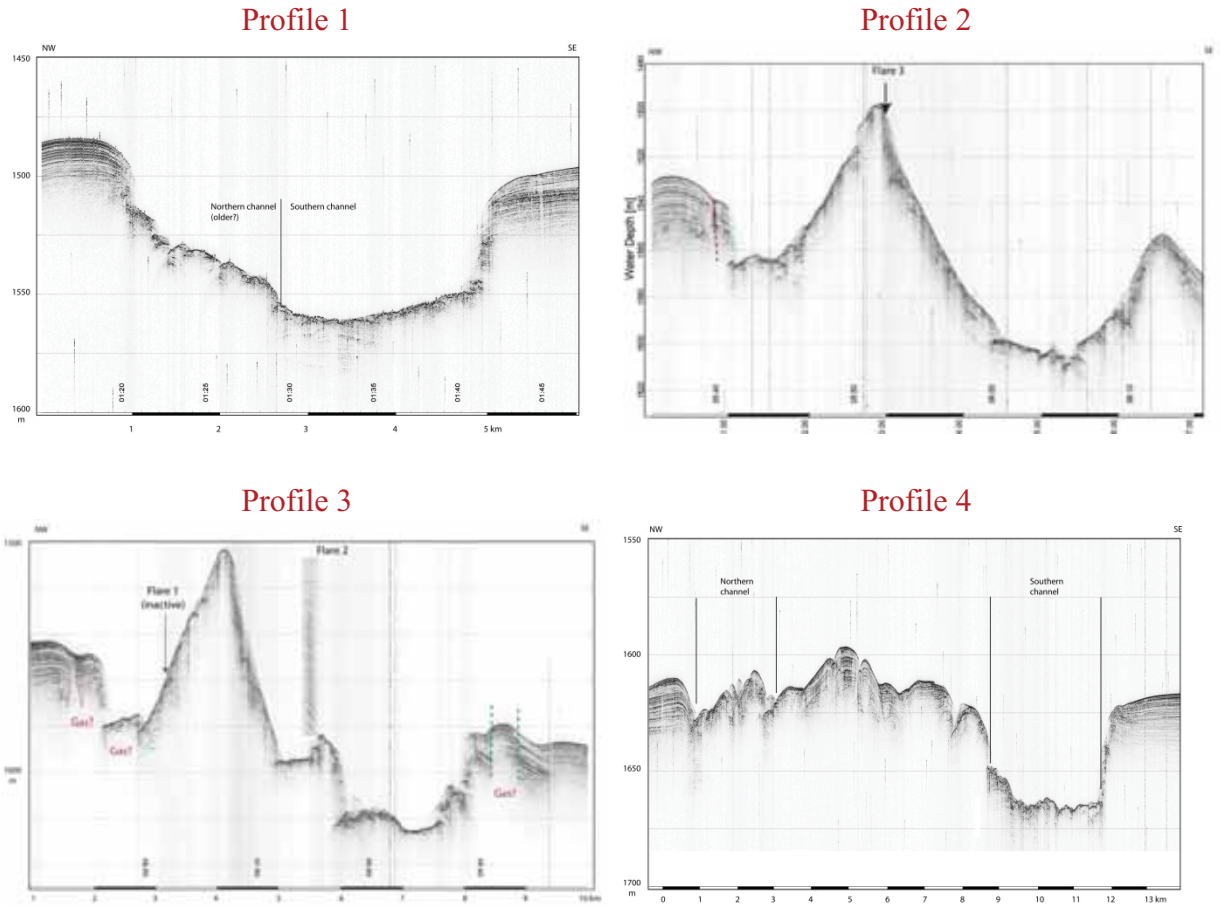

Fig. 16: Four echograms showing the subbottom profiles (Fig. 15) each NW to SE directed around Venere MV.

Profile over the accretionary wedge:

At the beginning of the second leg of M112 a more than 100 nm long profile has been conducted crossing the accretionary wedge from NW to SE (Fig. 17). Different morphologies and subbottom structures are shown in Fig. 18.

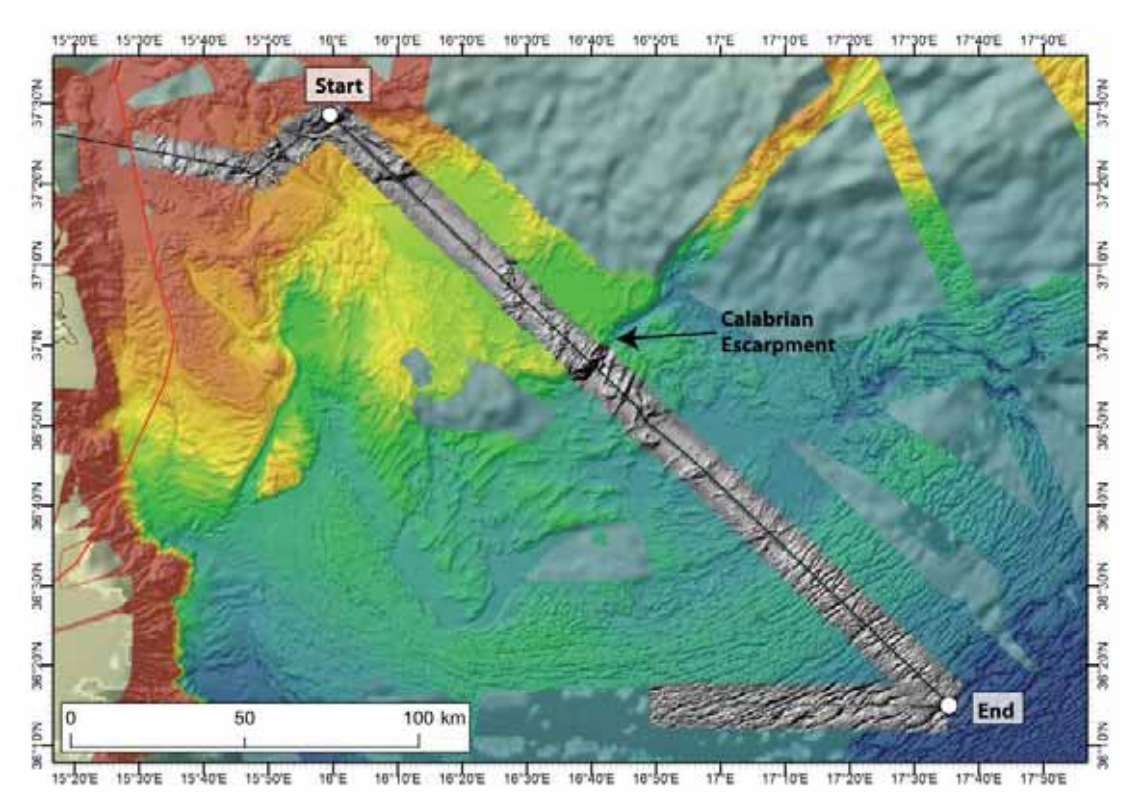

Fig. 17: Map showing the location of the subbottom profile crossing the accretionary wedge.

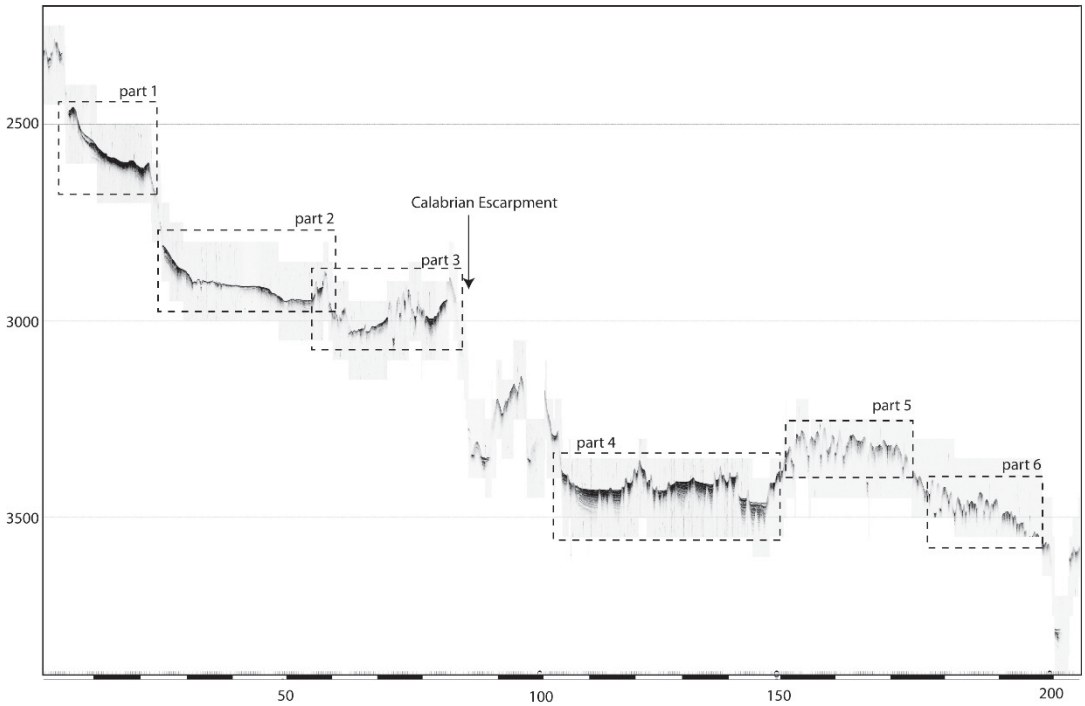

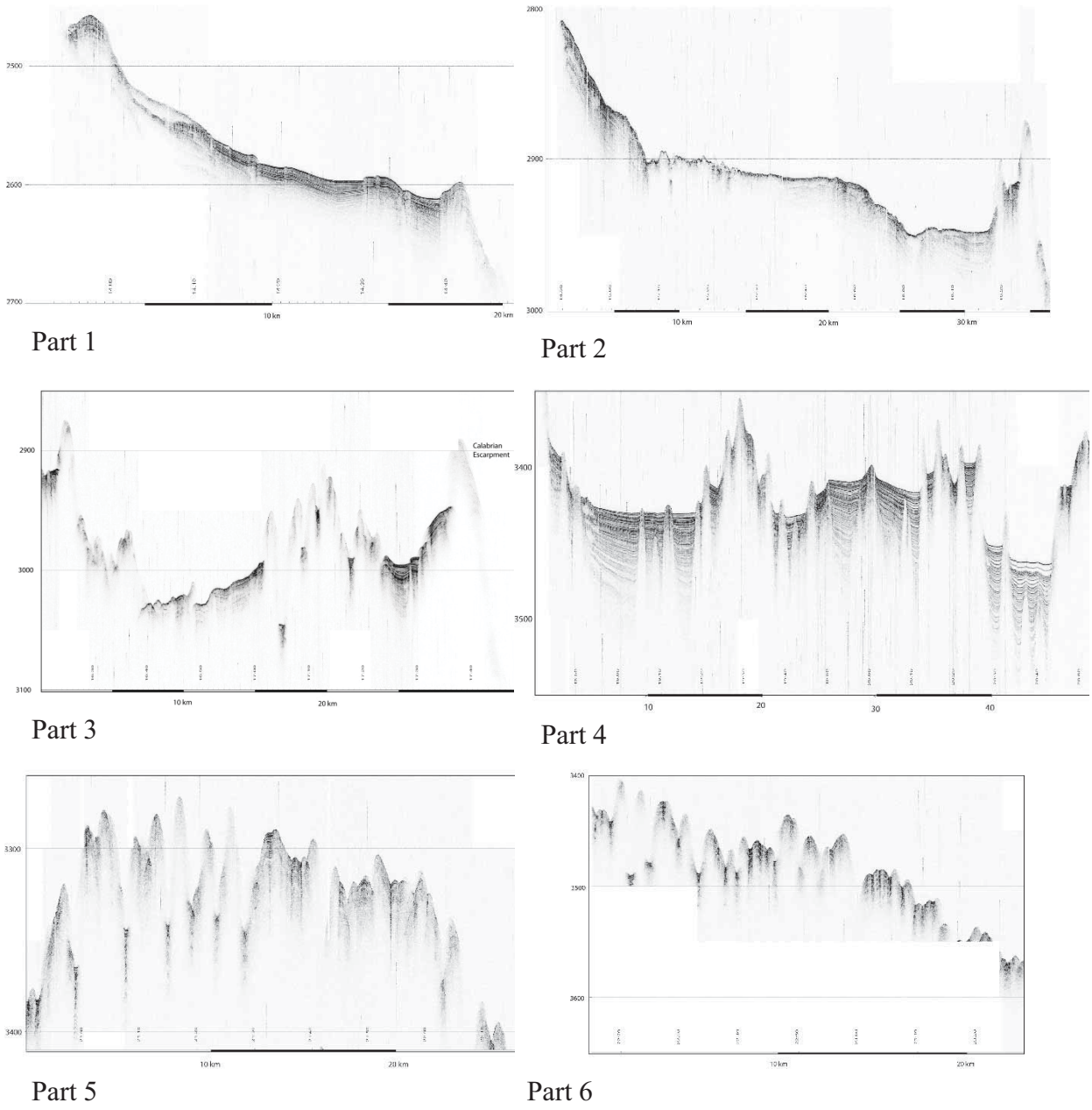

Fig. 18: Echograms showing the subbottom records of the profile crossing the accretionary wedge from NW (part 1) to SE (Part 6).

4.4 Flare Imaging

One of the major aims of the cruise was to explore gas bubble emission site ("flare sites") in the study area. Flare imaging surveys in this area were planned to access the temporal and spatial variability of the emissions. During M112 gas emissions were mapped by imaging the water column with three different techniques: (a) hull-mounted multibeam echosounder (Kongsberg EM122), (b) hull mounted parametric sub-bottom profiler (ATLAS PARASOUND), and (c) AUV-mounted multibeam (KONGSBERG EM2040). The water column data allowed determining the origin of gas emissions on the seafloor and the rising heights of gas bubbles in the water column. The flare origins could then be compared to seafloor and sub-seafloor features imaged with the multibeam echosounder and sub-

bottom profiler. Further visual analyses of the bubble streams were followed using the MARUM ROV QUEST 4000 m. With the ROV-mounted horizontally-looking sonar, single gas emission sites within a flare area were detected at the seafloor for detailed inspection and sampling. Finally, also temporal variability over one day has been documented using a seafloor installation of a sonar system, called ASSMO.

4.4.1 Multibeam Flare Imaging with EM122

During the cruise flares were mapped with the EM122 MBES. This system allows for a larger coverage compared to the PARASOUND, a single-beam sub-bottom profiler and a 3D-visualization of gas flares can be achieved. During the flare imaging surveys, the operator mapped flares in the water column data view on-the-fly (online) in a GIS (Global Mapper v.13). Therefore, the ships GPS position was streamed into Global Mapper. A point feature layer was created for each survey and for each flare a point was added. The location of the gas emission was estimated based on the ship position and the location of the flare within the MBES swath. This procedure allowed producing fast overview maps of flare distributions and maps for survey planning. The bathymetry and water column data was recorded in separate files (.all files for the bathymetry, .wcd files for the water column data) to avoid overly large files. Post processing of the water column data was done in Fledermaus Midwater (© QPS). Therefore, the .wcd files were converted into .gwc files using the "Convert Sonar Data" function. As navigation data the corresponding .all-files were loaded. The .gwc files were then viewed in the fan-view. For each gas flare the location origin on the seafloor was manually estimated based on the highest amplitudes. The corresponding xyz-coordinate was extracted with the geo-picking tool (Fig. 19). All flare locations picked in individual lines were exported as text file. These data were then imported and plotted in ESRI ArcGIS™ to generate accurate flare distribution maps. Data from surveys 15, 17, 19 and 22 have been postprocessed this way already during the cruise.

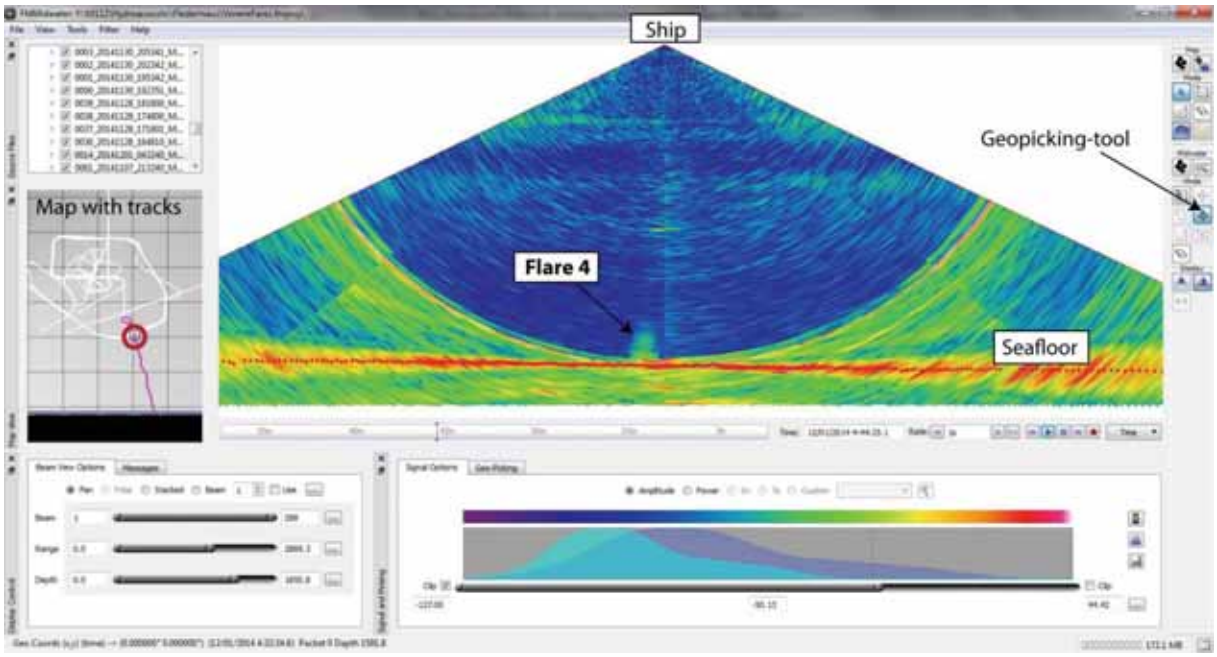

Fig.19: The Fledermaus Midwater interface (© QPS) with a fan view of a EM122 Ping that images a gas flare. XYZ coordinates of the estimated flare origin can be picked with the "Geo Pick" tool and exported as text file.

Despite intensive mapping of over 50 possible mud volcano structures with low speed (4-6 kn) and also passing several known tectonic structures, flares were exclusively detected at the Venere Mud Volcano. It should be noted, however, that those flares appeared rather weak in intensity and, although already known, still difficult to determine. The example shown in Fig. 19 is one of the best representations (in intensity and height) of a flare observation. In most cases they appeared even weaker and smaller in the multibeam swath, although the settings seem to be already optimized. We conclude therefore, that we might have missed possible flares, at least if we did not pass exactly in the center (where they would have been recognized in the PARASOUND).

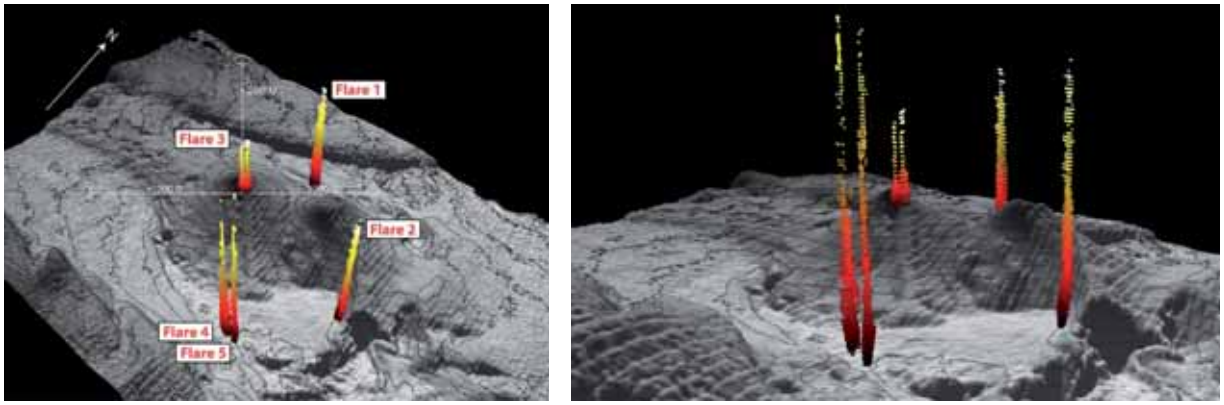

Fig. 20: 3D-compilation of all five detected flares during M112 in QPS Fledermaus in combination with the ship-based bathymetry acquired at Venere MV. The flares were extracted from the EM122 water column data and edited using the Midwater and DMagic toolboxes. Note that the data is compiled from several surveys and have not been active at the same time.

4.4.2 Single-beam Flare Imaging with PARASOUND

Although hydroacoustic evidence for gas bubble emissions (flares) were mapped over larger areas using the EM122, the 19 kHz signal (PHF) of the ATLAS PARASOUND was actually the more reliable information for flare activity and was recorded in addition during the entire surveys in the study area. The footprint is with ~7% of the water column is larger compared to the EM122, however especially relatively small flares show up much clearer due to the very high vertical resolution of PARASOUND. With respect to that fact, we passed several times with different directions over those mud volcanoes where we expected the highest possibility to be recently active. Nevertheless, none structure besides the Venere MV showed gas bubble emissions.

Indeed we detected in total five different flare locations during the first inspections of the Venere MV (Fig. 21). Following this finding, we scrutinized if the relative intensity between the flares is different and if their activity changes over time. Therefore, we prepared a short survey crossing all 5 flare locations with low speed (3-4 kn) in about 1.5 hours and repeated this survey frequently (Fig. 21). This flare-survey was performed 7 times during M112 and showed nicely (a) that the relative flare intensities are different (Fig. 22), and (b) that the intensities vary over days. A first analysis of the observed activities of every flare during the "flare-surveys" is given in Table 4.

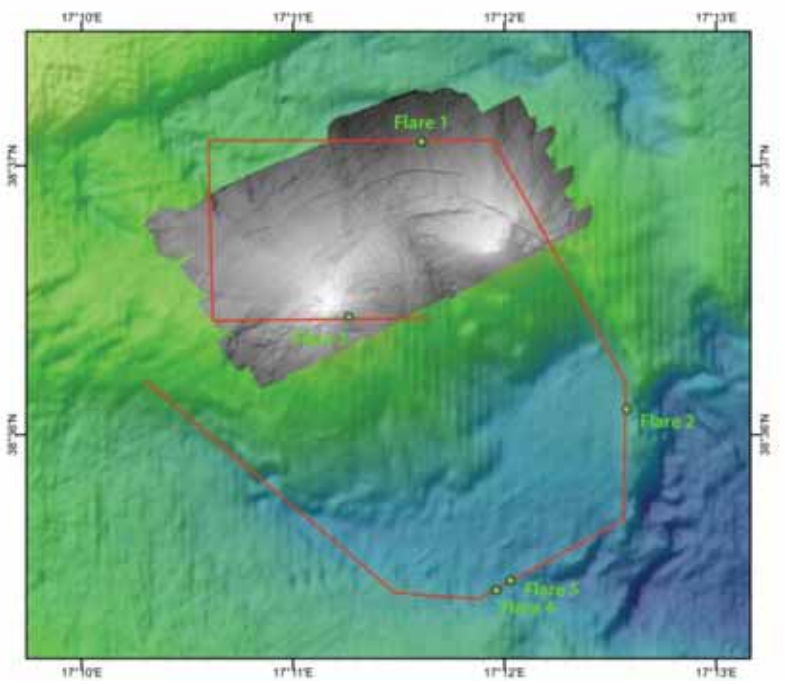

Fig. 21: Overview of the five flare locations and the survey to check their activity, which was performed 7 times during M112.

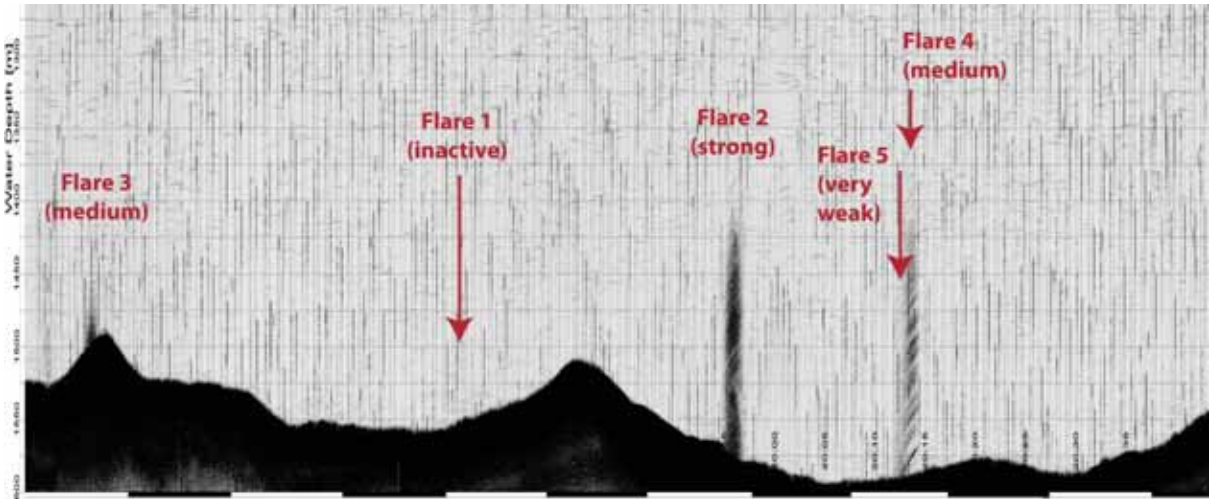

Fig. 22: Flare survey acquired on the 2/12/2014 (Survey 22) illustrating the different intensities of the five flares at Venere MV.

Table 4: Observations and activities of the five flares detected during the flare surveys. Intensity of the colour reflects relative intensity of the flare activity. *survey 32 was cancelled before crossing flare 4 and five but flares became visible during turning in the EM122 swath.

Flare	Survey 15	Survey 17	Survey 19	Survey 22	Survey 30	Survey 32	Survey 33
	28/11/14	29/11/14	30/11/14	02/12/14	08/12/14	10/12/14	10/12/14
1	on	on	off	off	off	off	off
2	on	on	on	on	on	on	on
3	on	on	on	on	on	on	on
4	on	on	on	on	on	on *	on
5	on	on	on	on	on	on *	on

Table 5: All flare observations during M112 detected with the PARASOUND system installed on R/V METEOR.

Flare1

09.11.2014	18:40	(medium)	
10.11.2014	01:40	strong	
10.11.2014	18:00	strong	
11.11.2014	00:00	strong	
12.11.2014	16:00	strong	
13.11.2014	05:50	(medium)	
13.11.2014	22:26	strong	
14.11.2014	04:30	strong	
14.11.2014	04:56	strong	
14.11.2014	21:05	strong	
18.11.2014	10:05	strong	
26.11.2014	05:18	off	
26.11.2014	19:38	very weak	
28.11.2014	21:48	weak	Survey 15
29.11.2014	17:46	very weak	Survey 17
30.11.2014	20:20	very weak	Survey 19
02.12.2014	06:50	(off)	
02.12.2014	19:28	off	Survey 22
07.12.2014	07:28	very weak	
08.12.2014	19:23	off	Survey 30
10.12.2014	06:21	off	Survey 32
10.12.2014	22:28	off	Survey 33

Flare 2

14.11.2014	04:18	medium	
17.11.2014	01:40	medium	
17.11.2014	03:55	(medium)	
26.11.2014	05:05	medium	
28.11.2014	22:14	strong	Survey 15
29.11.2014	18:13	medium	Survey 17
30.11.2014	04:28	weak	
30.11.2014	20:47	weak	Survey 19
02.12.2014	19:55	strong	Survey 22
07.12.2014	04:43	strong	
08.12.2014	19:42	weak	Survey 30
10.12.2014	06:38	very weak	Survey 32
10.12.2014	22:10	weak	Survey 33

Flare 3

12.11.2014	22:42	weak	
14.11.2014	21:13	weak	
26.11.2014	05:50	strong	
26.11.2014	17:07	weak	
26.11.2014	17:25	weak	
26.11.2014	18:00	weak	
28.11.2014	17:06	strong	
28.11.2014	17:27	medium	
28.11.2014	17:54	weak	
29.11.2014	17:15	medium	Survey 17
30.11.2014	19:43	strong	Survey 19
02.12.2014	18:51	medium	Survey 22
03.12.2014	10:30	weak	
03.12.2014	13:40	weak	
07.12.2014	09:30	(off)	
08.12.2014	05:40	off	
08.12.2014	18:56	very weak	Survey 30
09.12.2014	04:40	(very weak)	
10.12.2014	05:58	weak	Survey 32
10.12.2014	22:50	very weak	Survey 33

Flare 4

28.11.2014	22:30	strong	Survey 15
29.11.2014	18:28	strong	Survey 17
30.11.2014	04:44	strong	
30.11.2014	21:03	medium	Survey 19
02.12.2014	20:13	medium	
03.12.2014	20:52	strong	
03.12.2014	21:10	strong	
04.12.2014	10:35	strong	
08.12.2014	19:55	weak	
10.12.2014	21:57	strong	Survey 33

Flare 5

28.11.2014	22:29	strong	Survey 15
29.11.2014	18:27	medium	Survey 17
30.11.2014	04:43	medium	
30.11.2014	21:02	weak	Survey 19
01.12.2014	04:44	medium	
02.12.2014	20:12	weak	
03.12.2014	21:11	weak	
04.12.2014	10:36	weak	
08.12.2014	19:54	very weak	
10.12.2014	21:58	strong	Survey 33

Besides the observations during the dedicated flare surveys (Table 5), numerous further crossings allowed to evaluate the activity of the five flares (Table 4). In contrast to the observations during the flare surveys, these observations are not comparable due to different vessel speeds and because flares were passed in various directions or possible not exactly central. However, this information helps to define the general activity patterns of each flare. Flare 1 showed higher activity during M112 Leg 1 and very weak activity in Leg 2. Flare 3 was barely very intense and in the last week even almost inactive. Flares 2, 4 and 5 in contrast were always active when passed but show also variability. Although only known since Leg 2, flare 4 shows generally the most frequent and intense pattern.

4.4.3 AUV-based Flare Imaging with EM2040

Method

The multibeam data recorded with the AUV-mounted multibeam echosounder KONGSBERG EM2040 (used at frequency of 400 kHz) could be used to detect and locate gas flares in high accuracy. With the same method as with the ship-based multibeam water column data, the .wcd files were opened in Fledermaus Midwater, converted to .gwc and replaying either swath by swath or in the stacked view allows for detection of the flares (Fig 23). Screenshots of the flares detected were stored and the positions at the seafloor were picked and collected in a table. Due to navigation corrections, the positions were shifted after post-processing (Table 5).

Results from AUV Dive 62 at Venere MV

Water column recording was only acquired during Dive 62 at Venere MV, as storage problems arose due to the large data files collected. All further dives were deployed without water column storage and high-resolution flare positioning therefore not possible (but might be possible by particular post-processing of the bathymetric data). However, Dive 62 included the area of Flare 1 and the positions of individual bubble sites within that area could be determined (Table 4). The sites 1b and 1c have been also visually proven by ROV dives. Those sites are located very close to a high-backscatter patch in the AUV backscatter map (Fig. 14), which was proven to be a pronounced seep area with thick carbonate pavements in the central part. The gas emissions were found close to the edges of the carbonates.

First, the location of flare 1 surprised as there seemed to be no morphologic expression for a seep structure and no indication for a position at the flank of the mud volcano. However, the high-resolution bathymetry map shows ring structures around the main peaks of the mud volcano (Fig. 24), indicated by fractures visible as morphologic steps, which might facilitate fluid migration and seep formation at the seafloor.

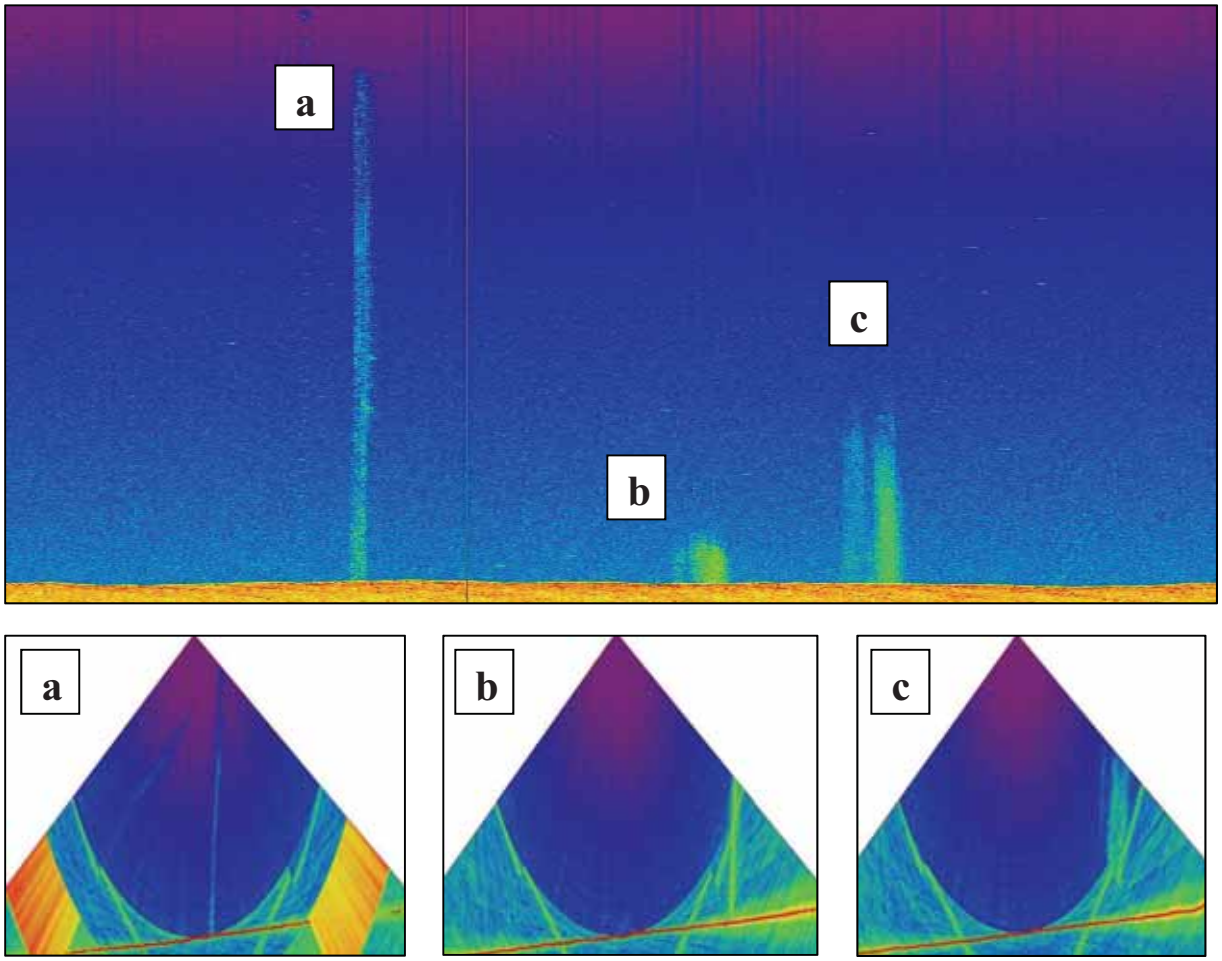

Fig. 23: Flare imaging of the AUV multibeam data (Dive 62) in the Fledermaus Midwater interface (© QPS). Above: Stacked view on a time axis illustrating the three flare clusters a, b and c shown below in the corresponding fan views.

Table 6: Flare positions picked in line 0016 of the AUV Dive 62 at Venere MV, Flare 1.

No.	Latitude (corrected)	Longitude (corrected)	Longitude (original)	Latitude (original)
1a	38.61826592550	17.19373375290	38.61890838000	17.19343751000
1b-1	38.61829339550	17.19368591290	38.61893585000	17.19338967000
1b-2	38.61828207550	17.19364856290	38.61892453000	17.19335232000
1c-1	38.61808961550	17.19345719290	38.61873207000	17.19316095000
1c-2	38.61834415550	17.19263142290	38.61898661000	17.19233518000

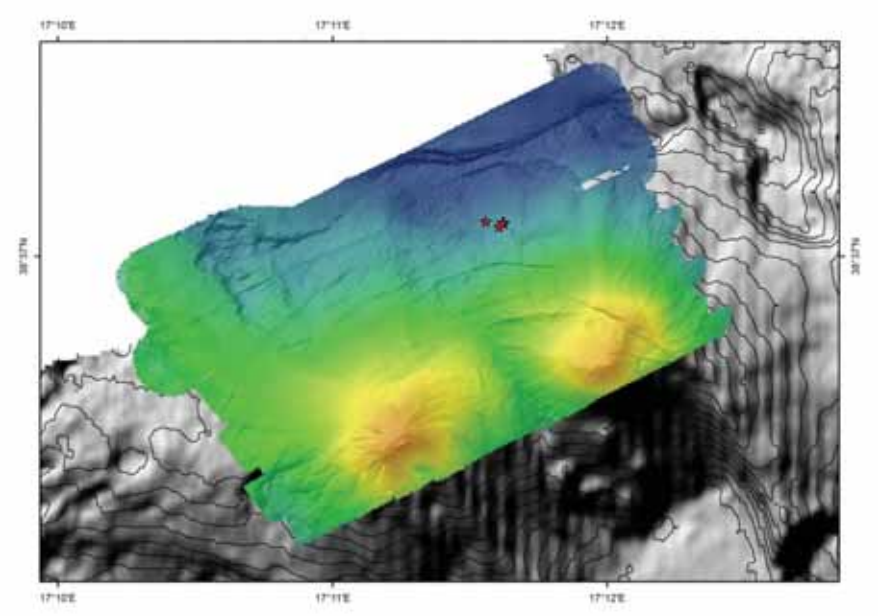

Fig. 24: Locations of the flares (red stars) detected with the AUV based multibeam records (Bathymetry combined of Dive 62, 63 and 64).

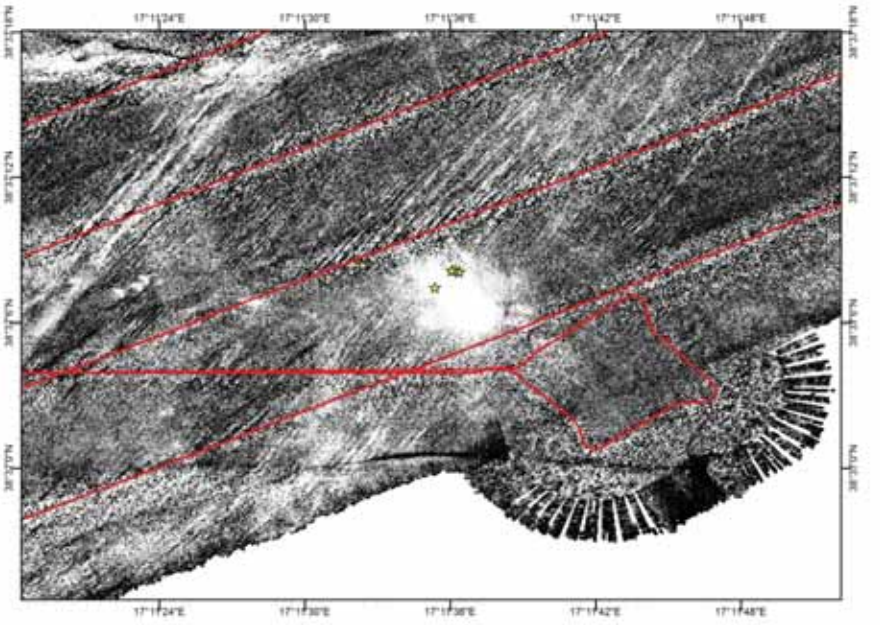

Fig. 25: The flare locations (yellow stars) correlate with a high-backscatter patch detected with the high resolution multibeam map of the AUV.

4.4.4 Gas Bubble Detection with the ROV-mounted Horizontally-looking Sonar

During ROV dives bubble stream detection is commonly supported by use of a horizontally-looking sonar mounted at the upper front of the vehicle. Due to the position of the installation on the vehicle, a sector of 180 degree in direction of the ROV heading can be imaged by scanning the water column. Finding gas bubbles streams with the sonar is much easier than visually with the cameras when you need to be already in front of a stream to recognize it. Rising bubbles become visible as

high-backscatter anomalies in the online view, depending on the stream intensity and sonar setting already at >10 m distance to the source.

However, during M112 the usually installed KONGSBERG MS1000 sonar head was defect (broke on the descent of the first dive) and could not be repaired until the end of the cruise. Therefore, another sonar head (IMAGENEX 881A, owned by AG Bohrmann) was installed instead for most of the other dives. But Dives 337, 345, 346, 347, 348 were acquired without a working sonar (and Dive 344 without recording the sonar).

The settings for finding gas bubble streams were defined while trying during Dive 338 (and by experience during earlier Cruise HE387), but modified depending on the record quality (especially the gain). The best performance was gained with the ROV in 15m altitude above seafloor and a range of 20m. The frequency was always set on 675kHz and the gain usually between 20 and 25dB. Scanning speed was chosen depending on the speed of the vehicle, i.e. when moving and searching for a signal on moderate or fast and when already detected a stream on low or lowest for a higher quality.

Gas emissions appeared depending on its intensity as small dots or bright sub-circular areas in the scans (Fig. 26). The records were useful for detection and general characterization but systematic mapping was not performed during M112. But, at the most vigorous emission site at Flare 1 several HD-recordings for visual quantification of a few bubble streams were made, which might be correlated for extrapolation with the simultaneously recorded sonar information (Fig. 26).

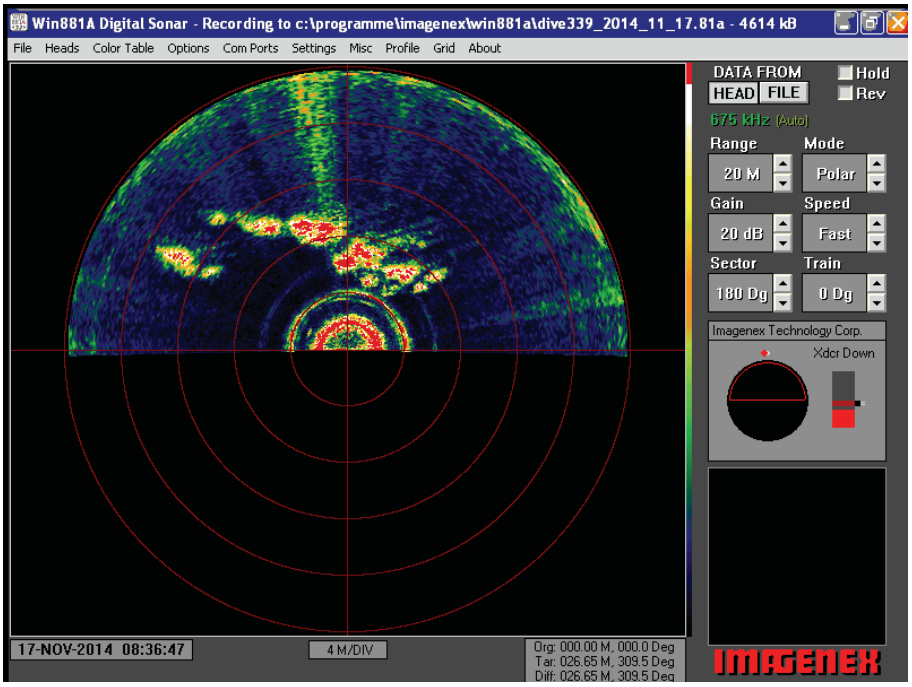

Fig. 26: Screenshot of the ROV-mounted Imagenex 881a illustrating several gas bubble streams at Flare 1.

4.4.5 ASSMO Deployment

The autonomous scanning sonar module (ASSMO) was built to observe and record the variability of gas bubble emissions at the seafloor over time. It was created and first deployed on Maria S. Merian

Cruise MSM15/2. The installation is made of a frame with a foldable arm that enables positioning a sonar in about 180 cm height above the seafloor and a chamber containing battery power as well as the programming module. It has to be deployed using an ROV, which transports and places the device on the seafloor, unfolds the arm with the sonar to a vertical position and after measuring brings it back to the vessel. The measurement, however, works autonomously and has to be programmed prior to the dive. The data need to be downloaded from the programming module and the files (*.81a) can be replayed with the respective software tool by KONGSBERG called 'win881a.exe'.

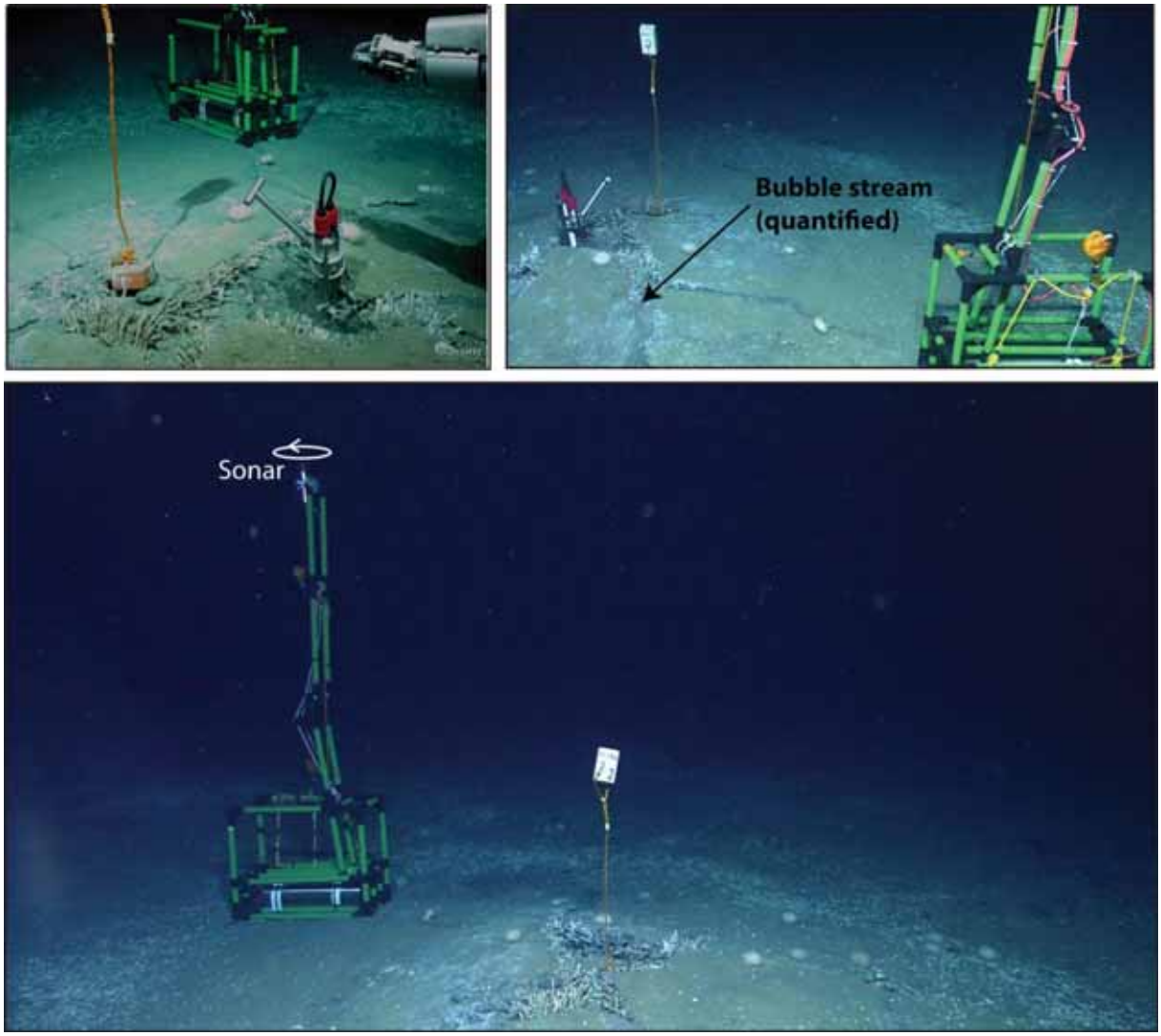

Fig. 27: Seafloor images illustrating the ASSMO deployment at Marker 2.

During M112 the ASSMO has been deployed for about 26 hours at the seafloor at Flare 5 recording the gas emission site at Marker 2 (Fig. 27). It was installed at the seafloor at the beginning of ROV Dive 345 at 3 Dec 2014 ~16:20 UTC and recovered at the end of ROV Dive 346 the following day, 4 Dec 2014 ~18:50 UTC. During deployment and recovery bubbles escaped in pulses from the same location through a crack in the seafloor, where carbonate plates overlain by a thin sediment cover are uplifted forming a mounded structure of approximately 3 m in diameter (Fig. 27). The cracks are most pronounced in the centre of this almost circular mounded structure and continue radial to their margin. During ROV Dive 343 a bursting bubble stream has been documented sourcing in the centre of the mound, however, during the ASSMO deployment the main activity came from a crack slightly down the slope of the mound. The distance of the ASSMO to the bubble stream was

~1.5m, to the centre of the mound ~2m. In addition to the ASSMO installation, also a T-stick has been placed in the sediment for the same duration. Due to the largely covering carbonates, the T-stick was placed at the centre of the mound, where the crack in the carbonates opens a possibility to penetrate into soft sediments (Fig. 27). It is the same location as for a short T-Stick measurement done during ROV Dive 343 (GeoB 19240-4).

The deployment as well as the recovery has been performed without technical problems and the set-up was satisfactory. Finally, the data were successfully recorded and can be interpreted. The general sonar settings were chosen on the experience with the sonar when mounted on the ROV during the earlier dives and as a first evaluation suitable for interpretation. Polar mode with a sector of 360 degree was chosen in order to record the entire surrounding. The range was set to 10m and the gain to 22dB. For later deployments it could be possible to change to only 5m range in case it is likely that the bubble emission is focused on a small area and the ASSMO can be placed such close again. The speed was fixed to 0.6 degree step size, which corresponds to 'medium'. An interval of scanning every 10 minutes was programmed, with a scanning time of 2 minutes. By replaying the data we calculated that ~3.8 rotations were scanned within 2 minutes, future deployments should be improved by programming full rotations.

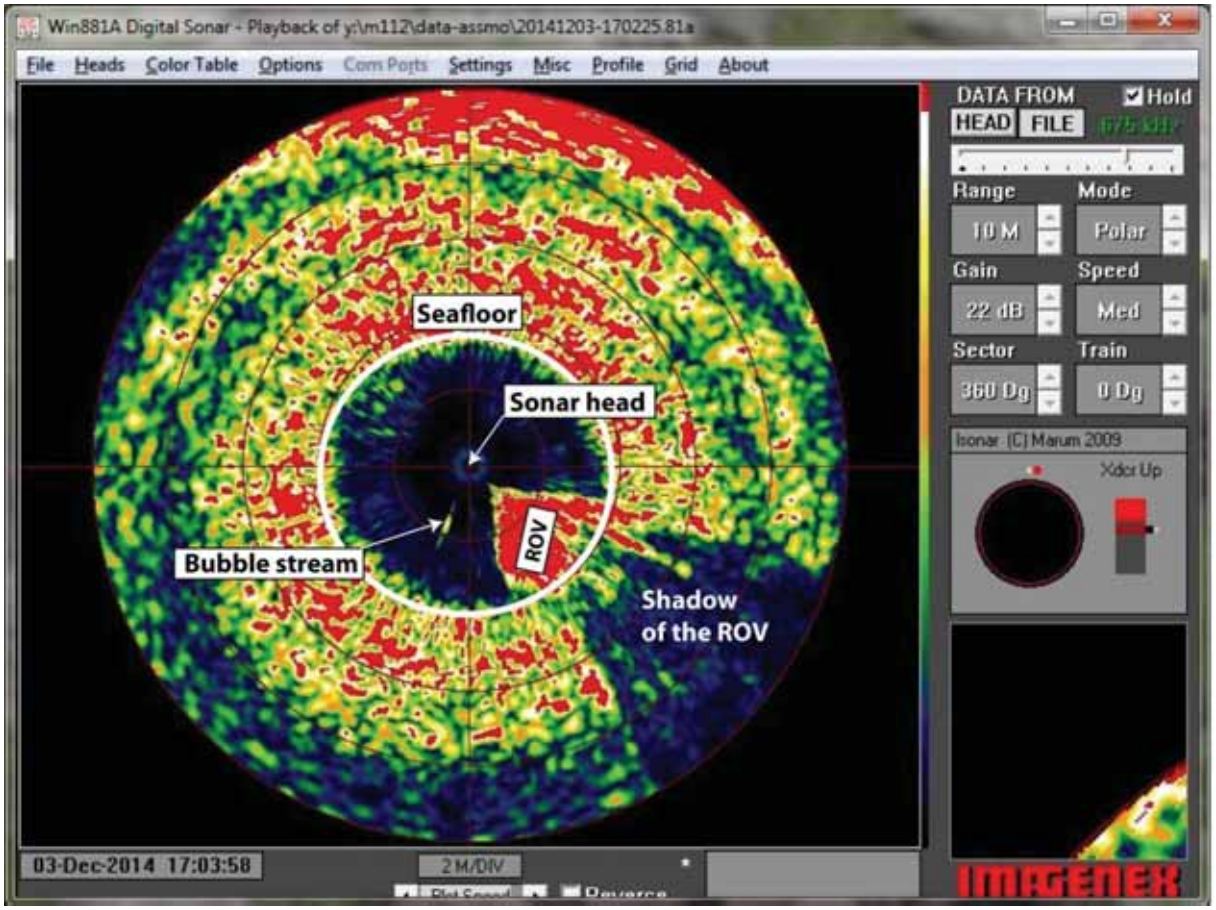

Fig. 28: Screenshot of a sonar scan showing the gas bubble stream at the same time visually quantified with the ROV.

Each of the 159 files useful for analyses shows three full scan rotations covering the emission site at the mound with Marker 2 placed at its center. An example is shown in Fig. 28, illustrating a

screenshot of the replay of one of the first files after deployment. The sonar head is seen in the center of the scan and the surrounding 4 meter of low reflectivity is the water column in which single bright reflections become visible interpreted mainly as bubble emissions but might be also sometimes passing fishes. Between 4 and 10m distance to the sonar head the high backscatter reflection of the seafloor itself is too strong to recognize any bubble emissions. After deployment and before recovery the bubble emission observed has been documented for visual quantification purposes and the ROV is clearly visible in the scans at the corresponding time (Fig. 28).

First analyses of the scans demonstrate a generally continuous activity of the bubble stream detected also visually with the ROV. However, this bubble stream emits bubbles in pulses with different frequencies. In the first hours of observation the frequency is clearly lower than at the end of the measurement. In addition, further infrequent bubble emissions were recorded besides this main bubble stream, whereas most of these occurred in the same sector (lower left from the sonar head). Especially those single occurring anomalies in other sectors might be interpreted as passing fishes. The amount of anomalies in the lower left sector has been plotted over time showing phases of up to 5 bubble streams active at the same time (Fig. 29). Nevertheless, any obvious trend can be detected so far and a correlation with the tidal information does not show a coherency (Fig. 29). More detailed analyses and interpretation are needed to correlate the activity with the temperature curves recorded simultaneously with the T-stick close to the bubble emissions (Fig. 29).

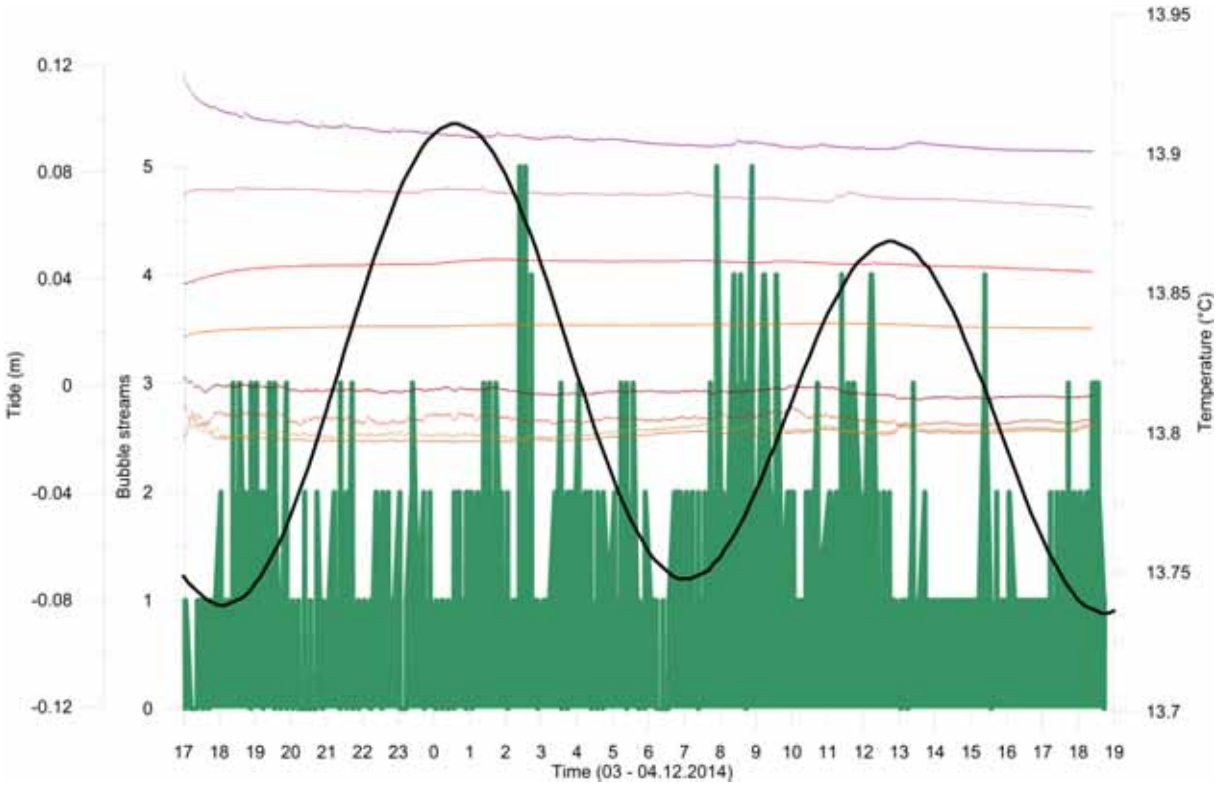

Fig. 29: Time series plot of the data analyzed from the ASSMO deployment (green) over 26 hours combined with the T-Stick records (colored lines) and the extracted tidal data (black curve) for comparison.

5 Underwater Navigation (Posidonia)

(H. Sahling)

The Ultra Short Baseline System (USBL) Posidonia (company IXSEA) was intensively used during the cruise M112 by ROV, AUV, and controlled deployment of tools such as CTD and GC. Posidonia is provided by the ships operator and maintained by the Wissenschaftlich-Technischer Dienst (WTD). Small transponders are available on board to be mounted on the cable or wire when using tools such as CTD and GC. The teams operating AUV and ROV have brought their own transponders. The antenna of Posidonia is permanently mounted on the ship's hull.

This short report intents to document our operation during cruise M112 and compiles the information available through communication with the WTD.

The Posidonia antenna was regularly maintained by service personal of IXSEA during times METEOR has been to the dockyard.

The system was last calibrated in 2010.

In order to receive good quality positions, it is necessary to import a sound velocity profile of the actual situation in the working area. This was done only during the mid-term of Leg 1. The values used are documented in Table 7 and shown in Figure 30. A SVP profile was first entered at 13 Nov 2014 ca. 19:00 UTC based on SVP-1 taken during the cruise. Unfortunately, a constant value of sound velocity was set for depths below 1500 m. That is why those values where changed to those shown in Figure 30 16 Nov 2014 around 15:00 UTC.

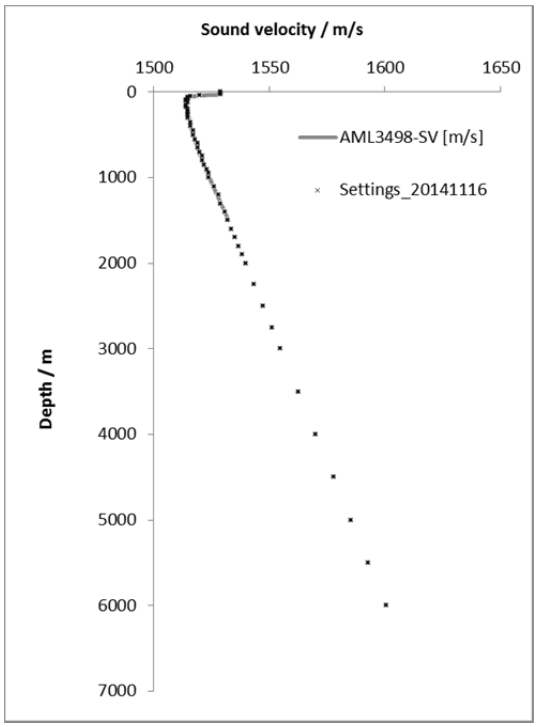

Fig.: 30: Sound velocity profile obtained during SVP-1 (line) and the values used for Posidonia (crosses).

Tab. 7: Values of sound velocity used during M112.

Pressure	Sv / m/s From 20141113	Sv / m/s From 20141116
0	1529	1529
10	1529	1529
20	1529	1529
30	1529	1529
40	1520	1520
50	1516	1516
60	1515	1515
70	1515	1515
80	1515	1515
90	1514	1514
100	1514	1514
125	1515	1515
150	1514	1514
175	1514	1514
200	1515	1515
225	1515	1515
250	1515	1515
275	1515	1515
300	1515	1515
350	1516	1516
400	1516	1516
450	1517	1517
500	1517	1517
550	1518	1518
600	1519	1519
650	1519	1519
700	1520	1520
750	1521	1521
800	1521	1521
850	1522	1522
900	1523	1523
950	1524	1524
1000	1524	1524
1100	1526	1526
1200	1528	1528
1300	1529	1529
1400	1531	1531
1500	1532	1532
1600	1532	1534
1700	1532	1535
1800	1532	1537
1900	1532	1538
2000	1532	1540
2250	1532	1544
2500	1532	1547
2750	1532	1551
3000	1532	1555
3500	1532	1563
4000	1532	1570
4500	1532	1578
5000	1532	1585
5500	1532	1593
6000	1532	1599

6 CTD and Water Column Work

(P. Geprägs, P. Wintersteller, S. Buchheister, T. Pape)

6.1 Introduction

At active mud volcanoes warm mud and fluids including volatiles are expelling. Previous studies at other mud volcanoes showed that near-bottom waters might be characterized by relatively high temperatures, high concentrations of dissolved methane and – occasionally – by low salinities (e.g. Charlou et al., 2003). During M112 five gas seepage sites have been observed in the region of the Venere MV. These sites were indicated by hydroacoustic anomalies caused gas bubble emissions from the seafloor (Chapter 4.4). The gas emission sites have been visited and sampled during several ROV dives and the water column above was sampled by hydrocasts lowered with a CTD.

The objectives of the water column work during M112 were:

- to evaluate the relation between physico-chemical parameters and concentrations of dissolved methane in near-bottom waters
- to determine the dimensions of the near-bottom water mass affected by fluid injection from the seafloor
- to assess the spatial extent of a methane plume sustained by seafloor methane seepage and diffusive methane injection.

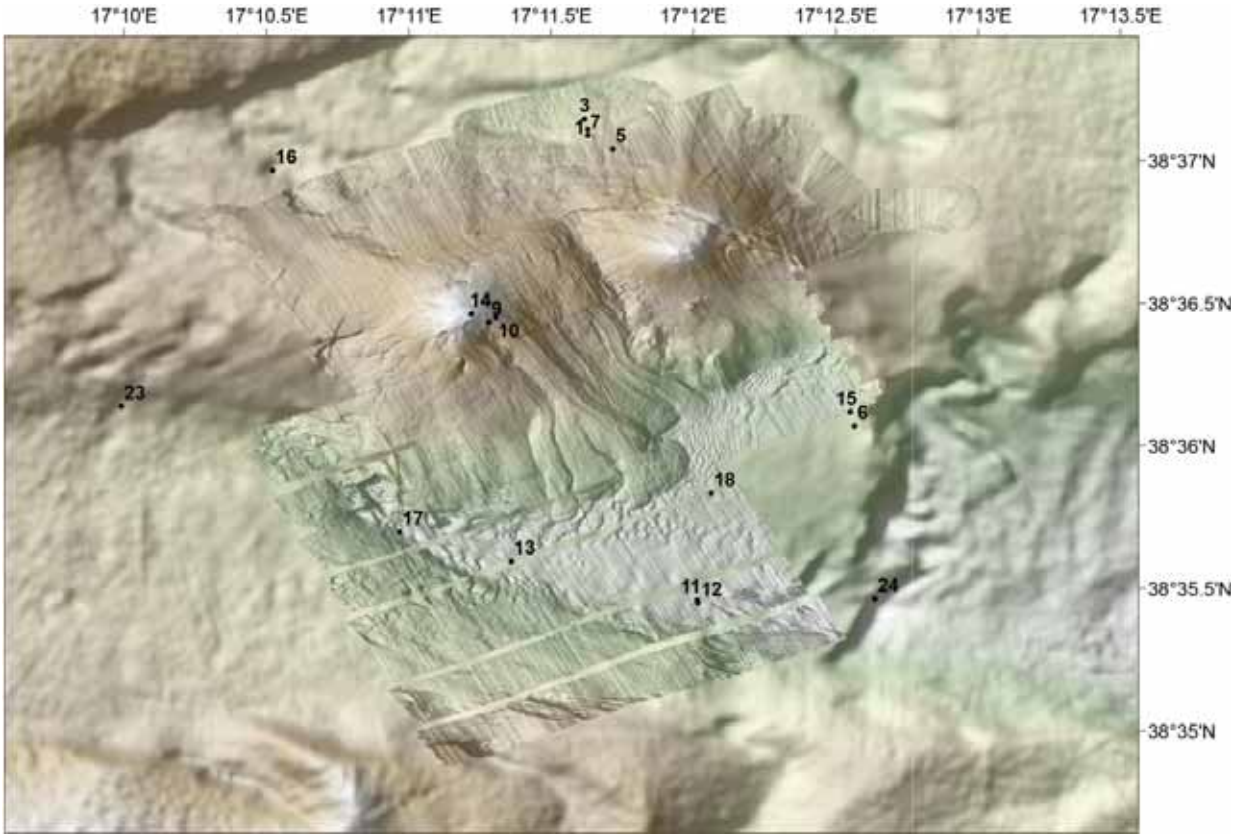

Fig. 31: Map of all CTD stations in the Venere Area where water samples were taken.

6.2 Methods

6.2.1 CTD

During M112 24 CTD stations which in most cases included water sampling for quantification of dissolved methane were performed (Table 8, map of all hydrocast stations: Fig. 31). For measurements of several physical-chemical parameters (e.g. conductivity, temperature, density) in the water column the ship-based Sea-Bird Electronics (SBE) SBE 9plus CTD probe equipped with two SBE 5T submersible pumps and a variety of sensors (2 x SBE 4C (conductivity), 2 x SBE 3plus (temperature), 1 x SBE 43 (dissolved oxygen), 1 x WetLabs FLNTURTD (combined fluorescence and turbidity)) and a Benthos PSA-916D altimeter mounted to a 24 Water Bottle SBE Carousel was used. All measured data were recorded and monitored online with a SBE 11plus V2 deck unit using the Seasave V.7.22.4 Software. During both legs of this cruise winch 02 or winch 03 of the R/V METEOR were used to lower and recover the CTD-Carousel system. The Posidonia IXSEA ultrashort baseline navigation system was mounted to the cable approximately 10 m above the carousel for exact position tracking for most of the casts.

Table 8: List of all CTD stations and samples

Hydrocast	GeoB	Water samples	Up-casts	Comment	Vacuum Extraction [amount of samples]	Syringe Headspace [amount of samples]
CTD-1	19204-1	X	1	LADCP failed	8	9
CTD-2	19207-1		3	CTD only, no LADCP		
CTD-3	19210-1	X	1		14	14
CTD-4	19214-1		1	LADCP+CTD only		
CTD-5	19216-1	X	3		8	20
CTD-6	19220-1	X	1		8	17
CTD-7	19223-1	X	3		11	21
CTD-8	19229-1	X	1	Background, no LADCP	18	21
CTD-9	19231-1	X	1		6	21
CTD-10	19233-1	X	3		6	20
CTD-11	19239-1	X	3		6	20
CTD-12	19241-1	X	3		6	21
CTD-13	19247-1	X	2		8	21
CTD-14	19250-1	X	7		7	21
CTD-15	19256-1	X	3		7	21
CTD-16	19262-1	X	2			21
CTD-17	19265-1	X	2			20
CTD-18	19271-1	X	2			21
CTD-19	19272-1		1	LADCP+CTD only		
CTD-20	19273-1		1	LADCP+CTD only		
CTD-21	19274-1		1	LADCP+CTD only		
CTD-22				Failed completely		
CTD-23	19281-1	X	2			21
CTD-24	19288-1	X	1			21
				In total:	**113**	**351**

6.2.2 Water Sampling, Gas Extraction and Analysis

Water samples from selected water depths were taken during the upcasts of 18 hydrocasts in total with 21 x 12L-water bottles (OceanTest Equipment Inc., OTE110B). Prior to deployment three water bottles out of 24 were removed from the carousel with respect to the space requirements of the LADPC, so only 21 bottles were in use. Since the focus was on the deeper water column some casts were divided into 3 lowerments at different locations which are marked with the number 1-3 behind the CTD number. In addition, near-bottom water from several decimeters above the seafloor was collected with the Gas Bubble Sampler (GBS) operated by the ROV MARUM Quest 4000 m. Bottom water was also sampled with the MIC (Mini Corer with 4 core liners).

6.2.2.1 Gas Extraction by Ultra-grade Vacuum

Immediately upon recovery on deck between 700 and 750 mL of the water samples were transferred into pre-evacuated 1 L gas tight glass bottles. The dissolved gas was prepared from the water samples by high-grade vacuum extraction. (Lammers & Suess, 1994; Rehder et al., 1999) within a few hours of collection. The released gas was taken with a gas-tight syringe via a septum of the extraction system and transferred into 20 ml serum glass vials pre-filled with saturated NaCl solution for on-board analysis by gas chromatography and long-term storage.

6.2.2.2 Extraction by Headspace Technique

In addition to the vacuum extraction – gas chromatography approach a new preparative-analytical method aiming a faster and easier analysis was tested during M112. This method comprised extraction and subsequent analysis of the gas phase for methane concentrations with the Greenhouse Gas Analyzer GGA.

Three 140 ml-syringes, provided with a valve, were taken of each bottle of the water rosette sampler. The syringes were flushed and filled with 100 ml of water, allowing for no air bubbles left in the syringe before closing the valve.

Two of these three syringes were used for the analysis, one as a spare. In the lab the syringes had to equilibrate to room temperature. Then 40 ml of Zero Air (synthetic air without methane) were added to the syringes. Both syringes were shaken for 1.5 min. With another syringe the headspace of the two samples was collected to end up with 80 ml of headspace gas. These 80 ml were injected in the GGA and diluted with 60 ml of Zero Air within the chamber of the instrument.

This method was also used to analyze the water samples from the Gas Bubble Samplers, which have a volume of about 400 - 500 ml. Three syringes were filled and some of the extracted gas was analyzed with the GGA and the rest of the extracted gas was stored in glass vials for onboard measurements with the GC and for isotopic measurements with a GC-MS at the MARUM.

6.2.2.3 Onboard Analysis of Molecular Gas Compositions and Concentrations of Methane

The gas samples were analyzed onboard for their molecular compositions and methane concentrations with a two-channel 6890N (Agilent Technologies) gas chromatograph (GC; (Pape *et al.*, 2010)). Light hydrocarbons (C_1 to C_6) were separated, detected, and quantified with a capillary column connected to a Flame Ionization Detector, while permanent gases (O_2, N_2, CO_2) as well as C_1 and C_2 hydrocarbons were determined using a stainless steel column packed with mole sieve and coupled to a Thermal Conductivity Detector. Calibrations and performance checks of the analytical system were conducted regularly using commercial pure gas standards and gas mixtures. The coefficient of variation determined for the analytical procedure was lower than 2%.

The second method to determine methane concentrations during M112 was called Off-Axis ICOS (Integrated-Cavity Output Spectroscopy) and was used the first time. This method is comparable to conventional Laser Absorption Spectroscopy where a laser beam is directed through a sample and the mole fraction or mixing ratio of the gas is determined from the measured absorption. But this analyzer, GGA-30r-EP from Los Gatos Research, uses high reflectivity mirrors in the absorption cell, which enlarges the optical path length by thousands of meters and thus the measured absorption of light is significantly enhanced (www.lgrinc.com). Only methane can be determined with this instrument and the sample is gone after the measurement. For the analysis 140 ml of gas is needed. On board 80 ml or less of the sample were injected and diluted with Zero Air to reach the required volume. Calibrations and performance checks of the analytical system were conducted regularly using commercial pure gas standards and gas mixtures.

6.2.3 LADCP (Lowered Acoustic Doppler Current Profiler)

With respect to further estimates of the distribution of dissolved methane and its transport in water as well as for further quantification of methane in water current measurements are necessary. An Acoustic Doppler Current Profiler (ADCP) uses the Doppler Effect by transmitting acoustic waves and receiving the backscattered echo from scatters in the water. A frequency of f = 300 kHz corresponds to a wavelength of $\lambda = c/f \approx 5$ mm, where a sound velocity in water of $c \approx 1500$m/s has been used. Particles of the same size as λ, such as plankton, are excited by the acoustic radiation and re-emit sound waves, which are received by the transducers of the ADCP. The crucial assumption is that the plankton moves with the same horizontal velocity as the water, i.e. it is transported by the water, but it does not move by itself. Because the scatters are usually moved by ocean currents, the backscattered acoustic wave is Doppler shifted. (RDI, 1996).

The velocity U_{ADCP} measured by the ADCP is a sum of the oceanic velocity U_{ocean} which is the magnitude to be determined, the velocity of the carousel water sampler with the CTD sensor U_{ctd}, and some background noise U_{noise} due to measurement noise and non-homogeneous flow in a depth cell.

$$U_{ADCP} = U_{ocean} + U_{ctd} + U_{noise}$$

Uctd depends on the winch speed in vertical direction but also on the ships movement over the time of deployment and recovery. It therefore equals the movement of the ship over the time.

$$DX_{\mathrm{ship}} = X^{T}_{\mathrm{ship}} - X^{0}_{\mathrm{ship}} = \overline{U_{\mathrm{ship}}}T = \int_0^T U_{\mathrm{ctd}}\,\mathrm{d}t,$$

T is the total time of the measurement.

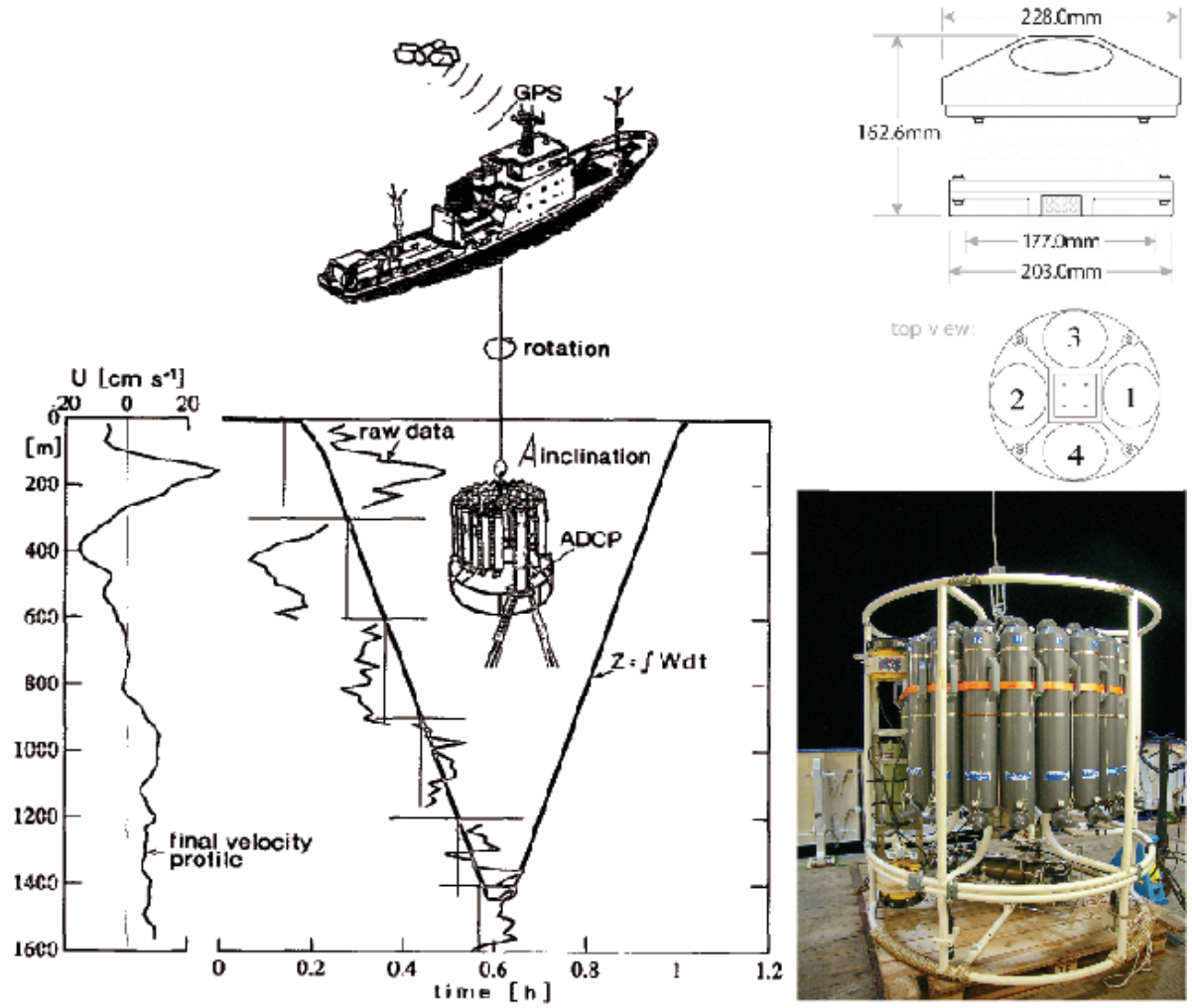

Fig. 32: Schema (Fischer and Visbeck, 1993) and setup for deployment of an up- and downward looking LADCP on R/V METEORS CTD Carousel.

The LADCP system consisted of two Workhorse Monitors with a frequency of 300 kHz built by RD Instruments, mounted with a rack on the shipside CTD Carousel of R/V METEOR (Fig. 32). They both possess high pressure cases for exposure to pressures at up to 6000 m depth and were mounted to a CTD/water sampling carousel with one at the top looking upwards (slave), and the other at the bottom and looking downwards (master). Narrowband Mode was used to achieve a maximum range, which means roughly 130 m. Thus the range of a profile from one ping is in the optimal case ca. 260 m. The true range depends on the scatteror density, which decreases with increasing depth. The manufacturer gives a measurement accuracy of 0.5 % of the water velocity relative to the ADCP ±0.5 cm/s. The standard deviation for a depth cell of size Δz = 8 m is according to the manufacturer 2.0 cm/s (cf. RDI, 1996). Prior to deployment the system has to be calibrated on land to adjust both compasses.

A MATLAB post processing toolbox by Christian Mertens (Universtiy of Bremen, 1998) was used to carry out the processing of raw data, aided by additional CTD-information and accurate GPS-positions for start and end of the casts. Detailed descriptions of the processing can be found in Fischer and Visbeck (1993) and Visbeck (2000).

Many thanks to Prof. Monika Rhein (Department of environmental Physics, University of Bremen) and her staff members Wolfgang Böke & Uwe Stöwer, for borrowing the hardware, giving introductions and for extensive support via mail.

6.3 Initial Results and Discussion

During M112 at least four major water masses could be distinguished:

1. surface water layer: high temperature, low salinity, intermediate oxygen, down to ca. 30mbsl
2. intermediate layer 1: intermediate temperature decreasing with depth, intermediate salinity increasing with depth, oxygen increasing with depth, down to ca. 50-80 mbsl
3. intermediate layer 2: low temperature decreasing with depth, high salinity increasing with depth, oxygen decreasing with depth, 180-250 mbsl
4. deep water layer: low temperature decreasing with depth, salinity decreasing with depth; oxygen decreasing with depth down to 1550 mbsl

Most interesting is the water column in the study area approximately 200 m above the seafloor. TS diagrams show little differences in these water depths, even when the profiles through the complete water column are looking very similar at all stations. Every salinity, temperature, sound velocity and oxygen profile of each cast is shown in the appendix.

6.3.1 Water Column Characteristics at the Background Station (Basin SE of Sicily)

At the water surface the temperature is with 20° C the maximum and decreases with depth (Fig. 33). At 1160 mbsl the lowest temperature of 13.758 °C is reached, a small increase of the temperature towards the seafloor can be observed. Salinity increases in the upper hundred meters and peaks at ca. 230 mbsl in 38.94 psu.

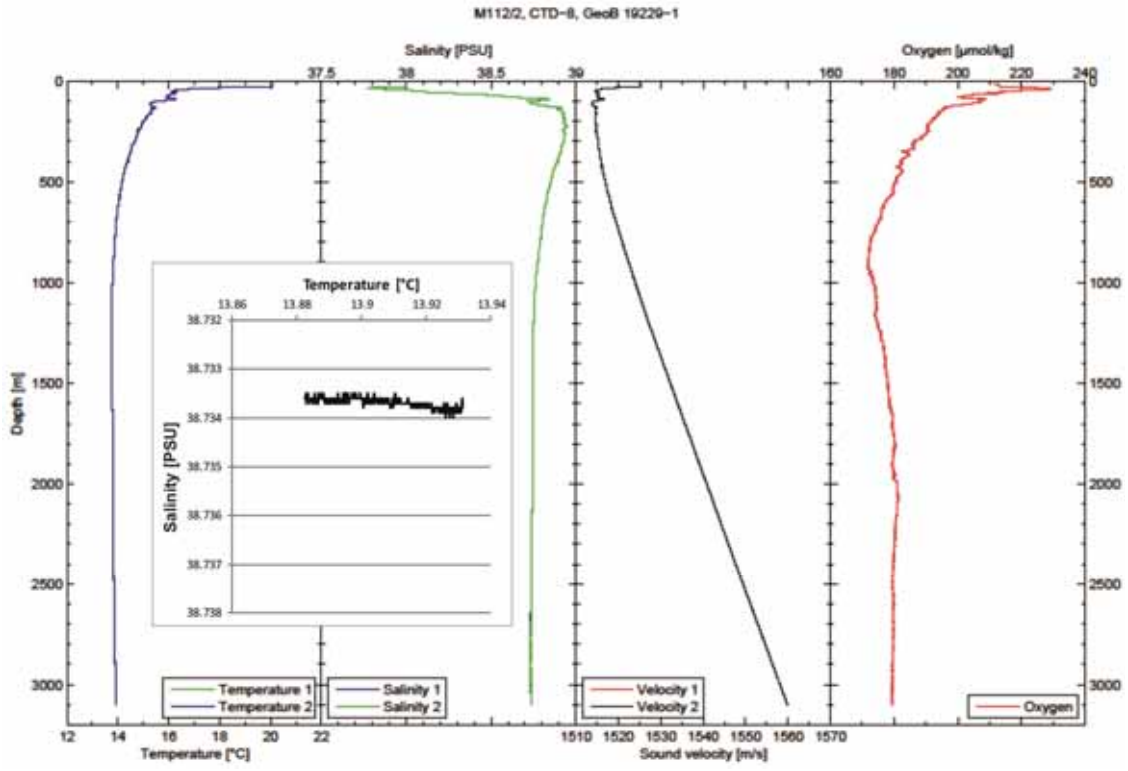

Fig. 33: Station CTD- 8 (GeoB 19229-1) SW of Sicily. Plot shows the temperature, salinity, sound velocity and oxygen profile over the complete water colum. TS diagram shows values from 2800 mbsl - 3104 mbsl (from left to right).

In greater water depth the salinity decreases and remains relatively constant at 38.7 psu. Oxygen shows two peaks in the surface water. The first peak, which is the maximum, is reached in ca. 50 mbsl with 215 µmol/kg and the second peak is in 90 mbsl with 208 µmol/kg. Then oxygen decreases to its minimum of 171.5 µmol/kg in 923 mbsl. The TS diagram shows the values of salinity and temperature 300 m above the seafloor. Salinity remains relatively constant whereby the temperature increase towards the seafloor is really significant. Compared to other stations the salinity is lower and the temperatures are higher by about 0.2° C.

The station for background concentrations was taken south of the study area in a sediment basin, where no methane source was expected. Background concentrations were around 2 nmol/l.

In Figure 34 a slightly increase in methane concentration is visible in the first hundred meters below the sea surface and in the last sample only a few meters above the seafloor. But these values are very low concentrated with 8 nmol/l and lower.

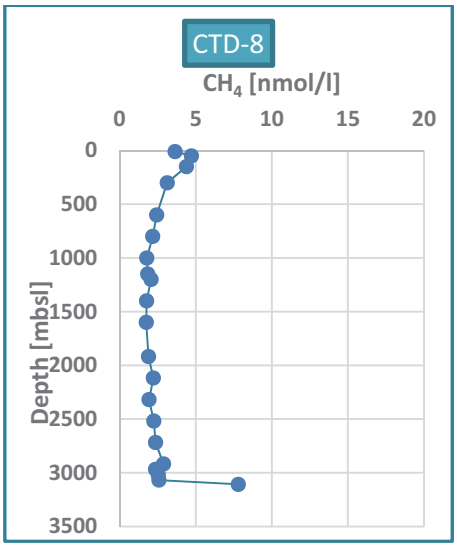

Fig. 34: Methane concentrations in the water column at the background station SE of Sicily.

6.3.2 Water Column Characteristics at Flare Sites

6.3.2.1 Venere Flare Site 1

The TS profile of CTD-7 in Figure 35 indicates two water masses, one showing an increase of salinity with increasing depth and temperature and the presence of a distinct ca. 50 m thick water mass, that is characterized by salinity decrease and temperature increase in 1450 – 1500 mbsl. Other profiles from Flare Site 1 show this layer as well, but with a broader expansion. The salinities at Flare Site 1 together with the stations on the summit have the highest salinities in the study area. The two diagrams on the right of Figure 35 show first results of the LADCP measurement demonstrated in two plots, the East velocity and the North velocity. Both together indicate a, according to the INVERSE-model, relatively small SE-ward current in this depth.

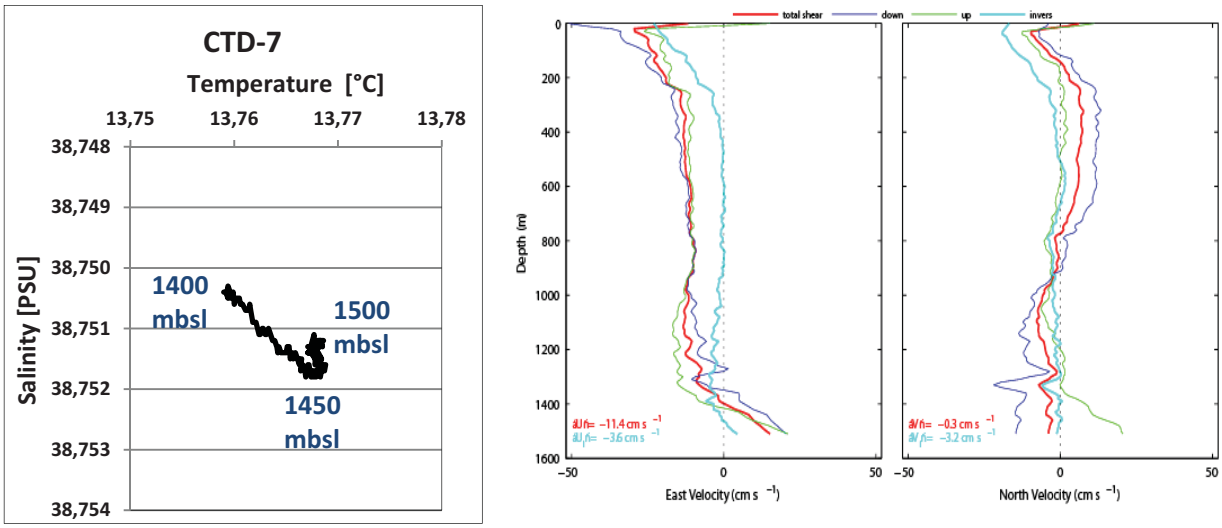

Fig. 35: TS diagram of Station CTD-7 with values from 1400 mbsl – 1500 mbsl (left) and preliminary LADCP results (right).

Water samples taken between the water surface and ca. 1400 mbsf showed concentrations of dissolved methane of less than 3 nmol /l that correspond to background concentrations as determined at station CTD-8. Below about 1450 mbsl enrichments in methane were observed for all water samples taken in that area (Fig. 36). In most cases methane enrichments were apparently restricted to a comparably thin water layer of about 20-30 meters in thickness between 1500 and 1560 mbsf. Only in CTD-1 the highest methane value was found close to the seafloor and then gets depleted within the next 60 m above the seafloor. Highest concentrations of all stations with ca. 10 µmol/L were determined for a water sample taken at station CTD-5 in 1542 mbsl.

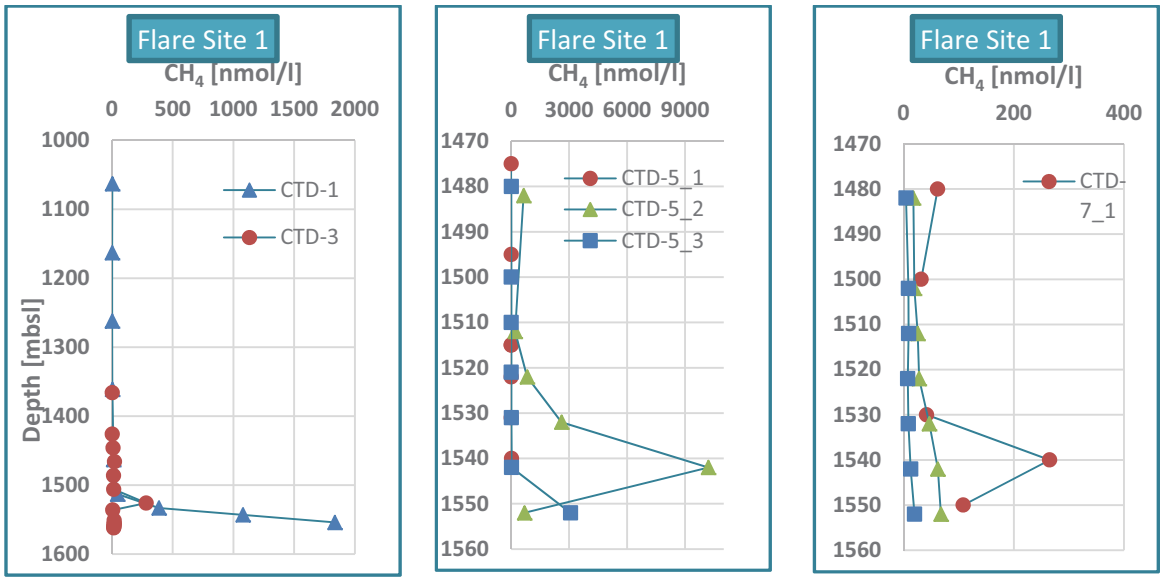

Fig. 36: Methane concentrations in the water column at Flare Site 1, containing Stations CTD-1, CTD-3, CTD-5 and CTD-7.

6.3.2.2 Venere Flare Site 2, 3 and 5

CTD-11 was taken at Flare Site 5, south of the Venere Mud Volcano and is almost identical to CTD-12, regarding the TS profiles (Fig. 7, left). It indicates only one water mass comparable to the water mass above the seafloor in CTD-7 (Fig. 34). The salinity decreases and temperature increases towards the seafloor. The measured temperatures at the seafloor with 13.773 °C are higher compared to the temperatures at Flare Site 1 and the salinities are lower. Highest temperatures are detected at Flare Site 2 in the East of the study area, they reach a maximum of 13.778 C directly above the seafloor. The currents at Flare Site 5 show the same SE-ward trend with low velocities (Fig. 37, right).

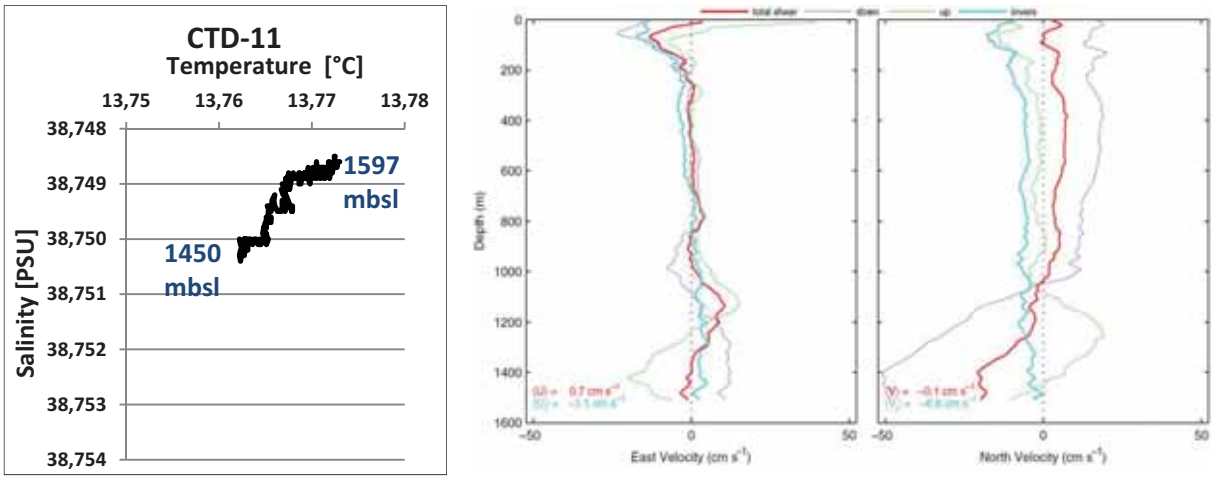

Fig. 37: TS diagram of station CTD-11 with values from 1450 mbsl – 1597 mbsl (left), LADCP Profile of CTD-11 (right).

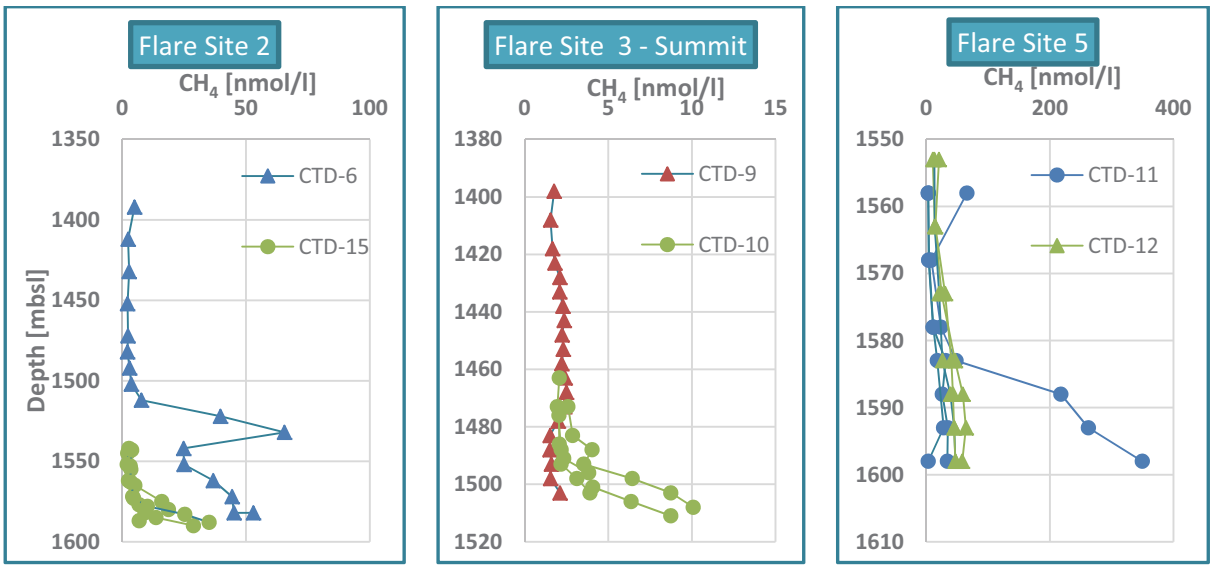

Fig. 38: Methane concentrations in the water column at Flare Site 2, 3 and 5.

Similar to observations at Flare Site 1 dissolved methane at Flare Site 2 peaked at water depths between 1530 and 1550 mbsf (Fig. 38). However, at station CTD-6 and CTD-15 the bottom water layer was also relatively enriched in methane. CTD-9 was taken above the summit of Venere MV and no clear peak can be identified, the methane values are with only 2 nmol/l background concentrations. A bit deeper at CTD-10, where Flare Site 3 was found, the methane concentrations

below 1489 mbsl get slightly enriched up to 10 nmol/l. These are the lowest methane concentrations detected in the water column in vicinity of an active and bubbling seep site. At Flare Site 5 all measured values are above the background concentrations. In the depth of 1580 mbsl all profiles show a soft peak and a little decrease towards the seafloor. There is just one cast of CTD-11 which shows a peak of 66 nmol/l in 1558 mbsl and then an increase of methane concentration up to 349 nmol/l below 1580m water depth.

6.3.3 Water Column Characteristics in the Venere Area off the Flares Sites

The TS diagram of station CTD-16 indicate lower salinities compared to Flare Site 1 but the values are also decreasing towards the seafloor (Fig. 39). CTD-16 is situated in the East, outside of the Venere structure, but even there the salinity decrease can be observed. Compared to CTD-11 the temperatures are lower and the change is not as significant. Figure 40 below shows the processed LADCP data acquired during CTD-16 cast and mirrors the mentioned layers in the water column with respect to different currents (Chapter 6.3 Initial Results, and profiles in the appendix). There is still a mismatch regarding the final water depth, due to wrong integration of the cell-bin-sizes over time/water depth. However, the small SE-ward current above the seafloor can be observed as well.

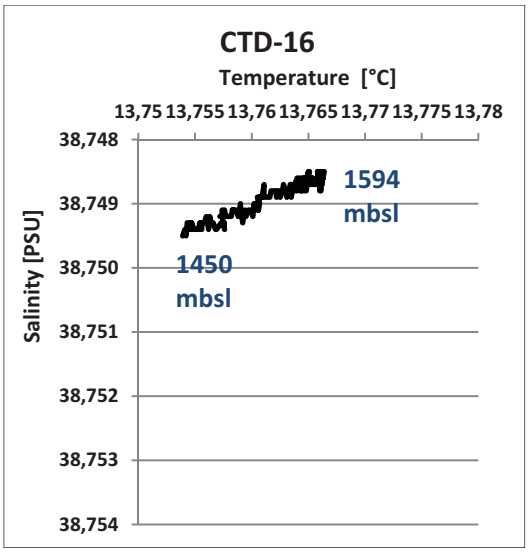

Fig. 39: TS diagram of station CTD-16 with values from 1450 mbsl – 1594 mbsl.

The regional background of methane is also around 2 µmol/l as observed in the southern sediment basin. But at some locations high methane values are measured even when there was no active flare site. For example, the stations CTD-13 and CTD-17 taken in the Canyon SSW of the Venere Summit (Fig. 41): they show concentrations up to 181 nmol/l. CTD-17 seems to be closer to a methane source showing one peak below 1550 m water depth. Whereas the samples of CTD-13 indicate two clear peaks, but with lower methane concentrations. In the elongation of this canyon CTD-23 was taken to eliminate another source from outside. In both hydrocasts of this station CTD-23 methane is below 4 nmol/l.

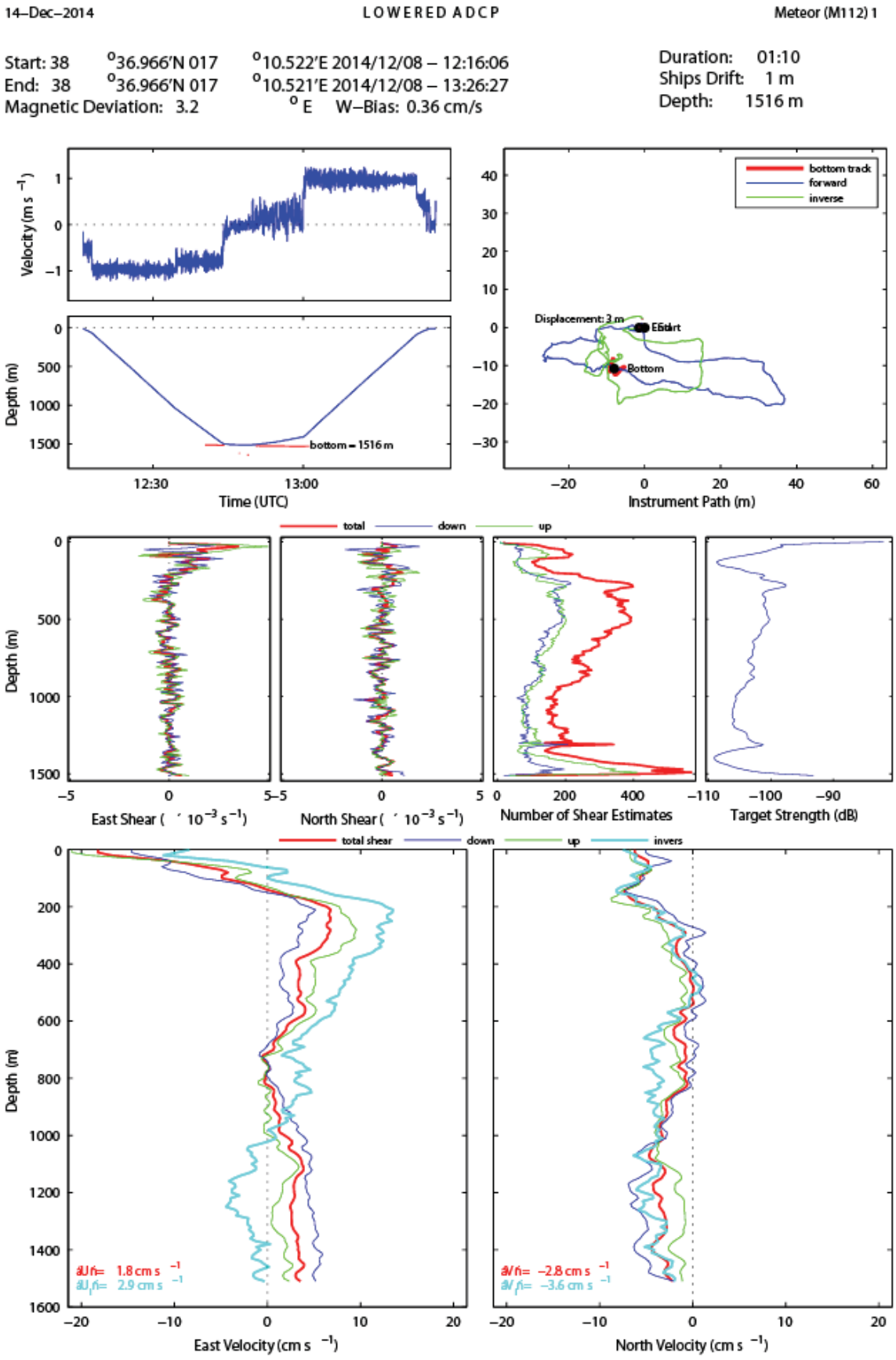

Fig. 40: Preliminary processed LADCP data from CTD-16 cast.

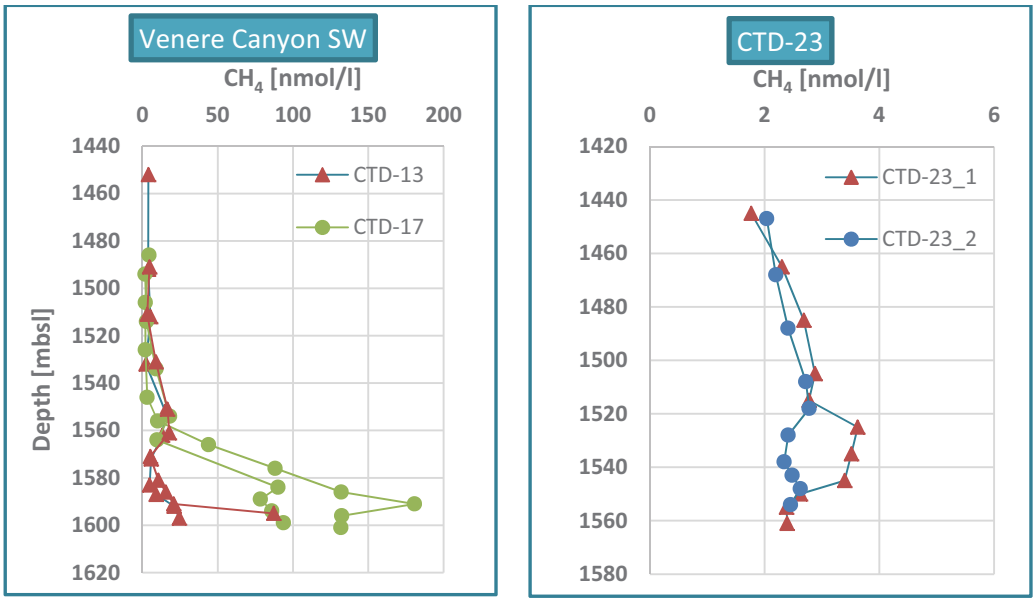

Fig. 41: Methane concentrations in the water column at Stations CTD-13, CTD-17 and CTD-23.

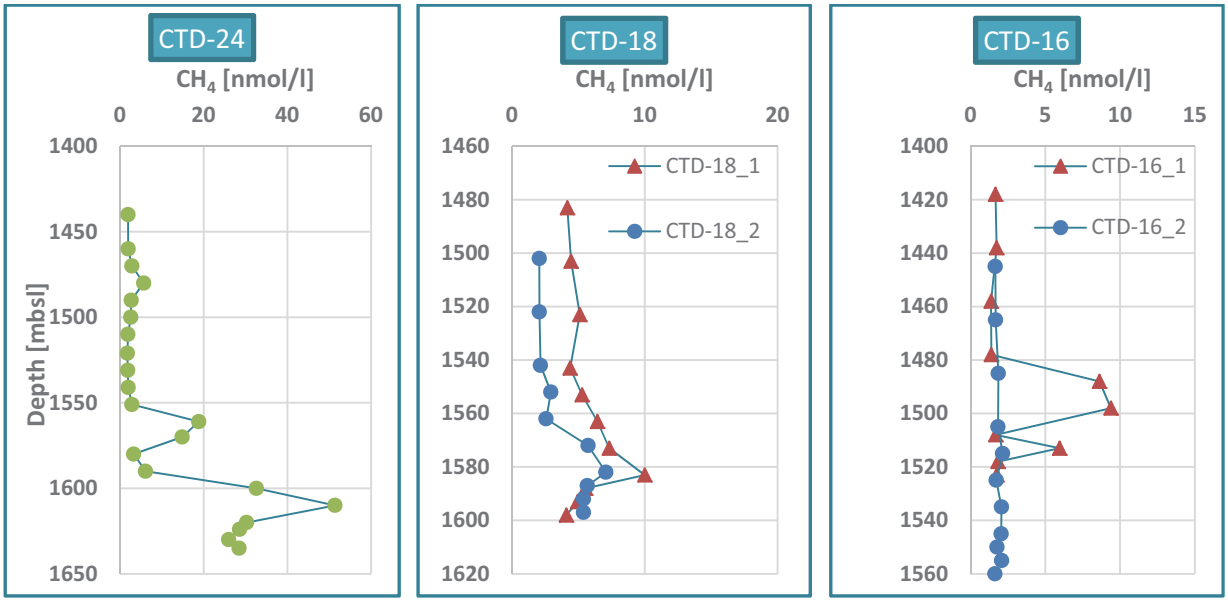

Fig. 42: Methane concentrations in the water column at Stations CTD-24, CTD-18 and CTD-16, SE-NW transect trough study area.

CTD-16 was taken NW from the Venere Summit and together with station CTD-18 and CTD-24 they built a transect through the study area where CTD-18 is in the center and CTD-24 is in the basin SE from the Venere Area (Fig. 42). Water currents are supposed to come from this direction, low methane concentrations analyzed in CTD-16.2 show that no methane is brought by water currents into the Venere MV area. Even when there is an enrichment in methane in CTD-16.1 up to 9 nmol/l, but this may be caused by another source further away from the study area. No methane was expected at station CTD-24, however, three peaks can be distinguished with increasing methane concentrations towards the seafloor with maximum concentrations of 51 nmol/l. In the center at CTD-18 the measured concentrations peak in 7 and 10 nmol/l in a water depth of 1582 mbsl.

6.3.4 Methane Concentrations in Bottom Water

Bottom water was sampled with the Gas Bubble Samplers a few decimeters to meters above the seafloor. Overall, the concentrations of methane range between 0.1 – 4574 µmol/l and are therefore remarkably enriched compared to the concentrations in the water column above (Table 9). The sample with the highest methane value was taken at Nikolaus MV with GBS-17, whereas the other Gas Bubble Samplers GBS-16 and GBS-18 at that location had only 0.3 and 1.7 µmol/l methane. At the summit of Venere MV, where fresh mud was extruded, methane concentrations are also really high with 1085 µmol/l in GBS-9 or with 225.2 µmol/l methane in GBS-20. Another location with high methane concentration was Flare Site 1, where the bottom water was sampled with GBS-3 during the first leg while this site was still active.

Table 9: Methane concentrations of water samples taken with Gas Bubble Samplers.

Station	Tool	CH4 [µmol/l]
GeoB 19221-7	GBS-1	22.8
GeoB 19224-3	GBS-2	6.6
GeoB 19230-2	GBS-3	849.2
GeoB 19230-11	GBS-4	0.6
GeoB 19232-8	GBS-5	35.1
GeoB 19232-9	GBS-6	1.2
GeoB 19240-7	GBS-7	0.3
GeoB 19240-14	GBS-8	165.5
GeoB 19242-5	GBS-9	1085.4
GeoB 19242-19	GBS-10	3.0
GeoB 19242-20	GBS-11	4.3
GeoB 19249-11	GBS-12	74.2
GeoB 19252-8	GBS-13	9.8
GeoB 19252-12	GBS-14	10.0
GeoB 19253-11	GBS-15	1.0
GeoB 19255-5	GBS-16	1.7
GeoB 19255-10	GBS-17	4574.2
GeoB 19255-13	GBS-18	0.3
GeoB 19258-3	GBS-19	0.7
GeoB 19258-19	GBS-20	225.2
GeoB 19258-20	GBS-21	0.9
GeoB 19267-2	GBS-22	0.1
GeoB 19267-11	GBS-23	0.4
GeoB 19267-12	GBS-24	3.1

7 Station Work with the Autonomous Underwater Vehicle (AUV) MARUM SEAL 5000

(G. Meinecke, J.Renken, U. Spiesecke, T. von Wahl)

7.1 Introduction

In the year 2006 the MARUM ordered a deep diving autonomous underwater vehicle (AUV), designed as a modular sensor carrier platform for autonomous underwater applications. The company International Submarine Engineering (I.S.E.) built this AUV in Canada. In June 2007 the AUV "SEAL" was delivered to MARUM and tested afterwards on the French vessel N/O SUROIT (June 2007) and the German R/V POSEIDON (November 2007) in the Mediterranean Sea. Since then, the AUV is in operational mode and was used 9 times on field cruises on-board research vessels (R/V SONNE, R/V METEOR, R/V M.S.MERIAN, R/V POSEIDON, N/O SUROIT, R/V OR5) and 2 times in Lake studies (Lake Constance, Lake Neuchatel). Therefore, this R/V METEOR cruise M112-1 is the 10th field cruise of MARUM SEAL.

7.2 SEAL Vehicle – Basics

The MARUM AUV Seal is No. 5 of the Explorer-AUV series from the company I.S.E. The AUV is nearly 5.75 m long, with 0.73 m diameter and a weight of 1.35 tons. The AUV consists of a modular atmospheric pressure hull, designed from 2 hull segments and a front and aft dome. Inside the pressure hull, the vehicle control computer (VCC), the payload control computer (PCC), 8 lithium batteries and spare room for additional "dry" payload electronics are located. Actually, the inertial navigation system PHINS and the RESON multibeam-processor are located as dry payload here. The tail and the front section, build on GRP-material, are flooded wet bays. In the tail section the motor, beacons for USBL, RF-radio, Flashlight, IRIDIUM antenna and DGPS antenna are located. In the newly constructed aluminium front section the Seabird SBE 49 CTD, the Sercel MATS 200 acoustic modem, the DVL (300 kHz), KONGSBERG Pencil beam (675 kHz), the recently implemented KONGSBERG EM2040 (200, 300, 400 kHz), the PAROSCIENTIFIC pressure-sensor and the BENTHOS dual frequency (100/400 kHz) side scan sonar are located (optional). Actually, the SEAL AUV has a capacity of approx. 15,4 KWh main energy, which enables the AUV for approx. 65 km mission-track lengths, which has to be reduced due to the more energy consuming EM2040 MBES compared to former cruises.

For security aspects, several hard- and software-mechanisms are installed on the AUV to minimize the risk for malfunction, damage and total loss. More basic features are dealing with fault response tables, up to an emergency drop weight, either released by user or completely independent by AUV time-relays itself.

MARUM put special emphasise on open architecture in hard- and software design of the AUV, in order to be as much as possible modular and flexible regarding the vehicle operations. Therefore, the VCC is based to large extend on industrial electronic components and compact-PCI industrial boards and only very rare proprietary hardware boards have been implemented. The software is completely built QNX 4.25 – a licensed UNIX derivate, to large extends open for user modifications. The payload PC is built on comparable hardware components, but running either with Windows and/or Linux.

On the support vessel, the counterpart to the VCC is located on the surface control computer (SCC). It is designed as an Intel based standard PC, also running with same QNX OS and a Graphic User Interface (GUI) to control and command the MARUM SEAL AUV. Direct communication with the

AUV is established via an Ethernet-LAN, either by hard-wired 100 mb LAN cable plugged to AUV on deck, or by Ethernet-RF-LAN modem – once vehicle is on water. The typical range of RF-communication is around 1 – 2 km distance to vehicle. Within this range the user has all options to operate the AUV in Pilot-Mode, e.g. to manoeuvre the AUV on water or change vehicle settings. Once the AUV is under water, all communication links were shut down automatically and the AUV has to be in mission-mode, means it is working based on specific user-defined missions.

Despite being in mission-mode it is necessary to communicate with the AUV when it's under water, i.e. asking for actual position, depth and status. To achieve this, on-board the support vessel an acoustic underwater modem with dunking transducer has to be installed (SERCEL MATS modem) communicating with the counterpart on the AUV, on request. Due to limited acoustic bandwidth only rare data sets are available.

7.3 Mission-Mode

The AUV - as dedicated autonomous vehicle - has to be pre-defined operated under water, by demand. As mentioned, only at sea surface a manoeuvring by the pilot is possible - once it dives, it will lose communication and therefore must be in a mission-mode. Initialized correctly, fault prevention mechanisms should prevent the AUV for damage/loss in that case.

Simplified, an AUV mission is a set of targets; clearly defined by its longitude, latitude, and a given depth/altitude the vehicle should reach/keep by a given speed of AUV in a distinct time. The AUV needs to be in a definite 3-dimensional underwater space to know exactly its own position over mission time in order to actively navigating on this. To achieve this basic scenario, the AUV is working at sea surface with best position update possible, e.g. DGPS position. Once it dives, it takes the actual position as starting point of navigation, looks for its own heading and the actual speed and calculating its on-going position change based on the last actual position, e.g. method known as dead reckoning. To achieve highest precision in navigation, a combination of motion reference unit (MRU) and Inertial Navigation System (INS) is installed on the MARUM SEAL AUV – the PHINS inertial unit from IXSEA Company. Briefly, the MRU is "feeling" the acceleration of the vehicle in all 3 axis (x,y,z). The INS is built on 3 fibre-optic gyro's (x,y,z) and gives a very precise/stable heading, pitch and roll information, based on rotation-changes compared to the axis. Even on long duration missions, the position calculating by the AUV will be very accurate based on that technique.

7.4 Mission Planning

In principle and very briefly, it would be accepted by the vehicles VCC to receive a simple list of waypoints as targets for the actual mission (the list has to be in a specific syntax). In order to arrange it more efficient and convenient a graphical planning tool is used for this mission planning. The MIMOSA (© Ifremer) mission-planning tool is a software package specially designed to operate underwater vehicles (AUVs, ROVs, Glider). The main goal of this software is to plan the current mission, observe to AUV once it is underwater and to visualize gathered data from several data sources and vehicles.

MIMOSA is mainly built on 2 software sources, e.g. an ArcView 9.1 based Graphical Information System (© ESFRI ArcGIS) and professional Navigation Charting Software (© Chersoft UK).

In order to plan a mission the user has to work on geo-referenced charts with a given projection (MERCATOR); either GIS-maps, raster-charts or S-57 commercial electronic navigational charts (ENCs). These basic charts could enlarge easily with user specified GIS projects, enhanced with already gathered data, e.g. multibeam data, points of interest. Once installed in MIMOSA, one can create AUV missions by drawing the specific mission by mouse or using implemented set of tools (MIMOSA planning mode). Missions created in that way are completely editable, movable to other geographical locations and exportable to other formats. In order to be interpretable by the MARUM SEAL AUV, the created mission will be translated in the I.S.E. specific syntax; a set of targets, waypoints, depths information and timer will be created and written into an export path. From here the mission file can be uploaded via the SCC (support vessel) into the VCC (AUVs control PC); the AUV has its mission and is capable to dive, based on a valid mission plan.

7.5 Mission Observing/Tracking

The MIMOSA planning tool is also used for supervision, e.g. to monitor the vehicle at sea surface and more interesting under water (MIMOSA observation mode). The MIMOSA software is client based, means one dedicated server is used for planning, while the others are in slave/client mode, picking up actual missions. Therefore, position data strings (UDP broadcast data) from the support ship (i.e. R/V METEOR / position, heading) are being sent to local network and fed into the MIMOSA software; the same is active for the AUV position data, e.g. DGPS signal once it is on sea surface. During dive the AUV can be tracked automatically via ship-borne ultra-short baseline systems (USBL), e.g. IXSEA GAPS or POSIDONIA, using the on-board AUV installed USBL transponder beacon responded signal (delivers position where the vehicle “actually” is).

In addition to this independent position source, vehicles own position (deliver where the vehicle “thinks” it is) can be displayed also. This position is based on transmitted data strings from MATS underwater acoustic modem, only sent from AUV on user request.

To summarize, usually you have displayed in tracking mode:
- position of support vessel (lon/lat and heading)
- either DGPS of AUV during surface track, or
- USBL position (GAPS or POSIDONIA)
- and MATS position (underwater acoustic on request)

7.6 Operational Aspects

In general, MARUM SEAL was used at least 10 times on field cruises so far. Thus, several different vessels have been in operation and on each vessel the handling of the AUV is quite a bit different. In principle, the A-frame seems to be the best position to launch and recovery the AUV, because the tendency to hit ships wall is minimized compared to sideward operation, based on experiences. On R/V METEOR M112-1 the AUV was operated successfully with the midship crane at starboard side of vessel, which works very well due to long elongation capability.

In principle, the AUV can be operated out of the lab, just with simple PC-console racks. On R/V METEOR M112-1 cruise, the AUV operations were run out of a 20” operation/workshop van, located on the main deck, midships. The consoles, file-server and printer are installed in the container, workbench, tools and spares as well.

The SERCEL MATS acoustic transducer was installed into the moon pool from R/V METEOR. For USBL positioning, the hull-mounted POSIDONIA system was used.

Prior to launch of AUV, the PHINS INS (on-board the AUV) needs to be calibrated. Therefore, it has to be reset and the support vessel has to be still standing for at least 5 minutes. After that initial phase (INS coarse align), the vessel needs to run a rectangular course; square-coarse, 5 minutes @ 3-5 knots each line (INS fine align). At the end of that time-span and course, the PHINS is in so called "normal mode", means it has its highest position quality.

7.7 Station Work on R/V METEOR M112-1

During R/V METEOR M112-1 cruise we did 5 dives, all without technical vehicle problems. In total, 280 km of track lines have been surveyed at bottom. During the first 4 dives, strange problems have been recognized related to the KONGSBERG EM2040 MBES system. Despite well-functioning AUV, the recording system of the EM2040 stopped erratically without any obvious reasons. Very limited logging options on the EM2040 system hampered the solving of the problem. Finally, the most probable fault option seemed to be located in the original SSD hard drive, implemented in the Kongsberg recording system. Obviously, the SSD hard drive firmware is not capable to flush all hard drive cache data before shutdown of hard drive. Due to this reason, the most used file on SSD (the file allocation table FAT) was handled mostly by the hard drive cache and therefore not regularly stored on SSD during shutdown – means the most actual one was/could be lost during shutdown. During dive 65, remnants of the recorded files could be found on the SSD – disregarding the lost FAT. For the last dive 66, the SSD hard drive was replaced by a standard spinning SATA hard drive, which recorded all data well.

Dive No. 62:
The first dive during R/V METEOR cruise M112-1 was located at Venere Mud Volcano. The track length at bottom was planned to 61.2 km. Due to detected MBES recording malfunction over mission time the mission was terminated after 31.5 km mission track.

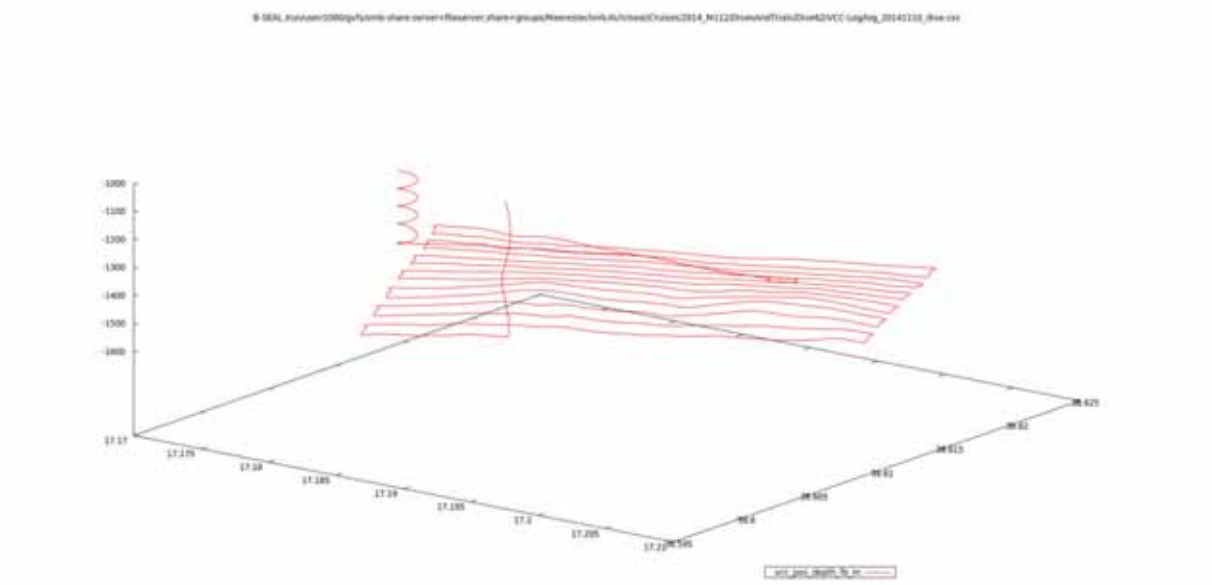

Fig. 43: Dive track of dive no. 62 (Venere MV), depth of AUV SEAL vs. longitude/latitude.

Dive No. 63:

The second dive during R/V METEOR cruise M112-1 was located at Venere Mud Volcano, again. The track length at bottom was planned to 58.7 km. Due to detected MBES recording malfunction over mission time the mission was terminated after 45.5 km mission track.

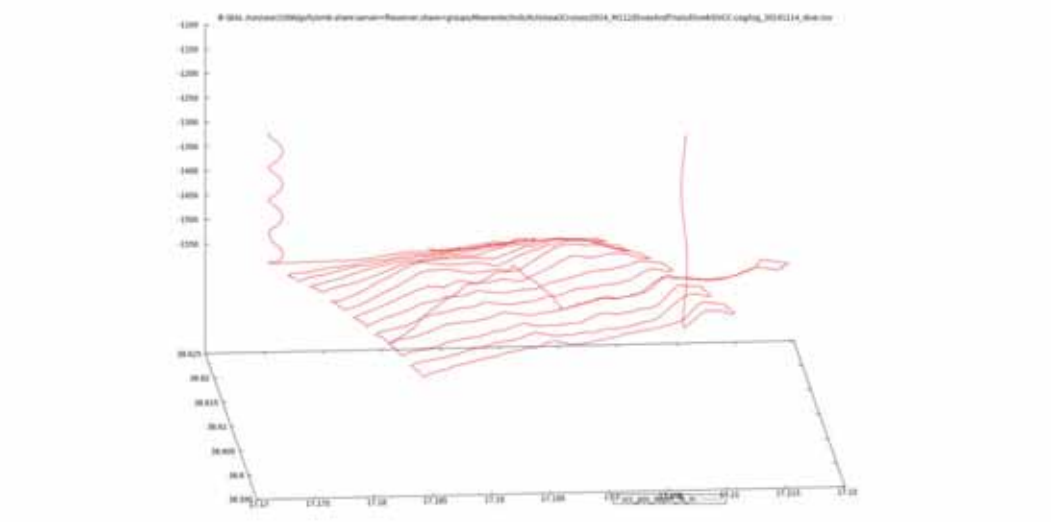

Fig. 44: Dive track of dive no. 63 (Venere MV), depth of AUV SEAL vs. longitude/latitude.

Dive No. 64:

The third dive during R/V METEOR cruise M112-1 was located at Venere Mud Volcano, again. The track length at bottom was planned to 59.9 km, starting south off the already mapped area from dive 63. In order to solve the problems with the MBES recording, after each complete mission line (back and forth) the MBES system was complete rebooted as mission task. After nearly 29 km track length, the AUV showed an irregular behaviour and added a circular pattern to the mission track. At the end of this specific track-line, the AUV didn't stop the track-line – instead it travelled further on straight line. We finally realized a collision with a fishing long line as only possible reason for such behaviour and terminated the AUV mission by acoustic abort. The AUV didn't come up in circular pattern (as programmed and expected) – instead it came up in roughly straight line and very slowly, because it was still connected to the long line and pulled it up to the sea surface. Finally, the AUV cut the long line at sea surface – the remnants has been torn into the propeller sealing.

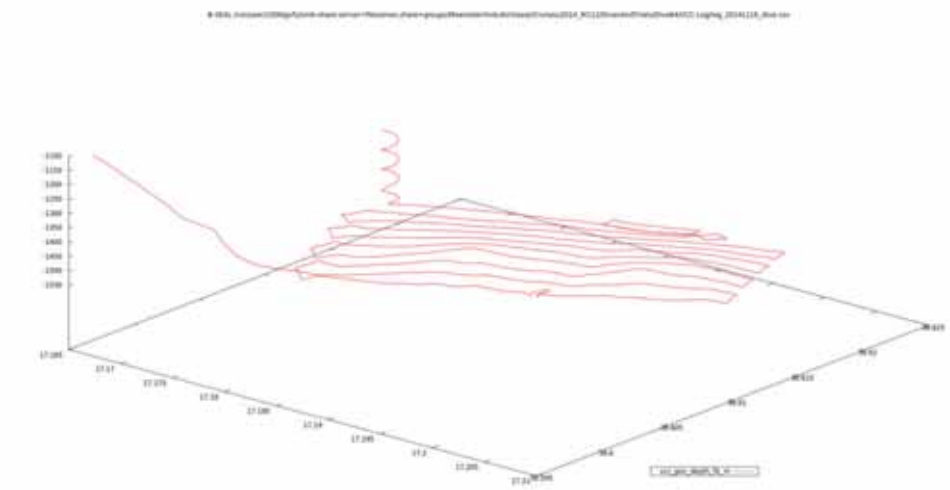

Fig. 45: Dive track of dive no. 64 (Venere MV), depth of AUV SEAL vs. longitude/latitude. Abort of AUV Mission, due to collision with fishing long line (circular pattern in last track –line).

Dive No. 65:

The fourth dive during R/V METEOR cruise was the repeated no. 64 at Venere Mud Volcano. The track length at bottom was 56.5 km. The AUV performed the complete mission without technical problems, despite the MBES recording problems, which was detected afterwards on deck.

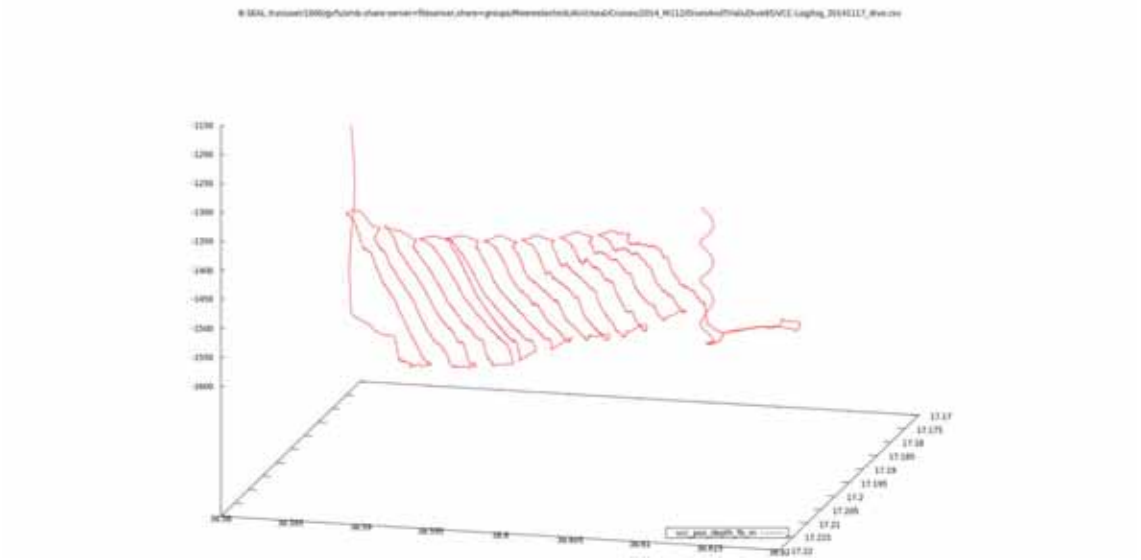

Fig. 46: Dive track of dive no. 65 (Venere MV), depth of AUV SEAL vs. longitude/latitude.

Dive No. 66:

The sixth dive during R/V METEOR cruise was planned at Cetus Mud Volcano. The track length at bottom was planned to 43.9 km. The dive could be started only on the 3rd retry, due to an erratic malfunction on the obstacle sonar in the first run and a bottom detection fault in mid water level in the second run, due to a prominent plankton layer at approx. 1000 m. Due the upcoming harsher weather and lower battery condition, we had the terminate the AUV dive at 23 km mission track.

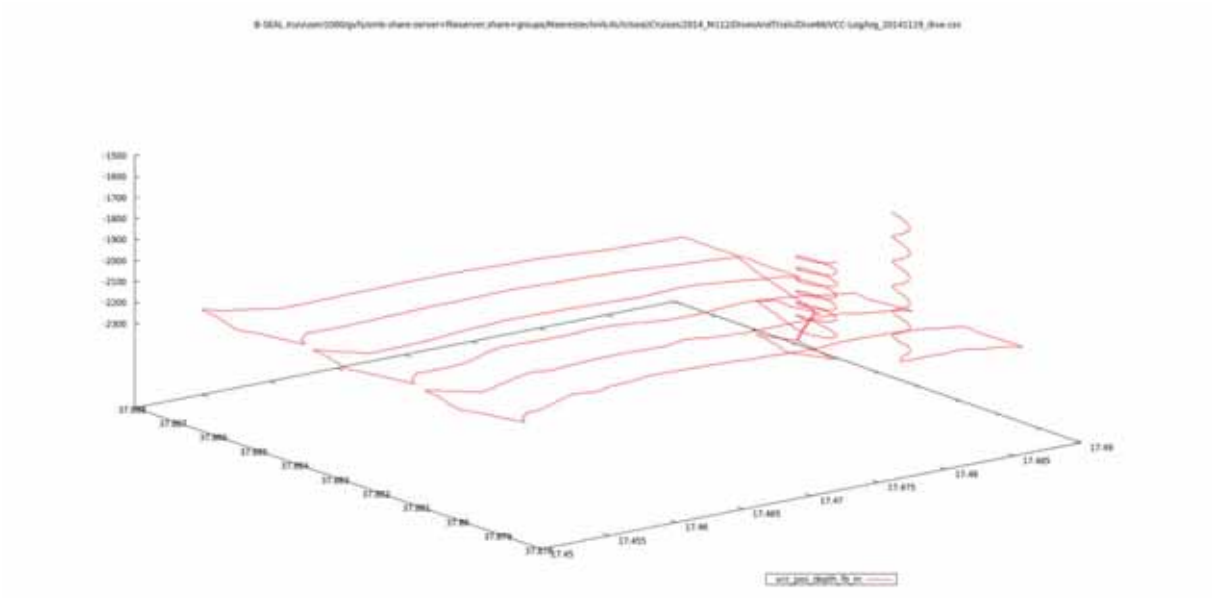

Fig. 47: Dive track of dive no. 66 (Cetus MV), depth of AUV SEAL vs. longitude/latitude.

8 Remotely Operated Vehicle (ROV) Quest

8.1 Technical Description and Performance

(C. Reuter, M. Zarrouk, S. Klar, H. Büttner, T. Leymann, D. Hüttich, N. Nowald, C. Seiter, R. Rehage)

The deep-water ROV (remotely operated vehicle) “QUEST 4000 m” used during M112 aboard the R/V METEOR, is installed and operated at MARUM, Center for Marine Environmental Sciences at the University of Bremen, Germany. The QUEST ROV is based on a commercially available 4000 m rated deepwater robotic vehicle designed and built by Schilling Robotics, Davis, USA. Since installation at MARUM in May 2003, it was designed as a truly mobile system specifically adapted to the requirements of scientific work aboard marine research vessels for worldwide operation. Today, QUEST has a total record of 350 dives during 31 expeditions, including this cruise.

During M112, QUEST performed 14 dives to depths between 1505 and 2860 m. There were technical issues with the manipulators during the first three dives, these were fixed during the cruise and there were no further major issues concerning the hydraulics. During the first dive we lost the Kongsberg MS1000 Sonar-head due to a short within the device. We integrated the IMAGENEX Sonar-head of the AG Bohrmann for most dives during the remainder of the cruise. Other than that, technical performance of the vehicle during dives was excellent, without any serious issues.

QUEST was operated by a team of 8 pilots/technicians. Close cooperation between ROV team and ship’s crew on deck and bridge allowed a quick gain of experience for the handling procedures during deployment and recovery. During diving, close cooperation allowed safe handling on deck and precise positioning and navigation of both ship and ROV at depth, which was essential for accurate sampling and intervention work such as instrument deployment and recovery. The ROV team is very grateful for the steady and highly professional support from the entire ship’s crew during the cruise.

QUEST System description

The total QUEST system weighs about 45 tons (including the vehicle, control van, workshop van, electrical winch, 5000 m umbilical, and transportation vans) and can be transported in four standard ISO 20 foot vans. Using a MacArtney Cormac electrically driven storage winch to manage the 5000 m of 17.6 mm NSW umbilical, no hydraulic connections are necessary to host the entire handling system.

The QUEST uses a Doppler velocity log (DVL, 1200 kHz) to perform stationkeep, displacement, and other auto control functions. The combination of 60-kW propulsion power with DVL-based auto control functions provides exceptional positioning capabilities at depth. Designed and operated as a free-flying vehicle, QUEST system exerts such precise control over the electric propulsion system that the vehicle maintained relative positioning accuracy within decimeters. Absolute GPS-based positioning is carried out using the shipboard IXSEA Posidonia USBL positioning system. Performance of the USBL system reached an absolute accuracy of somewhere between 3-8 m.

Table 10: Positions and times of M112 QUEST dives.

Dive No.	337	338	339	340	341	342	343
Area	Flare 1	Flare 1	Flare 1	Flare 2	Flare 1	Venere Top	Flare 4+5
GeoB Number	19202	19211	19221	19224	19230	19232	19240
Resp. Scientist	M. Römer	Y. Marcon	Y. Marcon	H. Sahling	M. Römer	G. Bohrm.	T. Pape
Date	09.11.14	13.11.14	17.11.14	18.11.14	26.11.14	28.11.14	30.11.14
Start bo (UTC)	21:02	09:13	08:24	12:18	08:26	10:05	09:26
End bo (UTC)	04:30	17:28	16:10	15:15	15:25	15:25	17:31
Bottom time	07:27	08:15	07:46	02:57	06:59	05:20	08:05
T-Stick	1		2		2	2	4
Mosaic		6			1		1
Push corer			3		8	3	6
GBS			2	2	2	2	3
Suction Sampl.			2				
Net					3	1	
Shovel							1
Marker			1				1

Dive No.	344	345	346	347	348	349	350
Area	Venere	Flare 4+5	Flare 4+5	Cetus MV	NikolausMV	Venere MV	Flare 2
GeoB Number	19242	19249	19252	19253	19255	19258	19267
Resp. Scientist	D. Präg	M. Torres	M. Römer	G. Bohrm.	D. Präg	M. Torres	M. Römer
Date	01.12.14	03.12.14	04.12.14	05.12.14	06.12.14	07.12.14	09.12.14
Start bo (UTC)	08:45	15:44	12:43	10:55	12:06	11:14	09:10
End bo (UTC)	16:39	19:17	19:09	17:37	18:11	18:16	13:11
Bottom time	07:44	03:33	06:26	06:37	06:05	07:02	04:01
T-Stick	5	3	1	12	3	4	1
Mosaic	3	1				4	1
Push corer	8	5	5	1	3	8	6
GBS	3	2	2	1	3	3	3
Suction Sampl.							
Net			2	1	3		
Shovel							
Marker							1
ASSMO		1					

The QUEST control system provides transparent access to all RS-232, network data and video channels. The scientific data system used at MARUM feeds all ROV- and ship-based science and logging channels into a real-time database system (DAVIS-ROV), a version of the database software commonly used aboard the German research vessels. During operation, data such as the sonar screen, DVL map and so forth plus most videos video including the HD feed are distributed to the lab and ships ethernet network in realtime to minimize crowding in the control van.

Post-cruise data archival will be hosted by the information system PANGAEA at the World Data Center for Marine Environmental Sciences (WDC-MARE), which is operated on a long-term base by MARUM and the Alfred-Wegener-Institute for Polar and Marine Research, Bremerhaven (AWI).

QUEST Video Setup and HDTV camera

Continuous PAL SD video footage was obtained with two color-zoom cameras (insite PEGASUS and DSPL Seacam 6500). In order to gain a fast overview of the dive without the need of watching hours of video, video is frame-grabbed and digitized at 5 sec intervals, covering both PAL and HD video material. For extremely detailed video close up filming, a near-bottom mounted broadcast quality (>1000 TVL) 3CCD HDTV 14 x zoom video camera was used (insite Zeus). Spatial Resolution of this camera is 2.2 Mega-Pixel at 59.94 Hz interlaced. Recording was carried out on demand onto tapes in broadcast-standard digital Sony HD-CAM format, using uncompressed 1.5 Gbit HD-SDI transmission over a dedicated fibre-optic connection. In addition, all video feeds were continuously recorded digitally based on H.264 compression, including HDTV and tiled pilot screen, and were transferred as digital files to the ships science server between dives. The files cover 30 minutes of video each for faster and easier access and contain a separate subtitle text-file with relevant vehicle data such as position, heading, depth and timestamp.

As a standard photo camera, a Scorpio Digital Still camera was used, providing 3.3. mega-pixel spatial image resolution and highly corrected underwater optics. For mosaicking and vertical downward view, a 24 mega-pixel digital photographic camera with two vertical external flashes was used. Video distribution was provided by dedicated CAT-6 based VGA transmission hardware, as well as by streaming the main tiled video image into the vessels network.

Scientific payloads:

During M112, the following scientific equipment was handled with QUEST:

- ROV based tools, installed on vehicle:
  - realtime Sea and Sun CTD
  - push cores for sediment sampling, max. 8 per dive
  - ROV portside drawbox basket
  - ROV starboard side fixed basket frame
  - 8-bucket suction sampler
  - vertical 24 MPix digital fotocamera and flash
  - nets with t-handle
  - a hammer with t-handle to crush carbonate crusts
  - a shovel with t-handle for digging up sediment
  - simple markers

- In situ instruments handled with QUEST:
  - ASSMO: autonomous scanning sonar
  - T-Lance
  - Gas Bubble Sampler

During R/V METEOR cruise M112 fourteen dives at Venere, Nikolaus and Cetus Mud Volcanoes have been performed with 88 hours and 17 minutes bottom time (Tab. 10). Several photo mosaic surveys were run using the new downward-looking camera (Prosilica GT6600C). During the dives 56 push corers were taken to sample sediments and the gas–tight gas bubble sampler was used 28

times for water (24 times) and gas (4 times). The T-stick was deployed 40 times to measure the local temperature gradient in the sediments. Ten times we used a net for sampling sediments and carbonate precipitates and rocks. We used the suction sampler and simple tools like a shovel or a hammer. Further activities have been the deployment and the recovery of the autonomous scanning sonar (ASSMO) and the deployment of markers.

8.2 Dive Summaries

8.2.1 Dive 337 (Station 1215-1, GeoB: 19202-1)

Area:	**Venere Mud Volcano, Flare 1**
Responsible scientist:	Miriam Römer
Date:	Sunday 09 November 2014
Start bottom (UTC):	21:02
End bottom (UTC):	04:30
Bottom time:	07 h 27 min
Start bottom (Lat/Long/depth):	38°37.085'N, 17°11.606'E, 1560 m
End bottom (Lat/Long/depth):	38°36.604'N, 17°11.228'E, 1515 m

Points of interest:

WP 1:	38°37.075'N	17°11.585'E	Flare area centre
WP 2:	38°37.099'N	17°11.554'E	Flare area NW limit
WP 3:	38°37.099'N	17°11.615'E	Flare area NE limit
WP 4:	38°37.051'N	17°11.615'E	Flare area SE limit
WP 5:	38°37.051'N	17°11.554'E	Flare area SW limit
WP 6:	38°36.677'N	17°11.950'E	Venere East
WP 7:	38°36.456'N	17°11.187'E	Venere West

Key results:

Bubble streams, reduced sediments and bacterial mats found in several places around WP3, strong bioturbation traces on the seafloor.

Technical description:

During the pre-dive check, a ground fault related to the mounted suction sampler appeared and could not be solved within short time. Therefore, we decided to unload the suction sampler in order to not delay the dive. On the descent to the seafloor in about 1000 m water depth the sonar connection got lost and could not be recovered during the entire dive. When reaching the seafloor some problems had to be fixed in order to hold the vehicle in a stable position, which was fixed after about 10 minutes. First images with the Scorpio camera resulted much too bright but have been adjusted for the rest of the dive. For photo-mosaicking the flashes did not work with the consequence that the images were mostly too dark. A workaround was to increase the exposure time. This, however, introduced motion blur in the images when the ROV was moving too fast. The major problem of the dive, however, appeared during the temperature measurement, as the manipulator could not be moved in certain directions. One hour was spent to find the reason and to

recover the function, which failed again. Nevertheless, the T-Stick could be finally recovered and stored in the box, but for the rest of the dive we were not able to do any more sampling.

Table 11: Samples and measurements taken during Dive 337.

GeoB	Instrument	UTC Start	UTC End	Position	Depth	Comment
19202-2	T-Stick	22:13:13	23:14:16	38°37.08373'N 17°11.59371'E	1567 m	Deployment lasted 1 hour

T-stick measurement in a dark patch of reduced sediments.

Mosaicking transect with downward looking camera (Prosilica GT6600C).

HD recordings of the forward-looking "Zeus" camera on HD tapes (ca. 40 minutes in total).

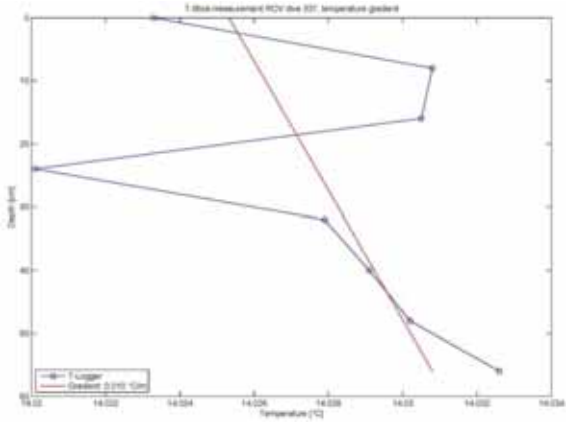

Fig. 48: Temperature gradient measured with the T-Stick during ROV Dive 337. Final calibration has to be acquired, however, the profile does not indicate elevated temperatures.

Dive description:

The first target for this ROV dive was dedicated to detecting the gas bubble emissions that were identified during the hydroacoustic survey mapping of the Venere MV. The first waypoint was therefore set to the position where the centre of the flare visible in the PARASOUND water column record (PHF, 18 kHz) has been located. It was planned to search for the gas bubble streams using the horizontally looking sonar mounted on the ROV. Unfortunately, the sonar lost communication during the descent and we started visual observations after reaching the seafloor. The first view of the seabed showed flat soft sediments in greyish colour with numerous slightly lighter coloured mounds and small holes, both probably related to bioturbation. All over the place were numerous clam shells, most probably representing empty chemosynthetic organisms. The ROV was moved in NE direction to WP3. The flare position we mapped using the multibeam system indicated that the location of the gas emission would be probably in that area. After only 20 m flying over the seafloor with a distance of about 1.5 m for having a good visual observation, the ROV reached an area with several dark patches (10-15) in an area of roughly 10 x 5 m. After documenting carefully by recording in high definition with the HD camera and taking several photos, we took a measurement with the T-Stick, directly placed in one of the dark patches. First results of this measurement did not reveal an elevated temperature gradient. Further on, we moved the ROV towards WP3 and passed another area characterized by dark sediments and whitish material, which we interpreted to be microbial mats. This area seems to continue to both sides, however, after documentation by doing photos we continued heading towards WP3. Another approximately 20 m the ROV reached another seep site, where we found several gas bubble emissions. Some gas bubbles were observed to be emitted individually, but a few bubble streams with relatively frequent emission could also be seen. The area with active degassing was just about 5-10 m.

From this point on, we switched on the new downward-looking still camera (Prosilica GT 6600C) in order to map parts of the seep area. This was the very first time that this camera was used on the ROV and some time was spent to find out the best settings for seafloor mapping. It turned out that the strobes failed to work and the first images were too dark. Brighter images were finally obtained by increasing the exposure time. However, lowering the shutter speed introduced additional blur in the images that was caused by the ROV motion.

Therefore, it was decided to dedicate the rest of the dive to exploration only, but to keep the Prosilica camera on anyway. Moving a further 40 m towards north-northwest (bearing: ca. 340°) from the gas emissions, we then turned west (bearing: 280°) for an additional 70 m. The observations showed that the seep area stretched at least as far as 40 m north and 70 m west of WP3. At this point, we finally headed south-southwest (bearing: ca. 203°) upslope towards the summit of Venere West (WP7) until the end of the dive. Because of the position of the ROV umbilical, progression in the direction of WP7 was slow and the summit of Venere West MV could not be reached before the end of the dive. However, we reached the southern limit of the seep area after about 100 m. Past the seep area the images showed soft and highly turbated hemipelagic sediments likely covering mud flows. A few rocks were observed (presumably clasts), very few clam shells, and no black sediment. One of the rocks which were observed seemed to be several metres large size and looked more like a rocky outcrop than a clast. However, this could not be confirmed from the images only. After about 500 m in the south-southwestern direction, we reached the area of high backscatter that surrounds Venere West MV. No clear change in seafloor morphology was observed at the transition to the high backscatter area, apart from the bioturbation, which seemed higher as we approached WP7. Unfortunately, the Prosilica camera failed to acquire photos shortly before the high-backscatter area was reached. The dive ended about 285 m before WP7.

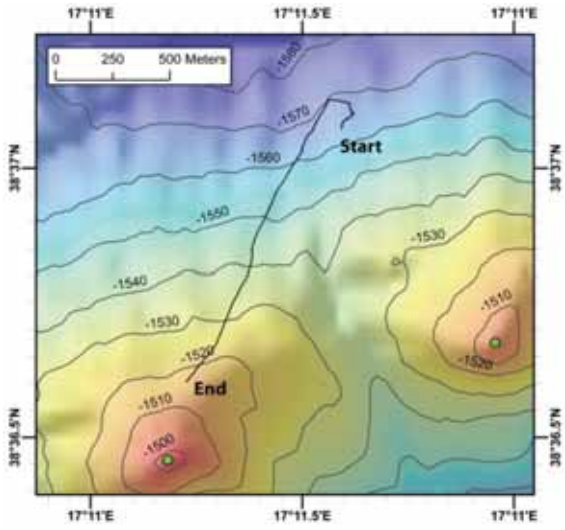

Fig. 49: Map of the dive track starting at the northern flank and ending almost at the top of the western peak.

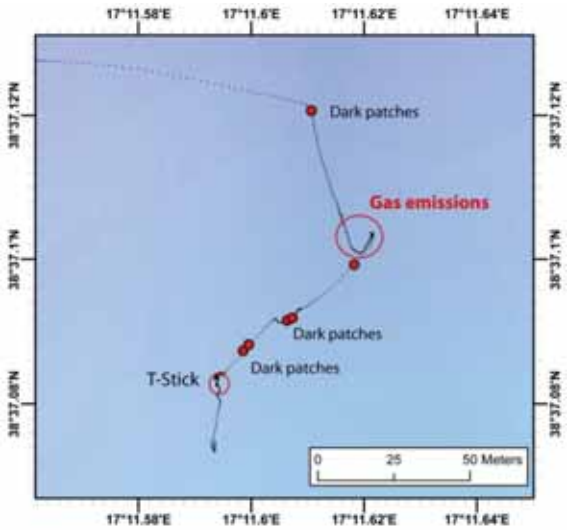

Fig. 50: Zoom of the first part of the dive investigating the seep area.

Fig. 51: Left: T-Stick measurement within a dark patch of reduced sediments. Right: Seafloor covered by microbial mats in the area with gas bubble emissions.

8.2.2 Dive 338 (Station 1221-1, GeoB: 19208-1)

Area:	**Venere Mud Volcano, Flare 1**	
Responsible scientist:	Yann Marcon	
Date:	Thursday 13 November 2014	
Start bottom (UTC):	09:13	
End bottom (UTC):	17:28	
Bottom time:	08h 15min	
Start bottom (Lat/Long/depth):	38° 37.08794' N	17° 11.63629' E, 1563 m
End bottom (Lat/Long/depth):	38° 37.09514' N	17° 11.61082' E, 1552 m

Points of interest:

WP 1:	38°37.102'N	17°11.621'E	Gas emissions from Dive 337
WP 2:	38°37.092'N	17°11.607'E	Dark sediments and bacterial mats
WP 3:	38°37.087'N	17°11.598'E	Dark sediments and bacterial mats
WP 4:	38°37.120'N	17°11.610'E	Dark sediments and bacterial mats
WP 5:	38°37.073'N	17°11.526'E	Rocky outcrop
WP 6:	38°36.677'N	17°11.950'E	Venere East
WP 7:	38°36.456'N	17°11.187'E	Venere West

Key results:

Authigenic carbonates, tubeworms, bubble streams, reduced sediments, bacterial mats found in several places.

Technical description:

A new forward-looking sonar was mounted on the ROV as replacement for the previous one, which broke down on Dive 337. This sonar allowed us to successfully visualize gas bubbles.

A new lighting system for the mosaicking cameras (Atlas and Prosilica cameras) had to be mounted onto the ROV after the failure of the strobes during Dive 337. The new system included two powerful lights, but no flashing light. Therefore, in order to get sufficiently bright photos with the Prosilica, we increased the exposure time up to 100 milliseconds. As a consequence, we had to lower

the speed of photomapping surveys down to 0.1 m/s to prevent motion blurring of the images. The altitude of the photomapping surveys was set to 2.5 m.

For this dive, we decided to record video footage from the downward-looking Atlas camera instead of the Pegasus camera as usual. The reason was to ensure full coverage during the mosaicking surveys, in case technical difficulties with the new Prosilica camera would arise. Indeed, the Prosilica camera is a new camera that was recently installed on the ROV, and our on-the-field experience with this camera is limited.

During the dive, USBL Posidonia positioning system failed to work correctly and produced an anomalously high amount of erroneous positions (Fig. 52). Although erroneous USBL positions could be filtered out in post-processing after the dive and correct absolute positions could be retrieved, this irregular behaviour made the USBL system unreliable for the navigation. Therefore, the DVL navigation was used instead of the USBL during the dive. It turned out to be very reliable for the mosaicking surveys. Indeed, the DVL produced high quality relative positioning and, in several cases, points of interests marked during the dive could be easily retrieved again later in the dive (e.g. the bubble streams). After failure of the USBL system, we decided not to reset the DVL system against the USBL data, in order to ensure that the accuracy of the relative positioning is preserved.

At 11:56 UTC, the manipulator arm failed to work during deployment of a push corer. From this point on, the manipulator was not operational and further sampling could not be done until the end of the dive. As a result, the push corer could not be recovered and was left on the seafloor (38° 37.10705' N, 17° 11.62427' E) at 1568 m water depth.

Table 12: Samples and measurements taken during Dive 338.
Six mosaicking lines across the high backscatter area with downward-looking still (Prosilica GT6600C) and video (Atlas) cameras.

Mosaic	Start	End
Line 1	13.11.2014 12:43:17 38° 37.0934' N 17° 11.6304' E Depth: 1565 m	13.11.2014 13:07:23 38° 37.0456' N 17° 11.6267' E Depth: 1558 m
Line 2	13.11.2014 13:32:01 38° 37.0485' N 17° 11.6202' E Depth: 1557 m	13.11.2014 14:01:31 38° 37.1156' N 17° 11.6208' E Depth: 1567 m
Line 3	13.11.2014 14:14:02 38° 37.1110' N 17° 11.6175' E Depth: 1568 m	13.11.2014 14:50:53 38° 37.0402' N 17° 11.6159' E Depth: 1557 m
Line 4	13.11.2014 15:07:54 38° 37.0417' N 17° 11.6089' E Depth: 1558 m	13.11.2014 15:38:22 38° 37.1020' N 17° 11.6125' E Depth: 1567 m
Line 5	13.11.2014 15:38:22 38° 37.1020' N 17° 11.6125' E Depth: 1567 m	13.11.2014 15:54:01 38° 37.0831' N 17° 11.5940' E Depth: 1564 m
Line 6	13.11.2014 15:54:01 38° 37.0831' N 17° 11.5940' E Depth: 1564 m	13.11.2014 16:27:46 38° 37.0904' N 17° 11.6249' E Depth: 1564 m

Recording of gas bubble streams with the forward-looking sonar.
HD recordings of the forward-looking “Zeus” camera on HD tapes (ca. 32 minutes in total).

Dive description:

The first target for this ROV dive was dedicated to detecting the gas bubble emissions that were identified during the ROV Dive 337 and AUV Dive 62. Therefore, the first waypoint was set to the position where gas bubbles had been observed during Dive 337. The forward-looking sonar was switched on while nearing the first waypoint in order to precisely locate the gas emissions. The work with the horizontally-looking sonar was conducted at an altitude of 15 m above the seafloor in order to avoid acoustic noise from the ground. The gas streams could be successfully imaged with the sonar. However, their activity appeared to be intermittent as they could not be imaged at all times, which hindered our ability to retrieve them.

Hence, it was decided to stop the search of the gas emissions and to carry on with the sampling program. Unfortunately, the manipulator arm stopped working during deployment of the first push corer in the centre of a large bacterial mat. To prevent damaging of other ROV components, the hydraulic pressure in the manipulator had to be released and the manipulator was deactivated. The push corer could not be recovered and was left on the seafloor at 1568 m water depth (38° 37.10705' N, 17° 11.62427' E).

From there on, the dive was dedicated to seafloor mapping with both downward-looking cameras (Atlas video camera and Prosilica photo camera) and six mosaic lines were conducted across the high backscatter area that was imaged during AUV Dive 62 (Fig. 53). Line 1 started from the push corer location and headed south (bearing: 180°) for about 110 m across the high backscatter patch. Line 2 started about 10 m to the west of the end of line 2 and headed north (bearing: 0°) for 150 m. Line 3 started 10 m to the west of the end of line 2 and headed south for 150 m. Line 4 started 10 m to the west of the end of line 3 and headed north for 120 m. Line 5 started from the end of line 4 and headed southwest to the start of line 6. Gas bubbles were observed during line 5 at 1566 m water depth (38° 37.09279' N, 17° 11.60369' E). Finally, line 6 started on the west side of the high backscatter area and crossed the first four lines with a heading around 47°. The mosaicking survey revealed occurrence of authigenic carbonate precipitates (Fig. 54 left) within the northern half of the high backscatter area. The northern limit of the carbonate area seems to match well with the northern limit of the high backscatter area. However, the southern limit of the carbonate area is unclear, as carbonates could not be observed in the southern half of the high-backscatter area. We believe that they may occur under a thin layer of hemipelagic sediments. Dense clam aggregations as well as many urchins were also observed within the high backscatter area. Finally, small tubeworms were observed approximately in the middle of the carbonate area, at 1562 m water depth (38° 37.08307' N, 17° 11.62262' E).

The rest of the dive, after ending the last mosaicking line (line 6), was devoted to finding the optimized settings for imaging gas emissions with the newly mounted forward-looking sonar. To that end, we moved towards the gas emission site that was observed during the mosaicking survey and could image the bubble stream in the water column from an altitude of 15 m and a distance of ca. 10 m (Fig. 54 right). The bottom time ended at 17:28 UTC.

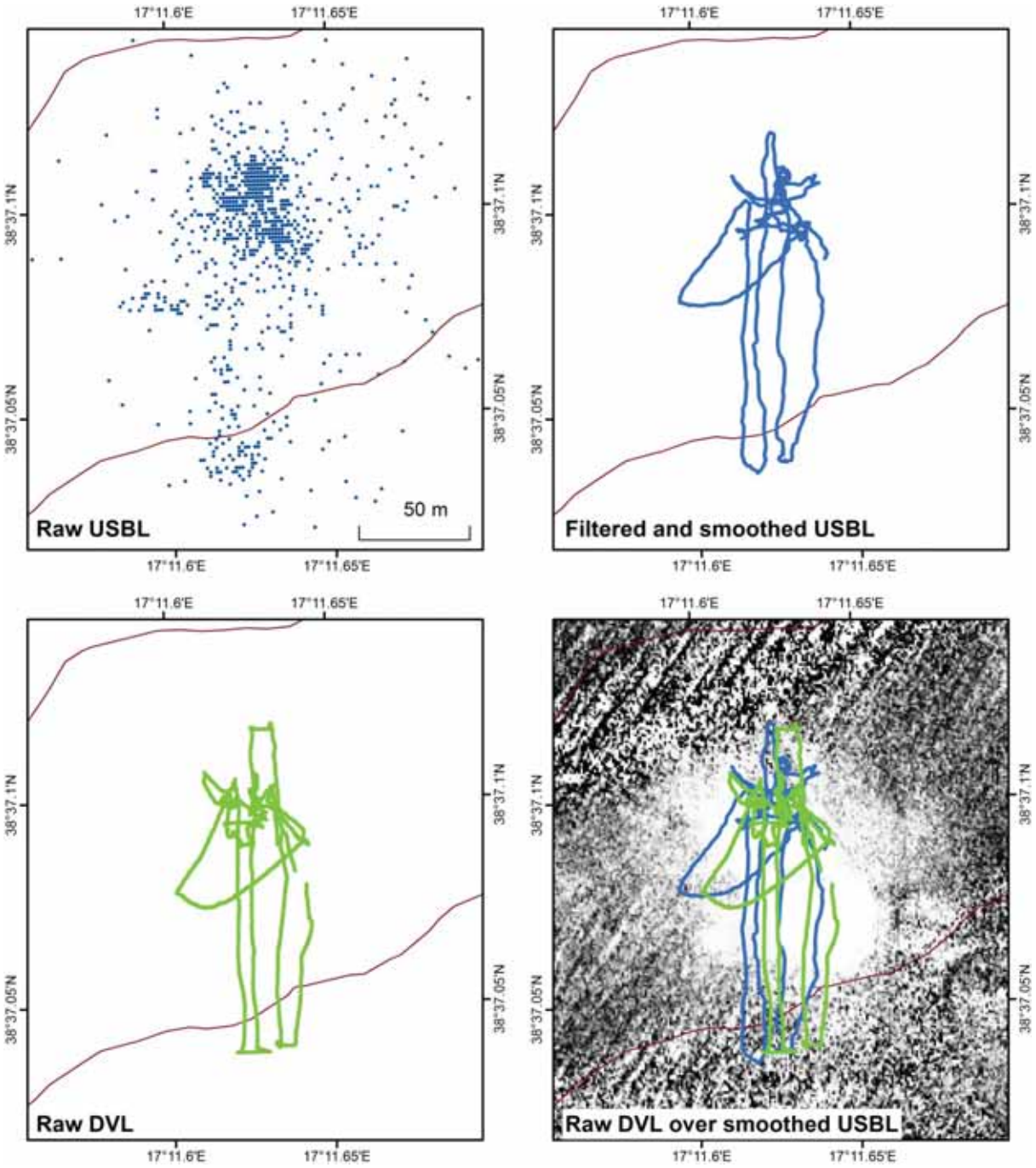

Fig. 52: Illustration of the different positioning systems. Although raw USBL (top left) did not allow accurate positioning during the dive, useful positioning data could be retrieved in post processing (top right). The raw DVL data (bottom left) proved efficiency for navigating during the dive. However, comparison with the USBL data (bottom right) showed that manual resetting of the DVL navigation against the USBL data caused offsets in the DVL timeseries that hindered its accuracy.

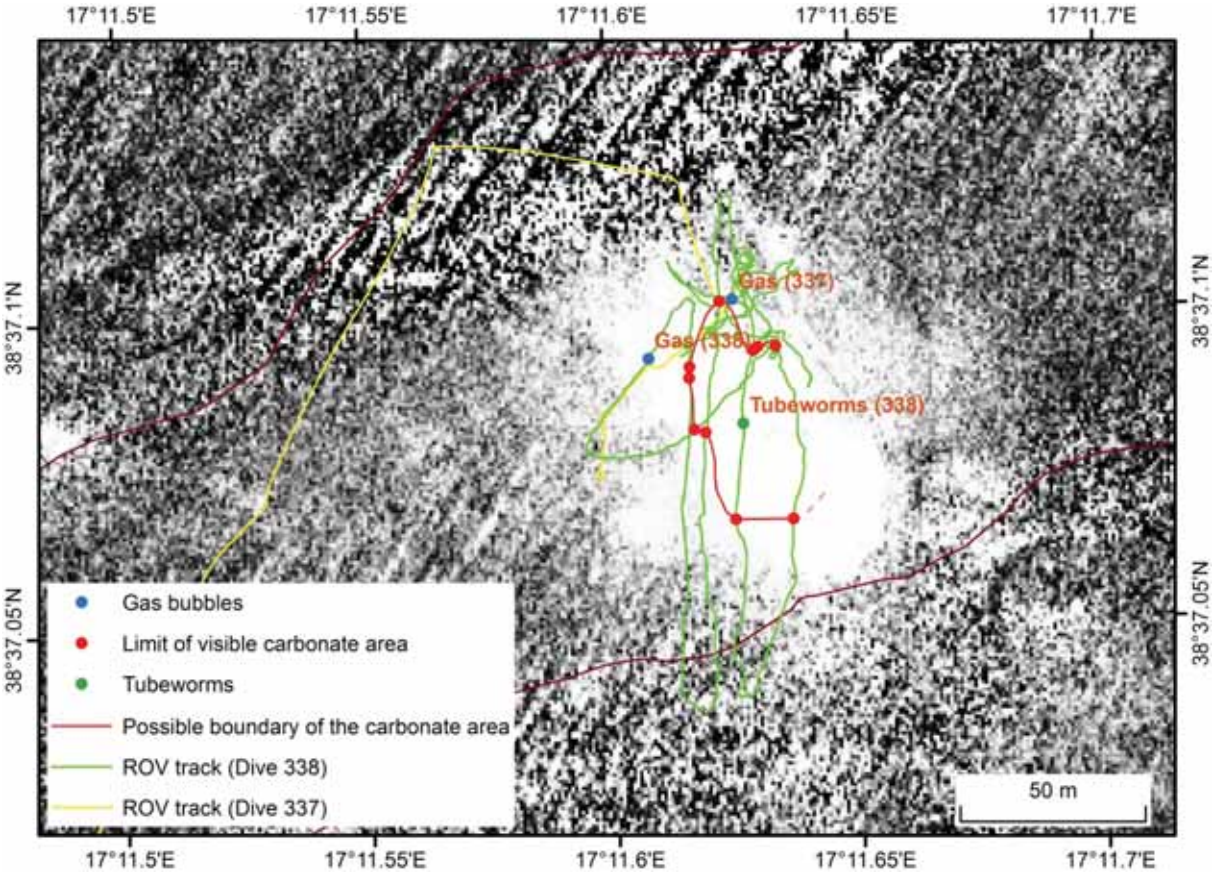

Fig. 53: Map of the dive track summarizing the main observations of the dive. Note that the absolute position of the background backscatter map (produced from AUV Dive 62) is not precisely known; therefore, the backscatter map may be offset from its true location by a few metres.

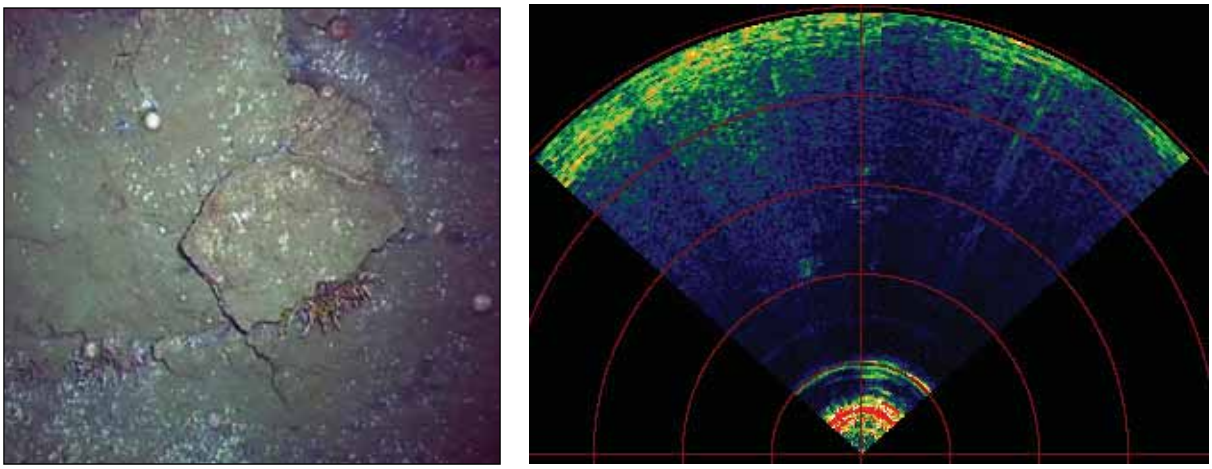

Fig. 54: Left: Carbonate slabs with tubeworms, urchins and clams. Right: Gas bubbles in the water columns as imaged by the forward-looking sonar.

8.2.3 Dive 339 (Station 1234-1, GeoB: 19221-1)

Area:	**Venere Mud Volcano, Flare 1**
Responsible scientist:	Yann Marcon
Date:	Monday 17 November 2014
Start bottom (UTC):	08:24
End bottom (UTC):	16:10
Bottom time:	07h 46min
Start bottom (Lat/Long/depth):	38° 37.0833' N, 17° 11.6063' E, 1561 m
End bottom (Lat/Long/depth):	38° 37.0795' N, 17° 11.6252' E, 1543 m

Points of interest:

WP 1	38° 37.1028' N	17° 11.6215' E	Gas 1 (Dive 337)
WP 2	38° 37.1049' N	17° 11.6164' E	Gas 2 (Dive 337)
WP 3	38° 37.0928' N	17° 11.6037' E	Gas 3 (Dive 338)
WP 4	38° 37.0831' N	17° 11.6226' E	Tubeworms
WP 5	38° 37.1071' N	17° 11.6243' E	Lost push corer

Key results:
Push cores in bacterial mats, gas samples, T-stick measurements, gas bubble imaging for quantification, faunal sampling with the suction sampler.

Technical description:
For this dive, the recurrence time of the Posidonia system was set to 6 sec. This resulted in a very good quality of the USBL positioning system with only few erroneous positions in comparison with the previous dive.

Furthermore, the manipulator of the ROV worked flawlessly during the entire dive, which enabled intensive sampling of the seep area and the bubble sites. However, issues with the auto-pilot mode caused navigation problems during the exploration surveys and the altitude of the ROV could not be kept constant.

Table 13: Samples and measurements taken during Dive 339.

GeoB	Instrument	UTC Start	UTC End	Position	Depth	Comment
19221-2	Gas Bubble Sampler	09:11	09:18	38°37.0949'N 17°11.6027'E	1568 m	No gas hydrates in the funnel
19221-3	T-stick	09:35	09:50	38°37.0947'N 17°11.6021'E	1568 m	In bacterial mat within bubble stream
19221-4	Push Corer	09:41	09:44	38°37.0945'N 17°11.6026'E	1568 m	In bacterial mat within bubble stream
19221-5	T-stick	09:58	10:09	38°37.0944'N 17°11.6000'E	1567 m	In bacterial mat without bubble stream
19221-6	Push Corer	10:03	10:03	38°37.0948'N 17°11.6026'E	1568 m	In bacterial mat at the rim
19221-7	Gas Bubble Sampler	10:25	10:26	38°37.0949'N 17°11.6024'E	1568 m	Just water, no gas

19221-8	HD-Camera (tapes 1-2)	10:57	11:10	38°37.0968'N 17°11.6064'E	1569 m	Bubble imaging
19221-9	HD-Camera (tape 2)	11:23	11:39	38°37.0955'N 17°11.6021'E	1569 m	Bubble imaging
19221-10	Push Corer	N/A	12:29	38°37.1053'N 17°11.6221'E	1568 m	PC lost during dive 338
19221-11	Suction Sampler	15:04	15:19	38°37.0795'N 17°11.6183'E	1564 m	Clams recovered in front of carbonates and tubes
19221-12	Suction Sampler	15:45	15:58	38°37.0800'N 17°11.6243'E	1564 m	Recovered a mussel and a tubeworm

Dive description:

The ROV dive was dedicated to sampling the gas bubble emissions that were identified in ROV dives 337 and 338. The first point of interest visited during the dive (WP3) was the position where gas bubbles had been observed in Dive 338 (Fig. 54). The forward-looking sonar was switched on while nearing the first waypoint in order to precisely locate the gas emissions. The work with the horizontally-looking sonar was conducted at an altitude of 15 m above the seafloor in order to avoid acoustic noise from the ground. The gas streams caused very strong acoustic anomalies, which could be clearly imaged with the sonar (Fig. 55). Those acoustic anomalies were considerably stronger than in Dive 338, which suggests that the intensity of the gas streams is variable. The gas emissions were found rapidly and were very intense. Most of the gas streams originated from large bacterial mats.

The next 2.5 hours following the finding of the gas emissions were dedicated to sampling activities. In summary, one gas sample, one bottom water sample as well as two push cores and T-stick measurements were taken within and around the bacterial mats and the gas emissions. Temperature gradients up to 0.2° C/m were measured in the bacterial mats (Fig. 56). A marker was left in order to facilitate the identification of the site in future dives (Marker 1: 38°37.09396'N, 17°11.6010'E). Finally, several gas bubble streams were recorded on HD tapes as well as with the forward-looking sonar for later quantifications of the gas fluxes.

From there we headed towards the gas streams that were observed in Dive 337 (WP 1 and WP2). Unfortunately, additional gas streams could not be found and the WP1 and WP2 sites could not be reliably identified. However, the push corer (R1) that was left on the seafloor during the previous dive was eventually found and could be recovered.

It was then decided to explore the area to the West and to the East in order to determine the extent of the carbonate area in these directions. The exploration was conducted at a fixed altitude, while the downward-looking video and photo cameras were recording. The exploration line was aimed at going from East to West through WP4. At WP4, we landed the ROV onto the carbonate pavements to get close-up views of the tubeworms (Fig. 57) and to sample the carbonates and the fauna. The carbonates turned out to be very hard and they could not be easily grabbed by the manipulator. However, small broken pieces could be collected with the suction sampler, together with clam shells, bacterial mats, a dead tubeworm, as well as a mussel. The use of the suction sampler exposed a blackish sediment layer that was underlying the thin top layer of brownish sediments. Finally, stirring the ground with the suction sampler triggered a new stream of gas bubbles from the sediments. The bottom time ended near WP4 at 16:10 UTC.

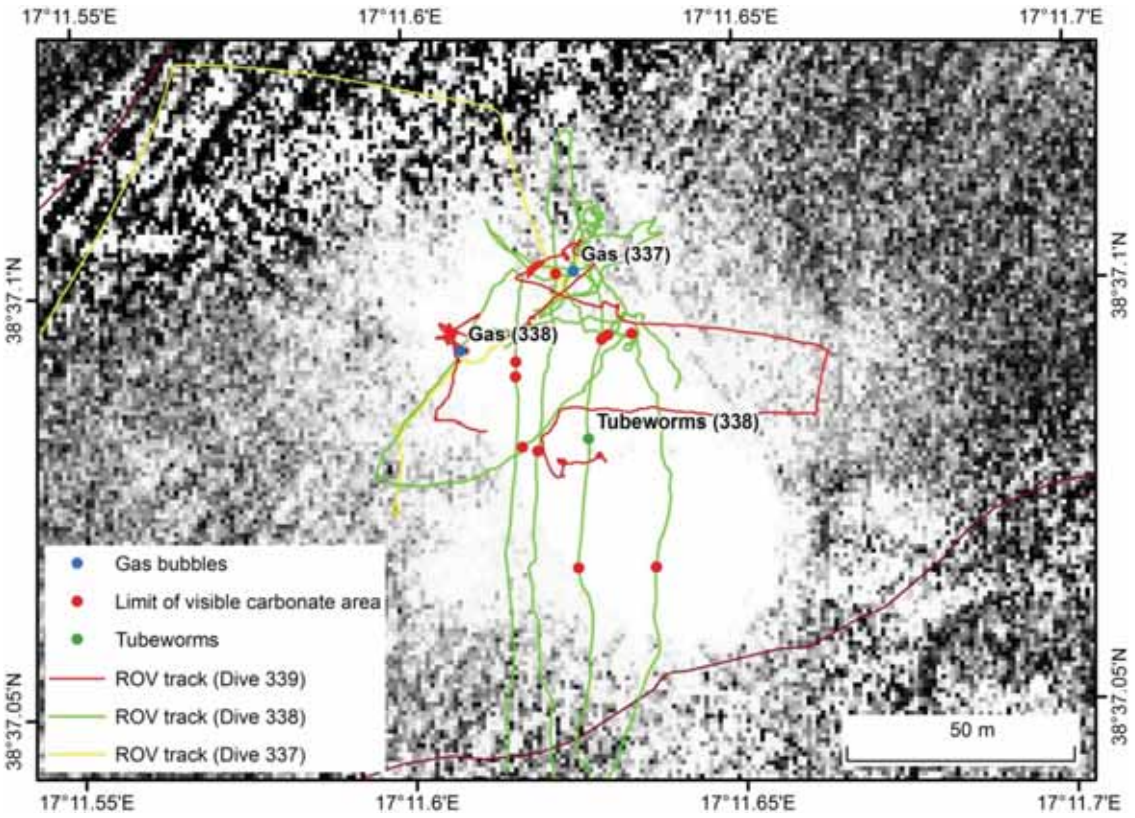

Fig. 54: Map of the dive track. Note that the absolute position of the background backscatter map (produced from AUV Dive 62) is not precisely known; therefore, the backscatter map may be offset from its true location by a few metres.

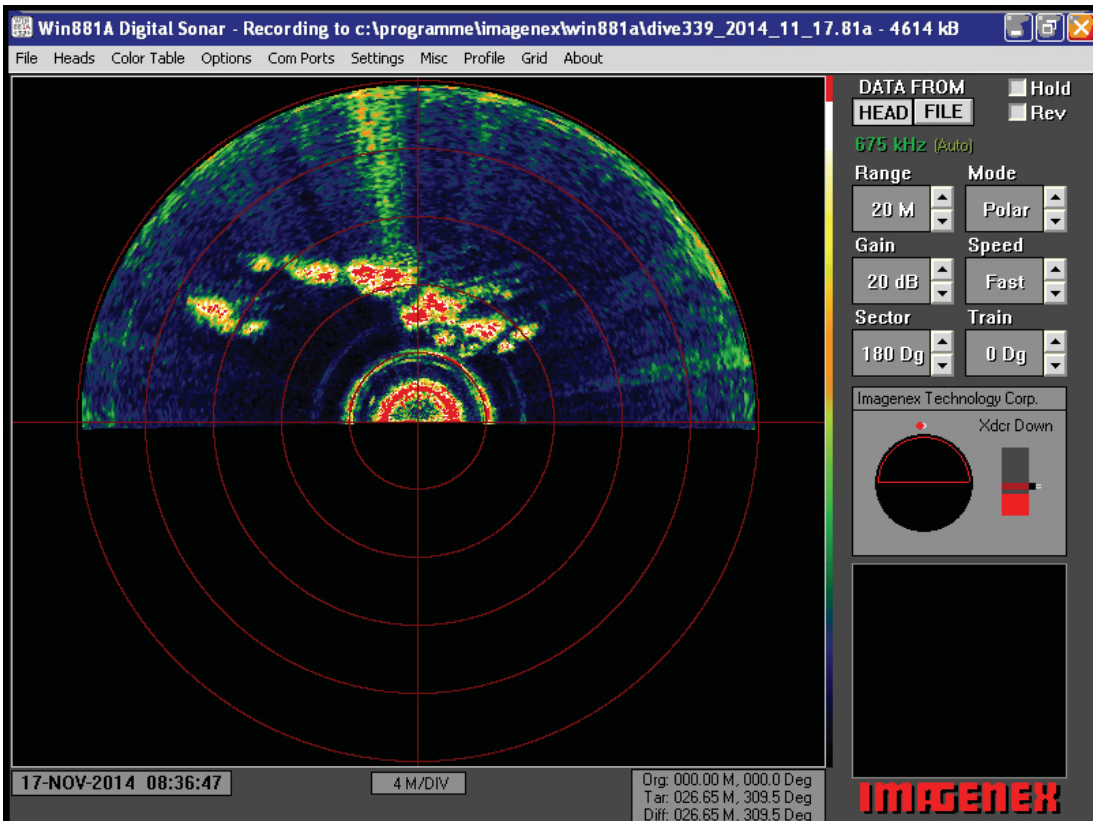

Fig. 55: Intense gas emissions caused strong acoustic anomalies on the forward-looking sonar, which help to localize the bubble streams rapidly.

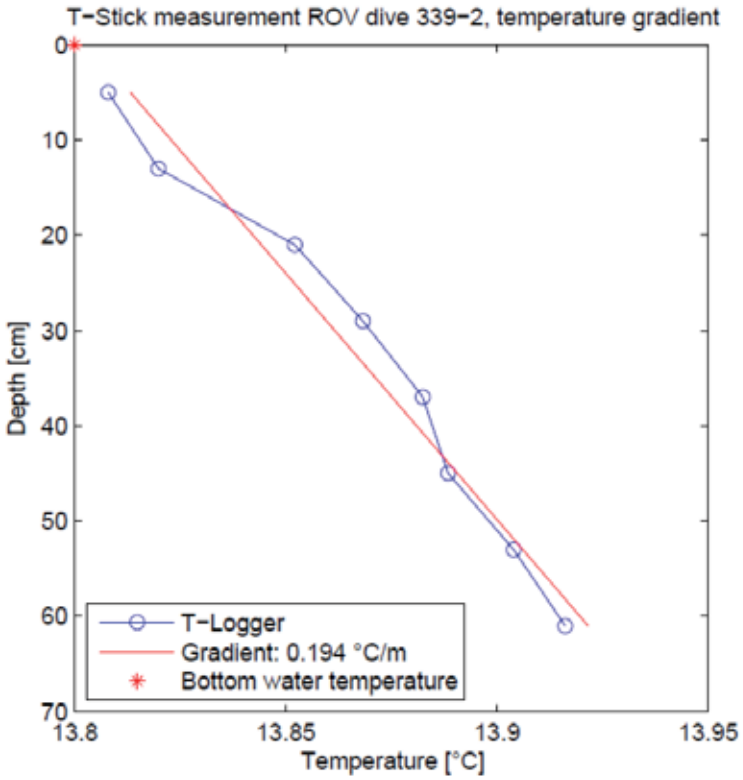

Fig. 56: Temperature gradient up to 0.194° C/m in the bacterial mats.

Fig. 57: Dense aggregation of living tubeworms.

8.2.4 Dive 340 (Station 1237-1, GeoB: 19224-1)

Area:	**Venere Mud Volcano, South Flare**
Responsible scientist:	Heiko Sahling
Date:	Tuesday 18 November 2014
Start bottom (UTC):	12:18
End bottom (UTC):	15:15
Bottom time:	07h 46min
Start bottom (Lat/Long/depth):	38° 37.0833' N, 17° 11.6063' E, 1561 m
End bottom (Lat/Long/depth):	38° 37.0795' N, 17° 11.6252' E, 1543 m

Points of interest:

WP 1:	38° 36.0464' N	17° 12.5812' E	PS flare (start)
WP 2:	38° 36.0958' N	17° 12.5417' E	PS flare (end)
WP 3:	38° 36.0961' N	17° 12.5685' E	EM122 flare

Borders of the discovered seep site:

W-limit:	38° 36.087’N	17° 12.561’E
S-limit:	38° 36.081’N	17° 12.571’E
E-limit:	38° 36.089’N	17° 12.5736’E
N-limit:	38° 36.099’N	17° 12.551’E

Key results:

Discovered 40 m wide seep field with clams, black patches, and bacterial mats immediately west of a morphological step; at the step carbonates are cropping out; step marks the limit of occurrence of carbonates eastward (high backscatter) and “regular” mud volcano sediments west of it. Bubbles were exactly found at EM122 predicted site, gas and water sample taken by GBS.

Technical description:

USBL positioning system worked well, manipulator worked well, flashes for Prosilica still camera worked and allowed taking good photos, Scorpio still images are generally too dark, HD camera with small smear spot at left side.

Table 14: Samples and measurements taken during Dive 340.

GeoB	Instrument	UTC Start	UTC End	Position	Depth	Comment
19224-2	Gas Bubble Sampler 2 (blue)	13:20	13:38	38°36.0959’N 17°12.5715’E	1596 m	Gas sample of sporadic bubble stream
19224-3	Gas Bubble Sampler 1 (yellow)	13:56	13:57	38°36.0966’N 17°12.5718’E	1595 m	Water sample close to bubble stream

Dive description:

The motivation of the dive was to look for seep-indications at the seafloor in an area characterized by a weak flare in PARASOUND echosounder. Based on the PARASOUND mapping, two coordinates along the ships track were picked to indicate the approximate position of the gas emission site (WP 1 and 2). Refined analyses of the EM122 swath also showing the flare suggested a slightly different

location (WP 3). Ultimately, the picked position from EM122 was surprisingly precise as we found a bubble site just a few meters off the predicted location!

Upon reaching the seafloor near WP 1 the ROV flew with the sea bottom in sight towards WP 3 and a ~40 m large seep area was discovered (see Figures). During the dive the seep was studied in order to define its limits and characteristics as summarized as follows. The main components of the seep are clamshells, dark patches with variable densities of filamentous bacteria, authigenic carbonates and one or more cluster with Lamellibrachia-type tubeworms. The southern area of the field appears to be the oldest part, with massive authigenic carbonate plates being broken apart in a crater-like feature of some meters in diameter and about one meter in depth. In the crater tubeworm tubes and rubbish has accumulated. In the area around the crater the seafloor is densely covered by empty vesicomyid shells. The shells may be the result of mortality of clams due to carbonate cementation of the sediments physically or chemically excluding the living infaunal clams from their habitat. The northern area of the field appears younger. Here the one and only bubble stream was observed. Dark patches surrounded by clamshells form a concentric pattern. It can be expected that somewhere here living clams are found in the sediments.

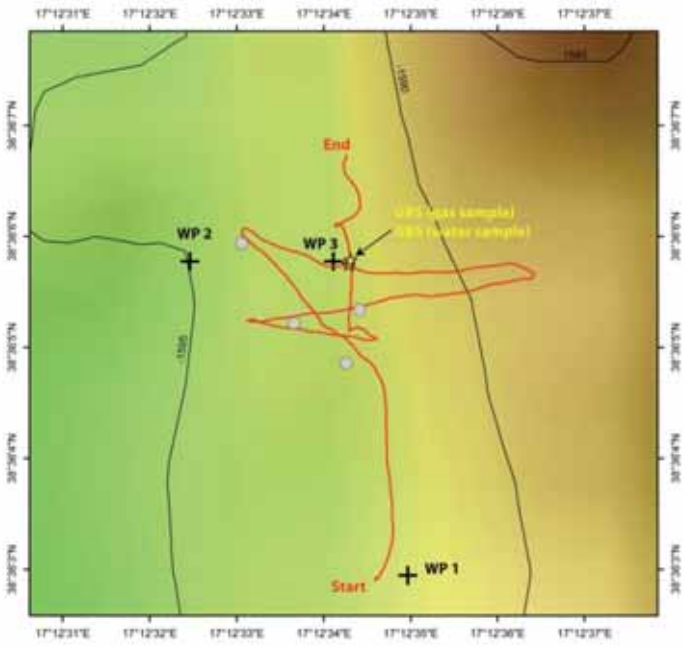

Fig. 58: Map of the ROV Dive 340 track with waypoints, the limits of the seep area (grey dots), and the gas bubble stream indicated by the sampling positions (stars).

To the east, the seep area is sharply limited by a NNW-SSE-trending boundary. This boundary was seen in the EM122 backscatter maps, with high backscatter eastward and medium backscatter westward. We could clearly see that eastward of the boundary the sediments are cemented by authigenic carbonates forming a flat layer within the sediments below a drape of soft sediments. At the boundary, we observed two places where the carbonates crop out: north of the seep area and at the site where the bubbles are released. The carbonates efficiently seal the system as suggested by the fact that no significant seep-indications were found in the sediments east of the boundary. The seep area is sharply limited along the boundary.

The gas bubble stream was found just a few decimeter west of the carbonate outcrop and visually documented. The bubble stream was transient, with burbs of bubbles of a few seconds releasing > 20 bubbles at a time followed by times of inactivity. The behaviour of the bubble release suggests that

bubbles are collected in the subsurface and periodically released when the collection chamber spills over. We managed to collect some bubbles by GBS and took a GBS about 30 cm away from the bubble stream.

Fig. 59: Left: ROV image approaching the seep area from the south. Dense shells at the seafloor in the foreground and the crater in the background. Right: ROV image of the crater (14:41:58 UTC) littered by rubbish and tubeworm tubes.

Fig. 60: Left: ROV image of the bubble emission site (13:14:15 UTC). The cemented sediments crop out at the site (view to the east). Above the carbonates (east) some dark patches cm in size indicate reducing conditions just above the carbonates but these signs disappear some meters further east. West of the carbonates the seafloor is blackish and bubbles are released from two sites roughly within the center of the black patch. Small tubeworms settle in the carbonates. Right: ROV image of the eastern limit of the seep area (14:55:08 UTC) viewing to the north. This lineament is in prolongation to the bubble site.

Fig. 61: Left: ROV image of the outcropping cemented sediments (15:13:33 UTC). This view is to the north, north of the bubble site. Right: ROV image of the northern area of the seep area (14:35:48 UTC) with concentric patterns of bacterial mats (center) in black patches surrounded by clams.

8.2.5 Dive 341 (Station 1243-1, GeoB: 19230-1)

Area: **Venere Mud Volcano, Flare 1**
Responsible scientist: Miriam Römer
Date: Wednesday 26 November 2014
Start bottom (UTC): 08:26
End bottom (UTC): 15:25
Bottom time: 06h 59min
Start bottom (Lat/Long/depth): 38°37.088' N, 17°11.604' E, 1564 m
End bottom (Lat/Long/depth):

Points of interest:

WP 1:	38°37.094'N	17°11.602'E	Gas emissions west (Marker 1)
WP 2:	38°37.102'N	17°11.621'E	Gas emissions east
WP 3:	38°37.080'N	17°11.624'E	Tubeworms
WP 4:	38°37.109'N	17°11.554'E	Third AUV-flare

Key results:
Inactive gas bubble emissions, elevated temperature gradients measured at gas emission site 1 and 2, pushcores taken for porewater characterization, up floating gas hydrates during t-stick and pushcore sampling at gas emission site 1, mosaic over central carbonate mound.

Technical description:
No technical problems during the dive.

Table 15: Samples and measurements taken during Dive 341.

GeoB	Instrument	UTC Start	UTC End	Position	Depth	Comment
19230-2	Gas bubble sampler	08:47	08:50	38°37.095'N 17°11.609'E	1568 m	Water sample at same location as 19221-7 (Marker 1)
19230-3	T-stick	09:04	09:14	38°37.095'N 17°11.609'E	1568 m	In gas emission site 1 (at Marker 1)
19230-4	Push corer	09:27	09:29	38°37.095'N 17°11.608'E	1567 m	Gas hydrates floating up
19230-5	Push corer	09:41	10:42	38°37.095'N 17°11.609'E	1567 m	Next to PC position as above
19230-6	Net	10:12	10:28	38°37.094'N 17°11.624'E	1566 m	Carbonate at the rim of the patch
19230-7	Mosaic	11:30	12:00	38°37.082'N 17°11.624'E	1568 m	Six lines of 15 m length and 1 m spacing. Over central carbonates
19230-8	Net	13:03	13:03	38°37.081'N 17°11.629'E	1564 m	Carbonate sample
19230-9	Net	13:10	13:10	38°37.082'N 17°11.629'E	1564 m	Carbonate sample
19230-10	T-Stick	14:03	14:26	38°37.102'N 17°11.630'E	1567 m	Close to bacterial mats at emission site 2
19230-11	Gas bubble sampler	14:11	14:12	38°37.102'N 17°11.630'E	1568 m	Water sample close to emission site 2
19230-12a	Push corer	14:42	14:58	38°37.102'N 17°11.630'E	1567 m	Within bacterial mat – for rhizons sampling

19230-12b	Push corer	14:44	14:56	38°37.101'N 17°11.628'E	1568 m	Within bacterial mat
19230-13a	Push corer	14:46	14:55	38°37.101'N 17°11.628'E	1567 m	Outside bacterial mat - for rhizons sampling
19230-13b	Push corer	14:49	14:53	38°37.101'N 17°11.627'E	1568 m	Outside bacterial mat
19230-14a	Push corer	15:16	15:23	38°37.100'N 17°11.623'E	1567 m	At another patch, within the bacterial mat - for rhizons sampling
19230-14b	Push corer	15:21	15:21	38°37.100'N 17°11.623'E	1569 m	Aside of previous PC

Dive description:

Dive 341 was planned at Flare 1 at the Venere Mud Volcano in order to complete the sampling at the seep site and the gas emission sites detected and characterized in the three dives before. However, we crossed the area just before the dive to confirm the flare position using the echosounder systems on board, but the flare disappeared. This observation showed that the gas bubble emissions at this flare site vary over time and during this dive, we did not expect to find bubble streams. Nevertheless we started the dive and went first to WP 1, where a Marker is positioned directly in gas emission site 1, which was found intensively bubbling during Dive 339. The Marker was found easily and indeed, the site showed no active bubble emissions.

For comparison with the water sample taken during Dive 339 taken very close to the bubble streams, we took again a water sample at the same location. Afterwards, a T-stick measurement was performed located just between the holes produced by our T-stick measurements made during Dive 339 (Fig. 64 a). The resulting gradient is with 0.31° C/m even higher than the already elevated gradients measured here before. In addition, we observed a white chunk floating up while recovering the T-Stick, which appeared to us to be gas hydrate. Therefore, a push corer was used to stick more into the sediments and several pieces of such material floated up (recorded in HD). A second push corer was taken aside without such a disturbation for porewater analyses. We headed on to WP 2 (gas emission site 2) and proved that also this formerly active site did not show any bubble streams at the moment.

On the way to WP3 we crossed the boundary to the carbonate paved area and broke a few pieces using the manipulator to sample them finally with the net. At WP 3 the mounded structure made of thick carbonates was found and a mosaic of 15 x 6 m (6 lines with 1 m line spacing and in 1.5 m height) was made before two pieces of carbonates were broken from the central area and sampled. First attempts to use a new tool, similar to a hammer, to break the thick carbonates failed. But by repositioning and trying to grab a thinner crust with the manipulator we were successful.

The last part of the dive was dedicated to sample close to WP2, where first a T-stick measurement was taken in a microbial mat and the gas bubble sampler was filled with water. Two pairs of push corers, one for porewater sampling, another for sediment analyses were taken afterwards. Finally, two more push corers were used to sample within another microbial mat just a few meters west.

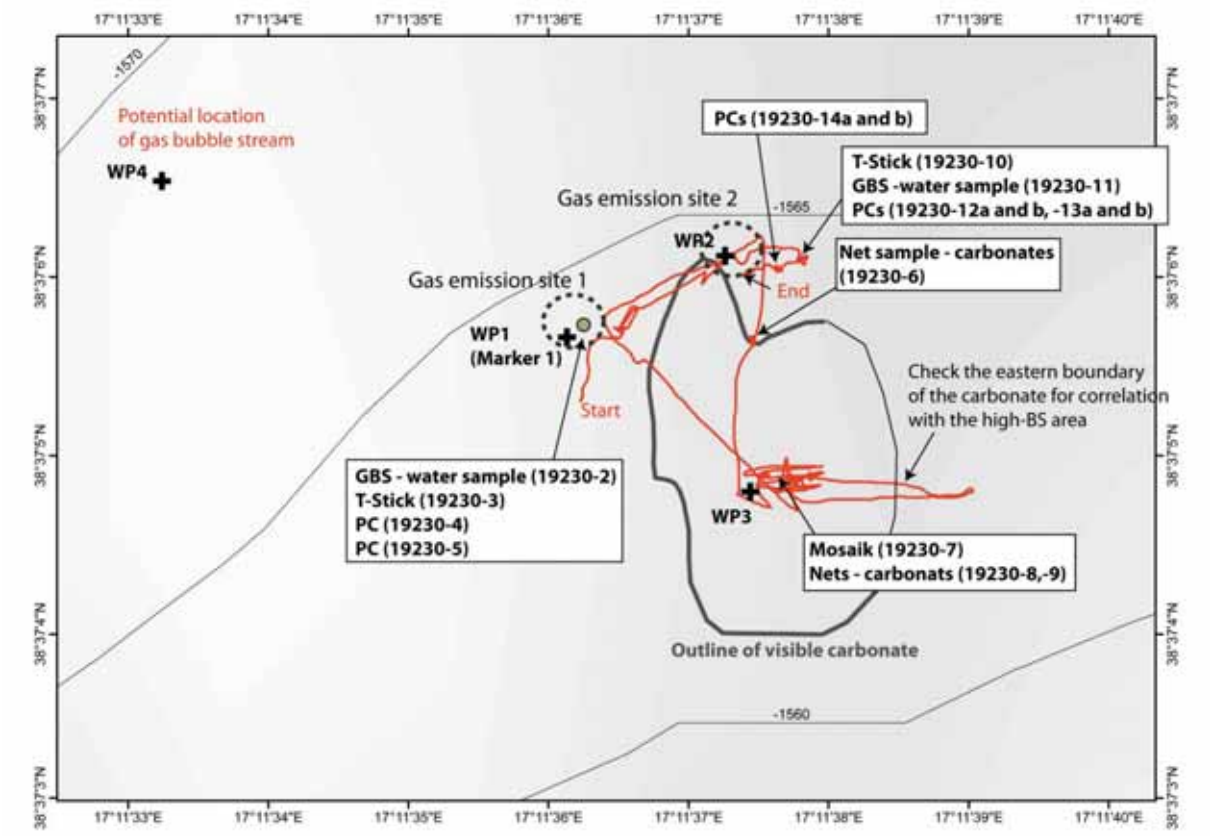

Fig. 62: Map of the dive track (red line - USBL). Sampling has been mainly done at WP1, WP2 and WP3, at and around the carbonate patch.

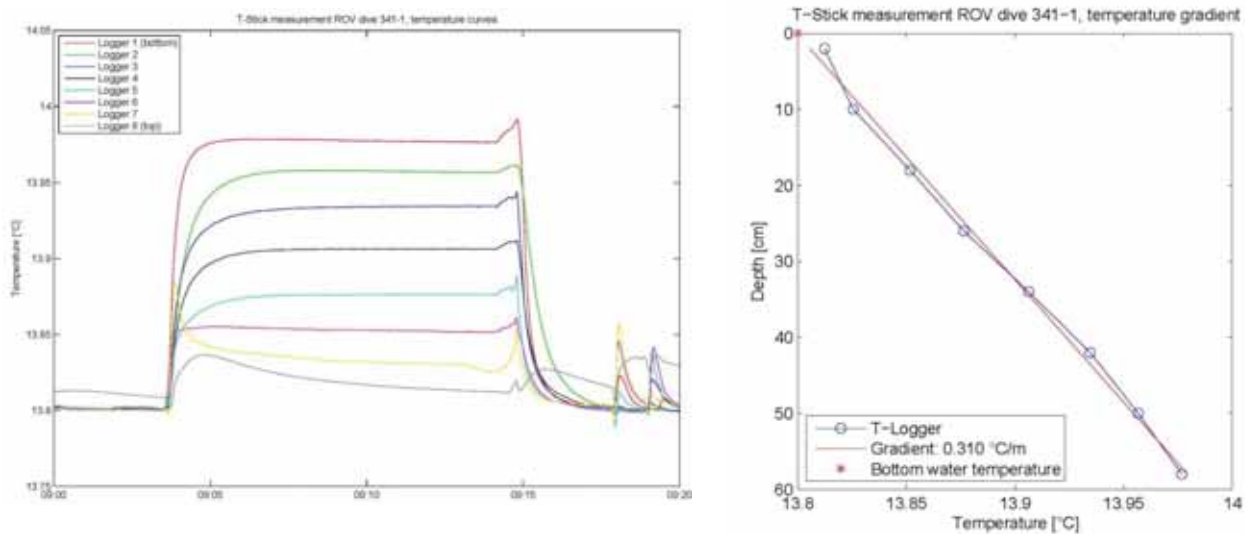

Fig. 63: Left: measurement of the T-stick shows different curves above and below ~15 cm depth, which might be correlated to gas hydrate occurrence in the shallow subbottom. Right: temperature gradient of up to 0.310° C/m in gas emission site 1.

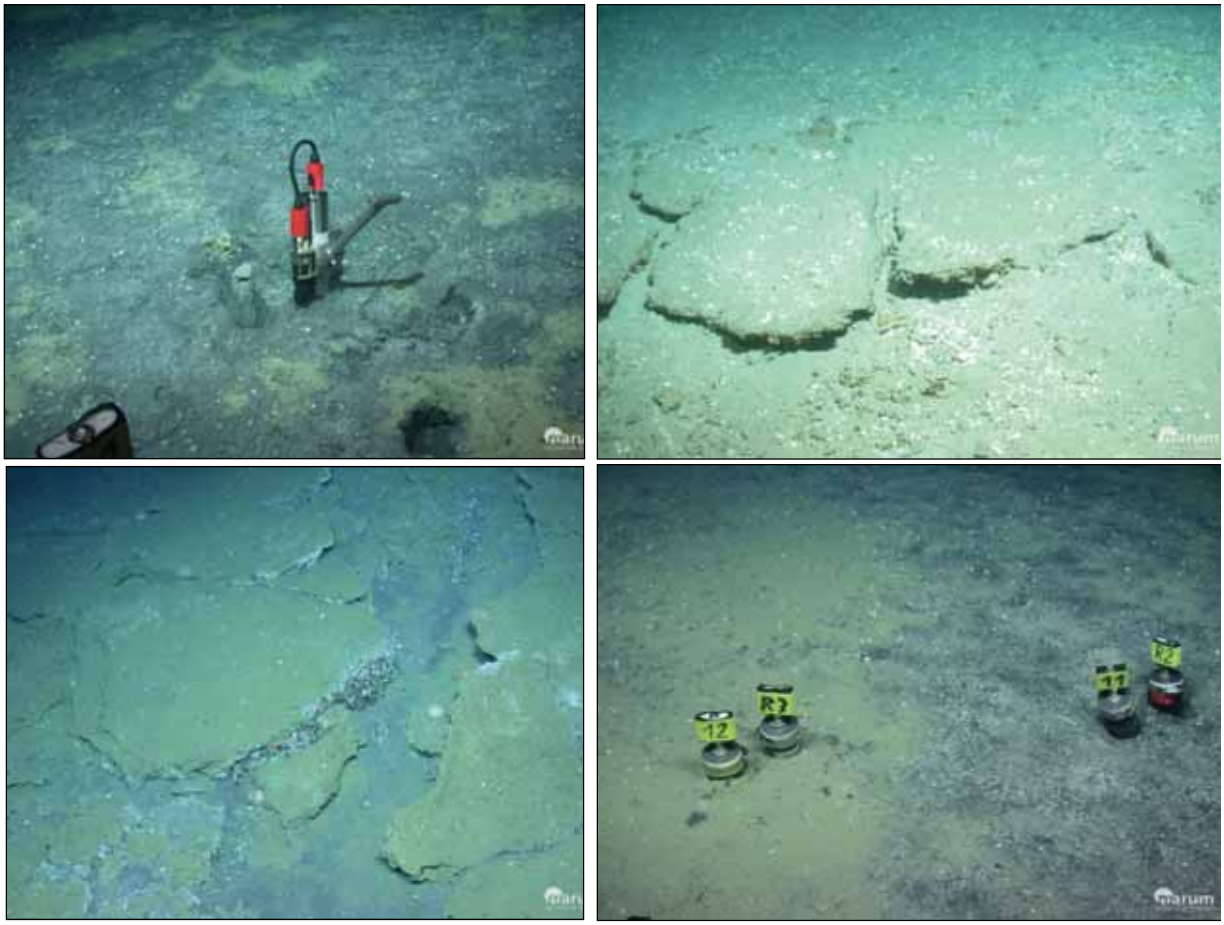

Fig. 64: Seafloor pictures taken during ROV-341. (a) T-stick measurement at (here inactive) gas emission site 1. (b) Outcropping carbonate pavements at the northern rim of the carbonate patch, where sample 19230-6 was taken. (c) Central area of the carbonate patch, where the mosaic was taken. (d) Push corer sampling close to emission site 2.

8.2.6 Dive 342 (Station 1245-1, GeoB: 19232-1)

Area:	**Venere Mud Volcano; western summit**
Responsible scientist:	Gerhard Bohrmann
Date:	Friday 28 November 2014
Start bottom (UTC):	10:05
End bottom (UTC):	15:25
Bottom time:	05:20
Start bottom (Lat/Long/Depth):	38°36.4782’N, 17°11.1794’E
End bottom (Lat/Long/Depth):	38°36.4631’N, 17°11.2924’E

Points of interest:

WP 1:	38°36.477’N	17°11.177’E	Starting point
WP 2:	38°36.466’N	17°11.196’E	potential top
WP 3:	38°36.458’N	17°11.303’E	potential flare position
WP 4:	38°36.428’N	17°11.254’E	location of bubble pulses

Key results:
During the dive fresh mud flows that spreads out from the summit of the mud volcano and flows according its downward slope first to the east and then to the southeast guided by the slope of mud volcano flank having been first investigated. An unknown seep-like white patch was sampled 30 m southeast of the summit outside sub-recent mud flows and water samples have been taken in the bottom water closely above young mud flows.

Technical description:
Due to the general breakdown of the forward looking of the ROV (Kongsberg MS1000) the IMAGENEX sonar-head was used during the dive.

Table 16: Samples and measurements taken during Dive 342.

GeoB	Instrument	UTC start	UTC end	Position	Depth (m)	Remarks
19232-2	T-stick	13:07	13:20	38°36.4332'N 17°11.2580'E	1512	On a white patch
19232-3	Push corer PC R1	13:12	13:13	38°36.4330'N 17°11.2580'E	1512	With crystal looking pieces
19232-4	Net (yellow)	13:28	13:31	38°36.4331'N 17°11.2581'E	1512	Sample white material in a net
19232-5	T-stick	14:29	14:40	38°36.4327'N 17°11.2580'E	1513	
19232-6	Push corer PC R2	14:33	14:36	38°36.4326'N 17°11.2580'E	1512	Low penetration
19232-7	Push corer PC R3	14:38	14:40	38°36.4327'N 17°11.2580'E	1512	Good penetration, much softer material
19232-8	Gas bubble sampler 2 (blue)	15:08	15:16	38°36.4491'N 17°11.3016'N	1509	On the rim south of WP3
19232-9	Gas bubble sampler 2 (yellow)	15:20	15:23	38°36.4628'N 17°11.2925'E	1506	A bit north of the rim not on the flow

Dive description:
According the dive plan the dive should explore the outflow area of fresh mud flows at Venere west summit. Peculiar flow structures were identified by small several decimeter-changes in the micro-bathymetry and an outflow area of the most recent mud flow could be defined right on the top of the summit (Fig. 65). Flow structures in two principle directions to the west/southwest or to the east/southeast became evident and the direct outflow area was imaged by a tiny circular elevation of 1-2 m high from where the most recent flow moved to the east. Circular flow pattern surrounded the outflow area and help to define the outflow region (Fig. 65).

ROV Dive 342 started NW of the summit outside the fresh mud flows. The seafloor was smooth and soft sediments covered the bottom. Some bioturbation traces have been identified. We tried to move in SE direction over the potential outflow area to the east by documenting the seafloor behavior with the ROV's cameras. By plotting the ROV track after the dive we found that we missed the outflow area of about 10 m, since we passed in the north of it (Fig. 65), however, during further exploration we reached the sub-recent flow approximately 30 m to the east and performed a profile perpendicular to the flow direction to the south until we clearly have left the recent flows. In order to surely distinguish between fresh flows and older structures we changed the direction at the

southern rim and followed a south to north trending profile until we have been back on the fresh flow. There the mud surface was broken in small scale chunks and the flow morphology was characterized by a higher elevation in the center of the flow and low-level edges (Fig. 66 left).

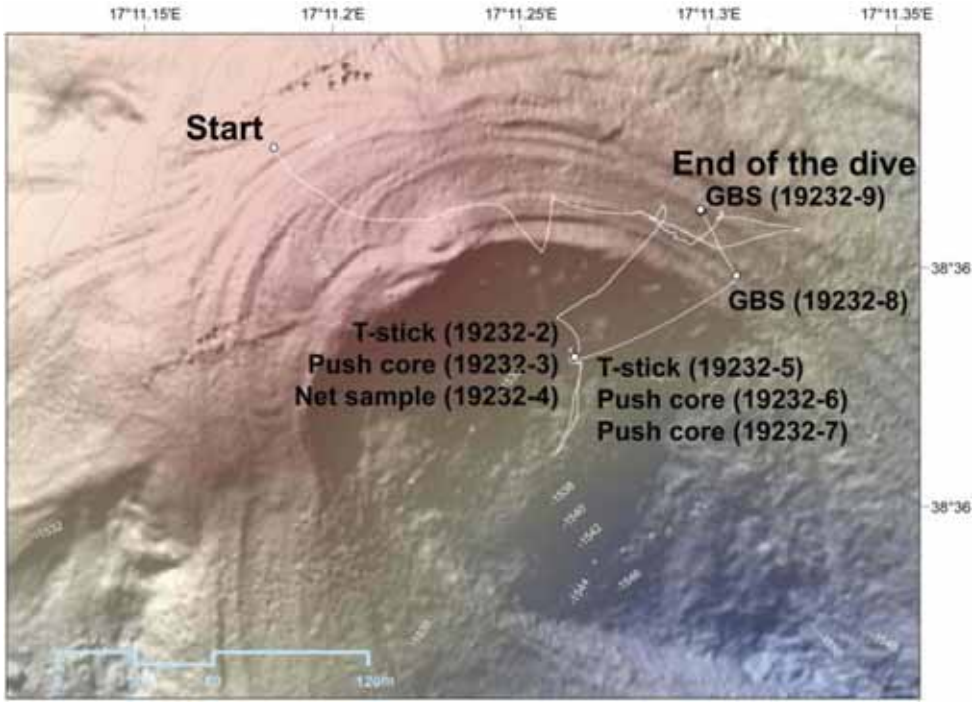

Fig. 65: Track and sampling locations of ROV Dive 342 at the summit of Venere West.

We followed the recent flow ca. 80 m to the east and surveyed the area north and northeast of the flow. Here we found pelagic sediments which covered the rougher topography of the underlying mud flows and adjusted its micromorphology. Due to the advanced bottom time we had to fly with the ROV to Way Point 3 which was a potential gas emission site documented by the weak gas flares during a hydro-acoustic survey in the night. The search with the sonar was difficult however by visual examination we found whity patches on the seafloor which remind us to a potential seep location (Fig. 66 right).

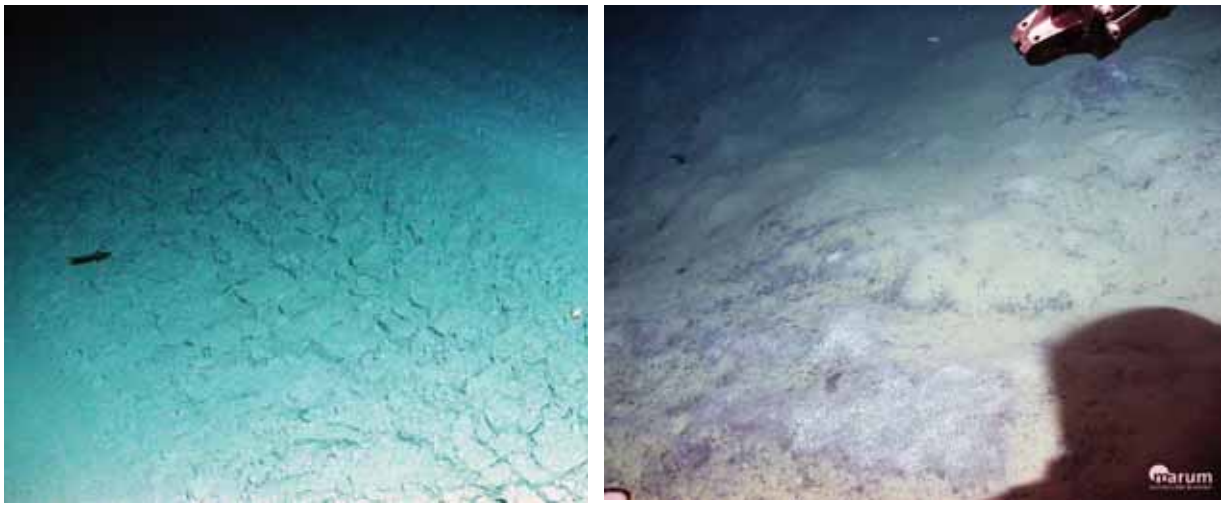

Fig. 66: Left: surface of a relative fresh mud flow sub-recently flown from Venere west summit (ROV Dive 342). Right: seafloor with white patch before T-stick and push core sampling (GeoB 19232-2 and -3).

A push core was taken (GeoB 19232-3) and a T-stick measurement was performed (GeoB 19232-2). After a more detailed examination of the white material on the seafloor we were no longer sure, that it represents bacterial mats and the white spots looked more like crystal grains. We therefore took another net sample from that place. Unfortunately after the net sample was recovered on deck of the ship and the sample was inspected, the white crystal-like grains could not be identified anymore.

After an excursion of 50 m downslope another T-stick measurement (GeoB19232-5) and two push cores (GeoB19232-6, -7) have been taken close by in an area that seemed to be characterized by an unknown seafloor disturbance. After inspecting the ROV images from that location the seafloor disturbance could have happened by the ROV itself and seems not to be the result of a natural seafloor event. Temperature gradients measured by the T-stick were calculated to be low of around 0,104-0,177°C/m (Fig. 67).

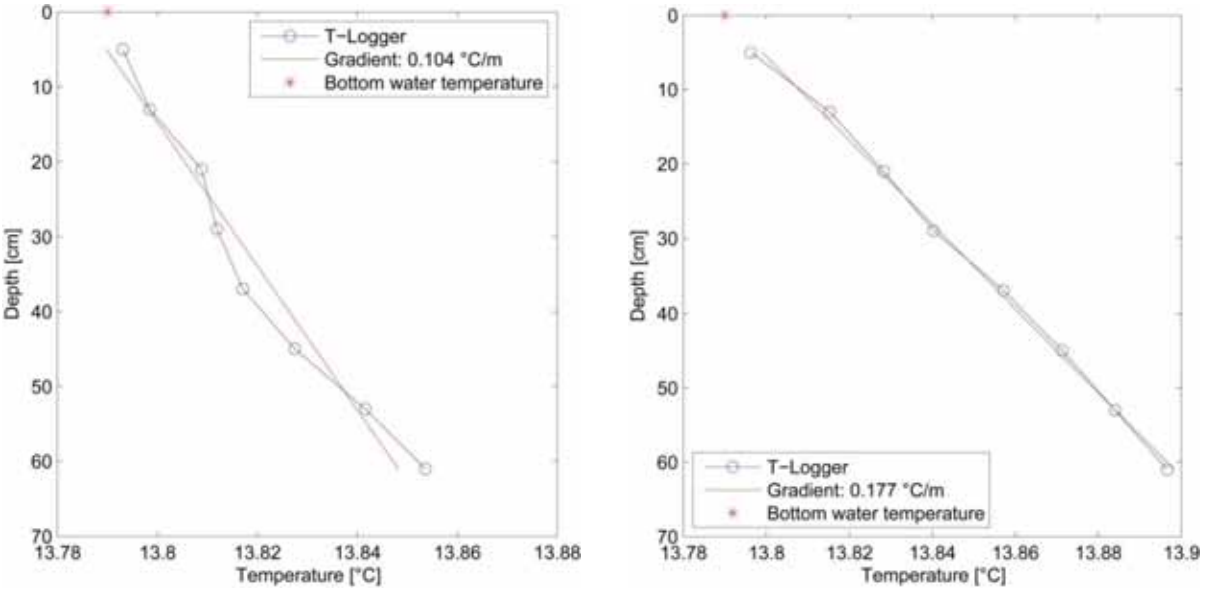

Fig. 67: Temperature profiles measured by T-stick during ROV Dive 342 at two locations where push cores have been taken GeoB Station 19232 (left) and GeoB Station 199232-5 (right).

The remaining half hour of the dive was used to fly in northeast direction to the sub-recent mud flow, where a gas bubble sample was used to take a water sample (GeoB 19232-8) close to the southern rim of the mud flow. A second water sample of near-surface bottom water was taken 50 m to the northwest on an older mud flow (GeoB19232-9; Fig. 65).

8.2.7 Dive 343 (Station 1252-1, GeoB: 19240-1)

Area:	**Venere Mud Volcano – Flares 4+5**
Responsible scientist:	Thomas Pape
Date:	Sunday 30 November 2014
Start bottom (UTC):	09:18
End bottom (UTC):	17:31
Bottom time:	08h 05min
Start bottom (Lat/Long/depth):	38°35.425'N, 17°11.967'E, 1605 m
End bottom (Lat/Long/depth):	38°35.426'N, 17°11.968'E, 1606 m

Points of interest:

WP 1:	38° 35.426' N	17° 11.960' E	Flare 4
WP 2:	38° 35.458' N	17° 12.020' E	Flare 5
WP 3:	38° 35.336' N	17° 12.028' E	High backscatter patch

Key results:

A mound-like structure covered by patchy microbial mats in the central area with clam shells was discovered. The structure was sampled with push corers. Digging in the blackish reduced sediments caused upfloating of subangular fragments of whitish material. The turbulent rising behaviour in the water column resembled that of gas hydrates. A larger mound-like structure was found afterwards. It was covered by fragmented carbonate pavements that were uplifted in the central area. Gas bubbles escaping the cracks at the summit of the mound, living tubeworms rooting below the carbonates and thick microbial mats associated to both substantiated persistent fluid seepage. Gas bubble streams were quantified by use of the HD camera and sampled. Two carbonate pieces, sediment push cores, and two near-bottom water samples were collected as well. T-stick measurements revealed a relatively steep geothermal gradient (ca. 0.210 °C/m) at the bubble emission site. Parallel tracks across the structure were followed with the ROV for acquiring seafloor photomosaic imagery. Marker 2 was placed on top of mound for recognition during subsequent dives in that area.

Technical description:

System worked properly during the entire dive; during intense digging in the sediment at WP 1 the QUEST shovel was bent.

Table 17: Samples and measurements taken during Dive 343.

GeoB	Instrument	UTC Start	UTC End	Position	Depth	Comment
19240-2	Gas bubble sampler 1 (blue)	10:37	10:56	38°35.457'N 17°12.022'E	1607 m	WP 2: Gas sample
19240-3	HD camera	ca. 10:45	ca. 10:55	38°35.457'N 17°12.021'E	1607 m	WP 2: Quantification of gas bubble stream
19240-4	T-stick 1	11:10	11:31	38°35.457'N 17°12.021'E	1607 m	WP 2: Within/ close to bubble emission site
19240-5	Claw of ROV-manipulator	11:14	11:18	38°35.457'N 17°12.021'E	1607 m	WP 2: Two fragments of authigenic carbonates
19240-6	Push corer R1	11:21	11:27	38°35.457'N 17°12.021'E	1607 m	WP 2: Sediments for pw analysis and sediment description
19240-7	Gas bubble sampler 2 (yellow)	11:45	11:46	38°35.457'N 17°12.021'E	1605 m	WP 2: Water sample ca. 2 m above seep structure
19240-8	Marker 2	11:51	11:53	38°35.457'N 17°12.021'E	1607 m	WP 2: Center of seep structure
19240-9	T-stick 2	13:11	13:22	38°35.486'N 17°12.075'E	1608 m	WP 3: Within microbial mat
19240-10	Push corer R2	13:13	13:20	38°35.486'N 17°12.074'E	1608 m	WP 3: Within microbial mat
19240-11	T-stick 3	13:23	13:35	38°35.485'N 17°12.074'E	1608 m	WP 3: Ca. 1 m east of microbial mat
19240-12	Push corer R3	13:26	13:27	38°35.486'N 17°12.074'E	1608 m	WP 3: Next to T-stick out of microbial mat

19240-13	Prosilica GT6600C camera	14:49	15:24	38°35.454'N 17°12.023'E to 38°35.456'N 17°12.026'E	1606 m	WP 2: Photo mosaic, heading 303°, alt. 1.4 m
19240-14	Gas bubble sampler 3(black)	15:39	15:41	38°35.458'N 17°12.022'E	1607 m	WP 2: Water sample close to seafloor
19240-15	Push corer R4	16:14	16:20	38°35.426'N 17°11.969'E	1606 m	WP 1: In-between clams and microbial mat for pw analysis and sediment description
19240-16	Push corer 18	16:22	16:28	38°35.425'N 17°11.969'E	1606 m	WP 1: Close to PC R4 for volatiles etc.
19240-17	T-stick 4	16:35	16:54	38°35.425'N 17°11.969'E	1606 m	WP 1: Top of microbial mound
19240-18	Push corers R5 and 16	16:40	17:08	38°35.426'N 17°11.969'E	1606 m	WP 1: Several attempts at the top; unsuccessful
19240-19	Shovel	17:10	17:29	38°35.426'N 17°11.969'E	1606 m	WP 1: Attempts to document presence of gas hydrate

PC = Push corer (R = dedicated for rhizon pore water sampling), PW = Pore water

Dive description:

Dive 343 was intended to explore and sample distinct areas to the south of the Venere MV summit that were characterized by high seafloor backscatter (see Chapter 7) and partially provided gas emissions into the water column (Flares 4 & 5; see Chapter 4; Fig. 68). According to data from the seafloor mapping and hydroacoustic surveys flare 4 & 5 should be less than 120 m distant to each other.

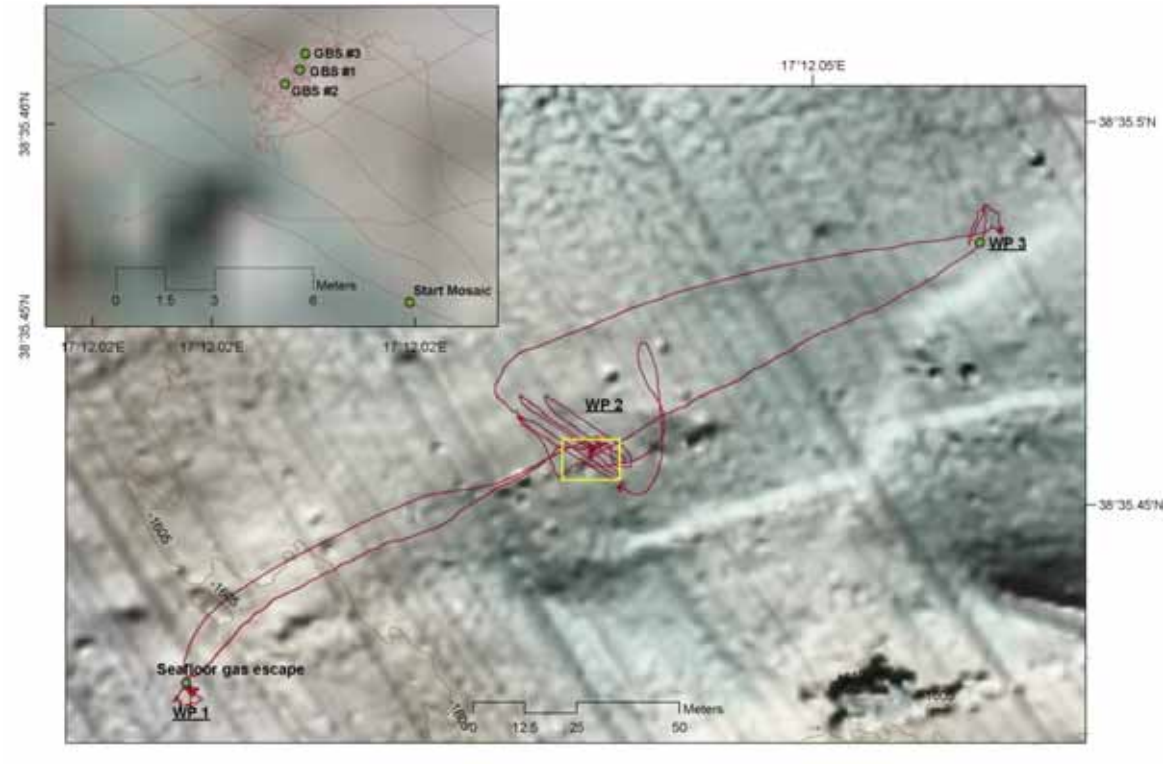

Fig. 68: Map of the dive track that started and ended in the southwest of the surveyed area (WP 1, likely origin of Flare 4) at the southern edge of the Venere MV. Positions of WP 2 (likely origin of Flare 5) and WP 3 ('backscatter patch') are highlighted as well. Yellow rectangle: Position of the close-up map.

Shortly after having reached the seafloor at WP 1 that was supposed to be located at the origin of Flare 4, a confined seafloor elevation of about 0.5 m in height and 3 to 4 m in diameter was

discovered (Fig. 69 left). At the foot of the mound-like structure a conspicuous concentric arrangement of clam shells was present. Patches of comparably thin, whitish microbial mats existed in its summit area and were likely indicators of upward fluid migration.

Fig. 69: Left: Seafloor photograph of the mound-like structure in the area where WP 1 (likely origin of Flare 4) was located. Note the patchy coverage by whitish microbial mats and the concentric arrangement of clam shells. Right: Seafloor photograph of the mound-like structure at WP 2 (likely origin of Flare 5). Note the patchy coverage by whitish microbial mats and the concentric arrangement of clam shells resembling that observed at WP 1 (left).

However, neither active seafloor gas bubble escape nor seafloor features (such as cracks or holes in the seafloor) pointing to gas seepage in the recent past from this site was found. In addition, outcropping massive authigenic carbonates did not become apparent. Sea urchins that likely grazed seep-associated microorganisms were present in comparably high density. After evaluation the structure dimensions by use of the laser lights the surrounding environment was inspected. An isolated bush of tubeworms diagnostic for significant fluid upward migration towards the seafloor was found about two meters NE of the mound and shells of dead clams were widely distributed on the seafloor. A few meters to the NE a subcircular cm-wide crack striking (sub)-parallel to the boundaries of the seafloor elevation and partially settled by whitish microorganisms was found. Gas bubbles escaping the crack were recorded with the ROV cameras and the sonar and dimensions of the crack were determined by use of the laser lights. While heading for about 120 m to the NE towards WP 2 (Fig. 68) strongly bioturbated hemipelagic sediment occasionally covered by isolated whitish microbial mats was observed. Additionally, the coverage by clam shells was less dense than that recognized close to WP 1.

Close to WP 2, the likely originating area of Flare 5, a network of seafloor cracks settled by whitish microorganisms was found. A few meters closer to the position of WP 2 tubes of dead tube worms rooting below a dislocated carbonate pavement became apparent.

At WP 2 a seafloor elevation about 1.0 m in height and 5-6 m in diameter was found (Fig. 69 right). Similar to the structure found at WP 1 whitish microbial mats existed in the summit area of the mound, while clams shells occurred accumulated at the foot of the structure. However, in contrast to the structure at WP 1 massive authigenic carbonates were exposed in the summit area. Such carbonates were fragmented and seriously dislocated (Fig. 70) potentially caused by uplift due to fluid overpressure below a former carbonate seal. Gas bubbles escaped regularly the seafloor through the respective crack. Moreover, live pogonophorans and clams were found to thrive close to

the bubble emission site (Fig. 70 left). In the surrounding of the mound sea urchins were recognized in comparably high density.

Fig. 70 Left: Close up of the bubble emission site of the mound-like structure at WP 2. Live tubeworms and clams rooted below the dislocated carbonate and stuck in the sediment, respectively, while attached white microbial tissues were waving in the water column. Right: Collection of a fragmented carbonate with the manipulator claw while measuring the in situ temperature with the T-stick (T measurement 1).

A sample of the gas discharged into the water column was collected by use of the Gas Bubble Sampler (GBS 1). For measurement of the in situ temperature with the T-stick close to the bubble emission site, several attempts were needed since the seafloor penetration was seriously hampered by resistant material. The final successful penetration (Figs. 70 right and 71) caused significant gas release from the seafloor. During the measurement two carbonate samples (1 and 2) and a push core (R1) were collected from the summit area. Those activities caused strong gas bubble ebullition from the seafloor. Because the push core tube was filled by a small sediment volume only, the material was removed and push core R1 was re-used at another site on top of the mound. However, during extraction of the push core from the sediment a greater sediment portion was lost again.

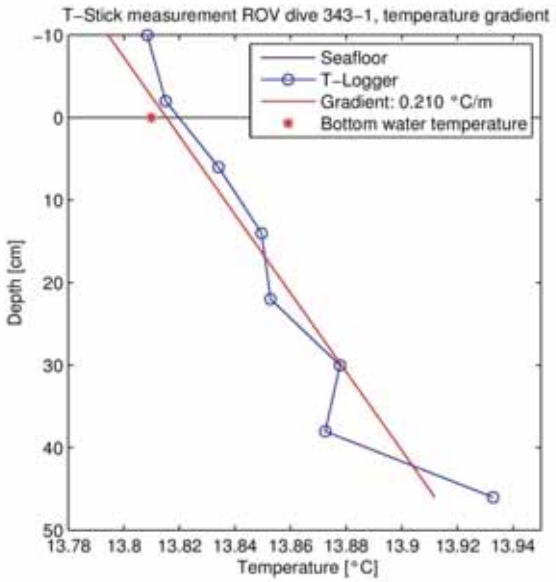

Fig. 71: Temperature measurement with the T-stick (1) close to the bubble emission site at WP 2 revealed a mean temperature gradient of ca. 0.21°C/m.

A near-bottom water sample was taken with the GBS (2) about 2 m above the mound top for analysis of dissolved methane concentrations. Finally, a marker (2) was placed on the ground for rapid recognition of the site during subsequent activities and dives. During passage from WP 2 to WP

3 (high backscatter area) with a heading of about 60° for ca. 40 m seafloor features pointing to fluid seepage did not become apparent. The seafloor consisted of bioturbated hemipelagic sediment sparsely covered by clam shells.

At WP 3 spatially confined patches of whitish microbial mats were found on the seafloor (Fig. 72 left). With regard to the relatively high seafloor backscatter intensity recorded during AUV dives, the area was explored for more pronounced indications of fluid seepage such as authigenic carbonates, or seep-associated clams and tubeworms. However, only assemblages of clam shells and few sea urchins that were also found at WP 1 and WP 2 during the dive were found in the surrounding area. It was therefore decided to move back to the microbial mats for detailed photo documentation (Fig. 72 right) and sampling.

Fig. 72: Left: Seafloor photograph of patchy microbial mats in the area of WP 3. Right: Detailed image of the microbial mat found at WP 3.

The T-stick was deployed within the microbial mat (2) and about 1 m distant to it (3; Fig. 73). During the respective measurements one push core each (R2 and R3) were taken close to the site of temperature measurement.

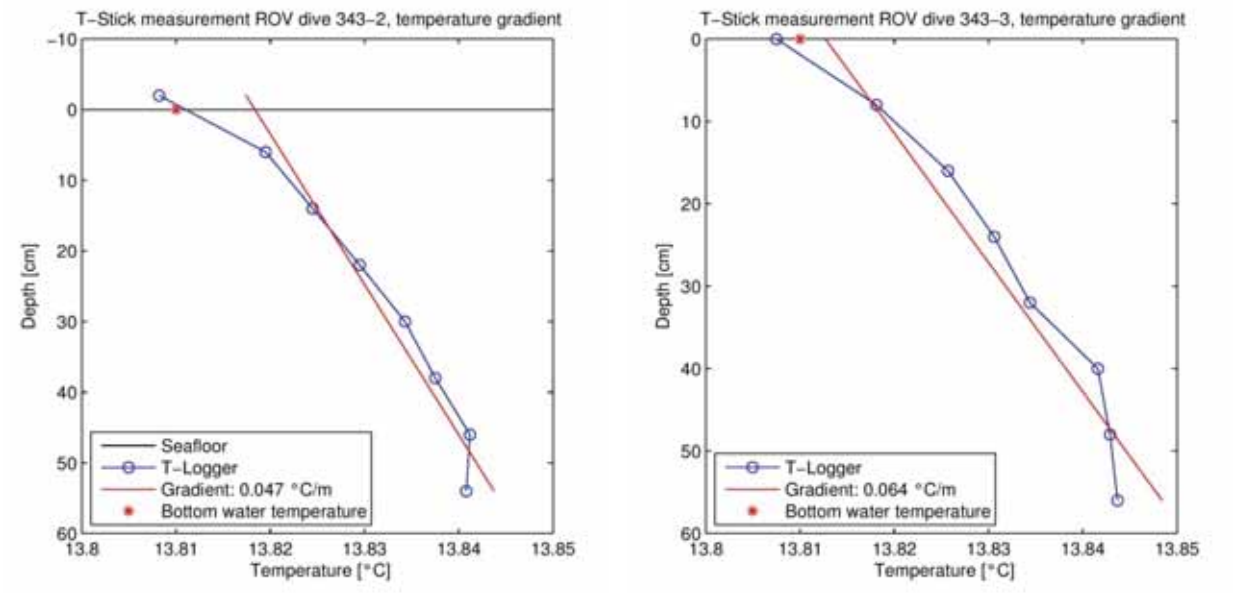

Fig. 73: Left: T-stick measurement (2) at WP 3; mean gradient of 0.047 °C/m below microbial mat. Right: T-stick measurement (3) at WP 3; mean gradient of 0.064 °C/m about 1 m distant to the microbial mat.

Finally, QUEST was moved back to WP 2 using a track positioned north of that followed during the earlier transfer from WP 2 to WP 3. Having approached WP 2 again, preparations for a seafloor photo mosaicking across the mound-like structure and surroundings by use of the Prosilica camera were

started. QUEST was finally moved with a velocity of 0.1 m/s and at an altitude of 1 m along six parallel track lines of 28 m in length each with a track distance of 1.5 m (Fig. 74 left). The track heading was set to 303° and the duration of the entire mosaicking station was about 35 mins. After an additional near-bottom water sample has been taken with a GBS (3) QUEST was moved back to WP 1. Similar to the strategy used for the return from WP 3 to WP 2 a track north of the forward run was chosen.

Fig. 74: Left: Plan view on the summit area of the mound-like structure at WP 2. Image taken during the photo mosaicking experiment with the Prosilica camera. Pogonophorans root below the fragmented carbonates. Area of bubble escape and former T-stick measurement highlighted by red circle. Dimensions of brick on the seafloor as part of the Marker 2 ca. 11 x 11 cm. Right: Deployment of the shovel used for potential detachment of gas hydrates

At WP1 two push cores (R4 for pore water sampling; 18 for analysis of volatiles etc.) were taken from an area between the patchy microbial mats on top and the accumulation of dead shells at the foot of the mound-like structure. Furthermore, a temperature measurement with the T-stick was conducted on top of the structure. However, because of very resistant material in the subseafloor the penetration of the tool was strongly hampered, so that several temperature loggers remained in the water column during the measurement. During penetration gas bubbles were escaping the seafloor. Remarkably, subangular whitish pieces were detached from the seafloor during tool penetration and extraction. The turbulent rise behaviour and comparably high ascending velocity of these pieces resembled those of gas hydrates investigated during former QUEST dives in other regions.

Several attempts with two push core tubes were made to obtain a sediment core from the top of the structure (station GeoB19240-18). However, either the core was too short because of restricted sediment penetration during the sampling procedure and/or the residual unconsolidated sediment was lost during transfer from the sampling site to the core container on QUEST.

In order to verify the potential presence of gas hydrates at this site it was decided to dig with the shovel designed for QUEST to improve the accessibility of deeper sediments (Fig. 74 right). During deployment of the shovel that lasted for about 15 mins, deposits as deep as about 20 cm below seafloor were excavated. During this procedure gas bubbles in significant amounts and very few pieces of whitish consolidated material were released. However, partially due to high sediment load in the water column caused by the sediment disturbance and/or the comparably small size of rising particles the presence of hydrates at this site remained unproven. Following this activity the dive was ended.

8.2.8 Dive 344 (Station 1255-1 , GeoB: 19242-1)

Area:	**Venere Mud Volcano; western summit**
Responsible scientist:	Daniel Präg
Date:	Monday 01 December 2014
Start bottom time (UTC):	08:44
End bottom time (UTC):	16:37
Bottom time:	07:21
Start bottom (Lat/Long/depth):	38°36.453'N, 17°11.243'E, 1500 m
End bottom (Lat/Long/depth):	38°36.453'N, 17°11.233'E, 1496 m

Points of interest:

WP 1:	38°36.452'N	17°11.249'E	Starting point on the seafloor
WP 2:	38°36.488'N	17°11.249'E	northern boundary of the flow
WP 3:	38°36.477'N	17°11.311'E	Flare 3a
WP 3corr	38°36.448'N	17°11.305'E	Flare 3a corrected
WP4:	38°36.412'N	17°11.278'E	Flare 3b

Key results:

The dive investigated the outflow center and fresh mud flows at the western summit of Venere Mud Volcano, acquiring photomosaic imagery, temperature measurements, bottom water samples at different heights above seabed and push-cores. Older mud flows with a bioturbated hemipelagic cover were distinguished from younger ones with an irregular, broken surface, consisting of soft mud with a tissue-like yellowish veneer. Bubbles were seen to rise from the mud at the outflow center when the ROV lifted off. Five T stick measurements in and next to the outflow center revealed gradients of up to 15.3° C/m.

Technical description:

There were no serious technical issues. The WP3 position provided for Flare 3a was in error, the correct position was substituted in the Global Mapper project. The sonar operated throughout the dive, but the data was not recorded. There was insufficient storage space for the Prosilica camera images, resulting in the loss of the last line of the summit mosaic, and no recording of images on the ensuing transit down the fresh mud flow. The ROV telemetry systems had to be reset several times, each time resulting in a brief loss of stability.

Table 18: Samples and measurements taken during Dive 344.

GeoB:	Instrument	UTC Start	UTC End	Position	Depth	Comment
19242-2	Mosaic	08:35	09:35	38°36.456 N, 17°11.245 E to 38°36.450 N, 17°11.237	1501 m to 1501 m	Transect of mud flows from S to N, and from N to S along a parallel line 15 m to the west
19242-3	Mosaic	09:54	11:09	38°36.453 N, 17°11.218 E to 38°36.460 N, 17°11.234	1499 m to 1500 m	Mosaic of outflow centre, 13 W-E lines 1.5 m apart
19242-4	T-stick 1	11:42	11:57	38°36.453 N, 17°11.223 E	1499 m	At top of outflow centre, soft seds (T stick sinks)

19242-5	GBS	11:47	11:49	38°36.453 N, 17°11.223 E	1499 m	GBS-2 (blue) - bottom waters
19242-6	Push core R5	11:55	11:57	38°36.453 N, 17°11.223 E	1499 m	Fresh mud flows at outflow centre, close to T stick
19242-7	T-stick 2	12:06	12:15	38°36.453 N, 17°11.223 E	1499 m	In depression next to outflow centre
19242-8	T-stick 3	12:48	13:06	38°36.456 N, 17°11.220 E	1500 m	Outside main outflow centre
19242-9	Mosaic	13:52	14:24	38°36.442 N, 17°11.297 E to 38°36.441 N, 17°11.291 E	1509 m to 1509 m	Transect of mud flows NE-SW (1st transect SW-NE Atlas did not record)
19242-10	Push core R6	14:47	14:50	38°36.463 N, 17°11.247 E	1502 m	North of youngest mud flow - hemipelagic drape?
19242-11	Push core R7	14:57	15:02	38°36.460 N, 17°11.243 E	1502 m	Paired with PC-15
19242-12	Push core 15	15:00	15:02	38°36.460 N, 17°11.243 E	1501 m	For volatiles, paired with PC-R7
19242-13	T-stick 4	15:29	15:39	38°36.454 N, 17°11.225 E	1499 m	Outflow centre, 2-3 m from summit
19242-14	Push core R8	15:30	15:34	38°36.454 N, 17°11.225 E	1499 m	As above, close to T-stick, paired with PC-16
19242-15	Push core R16	15:31	15:36	38°36.454 N, 17°11.225 E	1499 m	As above, close to T-stick, paired with PC-R8
19242-16	T-Stick 5	15:59	16:09	38°36.457 N, 17°11.226 E	1500 m	Outflow centre, 10 m from summit
19242-17	Push core R9	16:02	16:07	38°36.457 N, 17°11.226 E	1500 m	As above, close to T stick, sediment in core compresses
19242-18	Push core 17	16:04	16:04	38°36.457 N, 17°11.226 E	1500 m	As above, paired with PC-R9
19242-19	GBS	16:23	16:25	38°36.453 N, 17°11.223 E	1497 m	GBS-1 (yellow), 2 m above seafloor
19242-20	GBS	16:29	16:31	38°36.453 N, 17°11.223 E	1496 m	GBS-4 (yellow), 3 m above seafloor

Dive description

The objective of Dive 344 was to characterize a series of fresh mud outflows from the western summit of Venere Mud Volcano, which AUV data show begin at a small (<10 m wide) dome-like feature on the summit at 1499 m (Fig. 75) and extend 1.6 km to the base of the mud volcanic cone at 1600 m. The dive examined the mud flows over the upper 150 m of their length (Fig. 75), corresponding to the upper 10 m in depth below the summit (1499-1509 m). A secondary objective of the dive was to search for gas bubbles from the mud outflows, at a site 150 m from the summit detected by EM122 data (WP3corr, Fig. 75).

The dive began with a pair of N-S mosaic lines 15 m apart (GeoB19242-2), run transversely across the subparallel mud flows within 50 m of the summit (Fig. 75). As noted during Dive 342, the freshest mud flow, referred to as the 'highway', was easily recognizable from straight borders about 2 m apart and a rough surface (Fig. 76). Progressively older mud flows to either side changed from slightly less rough areas with a yellowish colour, to smooth areas of bioturbated hemipelagic sediment in the north (Fig. 76). Only a few possible clasts were observed. The ROV moved upslope to the outflow center along the 'highway', its surface becoming rougher near the summit with the appearance of

many broken plates that fit together (Fig. 77). The outflow center is an elongate amphitheatre about 2 m wide and <1 m in relief, formed by the borders of the 'highway' rising and curving around to meet behind the highest point (Fig. 77). A photomosaic was made of a 20 x 30 km area covering the summit, along 13 W-E lines 1.5 km apart (Fig. 75). During the mosaic acquisition, older mud flows outside the center were seen to have a yellowish discoloration (Fig. 78). Older flow lineations were seen to extend NW from the center (i.e. in the opposite direction of the present outflow) and curve around to flow east parallel to the 'highway' to the west and north beyond these flows was an area of chaotic relief with many visible clasts.

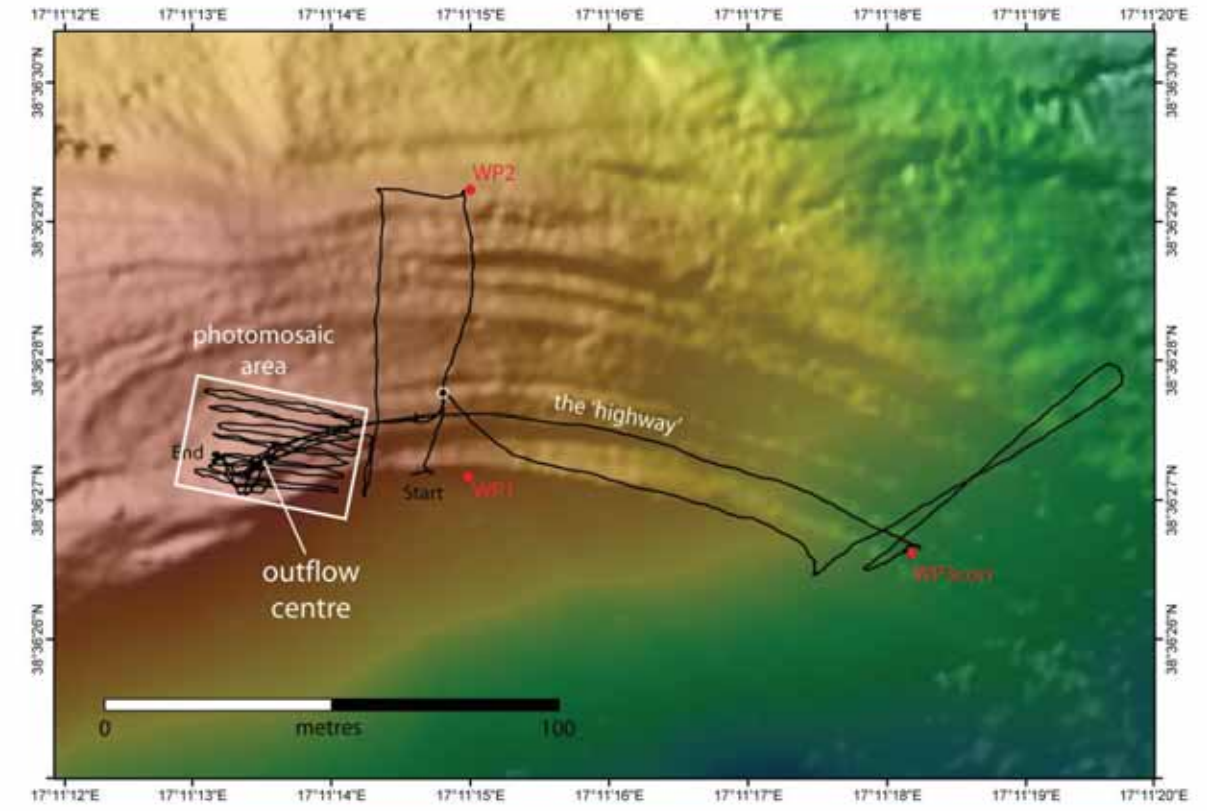

Fig. 75: Map of the dive track at the summit of the western cone of Venere mud volcano (black line – USBL positions). Sampling was mainly done within the photomosaic area on and next to the outflow centre (T sticks, push-cores, GBS water samples), save one push-core (white circle) taken next to the freshest mud flow, referred to as the 'highway'.

At the summit, the ROV landed on the top of the outflow center and acquired a T stick measurement, push core and GBS sample of bottom waters. The mud flow was fissured (Fig. 79), yet very soft, the T stick sinking slightly when released; on recovery the T stick was used to probe two nearby clast-like features, which consisted of soft, easily disaggregated mud. When the ROV rose to change position, several bubbles rose into the water column. A second T stick was deployed in the depression at the head of the outflow center, close to the first measurement, and a third T-stick 5 m north outside the outflow center, in an area of older flow lineations. The seabed in the latter area was observed to be covered by a yellowish tissue-like film; in addition, tiny circling animals were observed just above seabed, as had been seen near gas flare 5 during Dive 343. A panorama of Scorpio photos of the mud flows was taken (images 3392-3398).

The ROV then left the summit, following the curving 'highway' downslope to the east and then southeast, recording with the HD camera. The mud flow was observed to change in character

downslope; in the first 50 m, where it is a positive feature (convex in profile) separated by a depression from the elevated borders, it contained transverse ridges, perhaps due to compression; at greater distance, where the mud flow becomes a negative (channel-like) feature, transverse ridges were no longer observed. At a distance of 150 m the ROV stopped, and moved SW to run a mosaic line transversely across the mud flows, and across the location of a gas flare site observed on EM122 data (WP3corr, Fig. 75). The Prosilica camera did not record, so a second transect was run 5 m to the SE (GeoB19242-9). No gas bubbles were observed on the sonar.

The ROV then moved back towards the summit to acquire samples for geochemical analyses. On the way, a push core was taken just north of the 'highway' in what were thought to be older flows, but the core appeared to contain only greyish mud (Fig. 76). At the summit, paired push cores (one for pore waters, one for volatiles and porosity) were taken on the fresh mud flows at two sites: the first site 2-3 m below the landing site occupied earlier in the dive, the second site another 10 m downslope. T stick measurements were taken at both sites. At the last site, two GBS samples were taken of bottom waters at 2 m and 3 m above seabed, to obtain a high resolution water column profile to complement CTD data.

The total of five T stick measurements made at the summit during the dive proved to be remarkable. All four in the upper 10-15 m of the outflow center recorded increases of up to 8 degrees over the 60 cm length of the T stick, corresponding to gradients of 14.4-15.3° C/m (Fig. 80); the third measurement taken adjacent to the outflow center was slightly lower at 5° C/m. At all sites temperatures in each thermometer increased over time, such that equilibrium had still not been reached at the end of the measuring period (Fig. 80).

Fig. 76: Seabed photos across subparallel mud flows of differing characters. Left: freshest mud flow - the 'highway' - near outflow centre (view upslope) where it has positive relief, flanked by a depression, note irregular surface with large plates (Scorpio 11-13-25). Right: the 'highway' downslope from the summit (view downslope) where it has flat to negative relief, flanked by tractor-like tracks (Scorpio 13-32-49).

Fig. 77: Left: next mud flow to north of the 'highway', at location of push-core R6 (GeoB19242-10), note yellowish discoloration (Scorpio 14-46-56); Right: fourth mud flow to north of the 'highway', with bioturbated hemipelagic cover (Zeus 09-08-03).

Fig. 78: Summit of Venere Mud Volcano. Left: outflow centre, with crab, note broken plate-like surface of fresh mud outflow (Scorpio 09-47-26). Right: side view of outflow centre from the south, showing bordering depression and outer rim (Scorpio 11-26-58).

Fig. 79: Seabed photos of area around outflow centre at summit of Venere Mud Volcano. Left: older mud flows south of outflow centre, note yellowish discoloration (Scorpio 13-32-49).Right: older mud flows NW of outflow centre, note irregular relief in background (Scorpio 09-47-55).

Fig. 80: Seabed photos of area around outflow centre at summit of Venere mud volcano. Left: detail of irregular relief beyond mud flows, note exposed clasts (Scorpio 09-51-56). Right: T stick measurement in mud flows seen in b, note yellowish discoloration (Scorpio 12-52-47.

Fig. 81: Summit of Venere Mud Volcano. Left: side view of outflow centre, showing border depression and outer rim (Scorpio 11-26-58), arrows indicate locations of T stick sites, note crab at right. Right: T stick and push-core site on mud flow near crab, note fractures and mud clasts (Scorpio 11-55-54).

Fig. 82: Summit of Venere Mud Volcano. Left: bubbles in water column when ROV lifted to shift position (Zeus 12-01-58). Right: T stick measurement in depression (Scorpio 01 12-05-13).

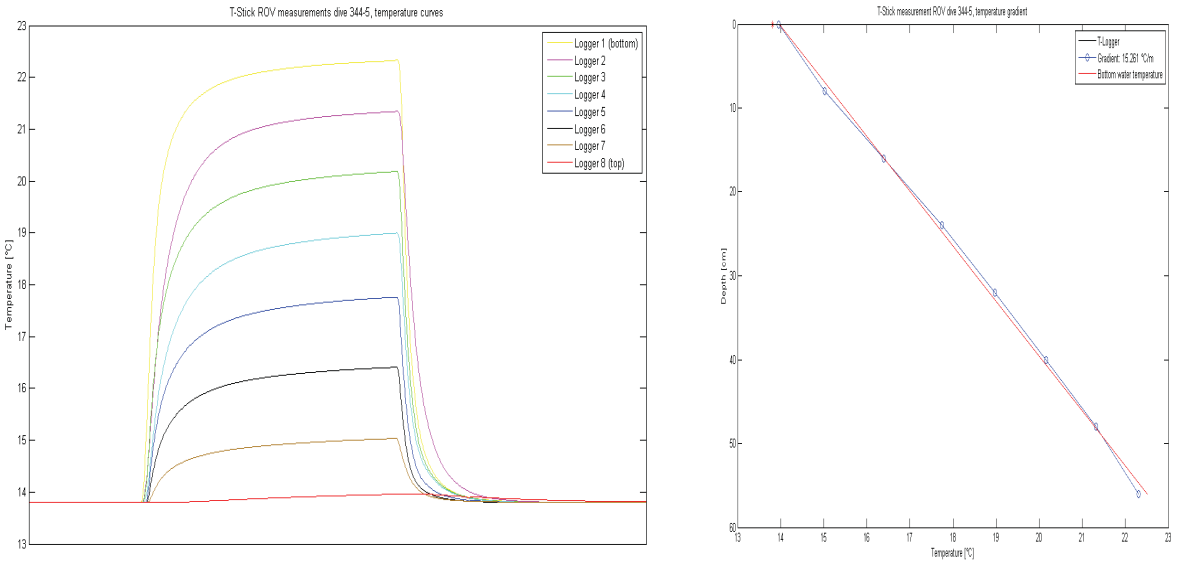

Fig. 83: Example of T stick measurement from the summit of Venere Mud Volcano, showing a gradient of over 15° C/m, note lack of evidence for advective flow; the time series at left shows that none of the thermometers heated to equilibrium during the measurement.

8.2.9 Dive 345 (Station 1262-1, GeoB: 19249-1)

Area:	**Venere Mud Volcano, Flare 4+5**
Responsible scientist:	Marta Torres
Date:	Wednesday 03 December 2014
Start bottom time (UTC):	15:44
End bottom time (UTC):	19:17
Bottom time:	03:33
Start bottom (Lat/Long/depth):	38°35.457'N, 17°12.016'E, 1605 m
End bottom (Lat/Long/depth):	38°35.426'N, 17°11.958'E, 1606 m

Points of interest:

WP 1:	38°35.457'N	17°12.021'E	(Marker 2)
WP 2:	38°35.428'N	17°11.969'E	
WP 3:	38°35.416'N	17°11.935'E	

Key results:

Successful deployment of the ASSMO sonar observatory and T-stick, to record 24 hours of bubble and temperature changes at Flare 5 (Marker 2). Bubble quantification at this location. Exploration of area west of Marker 2 and discovery of bubble streams at location of Flare 4, where Marker 3 was deployed, gas sampling and quantification of the flare as well as temperature measurements and push core sampling.

Technical description:

Dive was delayed because of problems with the data archiving system of the ROV. CTD on vehicle was not working during this dive. ROV sonar was also not operational. At the end of the dive, Scorpio was also not operational.

Table 19: Samples and measurements taken during Dive 345**.**

GeoB:	Instrument	UTC Start	UTC End	Position	Depth	Comment
19249-2	ASSMO	16:20	16:24	38°35.4563'N 17°12.0191'E	1607 m	Deployment of ASSMO at Marker #2
19249-3	T-Stick	16:42	16:48	38°35.4541'N 17°12.0202'E	1607 m	T-stick at Marker #2
19249-4	HD-quantification	17:16	17:37	38°35.4559'N 17°12.0212'E	1607 m	Quantification of gas stream using HD camera and 10-cm scale ROV arm and laser pointer
19249-5	Gas sampler, yellow	18:23	18:28	38°35.4287'N 17°11.9595'E	1606 m	Sampling of gas on high emission site at Flare #4. Potential hydrate forming in the funnel. HD on for quantification
19249-6	T-stick	18:34	18:42	38°35.4288'N 17°11.9595'E	1606 m	Close to bubble site, where sediments are soft
19249-7	Push core R1	18:37	18:40	38°35.4285'N 17°11.9590'E	1606 m	In proximity of bubbling site, paired with Core 15
19249-8	Push core 15	18:39	18:39	38°35.4285'N 17°11.9591'E	1606 m	In proximity of bubbling site, paired with core R1
19249-9	Marker #3	18:39	18:39	38°35.4285'N 17°11.9594'E	1606 m	At bubble stream
19249-10	T-stick	18:54	19:14	38°35.4277'N 17°11.9581'E	1605 m	Background station, ~ 5m from bubble stream on brown sediment
19249-11	Gas sampler-blue	18:57	19:02	38°35.4266'N 17°11.9579'E	1606 m	Background station, ~ 5m from bubble stream, close to the seafloor
19249-12	Push core R2	19:06	19:12	38°35.4266'N 17°11.9583'E	1606 m	Background station rhizon core paired with a core for volatiles, ~ 5m from bubble stream on brown sediment
19249-13	Push core 16	19:06	19:12	38°35.4266'N 17°11.9583'E	1606 m	Unsuccessful, sediment lost upon retrieval
19249-14	Push core 17	19:11	19:11	38°35.4266'N 17°11.9583'E	1606 m	Background station volatile core paired with a core for pore water, ~ 5m from bubble stream on brown sediment

Dive description

The main objective of the dive was to deploy the ASSMO sonar observatory coupled with a long-term (24-hour) deployment of a temperature stick on the bubble streams area demarked with Marker 2, as indicated in Figure. 84.

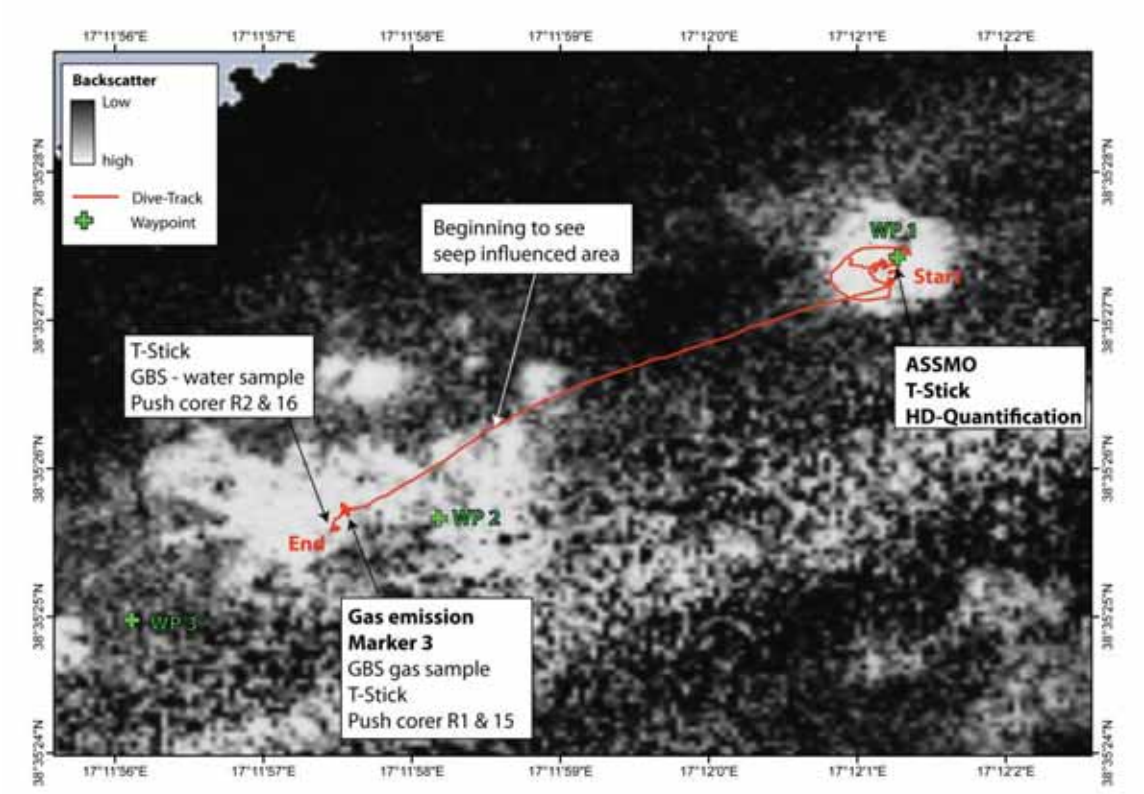

Fig. 84: Map of the area covered during Dive 345, showing locations of bubble emissions at the site of the ASSMO deployment (WP-1) and at Marker 3, a stronger gas emission site.

The deployment was very successful and the sonar and T stick are placed in an excellent position for recording (Fig. 85). Seafloor here is covered with bacterial mats, bivalve shells, tube worms and sea urchins. Bubbles emanate from the top of a broken carbonate covered mound, at intermittent streams of a few bubbles. The area is surveyed and video recorded with HD camera, as well as with the Prosilica camera. For the purpose of calibrating the sonar, gas emission quantification was undertaken, using the HD camera and the arm of the ROV that provided a 10-cm scale. Following these operations, the region surrounding Marker 2 was surveyed to determine the extent of seepage activity in relation to the backscatter map.

Fig. 85: Views of the ASSMO observatory site. Left: ASSMO deployed and positioned for bubble imaging, facing the emission site at marker #2. Right: overview of the site, with ASSMO base in the background and in front the T-stick at the bubble emission site and the foot of Marker 2. Tubeworms surround a crack in carbonate slabs and patches of clam shells on the seafloor in the background.

Upon completion of the program at Marker 2, we moved to WP2, heading 230 and keeping HD on to document the extent of each of the seep areas in relation to the backscatter map. At 18:01 we observed active bubbling, quite strong and regular at 38°35.42937'N and 17°11.96194'E. A photograph of the emitting site was taken with the lasers on. We proceeded to collect a gas sample at this site, during the collection we kept the HD camera on to allow for quantification based on the volume of gas on the gas sampler funnel, as illustrated in Fig. 86. A thin layer of hydrate was observed to form around some of the bubbles in the gas sampler funnel (Fig. 86).

Fig. 86: Left: gas bubble sampler used to estimate gas emission rate and collect a gas sample. A thin layer of hydrate is observed to form on the walls and around bubbles in the sampler. Right: push cores collected over black sediment in the vicinity of bubble streams.

At this location, we conducted two stations each included a temperature measurement, and rhizon push core for pore water sampling and a push core for volatiles, porosity and microbiology samples taken in close proximity to each other. One of the stations targeted the area very near the bubble emission site, over sediment that was clearly sulfide rich given its intense black color; the other station was ~ 5m away from the bubble streams, on top of brown sediment that did not appear influenced by seep activity (Fig. 87).

Fig. 87: Area of Marker 3. Left: location of marker 3, showing the holes after core and T-Stick removal, clearly illustrating the black sediment color. Right: core and T-stick on brown sediment.

The temperature data from both stations seems very similar, with a temperature gradient of 63°C/km and 61°C/km, and profile suggestive of an advective component (Figs. 88 and 89). The temperature distribution of these deployments show a different behaviour in the upper sensors that

do not display a decay with time following the friction pulse, and the deeper sensors that display the typical decay curve. This concluded the dive.

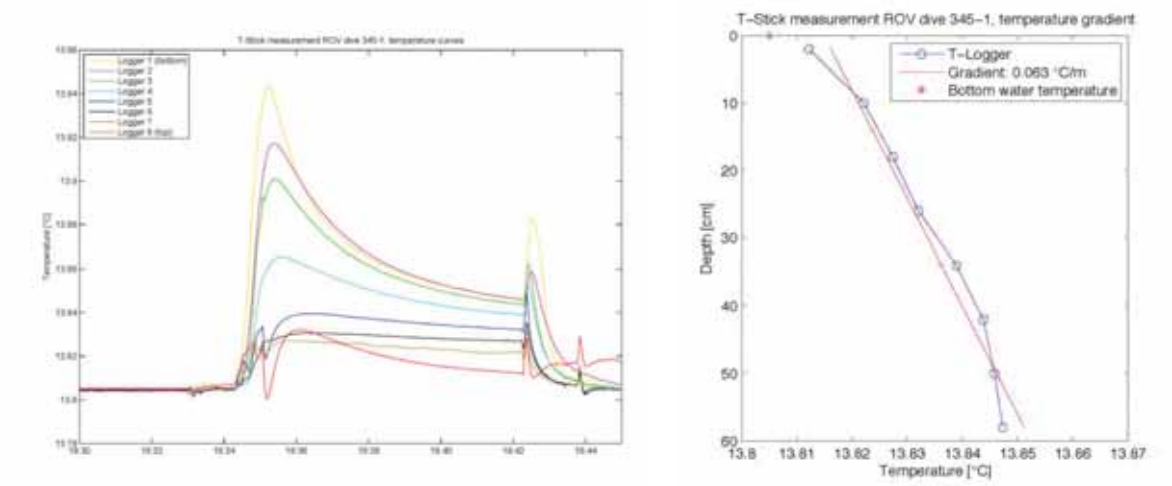

Fig. 88: Temperature data from the area in proximity to the bubble stream. Left: decay curves for the 8 sensors of the T-stick. Right: temperature-depth profile showing a temperature gradient of 63°C/km.

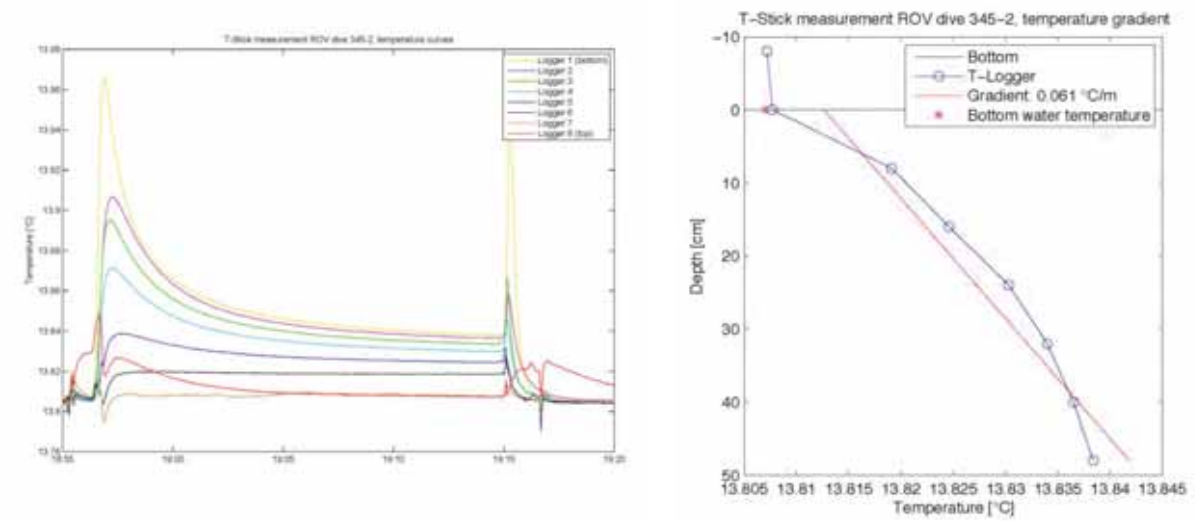

Fig. 89: Temperature data from the area ~ 5 meters away from the bubble stream. Left: decay curves for the 8 sensors of the T-stick. Right: temperature-depth profile showing a temperature gradient of 61°C/km.

8.2.10 Dive 346 (M112 Station 1265-1, GeoB: 19252-1)

Area:	**Venere Mud Volcano –Flare 4-5**	
Responsible scientist:	Miriam Römer	
Date:	Wednesday 03 November 2014	
Start bottom (UTC):	12:43	
End bottom (UTC):	19:09	
Bottom time:	6:26	
Start bottom (Lat/Long/depth):	38° 36.447’N	17°12.022’E 1605m
End bottom (Lat/Long/depth):	38° 36.457’N	17°12.020’E 1607m

Points of interest:

WP 1:	38°35.457'N	17°12.021'E	(Marker 2)
WP 2:	38°35.428'N	17°11.969'E	
WP 3:	38°35.416'N	17°11.935'E	

Key results:

Recovered the ASSMO and the T-Stick installed at Marker 2 after 24 hours. Explored the area of Flare 4 and found a circular collapse structure.

Technical description:

The forward looking sonar (Kongsberg) could not be installed on the ROV successfully for the dive and was not available to search for gas emissions. The Prosilica (downward looking photo-camera) did not save the images due to a storage problem determined after the dive.

Table 20: Samples and measurements taken during Dive 346.

GeoB	Instrument	UTC Start	UTC End	Position	Depth	Comment
19252-2	HD-Quantification	13:04	13:14	38° 35.4580' N 17° 12.0225' E	1607 m	At Marker 2, close to ASSMO installation
19252-3	HD-Quantification	14:15	14:20	38° 35.4293' N 17° 11.9711' E	1606 m	Bubble stream at WP2 in carbonate crack
19252-4	Carbonate sample	14:42	14:44	38° 35.4280' N 17° 11.9706' E	1606 m	From emission site at WP2, of the crack
19252-5	Bubble catcher	15:01	15:10	38° 35.4297' N 17° 11.9597' E	1606 m	Bubble stream at Marker 3
19252-6	T-Stick	15:17	15:17	38° 35.4298' N 17° 11.9602' E	1607 m	In the bubble stream, but did not penetrate
19252-7	Push corer (R1)	15:54	15:55	38° 35.4446' N 17° 11.9598' E	1607 m	North of WP2, short core, hard bottom
19252-8	GBS (blue)	15:57	15:57	38° 35.4444' N 17° 11.9595' E	1606m	North of WP2
19252-9	Push corer (R2)	16:19	16:21	38° 35.4325' N 17° 11.9436' E	1606 m	At whitish mat, lost upon retrieval
19252-10	Push corer (R3)	16:23	16:24	38° 35.4322' N 17° 11.9432' E	1605 m	At whitish mat, surface with white "crystals"
19252-11	Bubble catcher	16:26	16:30	38° 35.4323' N 17° 11.9433' E	1605 m	Whitish mat, an attempt to retrieve "crystals" again
19252-12	GBS (black)	17:15	17:15	38° 35.4280' N 17° 11.9506' E	1606 m	At collapse structure, close to bubble stream
19252-13	Net -Carbonate	17:33	17:54	38° 35.4277' N 17° 11.9504' E	1605 m	From the collapse structure
19252-14	Push corer (R4)	18:28	18:28	38° 35.4646' N 17° 12.0180' E	1607 m	At flare 5, north of Marker 2
19252-15	Push corer (18)	18:32	18:32	38° 35.4647' N 17° 12.0179' E	1607 m	At flare 5, north of Marker 2

Dive description:

The main intention of this dive was to recover the ASSMO and the T-Stick installed during Dive 345 about 24 hours before at Marker 2, the centre of Flare 5. However, the rest of the dive was dedicated to explore the area of Flare 4 just around 100 m southwest of it and to collect the installations at the end of the dive. Nevertheless, we started at Flare 5 and landed close to Marker 2 in order to prove

the gas emission activity and perform another quantification of the gas bubble stream close to the ASSMO, which would hopefully record still at the same time. This may allow later to correlate the estimated gas flux to the backscatter intensity recorded in the sonar scans. The same gas bubble stream as the day before was found, which was still pulsing. Just as a rough impression, we noticed that the pulsing frequency seems to be slightly higher than the day before during Dive 345. Afterwards we moved around the area and determined the northern, eastern and southern boundary of the seep area. We did not observe any further bubble emission but saw patchy distributed dark patches with whitish material, where we decided to take push corers at the end of the dive just before recovering the installations.

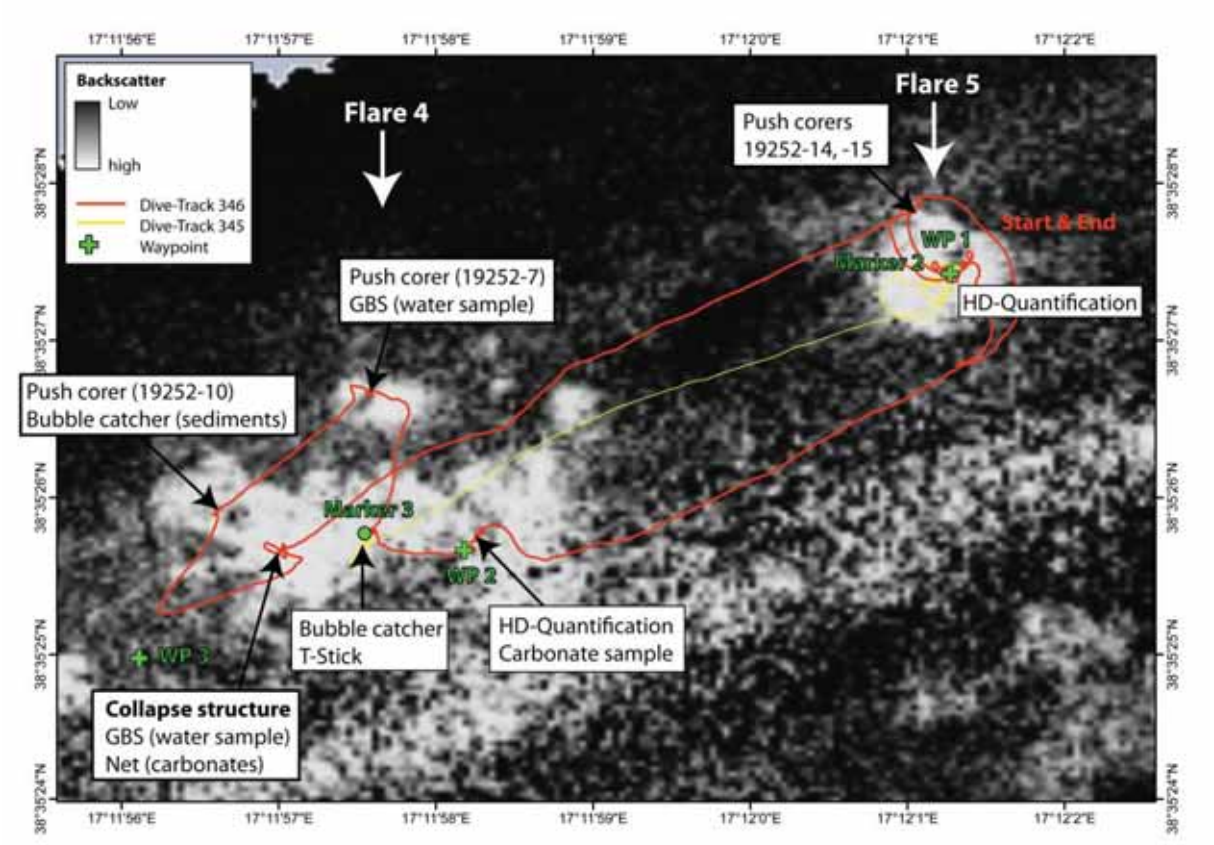

Fig. 90: Map of the dive track (red=Dive346). Flare 5 was both start and end of the dive. The seep areas of Flare 4 and 5 become clearly visible by high backscatter.

Before sampling Flare 5, we moved to Flare 4 along a line south of track of Dive 345 and reached WP2, where we found the bubble stream back detected during Dive 343. The bubbles emit through a crack in a carbonate pavement. The extent of the carbonates is not visible as the surface is covered by a sediment layer. A short documentation for flux quantification was performed and a piece of carbonate was broken from the crack and sampled.

Next stop was at Marker 3, deployed during Dive 345 at a steadily pulsing gas bubble emission. Due to the pulsing nature of the bubble stream, we performed a quantification using the bubble catcher instead of a visual scaling of single bubbles. It took ~9 minutes to fill about half a litre volume in the bubble catcher. Furthermore, the T-Stick was tried to place within the bubble stream, but the subsurface seemed to be hard in ~20 cm depth. After the second try the T-Stick was bended and could not be used for the rest of the dive and the measurement was not useful for interpretation. The following 1,5 hours of the dive was dedicated to investigate and explore the surrounding and

boundaries at Flare 4 and to search for further gas emission sites forming the hydroacoustic flare. The seep influenced area ended already about 15 m north of Marker 3.

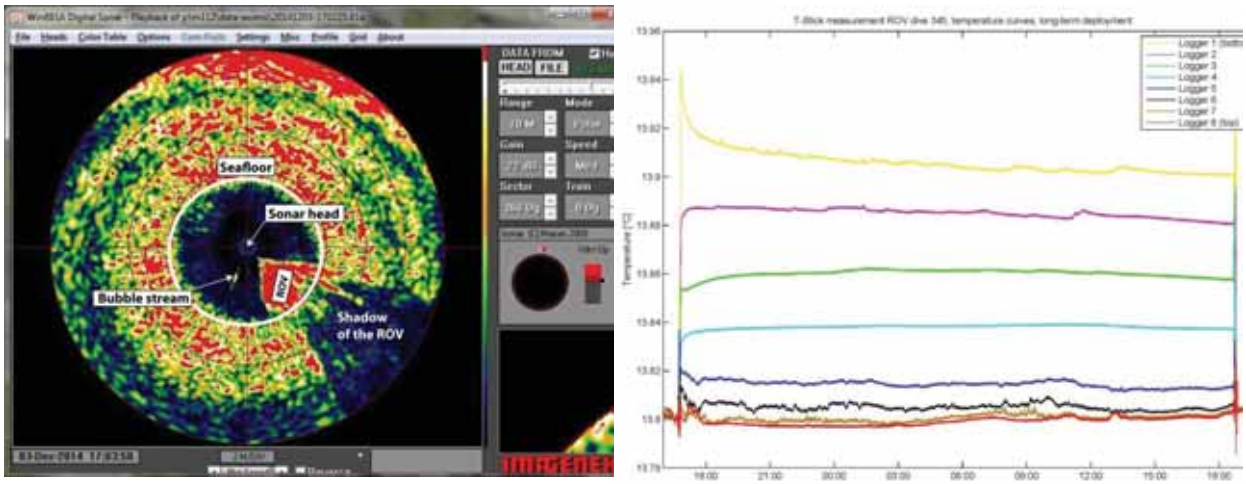

Fig 91: Left: sonar echogram during visual quantification of the bubble stream at Marker 2. Right: temperature curves during the ~24-hours deployment at Marker 2.

Turning in direction to WP3, we passed an area with dark patches, bacterial mats and surrounded by rims of clam shells. In that habitat we took a push core and filled the GBS with bottom water. The push corer could not penetrate entirely, indicating some hard material in the subbottom. Heading further southwest to WP3, another area with dark spots and whitish surface material was observed and sampled with two push corers. In order to collect the whitish material for analyses, the bubble catcher was used to sample the surface sediments. On-board observations suggest rather an organic origin than a precipitate. We reached the western boundary of the seep influenced area close to WP3 and headed back in a parallel line to the northeast. The elevated area already recognized in the background when sampling at Marker 3 was crossed and a collapse structure was detected on top of it. It is approximately 2 to 2.5 m diameter wide and has a several tens of centimetres deep depression. Several blocks of thick carbonate crusts lie within the depression. White bacterial mats cover parts in and around the structure. And a pulsing gas bubble emission was observed at the rim of the collapse structure. A bottom water sample was taken with a GBS and two blocks of carbonate could be grabbed using the manipulator and a net. Three parallel lines were flying over the structure that might be used for a small mosaic, but unfortunately the Prosilica did not record the pictures.

Fig. 92: Left: bubble stream quantification at Marker 2 (Flare 5). Right: Crack at the seafloor at Flare 4 with pulsing bubble escape.

The last part of the dive was finally moving back to Flare 5 (in a northern parallel track). Two push corers were taken north of Marker 2 in a dark spot with white surface material. As observed in the areas sampled with push corers, the penetration was just half of the depth of the core due to a hard resistant layer in the subbottom. Finally, the T-Stick and the ASSMO were recovered before ending the dive successfully.

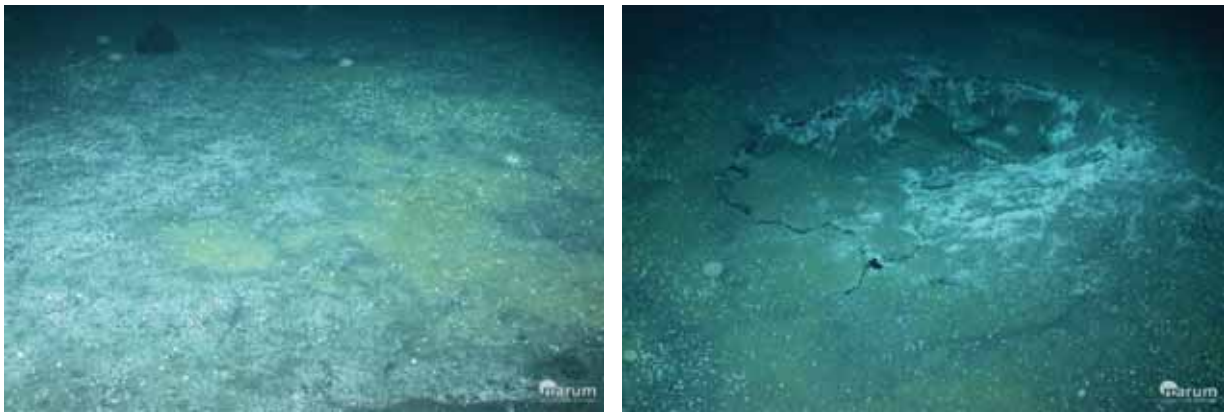

Fig. 93: Left: bacterial mats north of Marker 3 (Flare 4). Right: collapse structure at Flare 4.

8.2.11 Dive 347 (Station 1266-1, GeoB: 19253-1)

Area:	**Cetus Mud Volcano**
Responsible scientist:	Gerhard Bohrmann
Date:	Friday 5 December 2014
Start bottom (UTC):	10:55
End bottom (UTC):	17:32
Bottom time:	06:37
Start bottom (Lat/Long/Depth):	37°53.120'N, 17°27.751'E, 2267 m
End bottom (Lat/Long/Depth):	37°52.753'N, 17°27.768'E, 2233 m

Points of interest:

WP1:	37°53.123'N	17°27.747'E	Starting point, north of the caldera
WP2:	37°52.786'N	17°27.733'E	Center top
WP3:	37°52.606'N	17°27.728'E	Elevation, southern part of caldera
WP4:	37°52.794'N	17°28.260'E	Eastern mud outflow

Key results:

The dive on Cetus Mud Volcano clearly showed that in the central caldera no recent mud flow exists. The seafloor explored along the track was everywhere covered by pelagic sediments. A series of T-stick measurements show a higher heat flow in the center of the caldera which might document the proximity to the chimney in the mud volcano.

Technical description:

During this dive there was a hardware failure in the DVR system of the ROV. The failure was found after the dive, and all video recordings as well as the minifilms of the cameras were not stored. The only optical documentations are the images of the Scorpio and Prosilica cameras. As during other dives the forward looking sonar was not operational.

Tab. 21: Samples and measurements taken during Dive 347.

GeoB	Instrument	UTC start	UTC end	Position	Depth (m)	Remarks
19253-2	T-stick	11:12	11:22	37°53.116'N 17°27.744'E	2268	Outside the caldera
19253-3	T-stick	11:42	11:50	37°53.073'N 17°27.745'E	2243	On the rim
19253-4	T-stick	12:13	12:20	37°53.017'N 17°27.742'E	2250	In the ring depression
19253-5	T-stick	12:44	12:54	37°52.961'N 17°27.742'E	2243	On the mud flow
19253-6	T-stick	13:16	13:26	37°52.917'N 17°27.740'E	2239	Second T-stick on the mud flow
19253-7	T-stick	13:57	14:04	37°52.971'N 17°27.738'E	2236	T-stick in the area of higher backscatter
19253-8	T-stick	14:19	14:29	37°52.832'N 17°27.737'E	2231	
19253-9	Net	14:26		37°52.832'N 17°27.737'E	2231	Bunches of unknown animals
19253-10	T-stick	15:06		37°52.809'N 17°27.736'E	2231	
19253-11	GBS	15:08	15:11	37°52.809'N 17°27.736'E	2231	Water samples with the blue GBS
19253-12	Push core R7	15:15	15:16	37°52.809'N 17°27.736'E	2231	Ca. 1 m from the T-stick
19253-13	T-stick	15:30	15:42	37°52.786'N 17°27.735'E	2232	
19253-14	T-stick	15:56	16:06	37°52.768'N 17°27.733'E	2232	
19253-15	T-stick	16:16	16:25	37°52.754'N 17°27.734'E	2234	Southernmost station of profile
19253-16	T-stick	17:17	17:27	37°52.754'N 17°27.768'E	2234	Station to the east

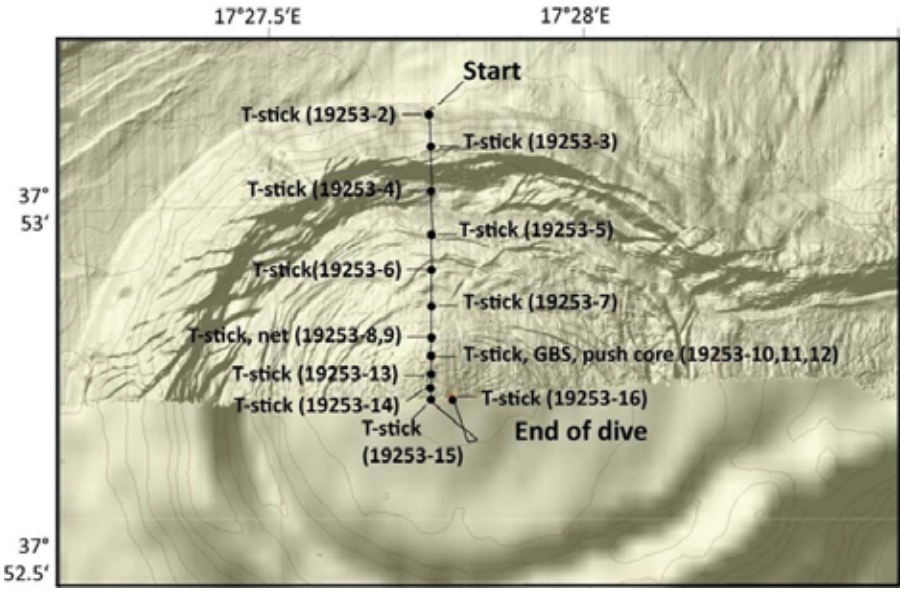

Fig. 94: Locations of sampling (GeoB numbers) on Cetus mud volcano during ROV Dive 347 on Friday 5 December. The northern part of the map shows the micro-bathymetry of the the AUV dive and the southern part is shown by EM112 data from the hull-mounted system of the R/V METEOR.

Dive description:

During the dive a north to south oriented observation profile was acquired along an approximately distance of 650 m (Fig.94). A clearly defined caldera structure of around 1200 m in diameter was well mapped during the Circee cruise on R/V Le Suroit in 2013 (Gutscher et al., 2013) which showed on its eastern side a ca. 400 m broad outflow. Several east to west oriented mud flow ridges are clearly connected to the mud flow activity of Cetus MV. Dive 66 of AUV SEAL 5000 mapped the micro-bathymetry of the northern half of the structure which is combined with ship's bathymetry measured during M112 in Fig. 94. The dive started at its deepest point at the foot of the ring wall which surrounds the central caldera of Cetus MV (Fig. 94), where the first T-stick measurement was performed. We ascended ~25 m height over the outer and shallower flank of the ring wall up to the rim and a further T-stick measurement (GeoB19254-3) was performed as well as in the inner ring depression (GeoB19254-4) after we descended around the steeper inner flank of the ring wall around 13 m. From this inner ring we headed over the other rise in seafloor morphology of about 10 m and did the next T-stick measurement (GeoB19254-5). From this site to the center of the mud volcano there was a continuously small rise in morphology of about 15 m over a distance of 350 m. Further 7 T-stick measurements were performed in much closer distances when coming closer to the summit of the structure.

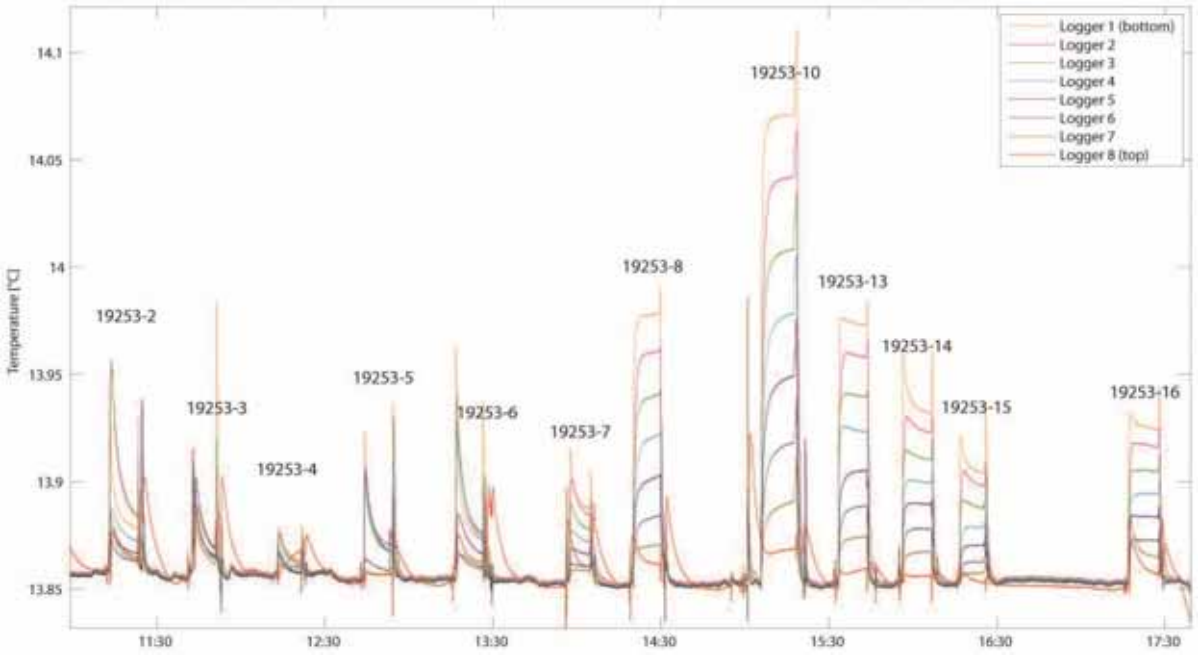

Fig. 95: Twelve temperature measurements acquired by T-stick deployments during ROV Dive 347 on Cetus Mud Volcano. For location of the GeoB numbers see Fig. 94.

Along the track we found a deviation in depths between the map and the ROV. The map gave depth information which was 16 to 25 m deeper than the depth of the pressure sensor of the ROV. The temperature measurements itself along this track showed clearly normal heat flow of around 0.024 – 0.035°C/m at the outer part of the caldera structure between Sites GeoB19253-2 and -6. A slightly increased heat flow of 0.051 °C/m was recognized at Site GeoB19254-7 just above a distinct ridge of 1.5 m (Fig. 95) and indicates may be the rim of the sub-recent mud flow activity on the summit. Six temperature measurements close and around the summit show heat flow values of 0.091 – 0.212° C/m (GeoB 19253-8, -13, -14, -15, -16) with the highest value of 0.363° C/m at Site GeoB19253-10 which seems to represent the location of the chimney of the mud volcano. Although

we recognized micro-morphological changes in seafloor bathymetry which we assign to former mud flow activities we observed on more or less most of the seafloor surface fine grained pelagic sediments and bioturbation traces throughout. On flanks of ridges we seldom could see clasts from mud breccia, however, the ridges itself were almost covered by pelagic or hemipelagic deposits. This observation clearly shows that Cetus Mud Volcano was not active recently. During the time when the T-stick measurement at Site GeoB19253-8 was performed we observed the seafloor using the HD-camera in high resolution. Several specimen of an unknown animal forming tree-like bunches were observed and sampled with a net (GeoB19253-9). Unfortunately these small animals have not been found anymore in the sediments which came onboard by net with the ROV. Furthermore at Site GeoB19253-12 a push core was taken and a water sample using the blue GBS was taken (GeoB19253-11) at the location where the highest high flow was measured (GeoB19253-10; Fig. 94).

8.2.12 Dive 348 (Station 1268-1, GeoB: 19255-1)

Area:	**Nikolaus Mud Volcano**
Responsible scientist:	Daniel Präg
Date:	Saturday 06 December 2014
Start bottom time (UTC):	12:06
End bottom time (UTC):	18:11
Bottom time:	06:05
Start bottom (Lat/Long/depth):	37°49.003, 17°58.231, 2676 m
End bottom (Lat/Long/depth):	37°48.776, 17°58.110, 2680 m

Points of interest:

WP1:	37°49.000'N	17°58.232'E	Starting point on rim of crater
WP2:	37°48.812'N	17°58.111'E	within the crater
WP2corr:	37°48.912'N	17°58.111'E	within the crater, corrected
WP3	37°48.842'N	17°58.023'E	western rim of crater
WP4:	38°48.887'N	17°58.131'E	deepest point of crater
WP5	38°48.813'N	17°58.125'E	southern rim of crater (col)

Key results:

This exploratory dive found evidence of past extrusive activity within the 300 m wide crater at the summit of Nikolaus Mud Volcano, the deepest part of which contained a field of rounded to elongate mounds locally up to 1.5 m high, consistent with mud flows buried beneath hemipelagic sediments. GBS samples of bottom waters from the crater and its rim contained significant quantities of methane. The seabed everywhere consisted of hemipelagic sediments, in places with semi-lithified mud clasts and carpets of diatoms.

Technical description:

The Prosilica camera system did not work so no photos were acquired.

Table 22: Samples and measurements taken during Dive 348.

GeoB:	Instrument	UTC Start	UTC End	Position	Depth	Comment
19255-2	TS-1	12:46	12:57	37°48.996 N 17°58.232 E	2677 m	Close to WP 1, soft sediments
19255-3	NT (red)	12:54	12:56	37°48.996 N 17°58.232 E	2677 m	Red net; clast next to T-stick
19255-4	PC-R6	13:03	13:05	37°48.996 N 17°58.232 E	2677 m	PC-R6, next to T-stick, not penetrating entirely
19255-5	GBS	13:11	13:11	37°48.996 N 17°58.232 E	2677 m	GBS-2 (blue) with water, at same location
19255-6	TS-2	15:04	15:15	37°48.896 N 17°58.131 E	2692 m	On a mound structure in center of crater
19255-7	PC-R5	15:08	15:13	37°48.895 N 17°58.131 E	2692 m	PC-R5, close to T-stick
19255-8	PC-19	15:10	15:12	37°48.896 N 17°58.132 E	2692 m	PC-19, paired with PC-R5
19255-9	NT (blue)	15:35	15:39	37°48.895 N 17°58.126 E	2692 m	Blue net, among mounds, clasts + pteropods(?)
19255-10	GBS	16:15	16:18	37°48.885 N 17°58.113 E	2692 m	GBS-1 (yellow) of bottom water, near pteropods(?)
19255-11	NT (yellow)	16:29	16:39	37°48.885 N 17°58.114 E	2692 m	Yellow net, sample of pteropods (?) and small clasts
19255-12	TS-3	17:21	17:31	37°48.814 N 17°58.128 E	2683 m	On southern rim of crater, among pteropods(?)
19255-13	GBS	17:25	17:26	37°48.814 N 17°58.128 E	2684 m	GBS-4 (black) of bottom water, close to T-stick

Dive description

The objective of Dive 348 was to explore Nikolaus Mud Volcano, a high backscatter cone up to 1 km wide and 50 m high with a central crater 300 wide at its summit (Fig. 96). The dive crossed the highest and lowest points of the rim of the crater, and the deepest part of the crater, a total vertical relief of 25 m (Fig. 96).

The dive began on the NW rim of the crater, where the seabed was observed to consist mainly of hemipelagic sediments of low relief, with signs of bioturbation. A brownish clast or crust was observed near the landing site, 50 cm long and slab-like with a tilted surface; when an attempt was made to sample with the ROV arm, it crumbled (Fig. 97); a sample was obtained using a net, releasing a fine cloud of 'dust' that flowed slowly across the low seabed relief for several minutes (Fig. 97). The net sample confirmed the clast to be semi-lithified sediment. Next to the clast, a T-stick measurement was acquired (Fig. 97), along with a push-core (that did not penetrate completely). The ROV then moved NW to the highest point of the rim, at 2668 m, across the same type of seabed: low-relief hemipelagic sediment with occasional brownish clasts, the latter commonly slab-like and tilted. From the highest point, the ROV descended into the crater towards WP2, still across the same type of seabed, then turned SW towards the deepest point of the crater, at 2692 m (WP4).

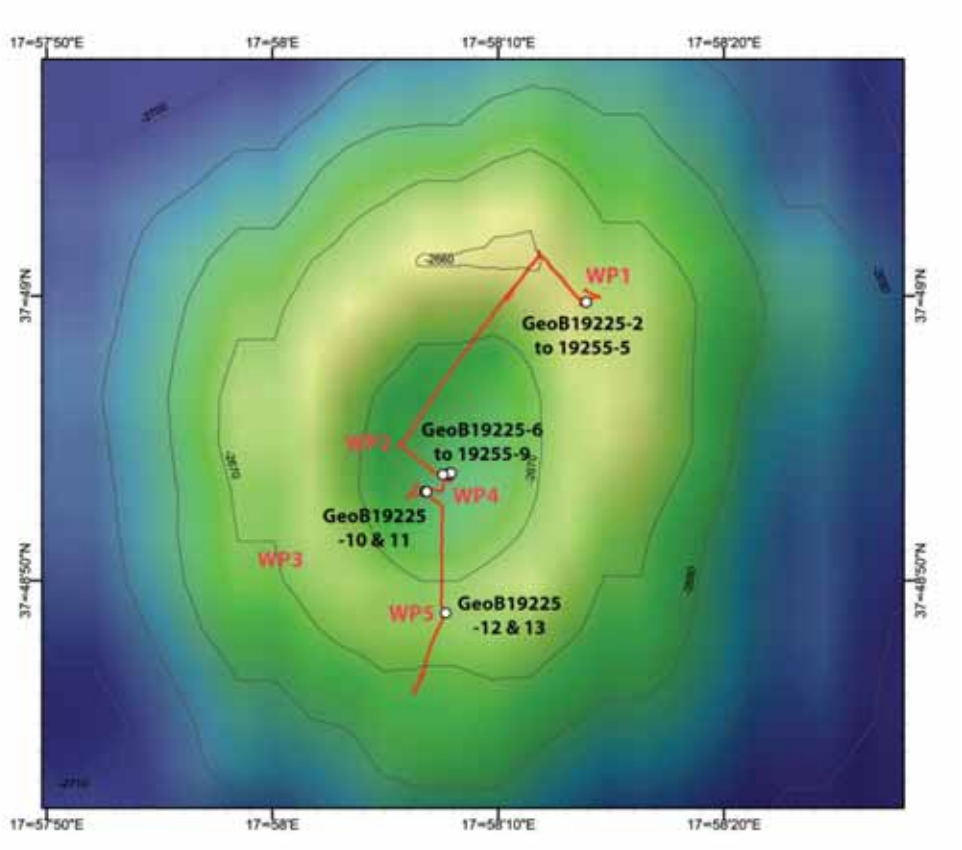

Fig. 96: Map of the dive track (red line - USBL), sampling was done at WP1, WP4 and WP5.

Near WP4 the ROV encountered an area of low (up to 50 cm) relief, with shallow depressions and small mounds, semi-circular to elongate, all draped by hemipelagic sediments (Fig. 98). The ROV landed near one of the mounds to take a T stick measurement together with a pair of push-cores (one for pore water, one for volatiles). The ROV then began to explore the extension of the mounds to the west, finding the area to be depth-limited, present below about 2690 m. Returning towards WP4, the ROV stopped to investigate another clast, which again broke when handled with the ROV arm and was sampled with a net. The ROV then made a 270° rotation, and observed larger mounds to the west: moving through them, they were seen to be equant to elongate and, estimating from the lasers, up to 1.5 m high, all draped in hemipelagic sediments (Fig. 98). The semi-lithified clasts were still present, and a beautiful bluish-white life-form was observed on top of one of them (Fig. 99). It was decided to take a GBS sample of bottom waters among the mounds nearby. This was done at a seabed depression next to one of the steep-sided mounds, which was seen to be covered with debris, thought to be pteropods, sampled using the last net (Fig. 100) and later identified as large diatoms. The ROV then moved SE and S across the mounds, which became smaller, and were no longer present above about 2690 m.

The ROV moved south, upslope towards the lowest part of the crater rim at 2680 m, across a seabed that once again consisted of low relief hemipelagic sediments. A number of elongate depressions were passed, their long axes transverse to the slope, each with tilted slab-like clasts on one or both sides, as though scoured (Fig. 97 left). The ROV arrived at the lowest point of the crater rim and on the open slope found a carpet of diatoms (Fig. 97 right). A T stick measurement was taken, and a GBS sample of bottom waters. The ROV then moved downslope across a lobate feature on the bathymetric data that could have been an old outflow from the crater, but observed only

bioturbated hemipelagic sediments. At 2686 m the dive ended; a push-core was taken for training purposes, but not given a GeoB number or retained.

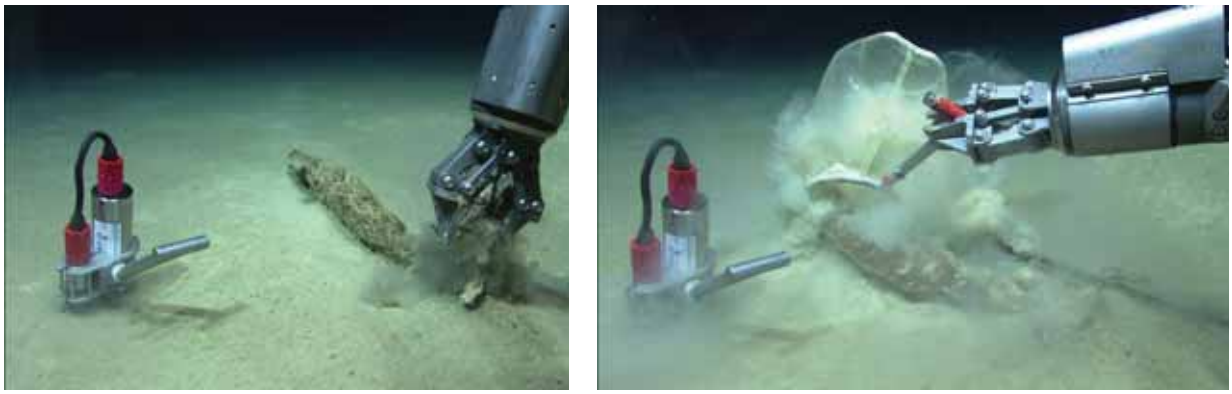

Fig. 97: Left: clast crumbling during sampling attempt with ROV arm (Zeus 12-48-37); Right: remains of clast after sampling, note cloud of 'dust' that has flowed into adjacent depression (Scorpio 12-56-12).

The temperature measurements made at three sites were non-linear and gave low or negative gradients. However, the three GBS samples of bottom waters were found to have elevated concentrations of methane, highest in the sample from the crater. Together with the buried seabed relief, this is consistent with past mud extrusion and on-going diffuse gas seepage at Nikolaus Mud Volcano.

Fig. 98: Area of mounds in deepest part of crater. Left: T stick and paired push-cores from a small mound (Zeus 15-12-06), Right: mounds over 1 m high (Zeus 15-49-07).

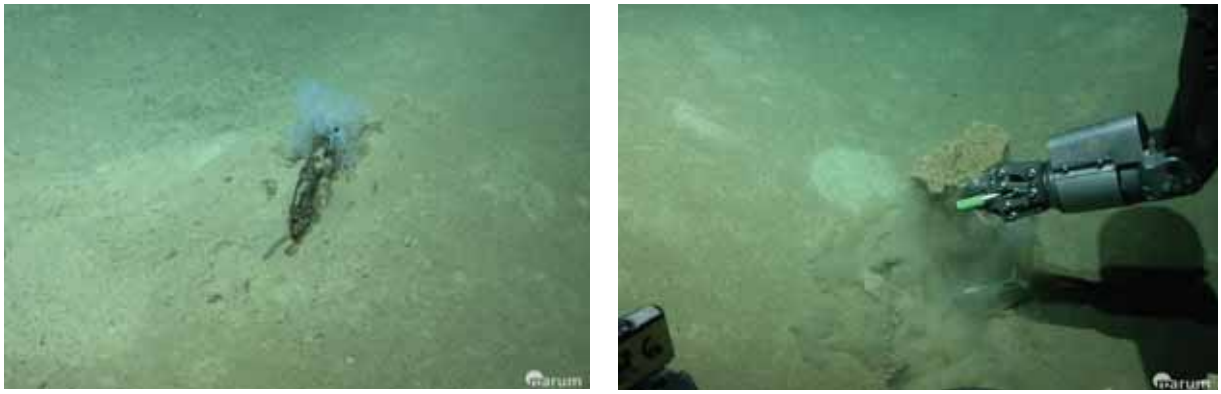

Fig. 99: Left: life on a clast (Scorpio 15-58-24); Right: close-up of debris, which sample showed to consist of diatoms and clasts (Zeus 16-11-53).

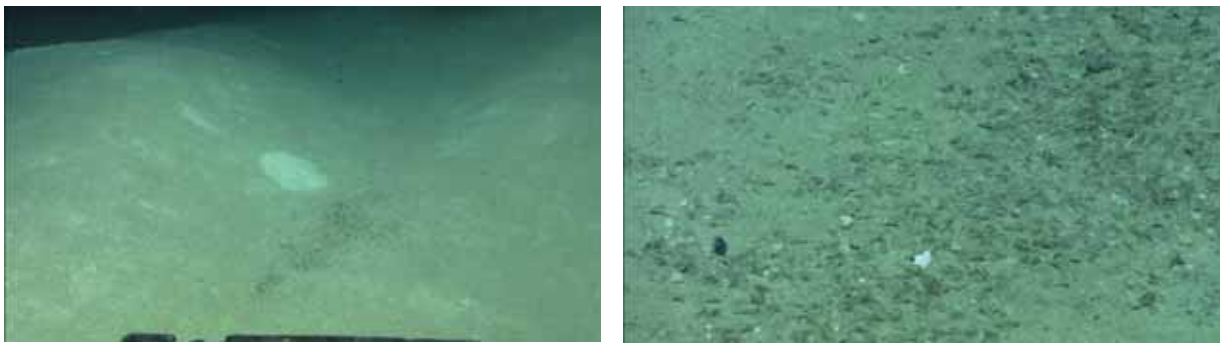

Fig. 100: Left: sampling area in depression between mounds, with debris (Zeus 16-21-38), Right: sampling using net (Scorpio 16-27-37).

Fig. 101: Left: Scour-like depression flanked by tilted clasts, on slope leading to south rim of crater (Zeus 17-03-23), Right: T-stick measurement on the south rim of the crater, within a carpet of diatoms (Zeus 17-30-54).

8.2.13 Dive 349 (Station 1258-1, GeoB: 19258-1)

Area:	**Venere Mud Volcano, Summit**
Responsible scientist:	Marta Torres
Date:	Sunday 07 December 2014
Start bottom time (UTC):	11:14
End bottom time (UTC):	18:16
Bottom time:	07:02
Start bottom (Lat/Long/depth):	38°36.3044'N, 17°11.1783'E, 1524 m
End bottom (Lat/Long/depth):	38°36.4517'N, 17°11.2170'E, 1498 m

Points of interest:

WP1:	38°36.307'N	17°11.177'E	W of mud flow
WP2:	38°36.385'N	17°11.122'E	E of mud flow
WP3:	38°36.407'N	17°11.277'E	potential flare area
WP4:	38°36.446'N	17°11.313'E	potential flare area

Key results:

A survey of the western rim indicates this to be an older flow. The center of the outflow area was also explored and seepage observations were limited to the north east flank, where bacterial mats indicate methane seepage in agreement with position of flares in the acoustic surveys. The location

of Flare 3 was investigated but no active bubbling was observed. Two mosaic surveys crossing the youngest flow were conducted to complete the mosaics across this feature. A sediment of push cores were collected along the most recent flow to investigate geochemical and microbiological evolution of the mud flow.

Technical description:
Light in the Atlas camera was not working, but there were no other technical problems during the dive, however after the last sample was successfully collected, there was a serious leakage of hydraulic fluid, which hindered closing of the sample drawer. However all samples were recovered successfully.

Table 23: Samples and measurements taken during Dive 349.

GeoB:	Instrument	UTC Start	UTC End	Position	Depth	Comment
19258-2	T-Stick	12:31	12:41	38°36.4282'N 17°11.2866'E	1514m	At bacterial mat on flank of Flare 3
19258-3	GBS blue	12:34	12:38	38°36.4285'N 17°11.2873'E	1514m	At bacterial mat on flank of Flare 3
19258-4	Push core R-4	12:38	12:41	38°36.4283'N 17°11.2872'E	1514m	At bacterial mat on flank of Flare 3
19258-5	Mosaik line 1	14:01	14:18	38°36.4411'N 17°11.3122'E	1513m	Crossing the mud flows, 70 m line towards the NE
19258-6	Mosaik line 2	14:22	14:34	38°36.4371'N 17°11.3597'E	1520m	Crossing the mud flows ~10 m SE of line 1
19258-7	Mosaik line 3	14:51	15:01	38°36.3825'N 17°11.3751'E	1526m	Crossing the mud flows at 60 degrees
19258-8	Mosaik line 4	15:07	15:21	38°36.3903'N 17°11.4135'E	1528m	Crossing the mud flows at 240 degrees, ~80 m long, ~15 m to SE of line 3.
19258-9	Push core R7	15:23	15:29	38°36.3769'N 17°11.3637'E	1526m	On the "older" mud flow west of the most recent flow, sediment apparent underneath hemipelagic cover
19258-10	T-stick	15:55	16:03	38°36.3948'N 17°11.3607'E	1525m	First of 3 stations along the most recent flow, ~ 150 m from the summit.
19258-11	Push core R8	15:57	15:59	38°36.3949'N 17°11.3609'E	1525m	Second of three stations ~140 m from the summit. Brown cover on the flow.
19258-12	Push core 3	15:59	15:59	38°36.3948'N 17°11.3607'E	1525m	Third of three stations ~150 m from the summit. Close proximity to core R8.
19258-13	T-stick	16:20	16:34	38°36.4179'N 17°11.3290'E	1519m	First of 3 stations along the most recent flow, ~ 110m from the summit.
19258-14	Push core R9	16:26	16:29	38°36.4185'N 17°11.3283'E	1520m	Second of three stations ~110 m from the summit.
19258-15	Push core 4	16:27	16:28	38°36.4186'N 17°11.3280'E	1520m	Third of three stations ~110 m from the summit. Core close to core R9.
19258-16	T-stick	17:20	17:29	38°36.4501'N 17°11.2832'E	1509m	First of 3 stations along the most recent flow, ~

						80m from the summit.
19258-17	Push core R10	17:23	17:26	38°36.4501'N 17°11.2828'E	1509m	Second of three stations ~80 m from the summit. Still brown cover on the flow. Very soft sediment
19258-18	Push core 5	17:24	17:25	38°36.4500'N 17°11.2827'E	1509m	Third of three stations ~80 m from the summit. Core for volatiles, in close proximity to core R10.
19258-19	GBS yellow	17:48	17:52	38°36.4582'N 17°11.2338'E	1501m	~10 meters from the summit along the most recent flow, ~0.5 m above seafloor
19258-20	GBS black	18:04	18:07	38°36.4523'N 17°11.2165'E	1498m	At the summit, site of most recent flow, ~0.5 m above seafloor

Dive description

The main objective of the dive was to explore the mud flows near the summit of Venere, including flows to the west, and to sample gas at Flare 3; however, the sonar data prior to the dive indicated Flare 3 not to be active. Transect and station locations are shown in Fig. 102.

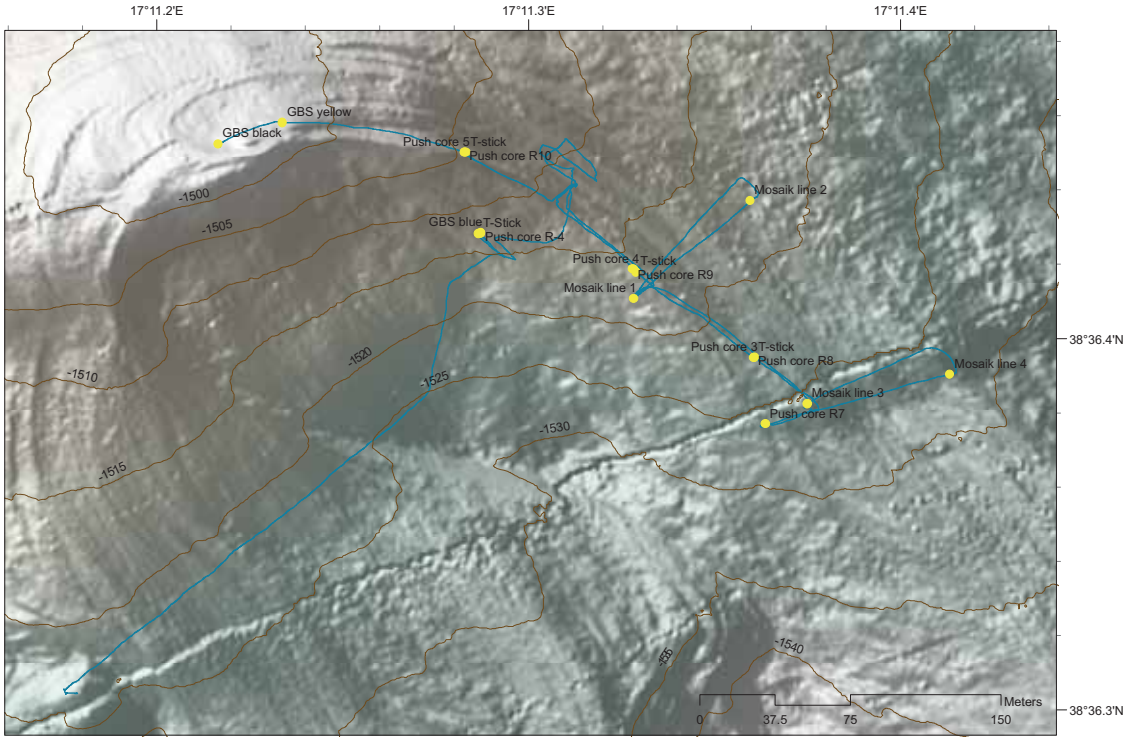

Fig. 102: Map of the area covered during Dive 348, showing locations of mosaik transects and sampling stations.

The beginning of the dive was set to explore the mud flow to the west of the summit to evaluate whether there was any indication of recent activity. A transect from west to east was undertaken to explore the characteristics of the seafloor, taking photo documentation along the way. The seafloor appeared highly bioturbated, with some variations in topography, but always showed a cover of pelagic sediment indicative of an older mud flow activity. There is a small escarpment at the NE

portion of the flow, which corresponds to the depth increase in the bathymetric map. Continuing across the caldera, bioturbation is significantly decreased and no evidence of flow.

As the vehicle approached the SE flank of the caldera, an increase in bioturbation is observed, followed by the appearance of some bacterial mat and black sediment patches indicative of seepage activity, along a fracture observed in the backscatter data (Fig. 103). The elongated area of bacterial mat coverage is estimated to be 15 to 20 meters long. This region corresponds to observations of flares in the Seabeam and Parasound surveys, however no gas emissions were observed from the ROV. The seep area was sampled with coring, temperature probe and bottom water sample were collected with the GBS.

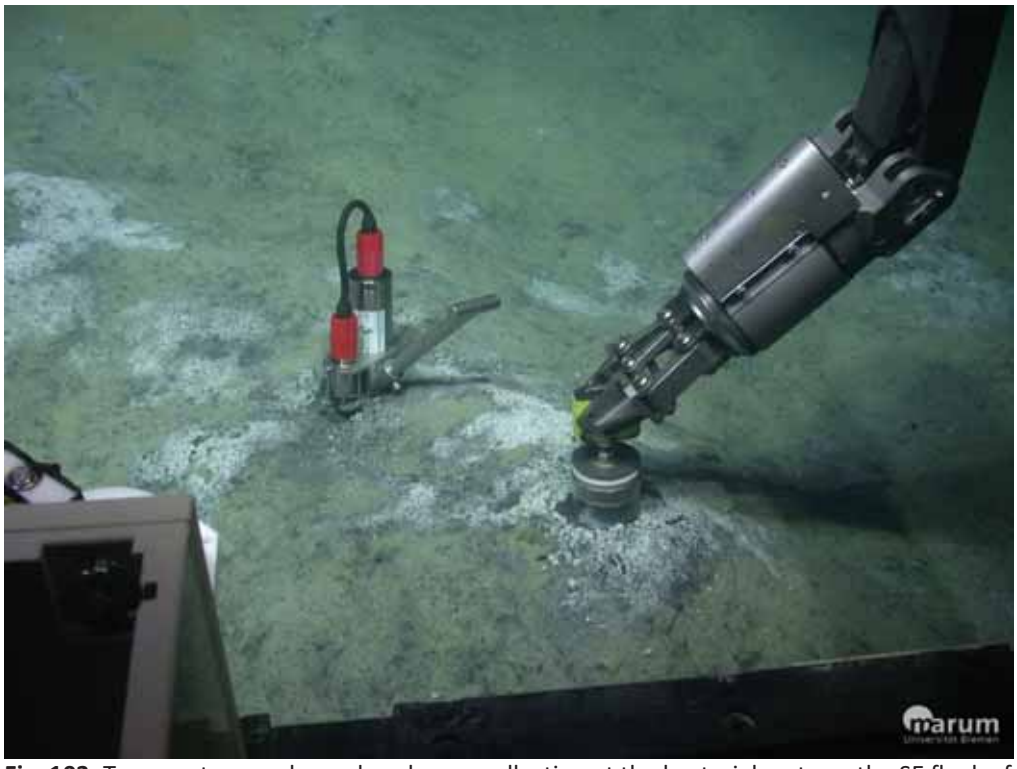

Fig. 103: Temperature probe and push core collection at the bacterial mats on the SE flank of the caldera.

The dive continued with a survey on the most recent mud flow in the area of Flare 3, in an effort to locate the gas emission on the seafloor. No bubbles were observed, and the mud flow is surveyed in this area with a photomosaic along two 70 m lines across the flow, separated by about 10 meters. Another 2-line crossing of the flow was conducted, ~80 m SE, in the region that lies at the edge of the AUV map, which may help bridge the AUV and shipboard datasets. These crossings were about 80 m in length, we mapped a well-defined edge of the flow towards the NE, but towards the SW the flows apparently continue towards the center, and beyond the mosaic line.

Upon completion of the mosaics, a series of three stations were conducted within the most recent flow, to obtain sediments and temperature profiles in a transect towards the summit. In each of these stations we deployed the T-stick and collected two cores: one for rhizon extraction of the fluids and another for analyses of volatiles, porosity and microbiology. A second survey of the around WP4 was undertaken to again look for bubbling activity in the area of Flare 3, but no bubbling activity was observed.

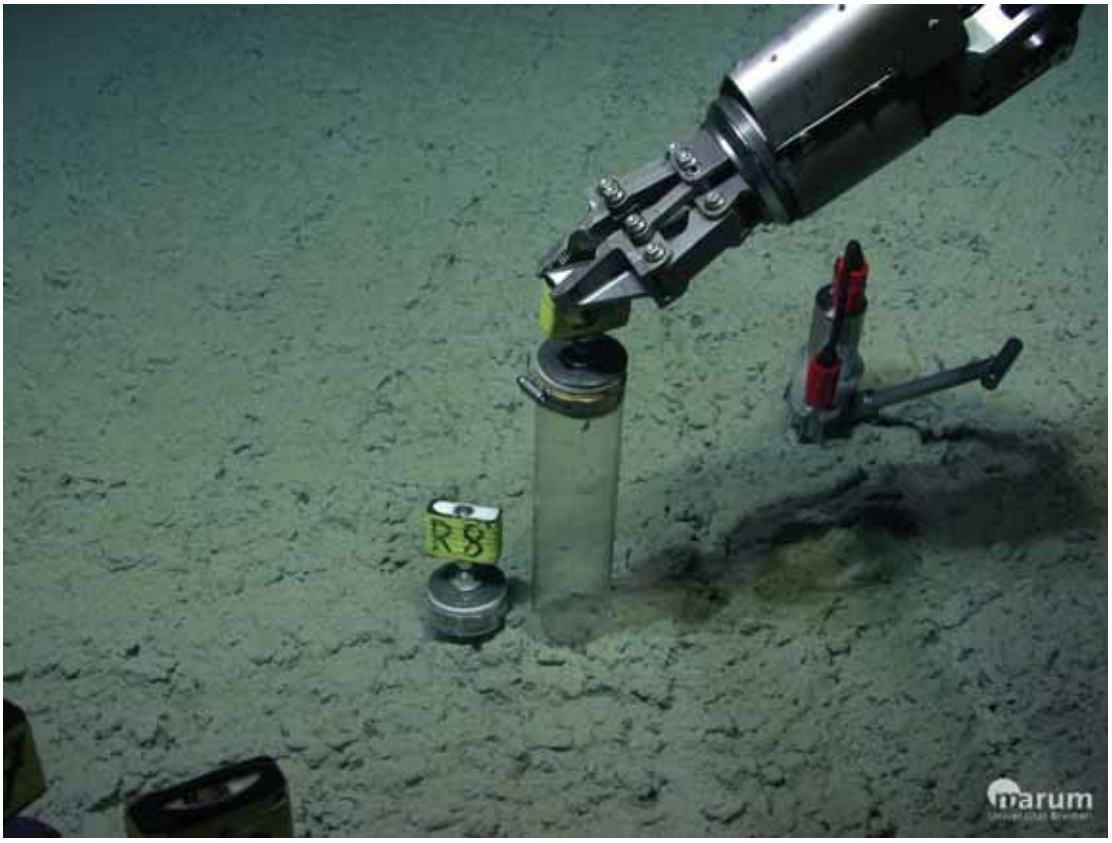

Fig. 104: Station with temperature probe and a pair of push cores, all collected in near proximity within the most recent flow at ~150 m away from the summit.

The dive concluded with the retrieval of two water samples ~0.5 meters above the seafloor, located 10 m from the summit and at the summit proper.

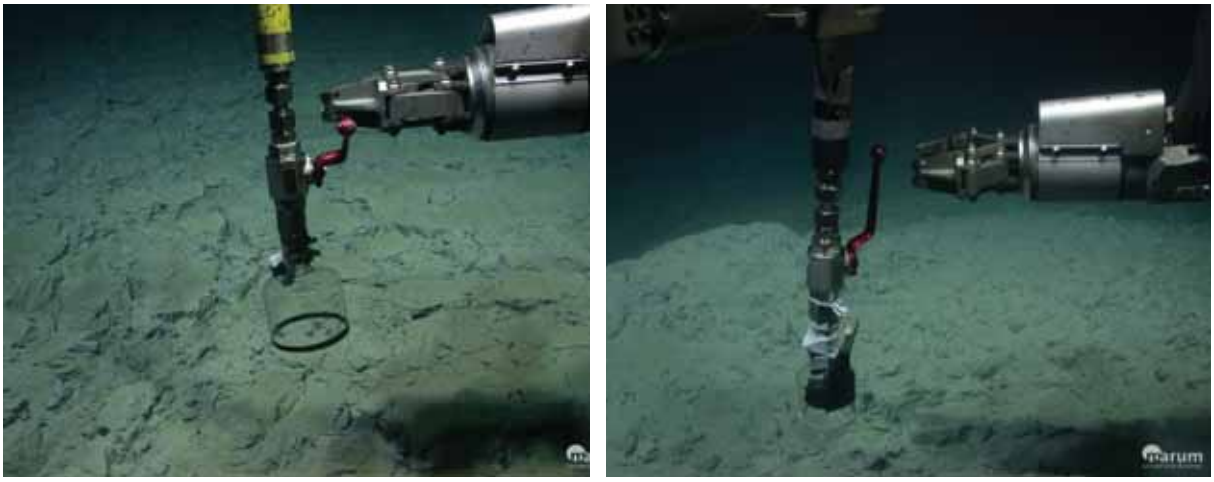

Fig. 105: Bottom water collection using the GBS at ~0.5 m above the seafloor Left: Station 10 m away from the summit, already showing a brownish sediment cover. Right: Station at the summit.

The temperature profiles and temperature gradient of the 4 stations collected during this dive is shown in Figs. 106 to 109. The temperature gradient in the NE flank of the caldera is already elevated relative to background, showing a value of 130° C/km. Within the most recent flow; however, are much higher temperatures, with a maximum value of 5453° C/km measured at the station 80 meters from the summit, the other stations in the flow are also elevated with values of 4820° C/km and 5453° C/km.

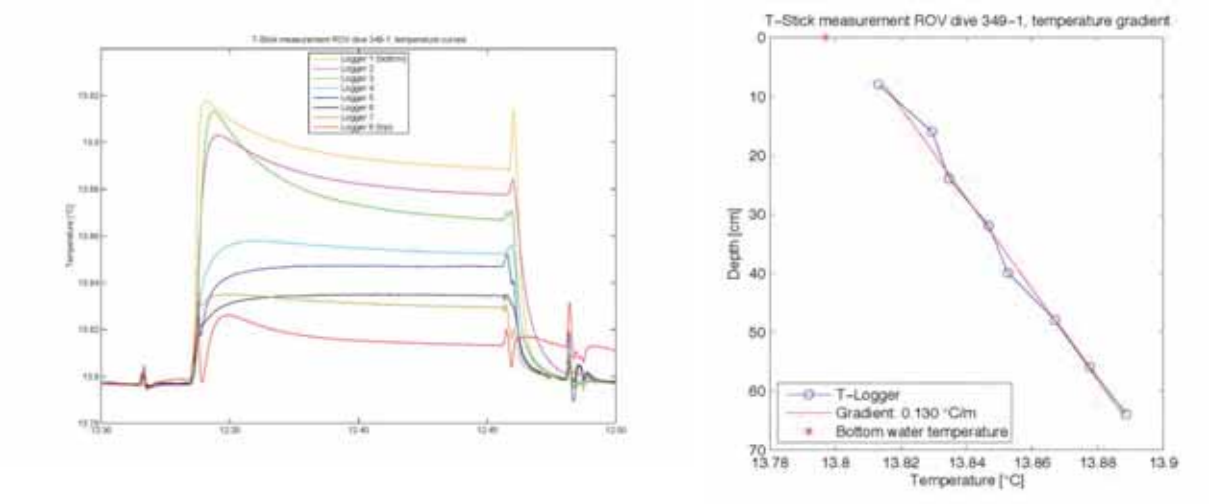

Fig. 106: Temperature data from the area in seep area on the eastern flank of the volcano. Left: decay curves for the 8 sensors of the T-stick. Right: temperature-depth profile showing a temperature gradient of 130° C/km.

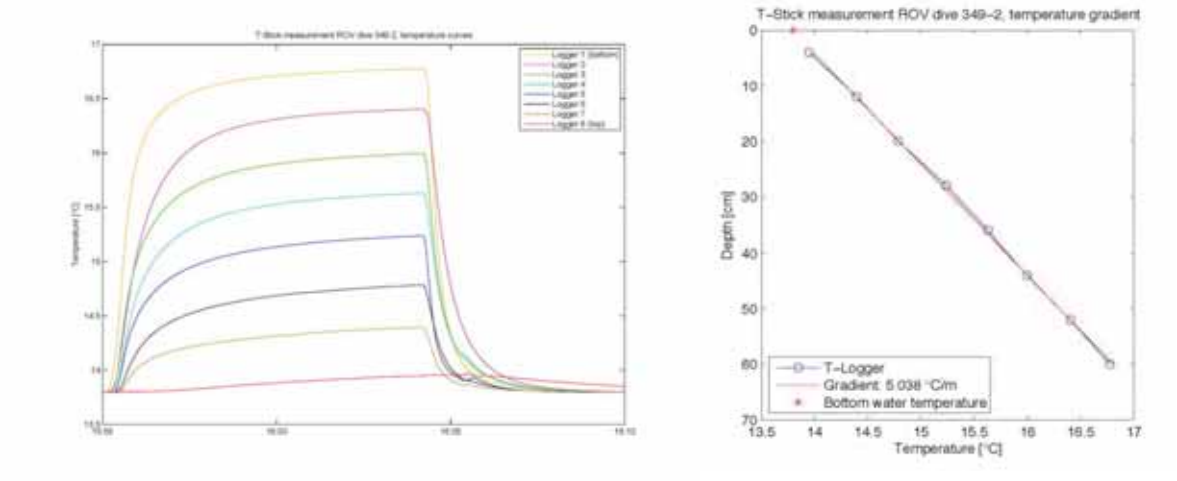

Fig. 107: Temperature data from the area ~ 150 meters away from the Venere Mud Volcano summit. Left: decay curves for the 8 sensors of the T-stick. Right: temperature-depth profile showing a temperature gradient of 5038° C/km.

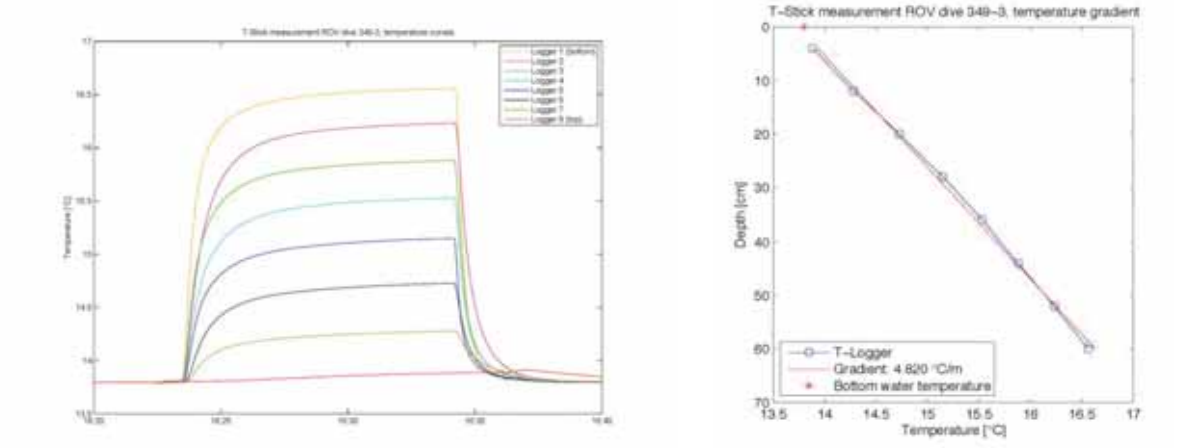

Fig. 108: Temperature data from the area ~110 meters from the summit. Left: decay curves for the 8 sensors of the T-stick. Right: temperature-depth profile showing a temperature gradient of 4820° C/km.

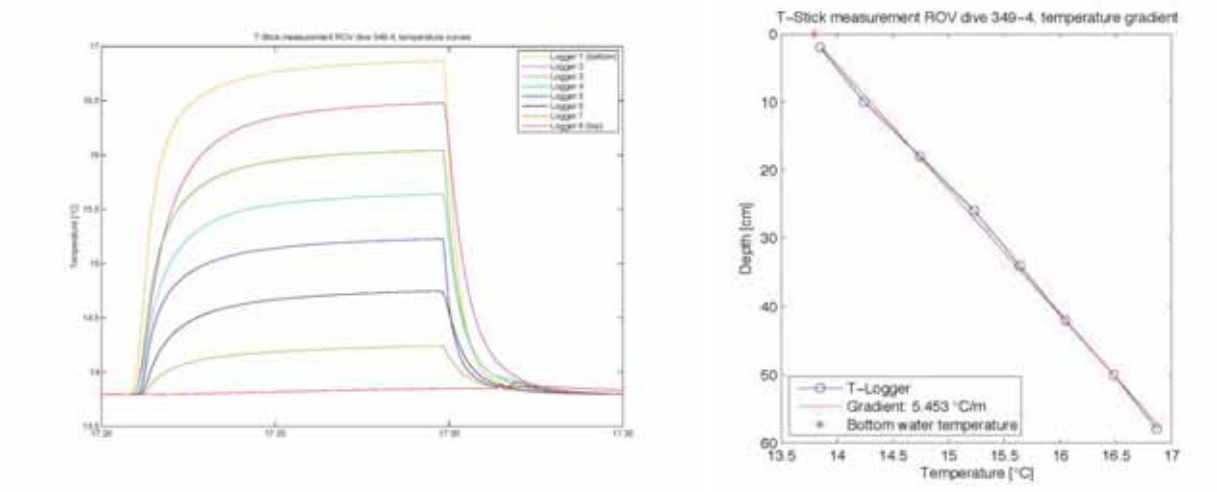

Fig. 109: Temperature data from the area ~ 80 meters away from the Venere Mud Volcano summit. Left: decay curves for the 8 sensors of the T-stick. Right: temperature-depth profile showing a temperature gradient of 5453° C/km.

8.2.14 Dive 350 (M112 Station 1279-1, GeoB: 19267-1)

Area:	**Venere Mud Volcano –Flare 2**
Responsible scientist:	Miriam Römer
Date:	Tuesday 09 December 2014
Start bottom (UTC):	09:10:34
End bottom (UTC):	13:11:17
Bottom time:	4 h 1 min
Start bottom (Lat/Long/depth):	38°36.093’ N 17°12.571’ E, 1593 m
End bottom (Lat/Long/depth):	38°36.101’ N 17°12.563’ E, 1595 m

Points of interest:

WP 1	38°36.0961’N	17°12.5717’E	Bubble stream (Dive 340)
WP 2	38°36.1160’N	17°12.5504’E	Flare 2 north
WP 3	38°36.0720’N	17°12.5762’E	Flare 2 south

Key results:

Found a young appearing seep area at the northern flare, mosaic of a collapse structure was taken, active gas bubble emission was detected close to the already sampled emission site during ROV Dive-340.

Technical description:

A major issue during this dive was the difference in the navigation relative to the last dive in that area (Dive 340). Similar to experiences during earlier cruises, this phenomenon seems to be related to the heading of the ship during the dive. During ROV-340 the heading of the ship was approximately south, whereas during this dive the heading was almost north. The difference was approximately 15 m, what made finding of targets set during the earlier dive difficult. It took also about an hour to recognize that we had this problem. Post-processing is also complicated, as the real positions cannot be defined doubtless.

Table 24: Samples and measurements taken during Dive 350.

GeoB	Instrument	UTC Start	UTC End	Position	Depth	Comment
19267-2	GBS (black)	10:53	10:53	38° 36.119' N 17° 12.556' E	1597 m	Water sample above young seep found in the northern area close to WP2
19267-3	Mosaic	11:31	12:00	38° 36.091' N 17° 12.560' E	~1595 m	20 m lines with 1.5 m spacing over carbonates and collapse structure
19267-4	Push corer (R2)	12:28	12:28	38° 36.100' N 17° 12.563' E	1596 m	In clam area
19267-5	Push corer (3)	12:30	12:32	38° 36.100' N 17° 12.563' E	1596 m	Aside R2
19267-6	Push corer (4)	12:35	12:36	38° 36.100' N 17° 12.563' E	1596 m	Close to R2 and 3 closer to bubble stream
19267-7	T-Stick	12:43	12:59	38° 36.100' N 17° 12.563' E	1596 m	Next to bubble stream
19267-8	Push corer (R3)	12:46	12:47	38° 36.100' N 17° 12.563' E	1596m	Next to T-Stick
19267-9	Push corer (5)	12:48	12:48	38° 36.100' N 17° 12.563' E	1596 m	
19267-10	Push corer (R5)	12:50	12:50	38° 36.100' N 17° 12.563' E	1596 m	
19267-11	GBS	12:55	12:55	38° 36.100' N 17° 12.564' E	1596 m	Water sample
19267-12	GBS	13:06	13:06	38° 36.101' N 17° 12.564' E	1595 m	Water sample
19267-13	Marker	13:15	13:15	38° 35.4277' N 17° 11.9504' E	1605 m	Christmas marker

Dive description:

The second dive at Flare 2 was dedicated to investigate the north and south of the seep area detected during the first dive (ROV-340). Detailed hydroacoustic observations during the cruise resulted, that not only one flare occurs at Flare 2. During the first leg of M112 just the central flare was active and investigated during ROV-340. However, during the second leg, several flare surveys showed different echograms, in which two flares are located close to each other, one north and one south of the former position. The dive started at the position, where gas bubbles have been detected during ROV-340 in order to check if bubble activity is visible. Unfortunately we could not find the same spot at the given position and searched for the seep area in the surrounding. About 20 m southwest a collapse structure was found (Fig. 114 left), which is probably the same as the one detected already during Dive 340. Following the seep influenced area we also found the site of the already investigated bubble stream. The position plots about 15 m northwest of the earlier position. The shift in the navigation is probably related to a different heading of the ship during both dives. Any bubble escape was recognized.

We followed the same escarpment of outcropping rocks in a northern direction and tried to find seep indications where the northern flare has been estimated. A young appearing seep area was passed, but due to the navigation inaccuracy and a possible shift of 15 m to the northwest we went on searching for further seep indications in that direction. However, without success. Therefore, we moved back to the small young appearing seep area to take a water sample with a gas bubble sampler (Fig. 112 left). Few small dark patches of reduced sediments were visible and partly covered

by whitish, most possible microbial mats. No gas bubble emission was observed although crossing the area several times and carefully watching for visual bubble observation and simultaneously scanning with the ROV-mounted horizontally-looking sonar (Imagenex 881). Afterwards, we moved back to the central flare area close to WP1 (where now a gas bubble stream was detected very close to the former position where gas bubbles have been sampled during ROV-340) and conducted a mosaic over the collapse structure using the downward looking Prosilica photo camera.

The last part of this relatively short dive was dedicated to sample the seep area. First, we tried to get a push corer into the sediments where whitish microbial mats on dark reduced sediments were visible (Fig. 113 left). But two attempts with the push corer failed as it penetrated not more than very few centimetres. Hard material (maybe carbonates) seems to lie just below the covering sediments. Touching with the manipulator revealed no further information. Final sampling was done close to the gas emission site. Six push corers were taken in different habitats and at the same time the T-Stick was placed close to the bubble site. By penetrating the T-Stick into the sediments a new quite intense gas bubble stream was created which lasted for almost the entire time of the measurement. The resulting temperature curves and also the calculated gradient reflect the influence of the gas bubble stream (Fig. 111): the curves do not come into equilibrium and also the gradient shows a zigzag curve, resulted by the heat transport of the pulsing gas bubbles. But the rough calculation shows an elevated gradient of 182° C/km. The dive ended with placing the Christmas marker at the seep site on bacterial mats.

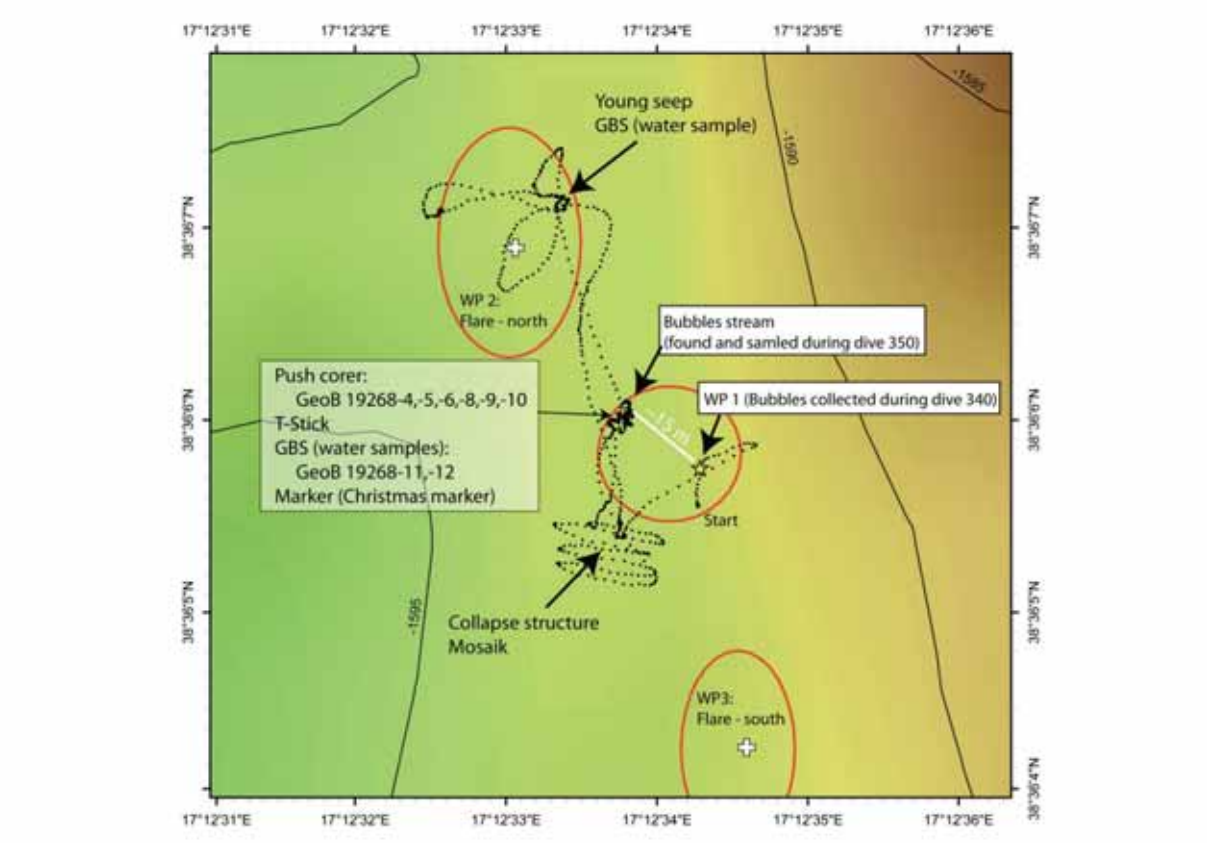

Fig. 110: Map of the area of Flare 2. The track is shown as black dots. Red circles indicate the approximate outline of the flares detected hydroacoustically. WP 1 is placed at the bubble emission site found during ROV-340, which was now found about 15 m shifted to the northwest.

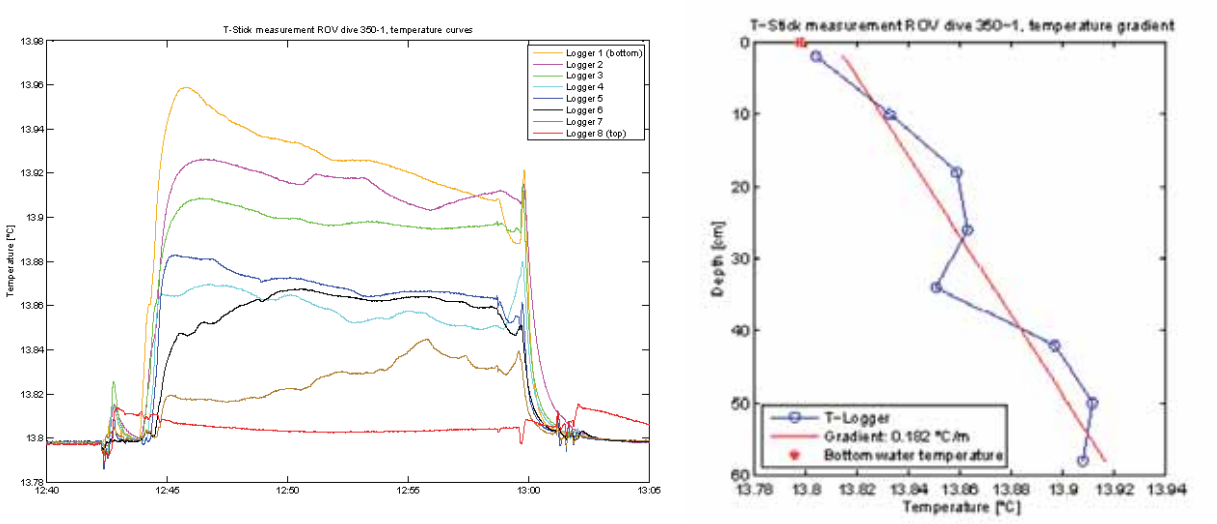

Fig 111: Left: temperature curves measured during T-Stick deployment close to a bubble stream, which produced a new source of bubble emission during the entire deployment. Right: the calculated temperature gradient of about 182° C/km is compared to the background value of 10° C/km clearly elevated.

Fig. 112: Left: GBS filled with bottom water over a young appearing seep area with dark reduced sediments and white bacterial mats. Right: bubble emission site at the edge of outcropping carbonates.

Fig. 113: Left: white bacterial mats close to WP1 (bubble emission site), where push corers could not penetrate due to a hard surface just few centimetres below the seafloor. Right: sampling with push corers very close to the gas emission site.

Fig. 114: Left: collapse structure in the central part of the central flare area. A mosaic was taken covering this area. Right: the Christmas marker placed on bacterial mats close to the bubble emission site.

9 Sediment Sampling

(L. Tamborrino, F. Mary, H. Sahling, S. Klüber, D. Praeg, S. Buchheister, M. Römer, M. Wiebe, C. Johansen, W. Menapace, O. Candoni, T. Pape)

9.1 Introduction and Methods

For sediment sampling several devices of MARUM were deployed during the M112 cruise: the gravity corer (GC), the minicorer (MIC), the dynamic autoclave piston corer (DAPC) and the ROV push corer (PC).

The GC (Fig. 115) had a top weight of about 2000 kg. It was equipped either with plastic liner or with plastic foil (or plastic bag – in German “Tütenlot”) for different purposes: plastic liner for keeping the sediments to describe and archive and plastic foil for a quick access of sediments if gas or gas hydrates were to be expected. In general, a core barrel length of 3 m was used during Leg 1. We used a 6 m long core barrel only one time successfully, during the second deployment it was bent.

The MIC is usually equipped with four cores of 7 cm inner diameter and 60 cm length. Due to technical problems the corer was reduced to only three cores during Leg 1. The MIC was deployed on the ships cable usually used for lowering the CTD (W2/W3). It was modified with four additional weights each 10 kg to make it heavier. Despite its low weight, it could be lowered with 0.8 to 1 m/s. It was also equipped one time with Posidonia showing that, despite its lightness, it was close to the ship and could be easily directed towards the target site at ~1500 m water depth. The MIC was lowered into the seafloor at a speed of 0.5 m/s and lifted out of the sediments with 0.3 to 0.5 m/s. In general, it yielded good recoveries of sediments.

Fig. 115: GC on deck prior to deployment.

Sediments collected by the dynamic autoclave piston corer were also described. For further details on the DAPC device are provided in the related chapter.

At some stations, MIC and GC were deployed with Posidonia navigation whereas the transponder was placed 10 m or 50 m, respectively, above the tool. As the officers at the bridge do not have the opportunity to see the Posidonia transponder position on a map relative to the ship, we provided this image via the MIMOSA screen operated by the AUV team, mirrored to the bridge. For this purpose, the corner coordinates of a rectangle were visually displayed, where we expected the ship to deploy the tool. Due to the dynamic positioning system present onboard, targeting the tools to the given locations was achieved with great precision.

The sampling strategy during Leg 1 was based on three different objectives: (1) to study the nature of backscatter as observed by AUV- or ship-based multibeam echosounders (BS); (2) to sample and study the occurrence of mud flows (MF); (3) to sample gas hydrate or gas rich sediments (GH).

9.2 Results from Core Descriptions

(F. Mary, L. Tamborrino, W. Menapace)

9.2.1 Gravity Cores

The gravity corer was deployed 38 times during M112 (Table 25) mostly at three different mud volcanoes, e.g. on Venere MV (Fig. 10). Only for two GCs (GC-6, GeoB19226-01 and GC-9, GeoB19229-03), the sampling activity failed.

Table 25: List of the gravity cores collected during the M112 cruise (core logs are shown in the appendix).

GC	GeoB #	Area	Plastic foil	PVC	Core recovery (cm)	Described on board	Not described
GC-1	19205-01	Venere MV (Flare 1)		X	262	X	
GC-2	19205-02	Venere MV (Flare 1)	X		176	X	
GC-3	19206-01	Venere MV		X	227	X	
GC-4	19212-01	Venere MV (Flare 1)	X		545	X	
GC-5	19213-01	Venere MV		X	232	X	
GC-7	19227-01	Cetus MV		X	165	X	
GC-8	19229-02	Deep-sea basin, SE of Sicily		X	215	X	
GC-10	19234-01	Venere MV (East)		X	194	X	
GC-11	19235-01	Venere MV (West)		X	262	X	
GC-12	19236-01	Venere MV (Flare 1)	X		220	X	
GC-13	19236-02	Venere MV (Flare 1)	X		97	X	
GC-14	19237-01	Venere MV (West)		X	119	X	
GC-15	19238-01	Venere MV (West)		X	131	X	
GC-16	19244-01	Venere MV (East)		X	96	X	
GC-17	19245-01	Venere MV (Western summit)	X		515	X	
GC-18	19245-02	Venere MV (Western summit)		X	326	X	
GC-19	19246-01	Venere MV (West)		X	194	X	
GC-20	19260-01	Venere MV		X	271		X
GC-21	19261-01	Venere MV (Mud flow 3)		X	257		X
GC-22	19263-01	Venere MV	X		275	X	
GC-23	19264-01	Venere MV (Mud flow 4)		X	163		X
GC-24	19269-01	Venere MV (Mud flow 1)		X	300		X
GC-25	19270-01	Venere MV (Mud flow 1)		X	255		X
GC-26	19275-01	Venere MV		X	93		X
GC-27	19276-01	Venere MV	X		195	X	
GC-28	19277-01	Venere MV (Western Flow)		X	38		X
GC-29	19278-01	Venere MV (NW flow)		X	293		X
GC-30	19279-01	Venere MV		X	404		X

GC-31	19280-01	Venere MV		X	286		X
GC-32	19282-01	Cetus MV		X	515		X
GC-33	19283-01	Cetus MV	X		293	X	
GC-34	19284-01	Cetus MV		X	570		X
GC-35	19285-01	Cetus MV		X	540		X
GC-36	19286-01	Cetus MV		X	480		X
GC-37	19289-01	Sartori MV		X	250		X
GC-38	19290-01	Sartori MV		X	500		X
Total Number of GCs (Length)			**8** (23,16 m)	**28** (78,38 m)	**99,54m**	**20** (47,39 m)	**16** (52,39 m)

Sediments from Venere MV flare sites

Four gravity cores were acquired from a seep site on the northern side of Venere MV (Flare site n. 1, Fig. 10), with a total of 1215 cm sediment recovery: GeoB 19205-1 (Fig. 116), 19205-2 (3 m long core), GeoB 19212-1, 19213-1 (6 m long core). Mud breccia was recovered in all these cores. It consists of a structureless mixture of a grey matrix (fine grain size, clay) and clasts (rock fragments). The mud breccia presents gas indicators such as a strong sulphidic smell and moussy texture. Rocks clasts are from millimetric to pluri-centimetric size, light grey to dark color, angular to sub-angular and of differing lithological compositions (sandstone, quartzite...). Bivalve shells, entire individuals or in fragments, and pteropod fragments were found in the mud breccia and are inferred to have been remobilized. A level of authigenic (?) carbonates, centimetric size, was found in the mud breccia at different depths in some of the cores. No distinction of mud flows could be made in these cores because of the absence of interbedded layers such as hemipelagic sediments, turbidites, sapropels or tephra layers. A study of the geometry or proportion of clasts, or a geochemical analysis could give more information on the extrusive activity.

In core GeoB 19213-1, two coarse layers with high concentrations of black to grey rock fragments up to millimeter size, were found at 80 cm and 110 cm depth. Above the layer at 80 cm, the mud breccia is composed of millimetric clasts and mud clasts. Between 80 and 110 cm, the mud breccia contains centimetric clasts and below 110 cm, there are larger clasts (pluri-centimetric).

Sediments from the western peak of Venere MV

Ten gravity cores were collected on the summit and the flanks of the western peak of Venere MV (Fig. 10), with 2517 cm of sediment recovery (1931 cm described during the cruise).

Three cores (GeoB19245-1, GeoB19245-2 and GeoB19263-1) were sampled at the summit of the western peak of Venere MV. Only moussy mud breccia composes these cores. It is a structureless mixture of a sticky grey matrix, of fine grain size (silty clay). Rock fragments are composed by millimetric to pluri-centimetric clasts, mostly hard, with different lithology (mudstone, sandstone, mud clasts, marly limestone, etc.) and colour. Two levels with a higher concentration of clasts (friable centimetric mud clasts at 78 cmbsf and hard sub-centimetric mudstone clasts at 165 cmbsf) are observed in the core GeoB19245-1. Also in GeoB19263-1, two levels of high concentration of pluri-centimetric clasts occur at 85 and 249 cmbsf.

Fig. 116: Left: Bivalve shells on the surface layer. Right: clast with calcitic veins.

Fig. 117: Example of moussy texture from mud breccia.

Only two cores (GeoB19235-1 and GeoB19276-1) of the south-western flank are described among the five collected. Only moussy mud breccia (Fig. 117) composes these cores. It is a structureless mixture of a sticky grey matrix, of fine grain size (silty clay). GeoB19235-1 has an oxidized portion at the top of the core. GeoB19235-1 and GeoB19276-1 are characterized by moussy texture from, respectively, 52 and 8 cmbsf to the bottom of the core. The uppermost 8 cm of GeoB19276-1 have a soupy texture. For these cores, rock fragments are composed by millimetric to pluri-centimetric clasts, mostly hard, with different lithology (mudstone, sandstone, etc.) and colour. The concentration of the pluri-centimetric clasts tends to increase with the depth or locally aggregated in the core GeoB19276-1.

GeoB19206-1 and GeoB19238-1 were taken from the northern flank of the western peak of Venere MV (Fig. 10). Only mud breccia was found in these cores. It is a structureless mixture of a sticky grey matrix, of fine grain size (silty clay), and different clasts. In GeoB19206-1, no gas indicators are observed in the first 170 cm. From 170 cm to the bottom of the core, the matrix texture becomes moussy and there is a sulphidic smell. No bioclast fragments were seen in this core. GeoB19206-1 shows a level, at 58.5 cmbsf, with high concentration of black, grey or dark green rock fragments up to millimeter size and dark friable rock clasts up to 0.7 cm size, similar to the coarse layers seen in the core GeoB 19213-1 (Fig. 118). The magnetic susceptibility data do not show obvious variation at this

level. An X-Ray analysis could be interesting to better understand this particular level. GeoB19238-1 has some hemipelagic sediment remains on the top of the core. At 104 cmbsf, a centimetric dark-black organic patch, characterized by a light sulphidic smell, was recognized.

Fig. 118: Coarse level of sub-centimetric clasts.

Sediments from the eastern peak of Venere MV

Three gravity cores (GeoB19234-1, GeoB19244-1, and GeoB19280-1) were collected in the proximity of the summit of the eastern peak of Venere MV (Fig. 10), with 576 cm of sediment recovery. GeoB19234-1 and GeoB19244-1 were described during the cruise. These cores share a similar hemipelagic sequence in the uppermost 50-60 cm. The surface layer is composed by structureless brown silty clays. Under the brown clays, a centimetric (5-6 cm of thickness) dark brown sandy layer is observed, overlying a segment of grey silty clays. The sandy layer give higher values in terms of magnetic susceptibility (see Appendix). The grey clays represent the bottom of the hemipelagic sedimentation: under the latters, the cores are composed by a structureless grey mud breccia with rock fragments. The mud breccia is composed by a fine grain size matrix with millimetric to pluri-centimetric clasts, mostly hard, of different lithology and colour.

In addition, one core (GeoB19279-1) was sampled as a reference in the eastern area of Venere MV, not involved by mud flows.

Sediments from the mud flows of Venere MV

From backscatter results, six mud flows have been distinguished at Venere MV. Seven gravity cores were sampled in the area covered by the mud flows of Venere MV (Fig. 10), with 1415 cm of sediment recovery. Only two cores (GeoB19237-1 and GeoB19246-1) from the mud flows were described during the cruise (tot. 313 cm). A surface layer (8-32 cmbsf) is composed by hemipelagic brown silty clays were observed only for GeoB19246-1. Under the surface layer, GeoB19246-1 shares the same sedimentological features of GeoB19237-1: structureless grey mud breccia with rock fragments. The mud breccia is composed by a fine grain size matrix with millimetric to pluri-centimetric clasts, mostly hard, of different lithology and colour.

Sediments from Cetus mud volcano and Sicily deep-sea basin
Nine gravity cores were collected in the area of Cetus MV, Sartori MV and the south-eastern deep-sea basin of Sicily. Two cores from Cetus MV (GeoB19227-1 and 19283-1) and from the deep-sea basin in the south-east of Sicily (GeoB19229-2) are described during the cruise.

GeoB19227-1 is characterized by a surface layer (0-40 cmbsf) of brownish hemipelagic sediments (silty clay). With the depth these clays become gradually darker in colour. A gradational inclined contact divides the uppermost sediment with the underlying structureless grey mud breccia (Fig. 119). This mud breccia has a fine grain size matrix with millimetric to pluri-centimetric clasts, mostly hard, of different lithology and colour.

Fig. 119: Gradational contact between the brownish hemipelagic sediment and the underlying grey mud breccia.

GeoB19229-2 comes from an area without mud volcanoes and for this reason is the only core described during the cruise without mud breccia. Until 176 cmbsf, the core is composed by muddy grey very fine sediment (clays). The bottom (176-215 cmbsf) of the core is composed by dark grey sandy sediment, very cohesive. These fine sands are similar to the sediment remains observed in the failed core GeoB19229-3. A probable reason for the failed sampling is the particular nature of the above described sands.

Only mud breccia was found in GeoB19283-1. It is a structureless mixture of a sticky grey matrix, of fine grain size (silty clay), and millimetric to pluri-centimetric clasts, mostly hard, of different lithology (sandstone, mudstone, marly limestone, etc.) and colour. The uppermost portion (0-15 cmbsf) is characterized by dark patches and a light sulphidic smell during the opening moment.

9.2.2 Mini Corer Sampling

GeoB19208-1 (MIC-1 and -2) was sample at flare site n.1. On top of the core, there is a fluid black fine-grained sediment surface layer with vesicomyd shells (entire or in fragments, up to 1 cm size), pteropod fragments and irregular pieces of authigenic carbonate. Sulphidic smell. White bacterial filament observed on the surface of MIC-2. Under the surface black fluid sediment, a dark grey moussy mud breccia was observed. Fine grain size matrix and millimetric clasts. Black organic portions were observed within the mud breccia segment.

GeoB 19209-1 (MIC-3) was taken on the northern flank of the western summit of Venere MV. A hemipelagic layer overlying a mud breccia was found in MIC-2. It is a brown silty-clay layer, with black

grain but no bioclast fragments. The contact with the mud breccia is progressive. The mud breccia has a fine grain size matrix and rock fragments of different size, lithology and colour.

GeoB19279-3 MIC-4) was sampled at Venere MV, but outside the area of the mud flow. It represents a reference for the normal hemipelagic sedimentation. The surface layers are characterized by silty clay sediment (0-4 cmbsf). A fine sands layer (4-6 cmbsf) represents the redox limit under the surface layer. Grey silty clays close the sequence at the bottom of the mini core (Fig. 120).

Fig. 120: Sandy layer in a splitted minicore.

9.2.3 Push Cores

Push corer is a specific tool of the ROV, widely used for sediment sampling of the shallow sub-seafloor (max 20-22 cmbsf). At hydrocarbon seeps, the sub-seafloor is the location of peculiar microbial biogeochemical processes. For these reasons, push cores have been sampled for further investigation about porosity, methane concentration-composition and microbiology. The sediment description and the magnetic susceptibility measurements (see Appendix) provide background information, useful for correlation with results of other analyses. During the cruise M112, three typology of sediment characterize the push cores sampled:

1) Black-dark grey fine sands with high sulphidic smell. Most of the sandy particles seem to be authigenic sulphide precipitates (pyrite?). All these push cores come from bacterial mats. In most of the cases, vesicomyds shells (single valves or fragments) are embedded in the uppermost portion. Few push cores show bioturbation elements.

2) Grey mud breccia with rock fragments. Fine grain size matrix. Millimetric to sub-centimetric clasts, mostly hard. Pervasive moussy texture observed mainly in the push core from the western summit of Venere MV. Most of the push cores with mud breccia have sulphidic smell, but few cores have dark bacterial patches.
3) Brownish hemipelagic sediment (silty clay). Only the push core from Cetus and Nicolas MV belong to this category. The cores from Nicolas are characterized by pteropod shells and fragments.

Most of the push cores collected during the M112/2 have been sample for further mineralogical analyses, with a frequency of 5 cm (see Table 26).

Table 26: List of the sub-samples of push cores for mineralogical analyses.

Number	0 cmbsf	5 cmbsf	10 cmbsf	15 cmbsf	20 cmbsf
GeoB19240-10	X	X	X	X	
GeoB19240-12	X	X	X	X	
GeoB19240-15	X	X	X	X	X
GeoB19242-06	X	X	X	X	
GeoB19242-10	X	X	X	X	X
GeoB19242-11	X	X	X	X	X
GeoB19242-14	X	X	X	X	
GeoB19242-17	X	X	X	X	
GeoB19249-07	X	X	X	X	X
GeoB19249-12	X	X	X	X	
GeoB19252-10	X	X	X	X	
GeoB19252-14	X	X	X	X	
GeoB19253-12	X	X	X	X	X
GeoB19255-07	X	X	X	X	
GeoB19258-04	X	X	X	X	X
GeoB19258-09	X	X	X	X	
GeoB19258-11	X	X	X	X	X
GeoB19258-14	X	X	X	X	
GeoB19258-17	X	X	X	X	
GeoB19267-04	X	X	X	X	
GeoB19267-08	X	X	X		
GeoB19267-10	X	X	X	X	

Fig. 121: Bioturbation structures and bivalves on push cores surfaces.

9.2.4 Carbonate and Rock Samples

(L. Tamborrino)

Most of the methane occurring in the seafloor sediments (independently if is biogenic, thermogenic, abiogenic or gas originated by gas hydrates destabilisation) is "consumed" in situ (Hoehler et al. 1994). Based on the quantitative analyses on the sulphate and methane content in the pore waters and verified by the isotope mass balance, geochemists have postulated the anaerobic oxidation of methane (AOM), through the sulfate reduction, such as the dominant biogeochemical process at cold seeps (Suess & Whiticar, 1989; Borowski et al., 1999). However for several years, the AOM question remained controversial because the microbes responsible of this reaction remained elusive, until microbiological associations of methanotrophic archaea (ANME) and sulfate-reducing bacteria (SRB) have been visualized by means of fluorescence in situ hybridization microscopy (FISH) from Hydrate Ridge (Boetius et al., 2000; Knittel et al., 2005) and confirmed also in cold seeps and clathrates deposits of Eel River basin (California, USA) (Orphan et al., 2004) and in the Gulf of Mexico (Joye et al., 2004). In general, the oxidation process is mediated by microbial consortia and consists of an inner sphere containing methanotrophic archaea (ANME) surrounded by sulfate-reducing bacteria (SRB). Metabolic reactions of this consortium could be summarized in the following equation, which shows the results of AOM processes, namely the generation of hydrogen sulphide (in aqueous solution as hydrosulfide anion HS−) and bicarbonate:

$$CH_4 + SO_4^{2-} \rightarrow HCO_3^- + HS^- + H_2O$$

As it was observed, one of the products of the AOM is the bicarbonate ion, increasing their concentration at cold seep. These chemical variations influence the alkalinity on the pore water, condition that induces the carbonate precipitations through a reaction with calcium ions from the seawater:

$$Ca^{2+} + 2HCO_3^- \rightarrow CaCO_3 + CO_2 + H_2O$$

In literature these carbonates are called "cold-seep carbonates" or "authigenic carbonates" (because minerals was generated where it is found or observed). In general, at submarine hydrocarbon seeps, two general facies of seep-carbonate can be observed:

1) Complete authigenic carbonate precipitates, forming layers within chemoherms (in case of anoxic bottom waters) or clotted/botroidal microbialite, precipitate in the sub-seafloor;
2) Authigenic carbonate cementing hemipelagic sediment.

The carbonate formations of Venere MV are mostly friable due a not complete cementation by carbonate precipitates. In general, lithification of these carbonates crusts decrease with depth and, few centimetres below the surface of the carbonate, the sediment is already completely incoherent and uncemented.

ROV observations and samples collected at Venere MV show that most of the carbonate crusts seems to be composed by background sediment cemented by authigenic carbonate minerals. The term "carbonate" could then result inappropriate. Until further petrographic-mineralogical investigations, the crusts observed will be defined as carbonate crusts or slabs (Figs. 10 a, b, c, d).

Most of the carbonate crusts are outcropping mainly at the flare sites of Venere MV, with different morphologies (see Figs. 122 and 123). The morphology of these carbonate crusts is clearly related to several key factors: Cementation grade and thickness are strictly related to the AOM rates and the consequent increase of alkalinity, responsible of the carbonate precipitation. Cementation directly influences the rheological characteristics (i.e. shear strength) of the carbonate crust.

At seep sites, methane and the other gaseous hydrocarbons can give a peculiar contribute to the fluid pressure. The cracks observed (Figs. 122 and 123) are probable related to an increase of the fluid pressure of the underlying sediments, thus exceeding the shear strength of the carbonate crust.

With cementation, permeability of the background sediment decreases, redesigning leakage pathways of fluids enriched of methane and/or hydrogen sulphide. Figure 122 right shows clearly the contrast of the biological activity on the surface of the carbonate (almost absent) and on the soft sediment (rich with bacterial mat and vesicomyds shells). The carbonate precipitation tends to reduce the possibility of migrating fluids to reach the seafloor, while in the soft sediment fluids can reach the surface, feeding the chemosynthetic ecosystem. But even under the carbonate slabs there are basic conditions for chemosynthetic ecosystems. In addition, carbonate crusts can be considered as local traps for fluids migrating upwards, favouring the accumulation under the carbonate crust. This phenomenon could help the increase of the fluid pressure, until the break of the carbonate crust. However, the carbonate crusts can be altered by elements of secondary porosity, like discontinuities (fractures), cavities related to micro-macrobiological activity and corrosion patterns. Secondary porosity represent an ideal degassing pathway. During the ROV dives, most of the gas flares observed came from fractured carbonate crusts. Rapid degassing can lead to a sudden decrease of fluid pressure in the underlying sediment, causing the collapse of the carbonate crust (Fig. 123 right).

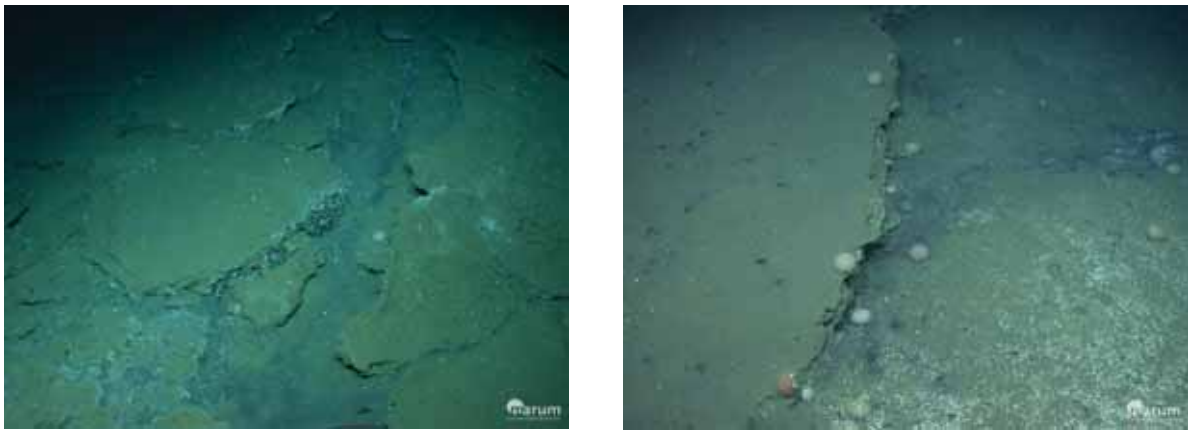

Fig. 122: Left: The “Carbonate Slab Drift”- Diverging carbonate slabs. Image taken during ROV dive 341- Flare 1. Similar picture was used for biology. Right: Carbonate slab- Contrast of biological activity between plain sediment and on the carbonate slab. Image taken during ROV dive 350 –Flare 2.

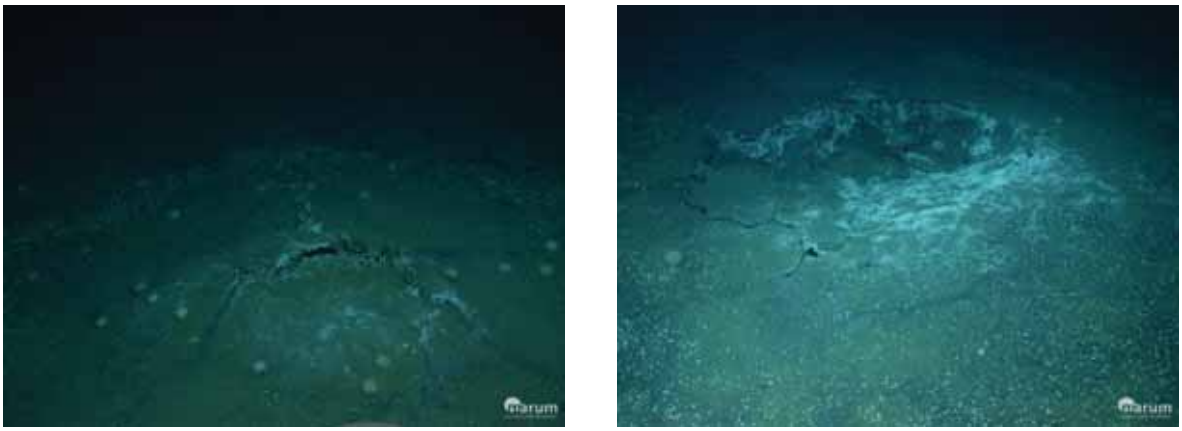

Fig. 123: Left: Carbonate mound with fractures filled by darker soft sediment. Gas bubbles from the carbonate. Image taken during ROV dive 343 at Flare 4-5. Right: Collapse structure of the carbonate crust. Gas bubbles from the internal wall of the depression. Image taken during ROV dive 346 at Flare 4-5.

Photo-mosaicking data and further investigation on the carbonate samples will provide a better understanding of the processes responsible of the carbonate crust morphology.

Chemosynthetic organisms have been founded mostly at the flare sites of Venere MV. Among the several macrofaunal organisms living in this context, ROV observations and samples collected confirm that only the tubeworm Lamellibrachia anaximandri and the bivalve Idas modiolaeformis strictly need the carbonate crusts for their protection and survival.

During the M112, several carbonate samples have been collected with ROV tools:
GeoB 19230-6. Two carbonate small samples (a, 6.3x5x3 cm; b, 6x3x2.5 cm). High concentration of vesicomyd shells (single valves or fragments) embedded in the samples.
GeoB 19230-8. One carbonate piece (13.5x8x4.5 cm) with rough surface with several millimetric bivalve shells. Altered surface is yellowish brown, while the fresh surface is grey. A green tubular organic element is observed on one side of the sample. Additional rock centimetric fragments (d. max 3-4 cm) compose the sample.
GeoB 19230-9. It is composed by three major samples (a, 10,5x8x4,5 cm; b,12x8x4 cm; c,9,5x6x3 cm) and other centimetric pieces d. max 3 cm). Carbonate colour: light yellowish brown on the altered surface (2,5Y 6/4) and dark greenish grey (10GY 4/1) on the free surface. Pieces a and b connected by two tubeworms L. anaximandri (middle-posterior portion, Fig. 124 left). Piece a is characterised by two holes (diameter ca. 0.5 cm) with a whitish inner coating and two holes occupied by the cutted lower portion of the tubeworms (reddish blood came out). On piece a, two yellowish shells of Idas m. (2x0.8x0.5 cm) were attached on the carbonate surface. The “tubeworm connection” between the two pieces is ca. 6 cm long. In this portion, tubeworms were damaged and it was possible recognise the outer chitinic wall (d. 0.5 cm) and the inner organic tissue.

On one side of piece b three brownish shells of Idas m. are present (1.5x0.6x0.4 cm). On the opposite side, there are the brachial apertures of two tubeworms (one was empty, the other was occupied by the organism, still living when it arrived on the deck). Authigenic carbonates minerals (probably aragonite) seem to cover a portion of the altered surface of piece b. Piece c has two yellowish hairy shells of Idas m. (1.5x0.6x0.4 cm and 0.9x0.4x0.3 cm). The surface of piece c seems to have biological remains, deeply eroded.
GeoB 19240-5. It is constituted by three samples (a, 28x18.5x7.5 cm; b, 19.5x15x5.5 cm; c, 7x6x4 cm). This sample comes from the carbonate mound-bubbling site of flare 4-5 of Venere MV. Piece a is the main sample and the following description refers to this piece. It represents a portion of the border of the carbonate crust, colonised by a small colony of tubeworm L. anaximandri and covered by a whitish bacterial mat (Fig. 124 right). The upper surface is smooth and greyish-brown in colour. The lower surface is rough with several holes and dark grey in colour. Most of the sample is composed by background sediment (fine sands, authigenic sulphide precipitates), cemented by authigenic carbonates. The grade of cementation decreases with depth. Sulphidic smell felt. The lower surface is also enriched by several elements linked to biological activity. Several holes (d. max 0.5 cm) are concentrated in the area covered by the whitish bacterial mat. These holes are probably associated to bioturbation or corrosion phenomena due to biogeochemical variations induced by microbial activity. Several (ca. twenty individuals) tubeworms L. anaximandri lived anchored to the piece a. All the portions of the tubeworm are observable in the sample: the anterior chitinic portions and the brachial apertures, the dark soft posterior portions (roots) and for some individuals, a colourless (or darkened by the surrounding sediment) jelly extremity, probably representing the early stage of the roots formation. The maximum length of the chitinic portion is ca. 4-5 cm. and the max

diameter is ca. 0.5 cm. Two shells of vesicomyds have been observed, attached to a reddish posterior end (16 cm long) of L. anaximandri. Few Idas m. individuals have also been discovered in cavities. Piece b show two surfaces: an olive brown altered upper surface and a black-dark grey bottom surface. Composition of this piece is similar to the piece a. Bioclasts of vesicomyds are embedded in the sediment matrix. One individual of L. anaximandri is also observed. Also the smallest piece c has bivalve shells and one tubeworm.

GeoB 19252-4. One sample (10x9x4 cm). Black background sediment, mainly composed by authigenic sulphide precipitates, cemented by carbonate. Rough surface. Sulphidic smell. One individual of vesicomyd observed.

GeoB 19252-13. It is composed by two samples (**a,** 39x30.5x9 cm**; b,** 22x15x10 cm). Both samples are characterised by a rough altered surface, mainly composed by bioclasts of different organisms cemented with seafloor sediment (Fig. 125 left). The thickness of the surface layer is ca. 2 cm. Above the surface, the samples are characterised by a semi-lithified background sediment (fine sands, mainly composed by authigenic sulphide precipitates). Low reaction with HCl (small amount of carbonate fraction). The grade of cementation decrease with depth and at the bottom is completely incoherent. Shells of vesicomyd of different stage of life and tiny reddish worms have been observed, mainly close to the surface layer. *Idas m*. shells have been also observed hidden in the cavities of the samples.

GeoB 19255-4. Three rock samples (**a**, 31x9x6 cm; **b**, 10x6x1.5 cm; **c**, 7.5x5.5x2 cm). These pieces are sampled at Nicolas MV (site with the highest concentration of pteropod shells) and they are not carbonates. The main sample (piece **a**) is covered by the incoherent hemipelagic sediment that characterised the seafloor of Nicolas MV. A dark brown (10 YR 5/4) crust composes the lithified upper surface of the sample (Fig. 125 right). The colour suggests the occurrence of oxidized minerals. Under this crust, the sample is composed by semi-lithified silty-sands. The cementation of the sands decreases with depth. Piece **b** shows similar features of piece **a**. Piece **c** is only composed by the semi-lithified sands.

In addition to carbonate sample, other rock samples (mainly clasts of mud breccia), have been also collected from gravity cores (for the complete list, see Table 27).

Further investigations, using petrography, mineralogy, stable isotope geochemistry and biomarker analyses, will be useful to better define the nature of the collected samples. The combination of these techniques could be used to confirm seep influence and other biogeochemical processes. Studies on recent seep carbonates on Venere Mud Volcano should be compared to both actual and fossil samples.

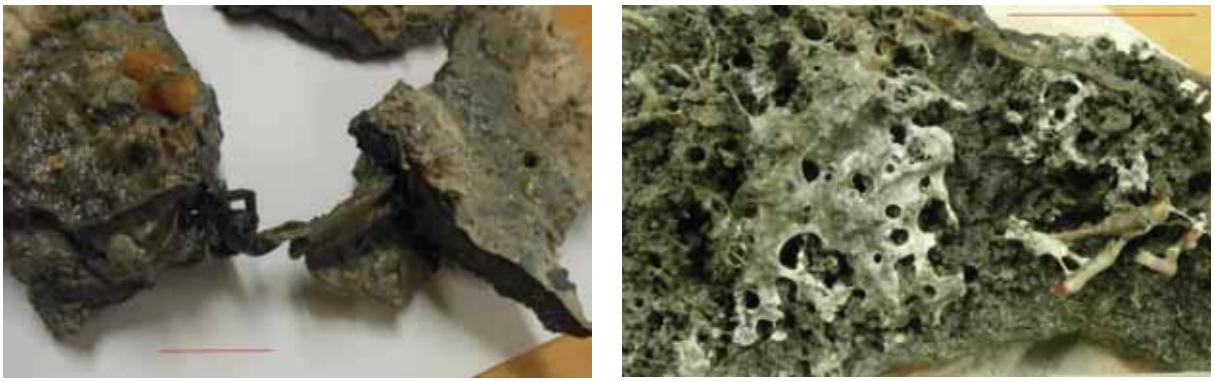

Fig. 124: Left: GeoB19230-9. The anterior portion of *L. anaximandri*, connecting the carbonate pieces (a and b). Scale bar: 2 cm. Right: GeoB19240-5. Bottom surface. Detail of the whitish bacterial mat covering the holes of the sample. Portion of tubeworms. Scale bar: 5 cm.

Fig. 125: Left: GeoB19252-13 (a). Upper surface. High concentration of bioclasts (mainly vesicomyd shells), responsible of the superficial roughness of the sample. Scale bar: 5 cm. Right: GeoB1955-4. Rock sample composed by altered crust, overlying semi-lithified sands. Scale bar: 5 cm.

Table 27: List of the rock samples collected during the cruise M112.

GeoB #	Area	Device	Description
19205-02	Venere MV (Flare 1)	Gravity corer (plastic foil)	Sandstone clasts (173-174 cmbsf) from the core catcher
19205-02	Venere MV (Flare 1)	Gravity corer (plastic foil)	Mud breccia clasts (shallow depth, not clean)
19205-02	Venere MV (Flare 1)	Gravity corer (plastic foil)	Limestone clasts and sediment from the outer surface of the gravity corer
19205-02	Venere MV (Flare 1)	Gravity corer (plastic foil)	Four section (0-40,40-90,90-120,120-176 cmbsf) of the core with mud breccia-Clast to clean
19206-01	Venere MV	Gravity corer (PVC)	Siltstone clasts (Sec. 2/3) with calcitic veins
19206-01	Venere MV	Gravity corer (PVC)	Millimetric to pluri-centimetric clasts of different lithology
19208-01	Venere MV	Mini-corer	Hemipelagic sediments (silty clay)
19209-01	Venere MV (Western peck)	Mini-corer	Hemipelagic sediment (silty clay) and mud breccia
19212-01	Venere MV (Flare 1)	Gravity corer (plastic foil)	Clasts of different lithology (siltstone with calcitic veins, Fossiliferous sandstone, friable mudstone
19213-01	Venere MV (Flare 1)	Gravity corer (plastic foil)	Limestone clasts from mud breccia
19221-11	Venere MV (Flare 1)	ROV- Suction sampler	Limestone clasts from push core (ROV dive 339)
19221-12	Venere MV (Flare 1)	ROV- Suction sampler	Limestone clasts from push core (ROV dive 339)
19230-06	Venere MV (Flare 1)	ROV- Arm/Net	Authigenic carbonate cementing background sediment and bioclasts.
19230-08	Venere MV (Flare 1)	ROV- Arm/Net	Authigenic carbonate cementing background sediment and bioclasts.
19230-09	Venere MV (Flare 1)	ROV- Arm/Net	Authigenic carbonate cementing background sediment and bioclasts.
19232-04	Venere MV (Western summit)	ROV- Net	Mud breccia clasts and shells (d. min. 4mm) from push core.
19232-04	Venere MV (Western summit)	ROV- Net	Sifted sediment (d. max 4 mm) from the push core of mud breccia
19240-05 A	Venere MV (Flare 1)	ROV- Arm/Net	Authigenic carbonate cementing background sediment and bioclasts.

19240-05 BC	Venere MV (Flare 1)	ROV- Arm/Net	Authigenic carbonate cementing background sediment and bioclasts.
19242-18/15/12	Venere MV (Western summit)	ROV-Push core	Millimetric to centimetric clasts of different lithology
19245-01	Venere MV (Western summit)	Gravity corer (plastic foil)	Pluri-centimetric clasts of different lithology from the whole core-Samples from every meter (1/2/3/4)
19252-04	Venere MV (Flare 4-5)	ROV-Arm/Net	Authigenic carbonate cementing sandy sediment.
19252-11	Venere MV (Flare 4-5)	ROV-Push core	Hemipelagic sediment from bacterial mat
19252-13 AB	Venere MV (Flare 4-5)	ROV-Net	Authigenic carbonate cementing background sediment (sands and sulphide precipitates) and bioclasts.
19255-03	Nikolaus MV	ROV-Net	Brownish crust and clast, overlying semi-lthified sands
19255-09	Nikolaus MV	ROV-Net	Brownish crust and clast, overlying semi-lthified sands
19257-01	Venere MV (Flare 1)	DAPC	Sandstone clast with calcitic vein from the core catcher
19261-01	Venere MV (Mud flow 3)	Gravity corer (PVC)	Friable mudstone clasts and hard siltstone from the core catcher
19263-01	Venere MV	Gravity core (plastic foil)	Pluri-centimetric clasts of different lithology from the whole core
19276-01	Venere MV	Gravity core (plastic foil)	Pluri-centimetric clasts with different lithology from the whole core
19277-01	Venere MV (Western flow)	Gravity core (PVC)	Black marly limestone and sandstone clast from the core catcher
19283-01	Cetus MV	Gravity core (plastic foil)	Pluri-centimetric clasts with different lithology from the whole core
19285-01	Cetus MV	Gravity core (PVC)	Black sediment with H2S smell from the core catcher (> 5mbsf)
19286-01	Cetus MV	Gravity core (PVC)	Sediment from the core catcher (> 5mbsf)
19290-01	Sartori MV	Gravity core (PVC)	Sediment from the core catcher (> 5mbsf)

10 Dynamic Autoclave Piston Corer and Molecular Composition of Volatile Hydrocarbons

(T. Pape, K. Dehning, T. Schade, P. Geprägs)

10.1 Dynamic Autoclave Piston Corer

During M112 both specimen of the Dynamic Autoclave Piston Corer (DAPC) owned by the MARUM, the DAPC I and DAPC II were used with the aim to recover gas-rich or even gas hydrate-bearing surface sediment cores under in situ hydrostatic pressure for the quantification of sediment-hosted gas. The inner diameter of the rigid PVC-liner in both tools is 8.5 mm while maximum core lengths are 265 cm (DAPC I) and 275 cm (DAPC II), respectively. Details on the technical specifications, on maintenance and handling on board, and on the degassing procedure of the DAPC are published elsewhere (Bohrmann, Pape et al., 2007; Heeschen et al., 2007; Abegg et al., 2008; Pape et al., 2011). During M112 seven DAPC stations were performed (Table 28). The DAPC was lowered via winch 10 and the movebar with a rope velocity of 0.5 m s^{-1} and heaved with 0.5-0.8 m s^{-1}. According to the DAPC working principle penetration of the core cutting barrel was conducted in the free fall mode. Upon completion of the controlled core degassing on deck, the PVC-liner containing the core was removed from the DAPC pressure chamber for subsequent pore water (Chapter 11.1) and sediment collection as well as macroscopic core descriptions (Chapter 9). Molecular compositions of volatiles released during core degassing were determined on board for cores GeoB 19251-1, 19257-1, 19268-1, and 19287-1.

Table 28: Overview of DAPC stations performed during M112.

GeoB	Area	DAPC	Pressure after recovery [bar]	Gas released [L]	Core recovery [cm]	Gas sediment wet volumetric ratio [L L^{-1}]	Remarks
19243-1	Flare Site 1	I	0	0	0	n. det.	no core, instr. likely fell on seafloor
19243-2	Flare Site 1	II	ca. 10	0	274	n. det.	pressure loss during recovery, no gas quantification
19251-1	West summit	II	164	41.3	210	3.68	
19257-1	Flare Site 1	II	25	42.9	182	4.41	
19266-1	West summit mud flow	II	0	0	0	0	instr. not released at seafloor
19268-1	West summit mud flow	II	148	67.9	253	5.02	
19287-1	West summit mud flow	II	169	3.2	n. det.	n. det	likely blockage of cutting barrel by mud clasts, few cm of sediment and numerous clasts in liner

n. det. = not determined

10.2 Molecular Composition of Volatiles at Venere MV

The main objective of this program was to assign the origin of volatile hydrocarbons (thermogenic vs. microbial) present in various mud volcano-associated deposits and/or expelled from the seafloor.

10.2.1 Shipboard Analysis

During M112 gas sufficient in concentrations for comprehensive analysis of its molecular composition was collected either with the Dynamic Autoclave Piston Corer (DAPC, Chapter 10.1) or with Gas Bubble Samplers (GBS) operated with the ROV QUEST (for locations see Table 29). While gas venting from the seafloor could be sampled with the GBS at flare emission sites at the rim of the Venere MV, gas emissions were not recognized from the mud flows. Nevertheless, during M112 the DAPC was successfully used for the first time to sample sedimentary gas from mud flows.

After recovery on deck, both the DAPC and the GBS were degassed under controlled conditions using a gas manifold system as described in Pape et al. (2011). At selected pressure stages prevailing in the DAPC- or GBS pressure chamber gas samples were taken with a gas-tight syringe and transferred into 20 ml glass vials prefilled with saturated NaCl solution for long-term storage and transport. The molecular composition of the gas was analyzed on board by use of a gas chromatograph (Agilent 6890N) equipped with a capillary column connected with a flame ionization detector and a mole sieve column connected with a thermal conductivity detector (Pape et al, 2011).

10.2.2 Preliminary Results and Discussion

During M112 76 gas subsamples were measured for their molecular composition. Hydrocarbon origins were assigned according to the classification based on hydrocarbon ratios and proposed by Bernard et al. (1976). All vent gas samples collected at the emission sites of Flares 1, 2, 4, and 5 were characterized by relatively moderate to high C_1/C_2 ratios. Such ratios signify a mixed origin with a slightly larger portion of microbial hydrocarbons (Table 29).

Table 29: Locations of gas samples taken with the Dynamic Autoclave Piston Corer (DAPC) or the Gas Bubble Sampler (GBS), range of C_1/C_2 ratios determined for the entire gas sample set prepared from the respective tool, and inferred hydrocarbon origin.

GeoB	Site	Tool/Gas type	C_1/C_2 (range)	Putative hydrocarbon origin
19221-2	Flare Site 1	GBS/ vent	1,780-1,910	mixed (microbial)
19257-1	Flare Site 1	DAPC/ sedimentary	1,210-1,600	mixed (microbial)
19224-2	Flare Site 2	GBS/ vent	895-1,080	mixed (microbial)
19249-5	Flare Site 4	GBS/ vent	1,060-2,370	mixed (microbial)
19240-2	Flare Site 5	GBS/ vent	1,130-1,220	mixed (microbial)
19251-1	Summit mud flow	DAPC/ sedimentary	95-121	mixed (thermogenic)
19268-1	Mud Flow	DAPC/ sedimentary	91-130	mixed (thermogenic)
19287-1	Mud Flow	DAPC/ sedimentary	82-122	mixed (thermogenic)

In contrast, C_1/C_2 ratios in gas obtained in the course of depressurization of mud were relatively low, indicating a prevalence of thermogenic hydrocarbons. Remarkably, differences in the composition of light hydrocarbons in the mud samples were insignificant, indicating that alterations in the gas composition during downslope movement were negligible at these sites.

11 Geochemistry

11.1 Pore Water Program

(M. Torres, S. Buchheister, R. Alvarez)

The main objective of the pore water program was to evaluate the nature and source of fluid flow in the mud volcanoes of the Calabrian arc, and establish the possibility for the presence of gas hydrate. In addition, changes in pore fluid composition may also illuminate the history of mud flow activity, by analyzing non-steady state profiles of pore fluid metabolites; as well as provide supporting data to studies of heterogeneity of seafloor habitats associated with areas of seepage.

Pore water samples were collected from 29 ROV push cores, 7 gravity cores, 4 DAPCs and one mini-corer using 3, 4 and 5 cm rhizons, depending on the core diameter. The location of the cores and general working area, showing the number of samples for geochemistry are listed in Table 31.

Because the bottom water temperature was ~18 degrees, we collected the fluids at room temperature. Volumes varied from 1 to 18 ml, after approximately 10 hours. The fluids were collected in 20 ml, acid washed syringes and subsampled as shown in Table 30, and when available fluids were analyzed shipboard for salinity, alkalinity and ammonium.

Table 30: Subsamples collected from rhizon samples.

Analyses	Volume (ml)	Treatment
Shipboard and major ions	0.3 to 8	Plastic scintillation vials, no treatment
Oxygen/hydrogen isotopes	2 to 4	4 ml glass vials (Chromatographic Services), no treatment
Anions	1 to 2	Plastic (Sarstedt) 2 ml and 1.5 ml cups
Cations (minors)	1 to 2	Plastic (Sarstedt) 2 ml and 1.5 ml cups, acid washed (10% HNO_3 overnight), acidified with 20 ul ultrapure concentrated (65%) HNO_3

11.1.1 Shipboard Analysis

When enough fluid was available, salinity was measured using a Kruss salinometer with a precision of ± 0.1 PSU calibrated daily against IAPSO standards of 9.989, 29.968, 34.993, and 38,022 PSU. For samples with limited volume, the salinity was measured using an ATAGO Master handheld refractometer, with limited resolution of only 1 PSU.

Alkalinity was determined with a pH-controlled titration to a pH just under 4. The pH electrode was calibrated against pH 4, 7 and 10 Hanna Instrument buffers. A 0.5 ml sample aliquot was diluted with 9.5 ml of distilled water, and sequential aliquots of 0.01M HCl standard were added while constantly stirring in an open beaker. The concentration and amount of acid used was recorded as well as the start and final pH value. Alkalinity was calculated using the equation:

$$\text{Alkalinity (mol/l)} = (H^{+}_{added} - H^{+}_{excess} + H^{+}_{initial}) / v_0$$

$$\text{Alkalinity (mol/l)} = [(v_{HCl} * c_{HCl}) - 10^{-pH}_{final} * (v_0 + v_{HCl}) / f_H^{+} + 10^{-pH}_{start} * v_0 / f_H^{+}] / v_0$$

v_{HCl} - volume of HCl added to final pH in mL
c_{HCl} - molar concentration of HCl added (usually 0.01molar)
pH_{start} - initial pH – may be neglectable if well above 7
pH_{final} - final pH – measure as precise as possible, should be between 3.9 and 3.5
v_0 - initial sample volume in mL
f_H^{+} - activity coefficient of H^{+} in seawater .. use 0.79

Ammonium was determined from a change in conductivity of across a PTFE membrane, using a conductivity meter with flow-through-cell (Amber science model 1056, cell 529). The sample is introduced to a 100 µL loop and pumped through the system using a Peristaltic pump (Ismatec IPC). On one side of the membrane, an alkaline buffer (NaOH+Na-citrate) converts ammonia to NH_3. NH_3 diffuses across the membrane, across which, an HCl solution that converts NH_3 back to NH_4^+, and the resulting conductivity drop was recorded in a strip-chart recorder. Standard curve was prepared daily using dilutions of a single element 1000 mg/l ammonium standard (Roth) to make 0.1, 0.25, 0.5, 1, 2.5, 5, 10 and 20 ppm standards. The method is reported not to have H_2S interference, however some samples showed a higher conductivity than baseline at injection and no detectable ammonium, suggestive of other interferences.

11.1.2 Preliminary Results

Venere Mud Volcano

A striking observation from the pore fluids is the general freshening of the fluids in the Venere mud volcano area, as illustrated in Figs. 126 and 127. The most extreme freshening was observed in the summit, where cores collected in the youngest flow show salinities down to 10 PSU as shallow as 20 cmbsf. Gravity and pressure (DAPC) cores collected in this recent flow also show fluids with 10 PSU salinities down to 500 cmbsf. A series of cores collected from the most recent flow, with increasing distance from the summit, revealed that magnitude of pore fluid freshening decreases as the flow ages. Pore fluids show values of 15 PSU in the upper20 cmbsf in stations >100 m away from the summit. Gravity and pressure (DAPC) cores also show a decrease in the magnitude of freshening away from the summit. Stations that sampled seeps on the NE flank of the caldera, as well as those that targeted nearby older flows, show significant less freshening, with minimum values of 25 or 35 PSU.

Pore fluids collected along the rim in the location of Flares 4 and 5, show a decrease of only ~2 PSU in the upper 15 cmbsf, even in areas of clear methane seepage (Fig. 129). Even less freshening is observed in the area of Flare 1, with no significant deviation from bottom water values (Fig. 128). Penetration at Flare 2 was more difficult, so cores are in general quite short. Nonetheless salinity decrease observed is approximately 1 PSU (Fig. 128). Figure 129 also includes data from a reference MIC core collected to the south of the Venere area, and shows salinity values consistent with bottom water values throughout the 20 cm recovered.

At all the cored sites, there is no significant difference in salinity values across a seepage area from highly active bubbling to more background sediments, indicating that the freshening is a more regional effect. In contrast to the salinity distribution, the alkalinity profiles show clear

heterogeneity, indicating that alkalinity is controlled by methane seepage activity, most likely reflecting alkalinity production by AOM at the seepage sites (Figs. 131-134). Pore water collected in areas of bacterial mat or clam communities show enhanced values, up to 50 mM, and in contrast, cores collected just 1 meter away from the seepage area, with no signs of seepage, have alkalinity values of less than 10 mM. It is interesting to note that in some cases, a brown sediment cover is not indicative of a real background situation, as observed in Dive 341 in the area of Flare 1. Cores collected over "background-looking" areas still show high alkalinity, but at close inspection of the sites sampled by the ROV show that the sediments immediately below the surface have a black coloration indicative of sulfide minerals. Figure 134 also includes data from a reference MIC core collected to the south of the Venere area, and shows low alkalinity values consistent with limited organic carbon cycling, probably from organic carbon diagenesis.

Cetus and Nikolaus MVs

Seafloor observation at these two mud volcanoes indicated the flows to be generally old, and no sign of recent gas seepage was observed, consistent with a lack of flare images after repeated acoustic surveys of the area. However bottom water samples collected near the seafloor indicate presence of methane in the crater of both volcanoes (Fig. 130). Salinity data in push core from Cetus MV has almost near seawater values throughout the core; however a gravity core from this area has a clear indication of pore fluid freshening at depth, showing values down to 15 PSU below 50 cmbsf. This striking observation indicates that whereas at present this mud volcano is inactive, it has experienced upward advection of deep-sourced fluids, with low salinities in the recent past.

Salinity values of a push core retrieved from Nikolaus MV are consistently freshened, with an overall decrease of 2 PSU relative to bottom seawater. At this location there is also high methane concentration of a sample collected near the seafloor, indicating that this is indeed a mud volcano, and that it experiences upward advection of deep-sourced fresh and methane-rich muds, even though at a much reduced activity than observed Venere.

Alkalinity in push cores from both Cetus and Nikolaus MVs are quite low, at about 5 mM (Fig. 135). However consistent with the salinity data from the gravity core recovered from Cetus, alkalinities here also show a dramatic increase from near surface low values to ~ 23 mM below 40 cmbsf. These data most likely reflects generation of alkalinity by AOM in the methane rich fluids.

Table 31: Summary of samples taken for geochemistry, microbiology and physical properties during Exp. M112.

Push cores

Dive 339 Venere MV Flare 1

GeoB	PW Sample number	DNA (#)	FISH (#)	Volatiles	Mag suscept	Porosity	Comment
19221-4				1			In bacterial mat within bubble stream
19221-6				1			In bacterial mat at rim

Dive 341 Venere MV Flare 1

GeoB	PW Sample number	DNA (#)	FISH (#)	Volatiles	Mag suscept	Porosity	Comment
19230-5	17-22				Y		Next to Marker 1 emission Flare 1

19230-12a	29-35				Y		Within bacterial mat – for rhizons sampling
19230-12b		9		10		10	
19230-13a	23-28				Y		Outside bacterial mat - for rhizons sampling
19230-13b		5		7		7	
19230-14a	11-16				Y		At another patch, within the bacterial mat - for rhizons sampling
19230-14b		8		10		14	

Dive 342 Venere West Summit (no cores for volatiles or microbiology)

GeoB	**PW Sample number**	**DNA (#)**	**FISH (#)**	**Volatiles**	**Mag suscept**	**Porosity**	**Comment**
19232-3	35-40						White patch, apparent crystals
19232-6	41-42						Inside caldera, low penetration
19232-7	43-48						Inside caldera softer sediment

Dive 343 Flare 4 and 5

GeoB	**PW Sample number**	**DNA (#)**	**FISH (#)**	**Volatiles**	**Mag suscept**	**Porosity**	**Comment**
19240-10	77-81				Y		Within bacterial mat, ~100 m NE of Flare 5
19240-12	73-76				Y		~1m east of bacterial mat (out of the mat)
19240-15	67-71				Y		Edge of mat and clam structure R4
19240-16		4		5		6	PC 18 volatile, 1 ASS for mineralogy

Dive 344 Venere west summit

GeoB	**PW Sample number**	**DNA (#)**	**FISH (#)**	**Volatiles**	**Mag suscept**	**Porosity**	**Comment**
19242-6	92-96				Y		Fresh mud flows at outflow center, close to T stick
19242-10	82-86				Y		North of youngest mud flow - hemipelagic drape? Near vicinity of Flare 3
19242-11	98-102				Y		Paired with PC-15
19242-12		9		7		7	Volatile core. Some samples taken for minerals as well
19242-14	87-91				Y		Outflow centre, 2-3 m from summit close to T-stick, paired with PC-16
19242-15		7 + 1 of surface water		7		6	Core for volatiles. Film of organic looking stuff floating on top. Sampled on centrifuge tube. Aerobic methane oxidizers?
19242-17	103-107				Y		Outflow centre, 10 m from summit, close to T stick, sediment in core compresses
19242-18		7		6		6	Outflow centre, 10 m from summit, sediment in core compresses, for volatiles PC 5, paired with PC R5 above

Dive 345 Venere Flares 4 and 5

GeoB	PW Sample number	DNA (#)	FISH (#)	Volatiles	Mag suscept	Porosity	Comment
19249-7	135-139						In proximity of bubbling site, rhizon core, paired with core 15. LOTS of clams throughout the core length.
19249-8		11		13		12	LOTS of clams throughout the core, no "clean" sediment to sample
19249-12	140-143						Background station rhizon core paired with a core for volatiles, ~ 5 m from bubble stream on brown sediment
19249-14		5		6		4	

Dive 346 Venere Flares 4 and 5

GeoB	PW Sample number	DNA (#)	FISH (#)	Volatiles	Mag suscept	Porosity	Comment
19252-7		5	6			5	North of WP2, short core, hard bottom. Push core R1 but had no pre-drilled holes, used for volatiles and FISH
19252-10	144-148						At whitish mat, surface with white "crystals"
19252-14	149-153						At Flare 5, north of Marker 2- rhizon core
19252-15		6		7		6	At Flare 5, north of Marker 2, volatile core. PC18

Dive 347 Cetus Mud Volcano

GeoB	PW Sample number	DNA (#)	FISH (#)	Volatiles	Mag suscept	Porosity	Comment
19253-12	154-158						No mud flow or seepage activity apparent. Brown hemipelagic material

Dive 348 Nikolaus Mud Volcano

GeoB	PW Sample number	DNA (#)	FISH (#)	Volatiles	Mag suscept	Porosity	Comment
19255-7	180-183						Push core R5- no seep activity. Very hemipelagic looking, "background"?
19255-8		4	2	7		6	PC19 for volatiles, paired

Dive 349 Venere Summit flows

GeoB	PW Sample number	DNA (#)	FISH (#)	Volatiles	Mag suscept	Porosity	Comment
19258-4	195-199						Push core R4. At bacterial mat on flank of Flare 3
19258-9	200-204						Push core R7. On the "older" mud flow west of the most recent flow, some darker sediment apparent underneath hemipelagic cover
19258-11	205-208						Push core R8. Second of three stations ~140 m from the summit. Brown cover on the flow. Very

							"fluid" sediment
19258-12		10		11		10	Push core 3. Third of three stations ~150 m from the summit. Core for volatiles, in close proximity to core R8.
19258-14							Push core R9. Second of three stations ~110 m from the summit. Still brown cover on the flow. Very soft sediment
19258-15		9		10		10	Push core 4. Third of three stations ~110 m from the summit. Core for volatiles, in close proximity to core R9.
19258-17	215-219						Push core R10. Second of three stations ~80 m from the summit. Still brown cover on the flow. Very soft sediment
19258-18		7		8		8	Push core 5. Third of three stations ~80 m from the summit. Core for volatiles, in close proximity to core R10.

Dive 350 Venere Mud Volcano – Flare2

GeoB	PW Sample number	DNA (#)	FISH (#)	Vola tiles	Mag suscept	Poro sity	Comment
19267-4	235-239						Push core R2. Area with clam shells, gas bubbles at the edge of a carbonate slab. Paired with core 4 below
19267-6		2		2			Area with clam shells, gas bubbles at the edge of a carbonate slab. Paired with rhizon core. Core came out of liner, so depths are highly unconstrained and there may be contamination
19267-8	240-242						Push core R3. Near gas bubbles, T stick inserted in proximity resulted in lots of bubble release. Paired with core 9 below
19267-9		5		6		6	Push core 5. Near gas bubbles, T stick inserted in proximity resulted in lots of bubble release. Paired with rhizon core above
19267-10	243-246						Push core R5. Over brown looking sediment in close proximity (~1m) to the bubble site

Gravity and DAPC cores

GeoB	PW Sample number	DNA (#)	FISH (#)	Vola tiles	Mag suscept	Poro sity	Comment
19205-1				4			GC-1, Venere MV Flare 1
19205-2				3			GC-2, Venere MV Flare 1
19206-1				3			GC-3, Venere MV
19227-1						12	GC-7, Cetus MV
19229-2	1-10	3		5		5	GC-8. Basin SE Sicily
19234-1				2			GC-10, Venere MV (East)
19236-1	46-60	10	10 (but 2 were lost	10		10	GC-12 in a bag, Venere MV Flare 1, looking for hydrate.

			during pro cessing)				NOTE microbiology samples were mislabelled as 19235-1 but already in liquid nitrogen could not fix
19236-2	61-66						GC in a bag, Venere MV Flare 1. ANOXIC SEDIMENT SAMPLES at 15-20 and 62-68
19237-1				1			GC-14, Venere MV (West)
19238-1				2			GC-15, Venere MV (West)
19243-2	130-134						DAPC-2 1at Flare 1. Some pressure and gas loss
19244-1				1			GC-16 , Venere MV (East)
19245-1	108-129	16	7	21		20	GC-17 in a bag, Venere MV summit. Bubbles observed upon recovery. VERY gassy core,
19251-1	159-179						DAPC-3 core at Venere MV summit, ~20 L gas
19257-1	184-194						DAPC-4 Venere MV Flare 1
19260-1				3			GC-20, Venere MV Flare 2
19263-1	220-234	9	5	13		13	GC-22 in a bag, Venere MV mud flows, ~80 m from summit.
19264-1				2			GC-23, Venere MV (mud flow 4)
19268-1	262-277						DAPC-6, Venere MV mud flows ~80 m from summit. Gassy and perhaps gas hydrate?
19269-1				3			GC-24, Venere MV (mud flow 1)
19270-1				3			GC-25, Venere MV (mud flow 1)
19275-1				1			GC-26, Venere MV (flank)
19276-1	144-162	9	7	10		10	GC-27 in a bag, Venere MV mud flows, ~150 m from summit
19278-1				3			GC-29, Venere MV (NW flow)
19279-1				3			GC-30, Venere MV
19280-1				3			GC-31, Venere MV
19282-1				2			GC-32, Cetus MV
19283-1	278-294	8		15		15	GC-33 in a bag, Cetus MV center. Core over penetrated
19284-1				4			GC-34, Cetus MV, Core over penetrated
19285-1				6			GC-35, Cetus MV, Core over penetrated
19286-1				5			GC-36, Cetus MV
19289-1				3			GC-37, Sartori MV
19290-1				5			GC-38, Sartori MV

Mini-corer

GeoB	PW Sample number	DNA (#)	FISH (#)	Vola tiles	Mag suscept	Poro sity	Comment
19208-1				2			MIC-1, Venere MV (Flare 1)
19279-3	257-261	9	7	14		13	MIC-3. Background station in vicinity of Venere, away from mud-volcano influence

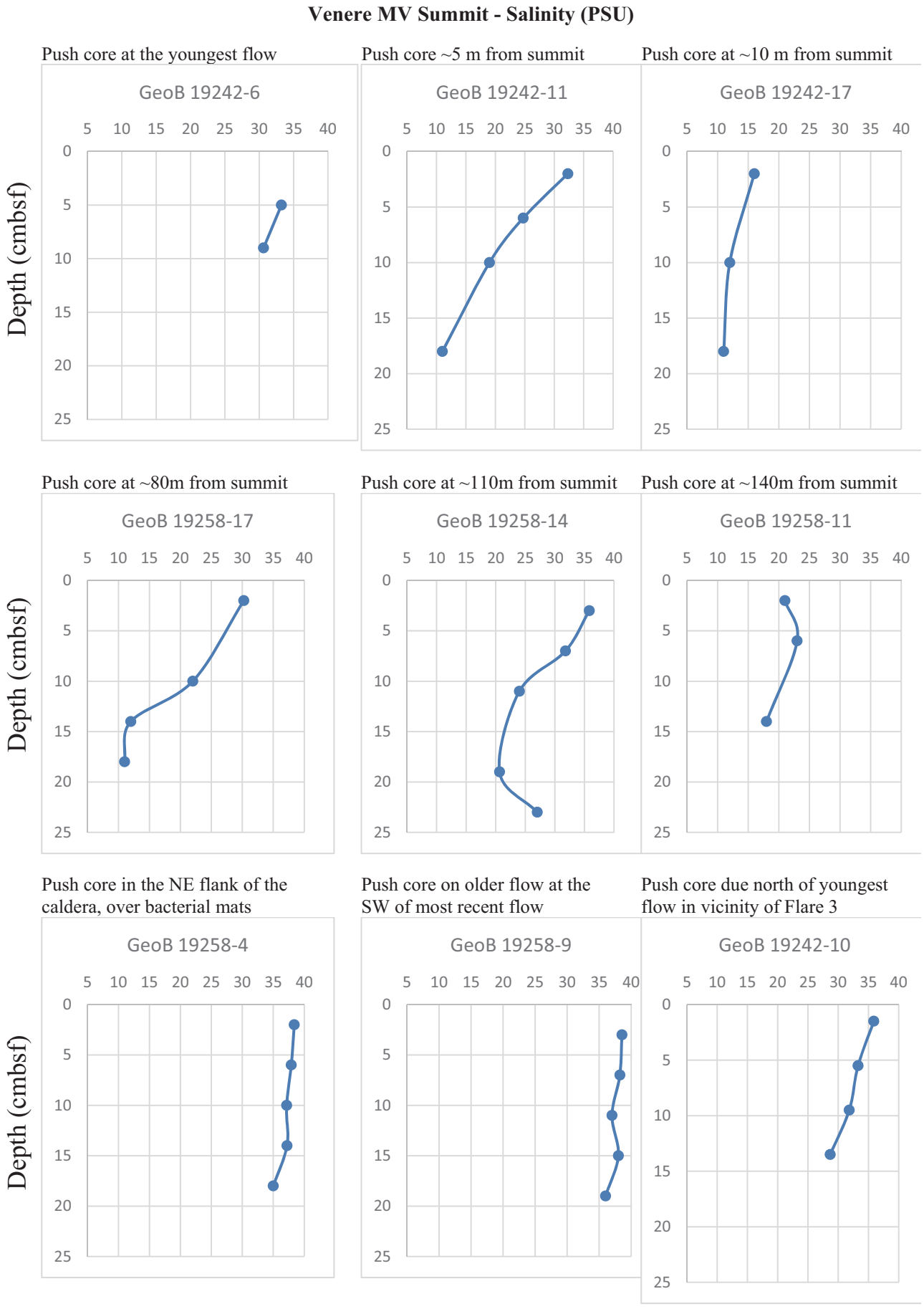

Fig. 126: Salinities at summit of Venere mud volcano from push cores.

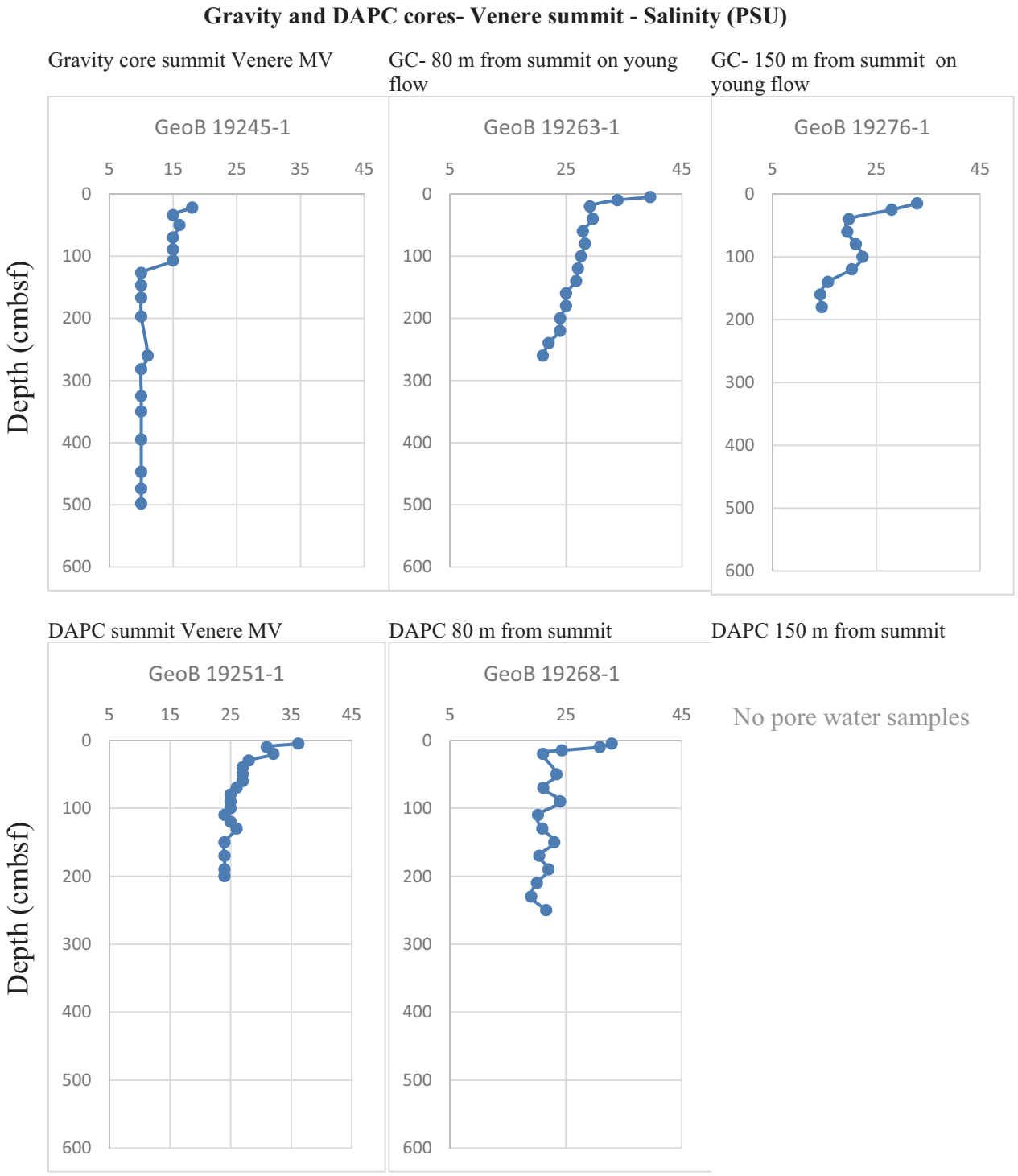

Fig. 127: Salinity data from gravity and DAPC cores recovered from summit of Venere Mud Volcano.

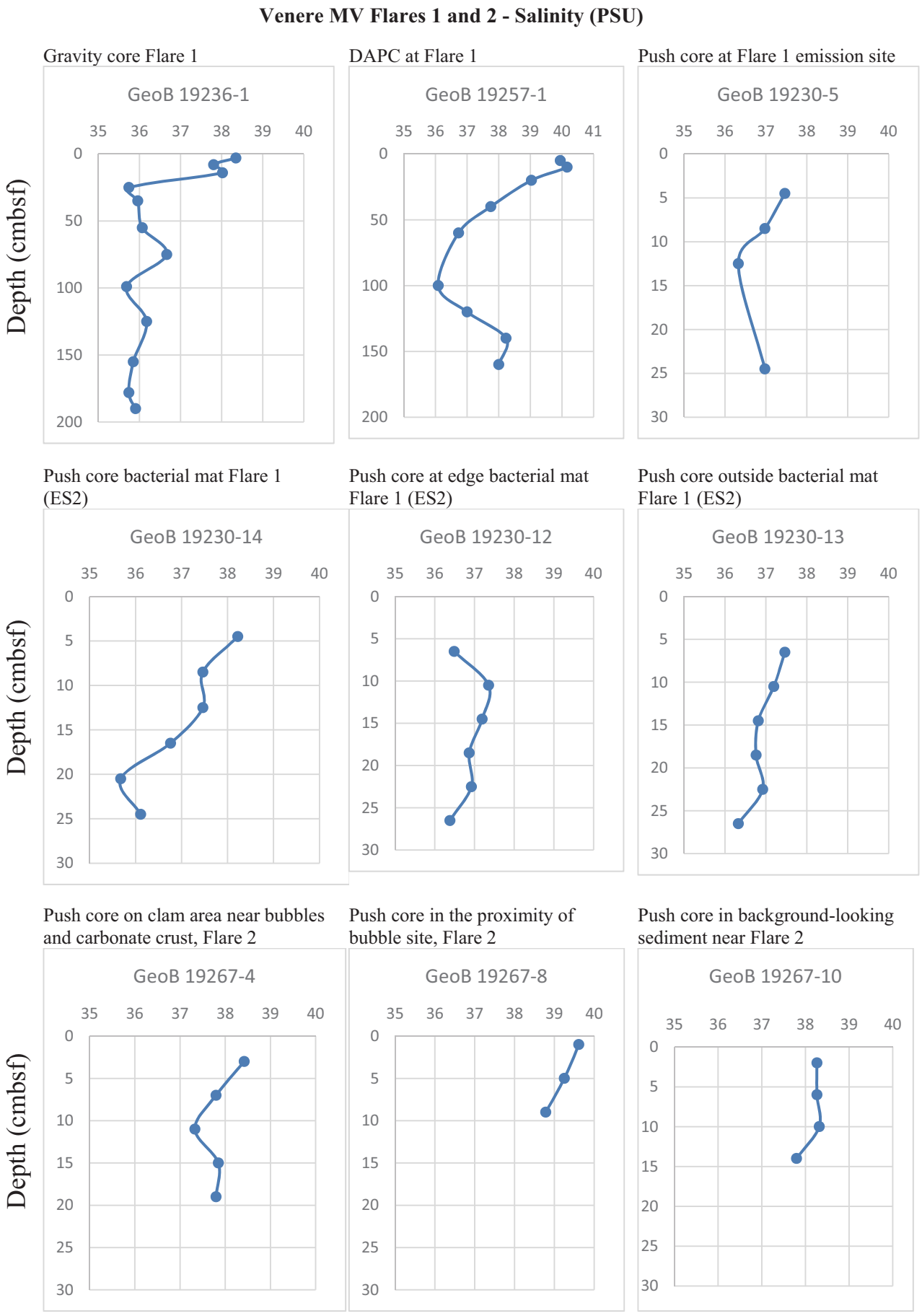

Fig. 128: Salinity in push cores, a gravity core and a DAPC recovered from Flares 1 and 2.

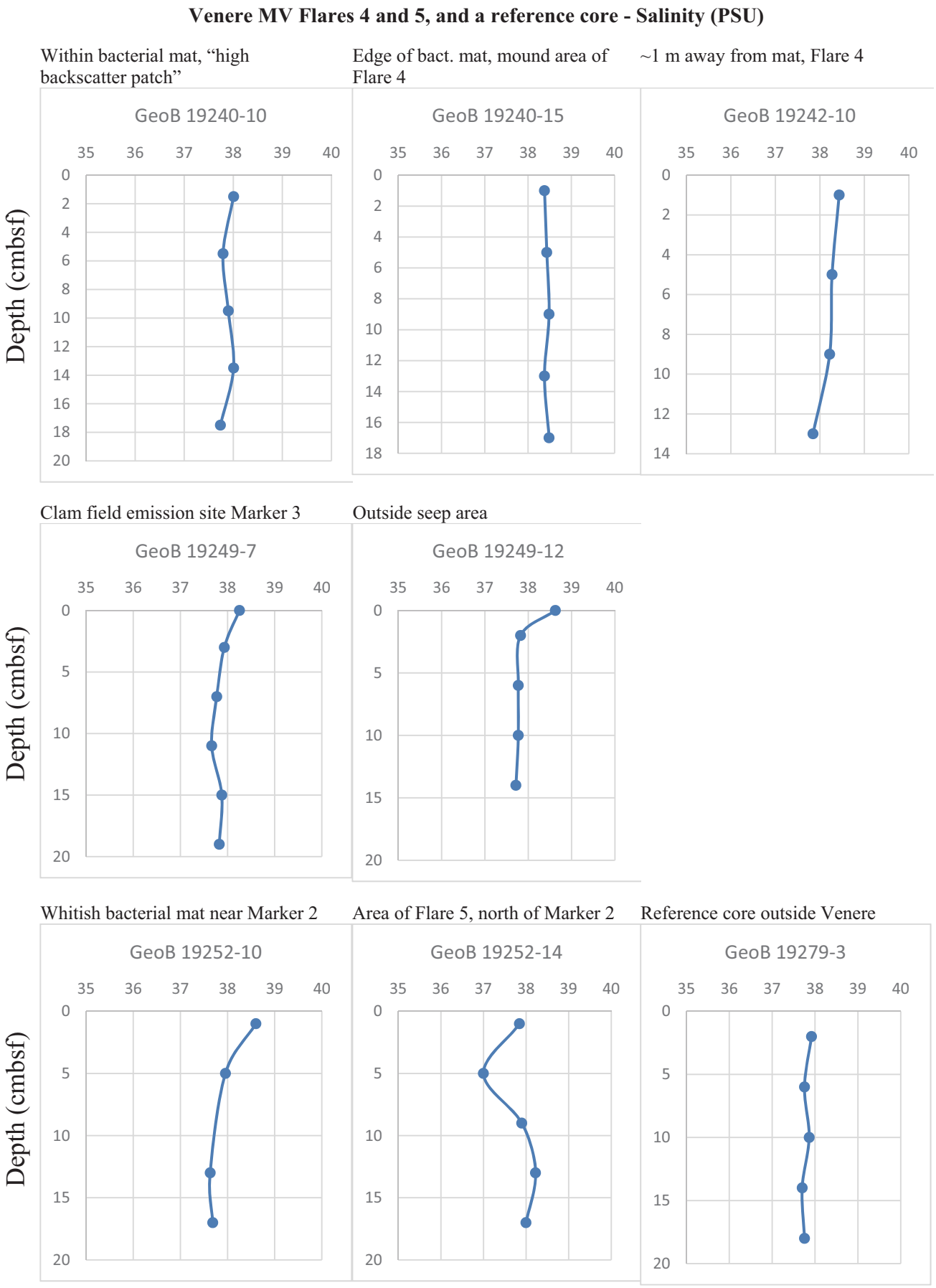

Fig. 129: Salinity in ROV push cores recovered from areas of Flare 4 and 5, and from a reference MIC core outside the Venere area.

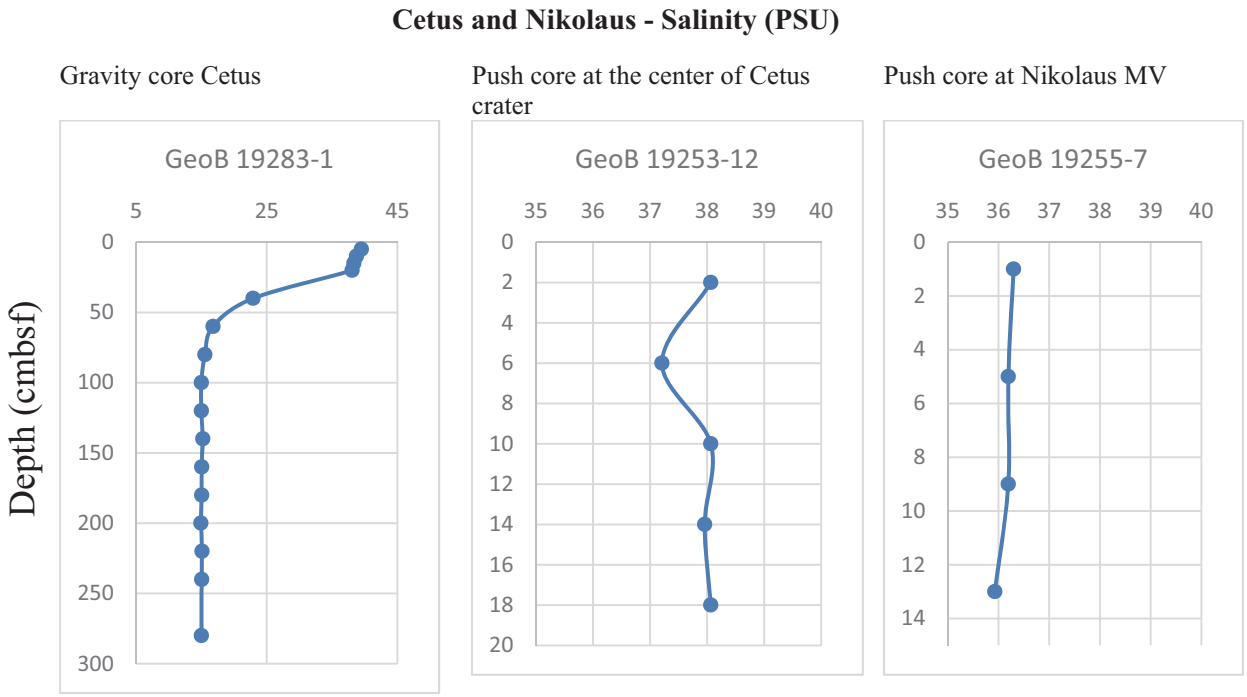

Fig. 130: Salinity in a gravity core and a push core from center of Cetus Mud Volcano and a push core from the center of Nikolaus Mud Volcano. Note the different scales used in gravity and push core data.

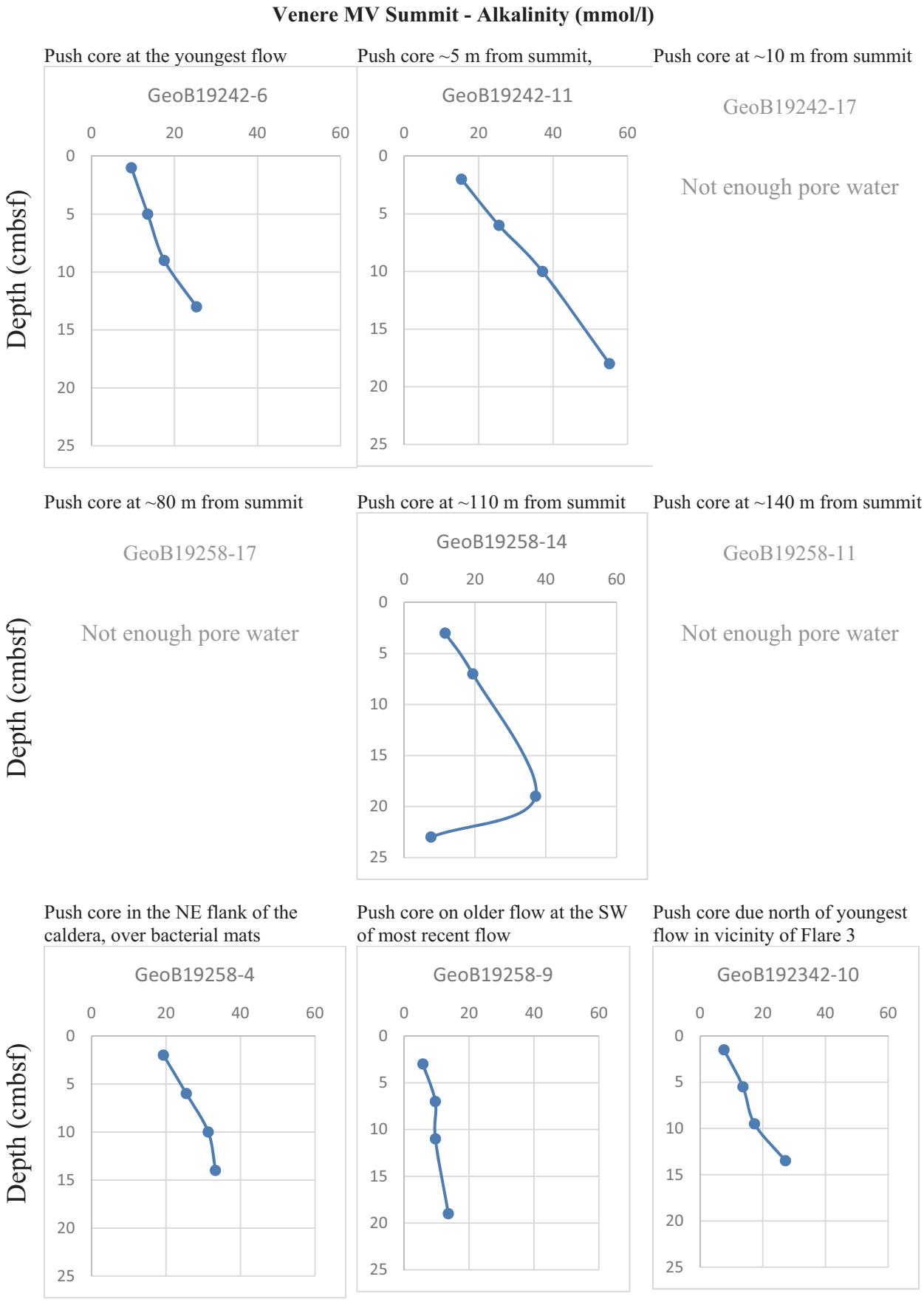

Fig. 131: Alkalinities in ROV push cores from the Venere summit.

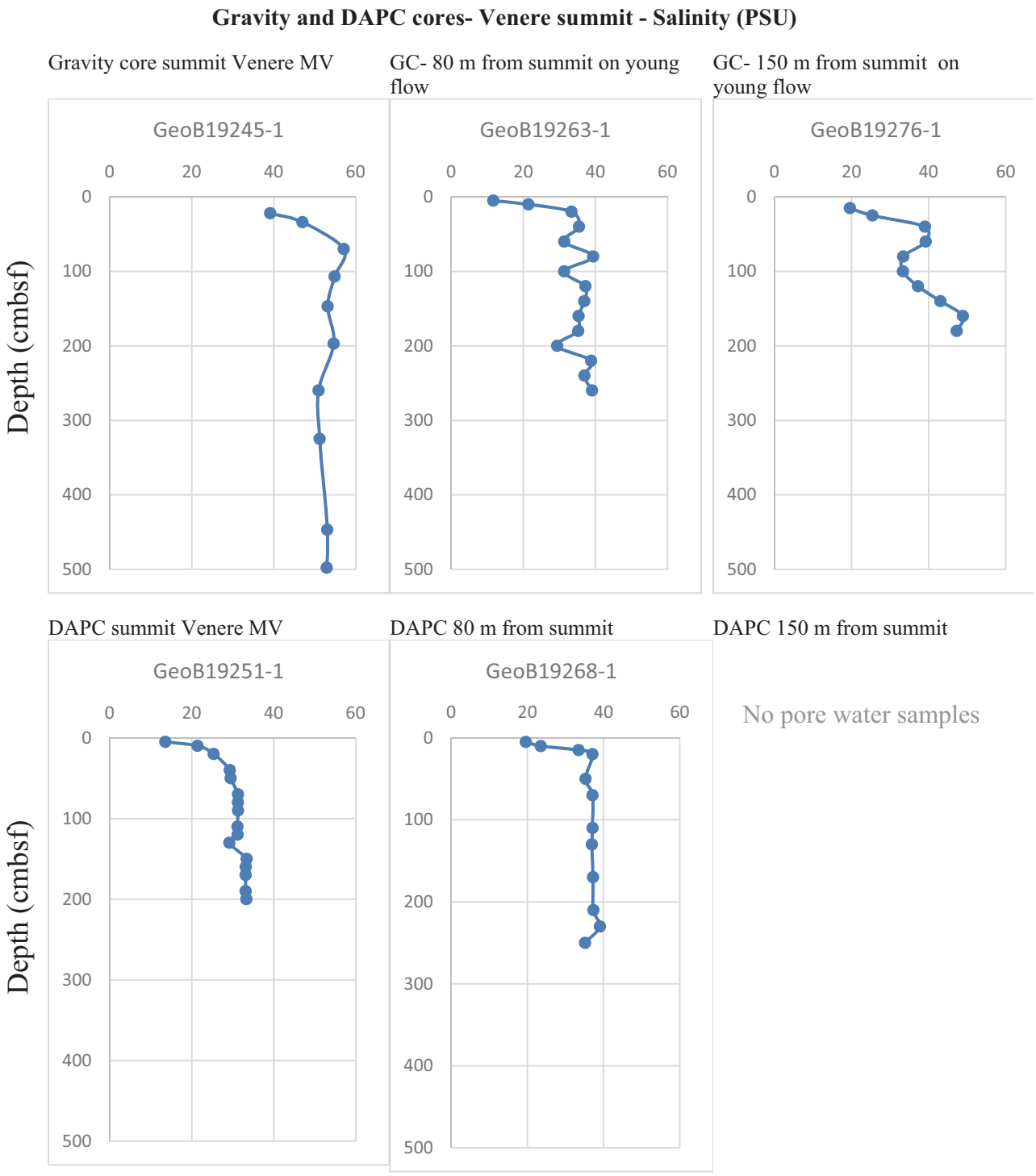

Fig. 132: Alkalinity data from gravity and DAPC cores recovered from summit of Venere Mud Volcano.

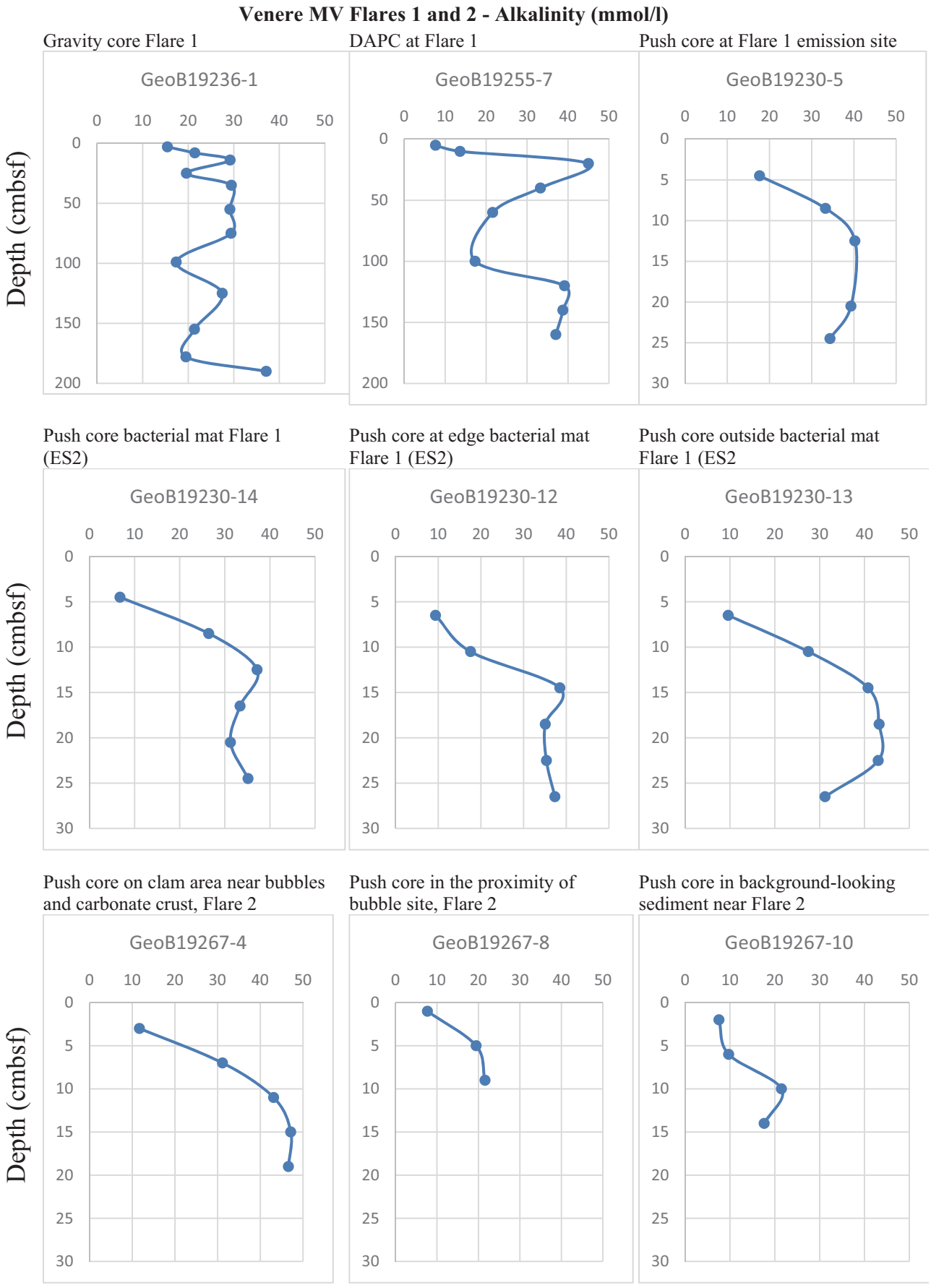

Fig. 133: Alkalinity in push cores, a gravity core and a DAPC recovered from Flares 1 and 2.

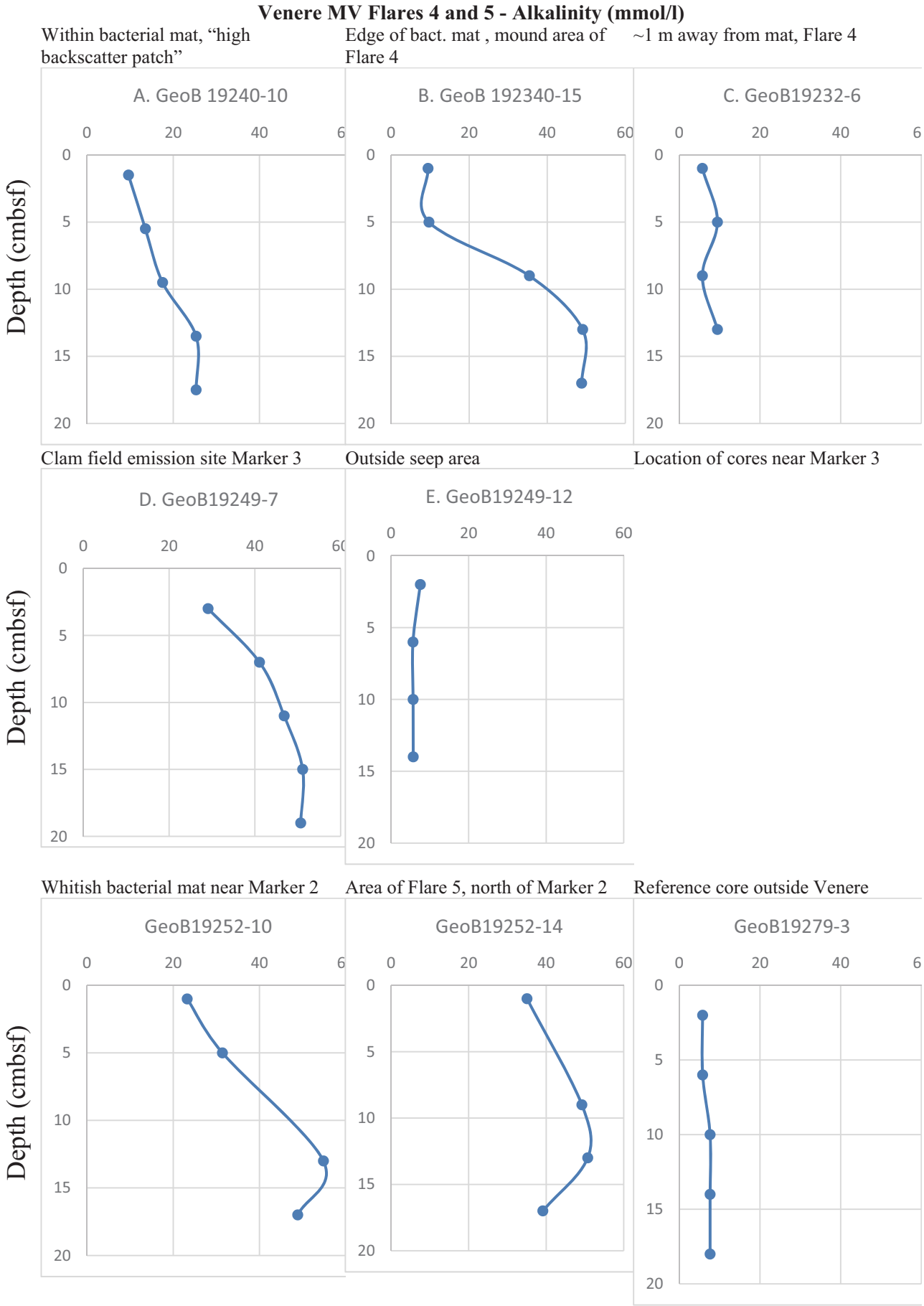

Fig. 134: Alkalinity in ROV push cores recovered from areas of Flare 4 and 5, and from a reference MIC core outside the Venere area.

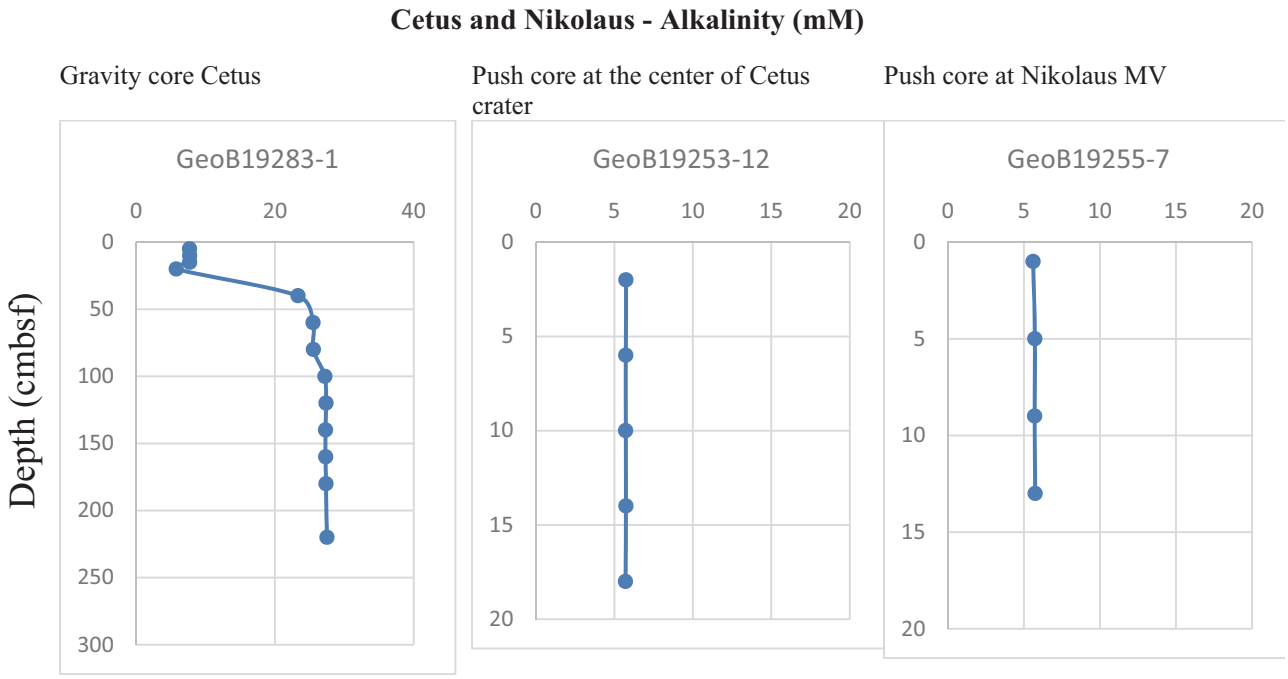

Fig. 135: Alkalinity in a gravity core and a push core from center of Cetus Mud Volcano and a push core from the center of Nikolaus Mud Volcano. Note the different scales used in gravity and push core data.

11.2 Vertical Concentration Profiles of Methane Dissolved in Pore Water

(T. Pape, S. Buchheister, P. Geprägs)

11.2.1 Introduction

The major objective of the works on dissolved methane concentrations in pore waters was to characterize geochemically the nature, strength and history of methane upward migration associated to mud volcanic activity at specific mud volcano sites on the Calabrian arc. Because transport and fate of methane are closely connected to those of other pore water ingredients methane profiles established here and pore water data (Chapter 11.1.) will be jointly evaluated.

11.2.2 Shipboard Analysis

For analysis of methane dissolved in pore water, the headspace technique was used. For this, 3 ml of bulk sediment retrieved with the gravity corer, mini corer (MIC) or push cores during ROV dives were transferred to 20 ml glass vials prefilled with 5 ml NaOH, thus creating a headspace volume of 12 ml. Samples were taken according to selected depth intervals (2-3 cm for push cores and MICs) or 15 to 25 cm for gravity cores in flexible bag liners. For gravity cores in unopened rigid PVC liners, sediment samples were only taken from the segment cuts (1 m distance).

Sediment samples for methane analysis were obtained from 18 push cores (9 ROV dives, 124 samples), 28 gravity cores (138 samples), and two mini cores (16 samples; for location of cores and numbers of samples see Table 31). The majority of push cores recovered from the gas emission sites

at Venere MV contained clam shells in high density often throughout the entire core that made sediment sampling with syringes for analysis of volatiles difficult.

Methane concentrations in the headspace volume were determined using the gas chromatographic system described in Chapter 10.

11.2.3 Preliminary Results and Discussions

Venere Mud Volcano

Push cores and gravity cores taken in the youngest mud flow in the summit area of Venere MV revealed high ex situ concentrations of dissolved methane (> 4.5 mmol L^{-1}; Fig. 136). Remarkably, a tendency of decreasing methane concentrations with increasing depth was observed for a ca. 5 m-long gravity corer (GeoB19245-1) taken in this area (Fig. 137). This trend in methane concentrations hints to mud flow(s) in the recent past that initiated overflow of older, comparably gas-poor sediments by younger gas-rich muds. Diffusion and/or anaerobic oxidation of methane in uppermost deposits were still too uneffective to cause steady-state methane concentrations profiles. Comparably high methane concentrations (> 3 mmol L^{-1}) were also found in push cores and gravity cores recovered from the mud flow several tens of meters distant to the summit (Figs. 136 & 137). Therefore, a high methane storage capacity can be assumed for the mud expelled at the Venere MV. Enrichments in dissolved methane, but generally with ex situ concentrations < 1.5 mmol L^{-1}, were also observed for push cores taken along the MV rim at the emission sites of Flares 1, 2, 4 and 5 (Fig. 138). Cores collected within and outside microbial mats at the emission sites of Flares 1 and 2 did not show significant differences in the extent of dissolved methane concentrations. Moreover, for most cores a trend of increasing concentrations with increasing depth might be attributed to the microbial anaerobic oxidation of methane.

The three push cores collected in the area of Flare 4 showed relatively moderate (< 0.5 mmol L^{-1}) to low methane concentrations in the sediment (Fig. 139). Highest concentrations in the sediment were found for a push core taken in the clam field close to a bubble emission site, while the comparably short core from the assumingly inactive mound close to the emissions site of Flare 4 did not show methane enrichments. Interestingly, for all three cores relative methane enrichments were found in near-bottom water samples. A similar observation with highest methane concentrations close to the seafloor was made for a push core collected at the emission site of Flare 5.

Cetus and Nikolaus Mud Volcanoes

The single gravity core recovered from the central part of the Cetus MV showed enrichments in dissolved methane with ex situ concentrations exceeding 1.0 mmol L^{-1} in samples deeper than 50 cmbsf (Fig. 140). This observation is consistent with significant pore water freshening found at this site and corroborates the assumption of upward advection of deep-sourced fluids in the recent past (Chapter 11.1). The single push core retrieved from the Nikolaus MV did not show methane enrichments in the uppermost 13 cm of sediment (Fig. 140).

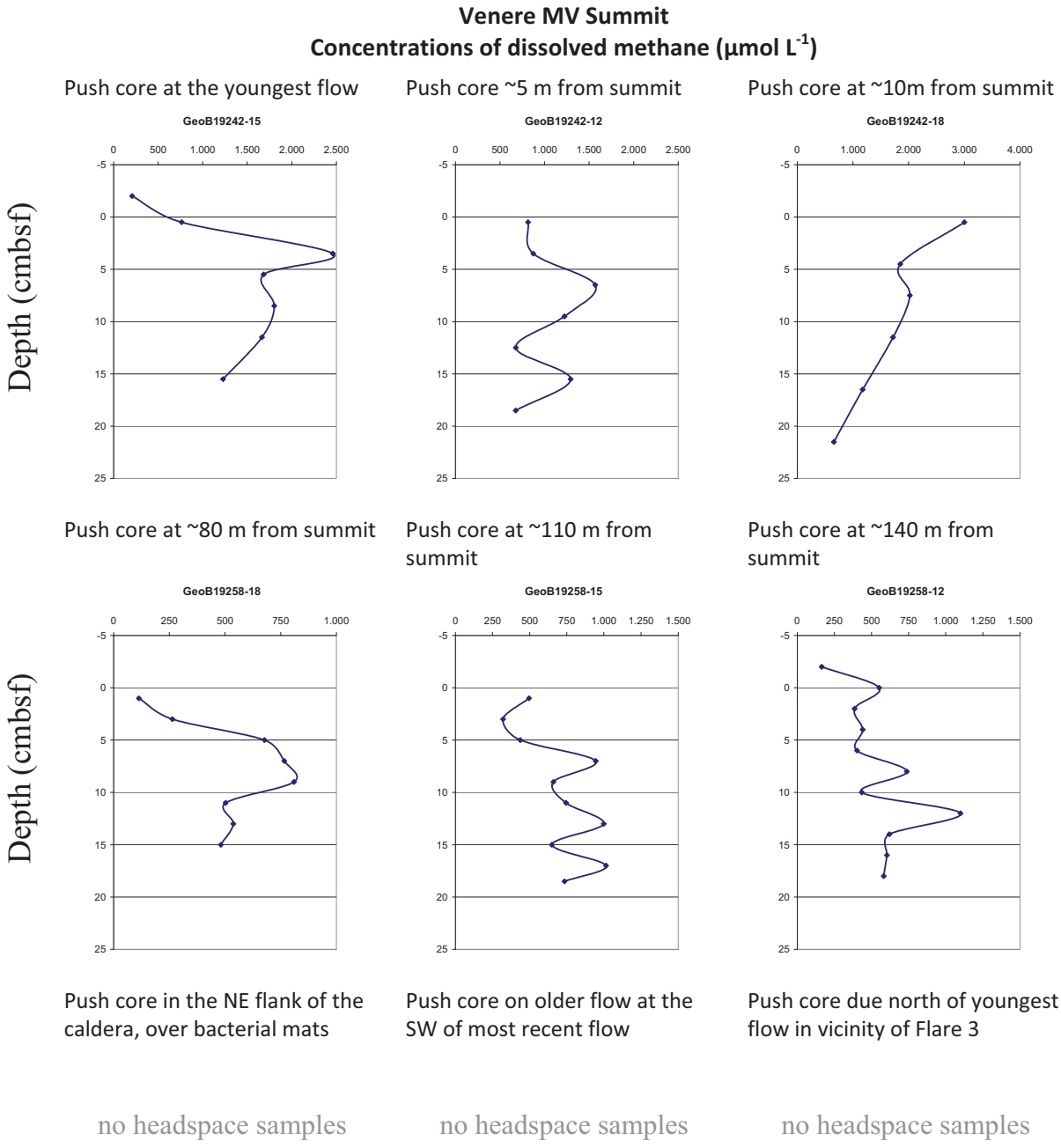

Fig. 136: Concentrations of dissolved methane from push cores recovered from the summit of Venere Mud Volcano.

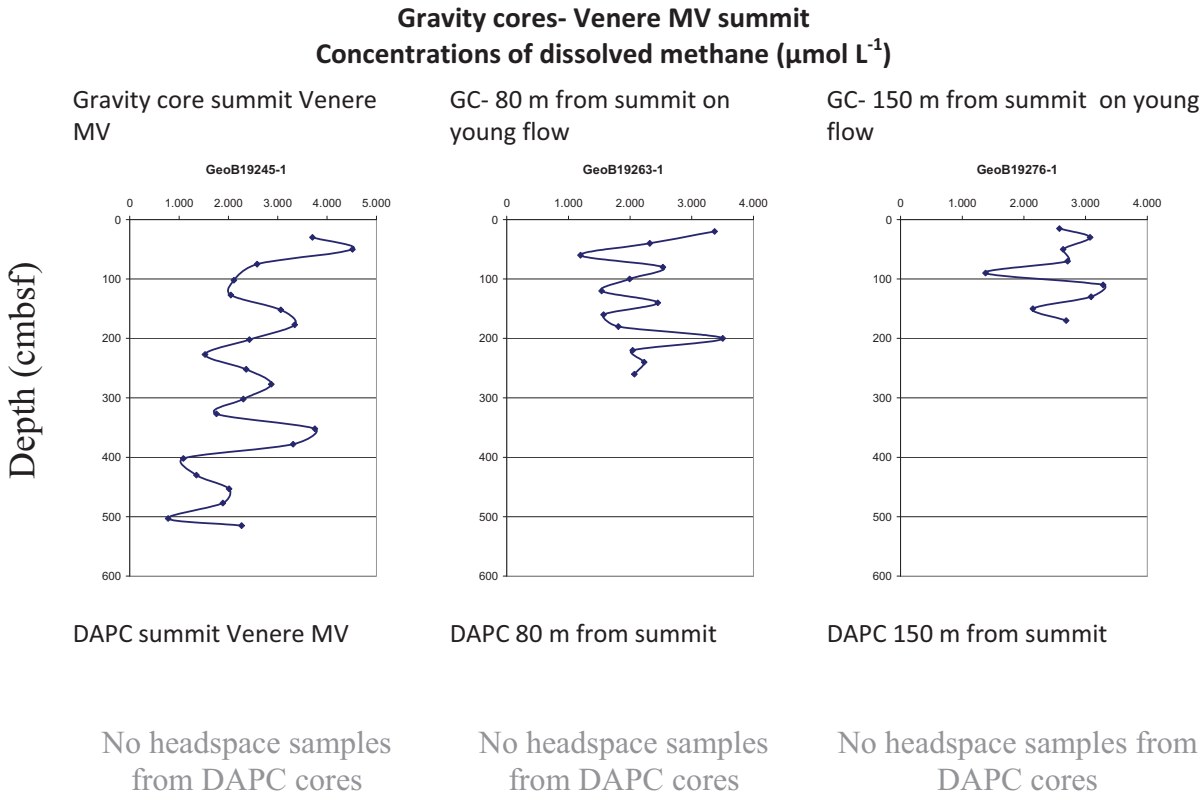

Fig. 137: Concentrations of dissolved methane from gravity cores recovered from the summit of Venere Mud Volcano.

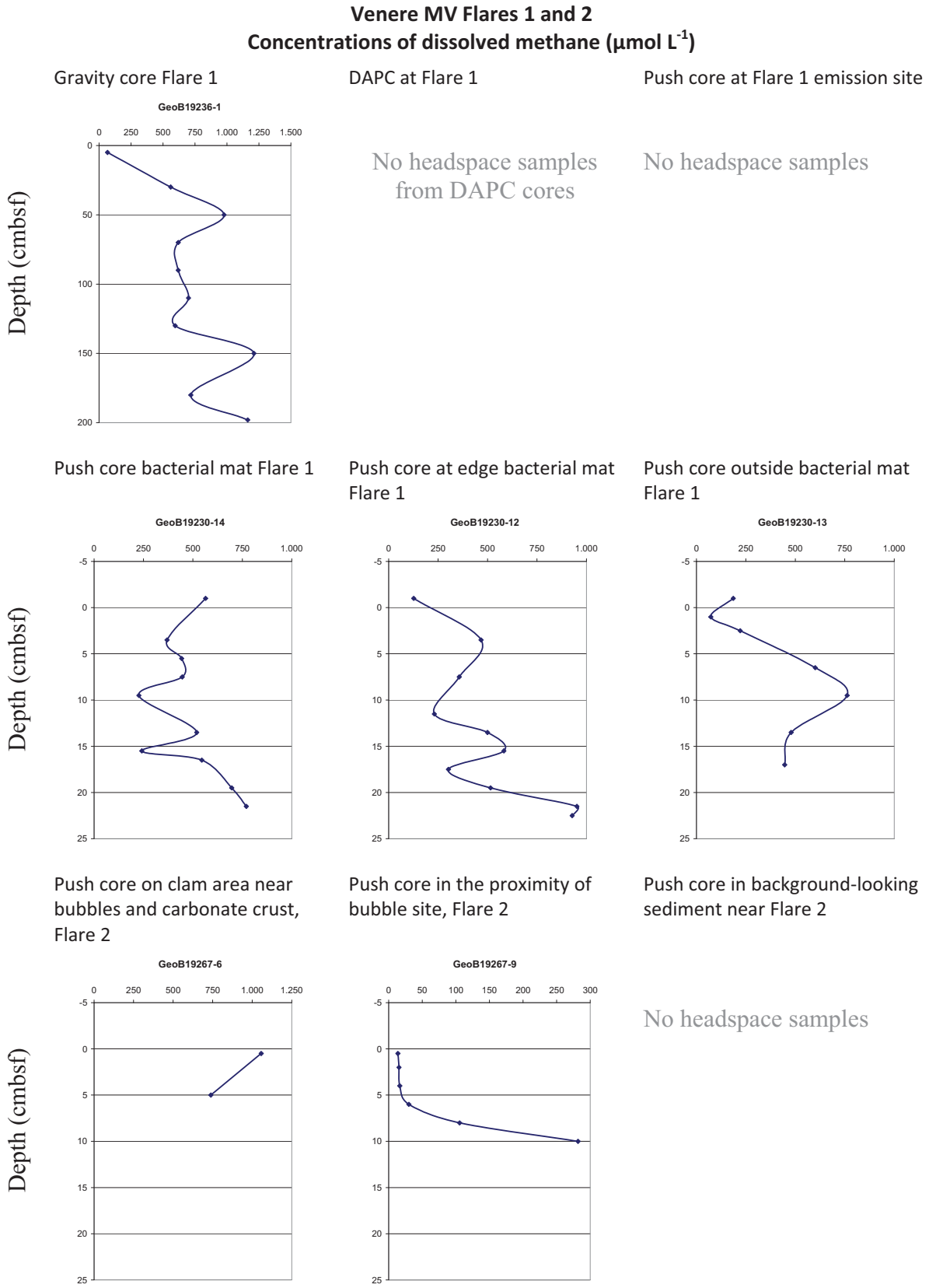

Fig. 138: Concentrations of dissolved methane in push cores and a gravity core recovered from Flares 1 and 2. Note the different scales used in gravity and push core data.

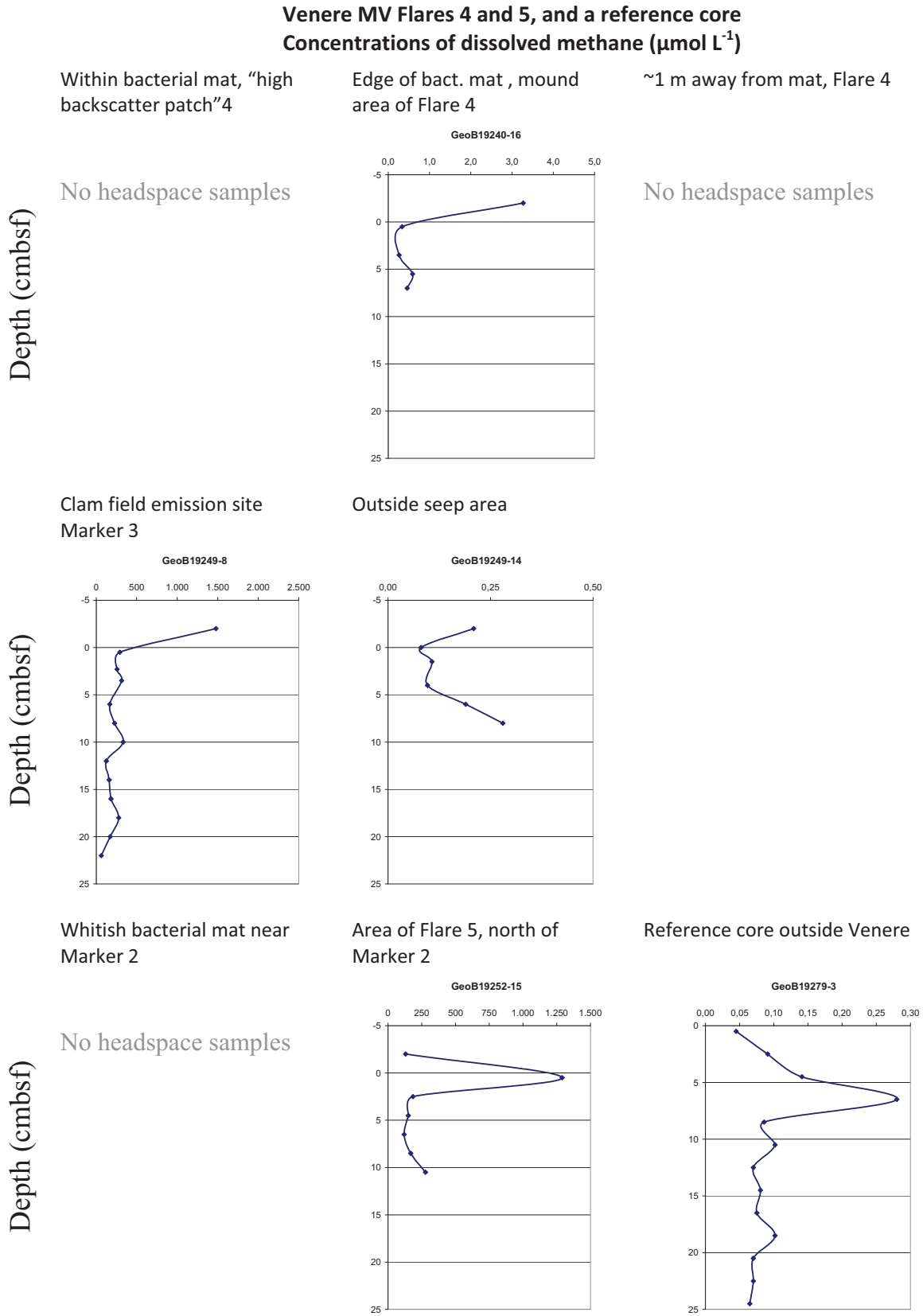

Fig. 139: Concentrations of dissolved methane in push cores recovered from areas of Flare 4 and 5, and from a reference MIC core outside the Venere MV area.

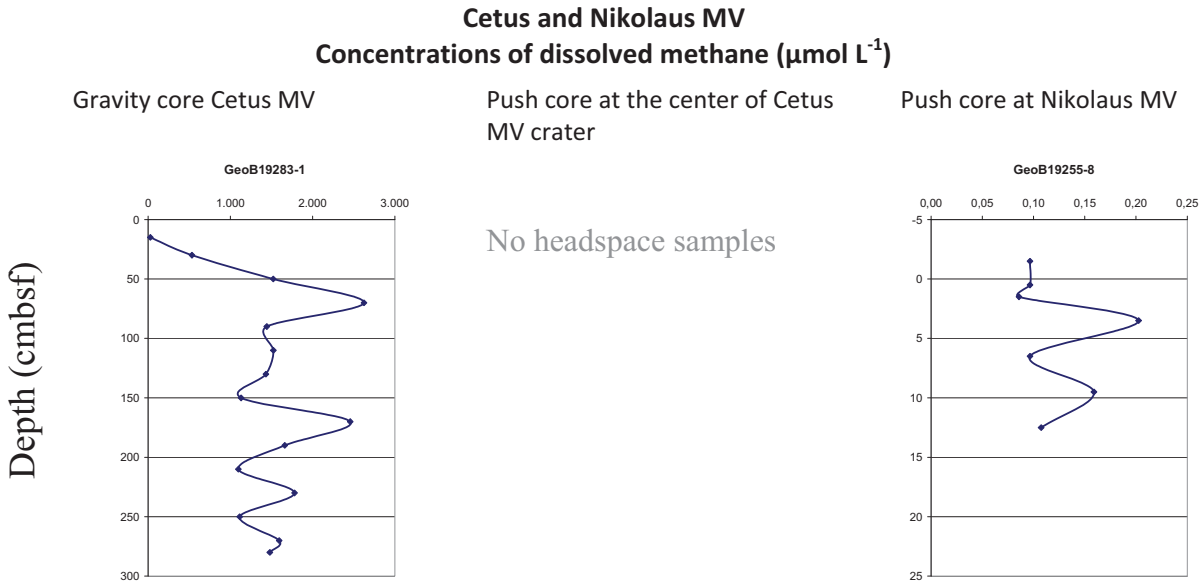

Fig. 140: Concentrations of dissolved methane in a gravity core from the center of Cetus Mud Volcano and a push core from the center of Nikolaus Mud Volcano. Note the different scales used in gravity and push core data.

12 Heat Flow Measurements

(C. Sans I Coll)

12.1 T-Lance

During the second leg of this cruise, 13 positions were selected to conduct heat flow determinations, to get a first impression of heat flow distribution on two different mud volcanoes.

For heat flow density determination, information about the undisturbed temperature gradient is essential as well as the thermal conductivity of the respective material. During this cruise, temperature gradient is measured using a temperature gradient lance (see Fig. 141). Thermal conductivity *k* is measured on core material, sampled at or close to the locations of the gradient lance positions using the using the KD2 Pro instrument.

Fig. 141: Temperature gradient probe equipped with five temperature loggers on the lance and one above the head for bottom water reference temperature.

For temperature measurements, five ANTARES autonomous temperature loggers are mounted onto the lance of a dedicated tool plus one additional for bottom water reference. These loggers have a resolution of approximately 0.001 K and an accuracy of approximately 0.1 K. They were deployed with CTD-17 (GeoB 19265-1) during this cruise for later calibration. This has however not been done yet, and all present results derive only from inter-calibration between the sensors. The relative depth positions on the instrument are: 4.69, 3.98, 3.28, 2.58, 1.88, 0 m with respect to the uppermost water sensor, resulting in 0.7 m spacing for almost all sensors.

For thermal conductivity measurements, the DECAGON DEVICES thermal properties meter KD2 Pro is employed together with the smaller single-needle. The instrument is rated at 5 % accuracy in conductivity.

Table 32: List of all T-Lance measurements conducted on M112.

Meteor Station	HF Station	GeoB	Instrument	Location	Latitude N	Longitude E	Depth [m]
1261-1	HF1470	19248-1	HF-1	Venere MV	38º 36.445'	17º 11.229'	1498
1261-2	HF1471	19248-2	HF-2		38º 36.452'	17º 11.221'	1500
1261-3	HF1472	19248-3	HF-3		38º 36.452'	17º 11.223'	1499
1261-4	HF1473	19248-4	HF-4		38º 36.455'	17º 11.226'	1495
1261-5	HF1474	19248-5	HF-5		38º 36.456'	17º 11.227'	1496
1267-1	HF1475	19254-1	HF-6	Cetus MV	37º 52.959'	17º 28.450'	2258
1267-2	HF1476	19254-2	HF-7		37º 52.806'	17º 28.513'	2254
1267-3	HF1477	19254-3	HF-8		37º 52.754'	17º 28.631'	2250
1272-1	HF1478	19259-1	HF-9	Venere MV	38º 36.461'	17º 11.255'	1494
1272-2	HF1479	19259-2	HF-10		38º 36.455'	17º 11.285'	1499
1272-3	HF1480	19259-3	HF-11		38º 36.436'	17º 11.323'	1505
1272-4	HF1481	19259-4	HF-12		38º 36.400'	17º 11.372'	1515
1272-5	HF1482	19259-5	HF-13		38º 36.430'	17º 11.406'	1519

Cetus MV

The three measurements were conducted across the eastern summit of Cetus Mud Volcano. Both first and last measurements show gradients of 0.02 ºC/m, with a relatively linear profile. The second measurement HF-7, positioned closer to the centre of this smaller mount, has a zigzag behaviour (see Fig. 142).

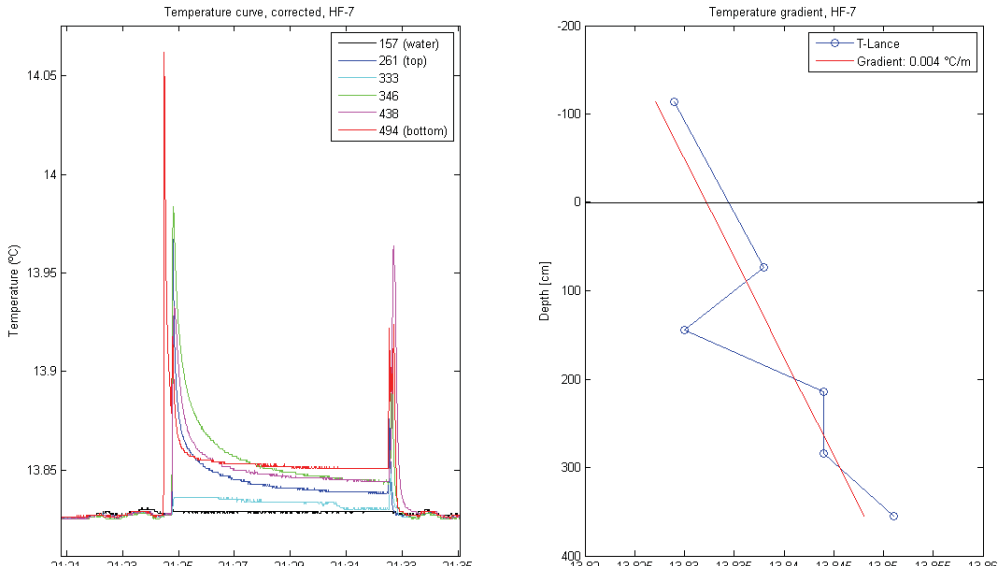

Fig. 142: Second measurement on Cetus MV, showing a zigzag temperature gradient profile.

Venere MV

NOTE: At some point of the GeoB Station 19259 the bottom-most logger got damaged, probably hitting some harder clust, and data could not be read on board. Attempts to read the stored data will be conducted on the lab. For the moment, only the other five could be used.

The first five measurements were conducted on the western summit of the Venere Mud Volcano, and were intended to match the positions of the T-stick measurements at Dive 344 that showed high gradient values in the first meter of sediment (see 12.2 T-stick).

At HF-2, HF-4 and HF-5, temperature values of ca. 26-27 ºC were measured at approximately 5 m depth, while HF-3 showed ca. 24 ºC and HF-1 ca. 20°C. The first three of these profiles (HF-1 to HF-3) show a very linear behaviour, with gradient values of 1.624, 2.878 and 2.405 ºC/m, respectively. Profiles HF-4 and HF-5 show on the other hand a slightly concave behaviour, with gradient values of 2.863 and 2.702 ºC/m, respectively.

The following four measurements were conducted on the eastern mud flow of the western summit, going downwards. Measurement HF-9 shows a concave shape, with ca. 4 ºC/m on the first 2 meters of depth and of ca. 1 ºC/m from 2 to 3 m. The bottom sensor measures a slightly colder temperature than the preceding one. Measurements HF-10 and HF-12 show clearly linear behaviours, with gradients of 1.269 and 0.235 ºC/m. Measurement HF-11 has a very irregular behaviour with a negative gradient, more difficult to interpret (see Fig. 143); the temperature difference between the bottom sensor and the top one is of approximately -0.05 ºC, with a vertical spacing of approximately 2 m. The absolute depth is hard to interpret but given the temperature increase of the water sensor, we consider this was also inside the sediment.

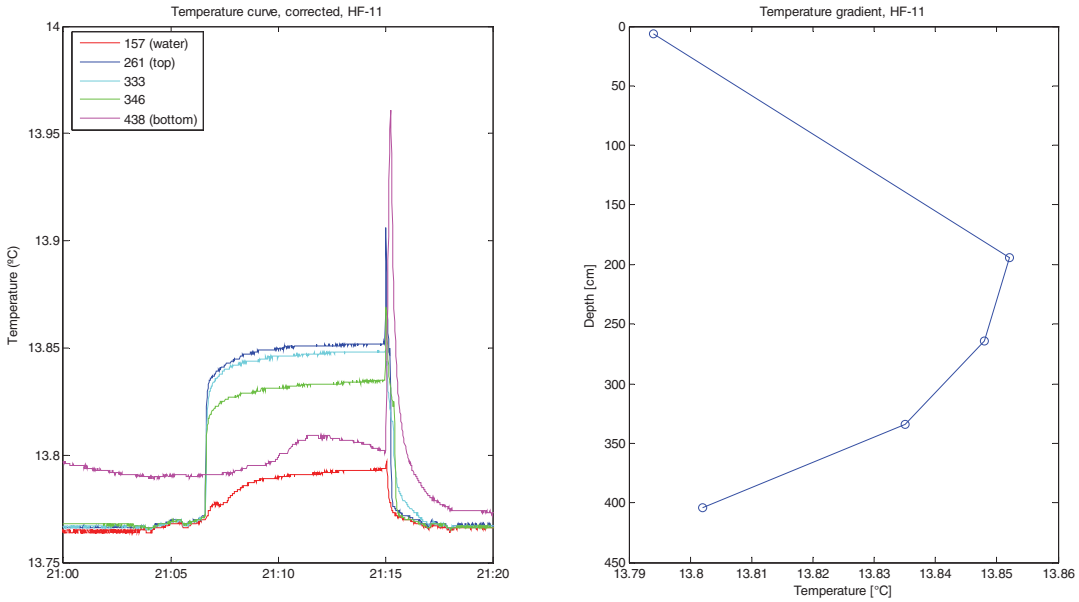

Fig. 143: Irregular gradient of HF-11. Depth values are an interpretation given the increased temperature of the water sensor (red line).

The last measurement was conducted outside of the flow, for comparison purposes. The data suggests that penetration was not complete and the top sensor was still in bottom water. The value of the temperature gradient is 0.041 ºC/m (see Fig. 144).

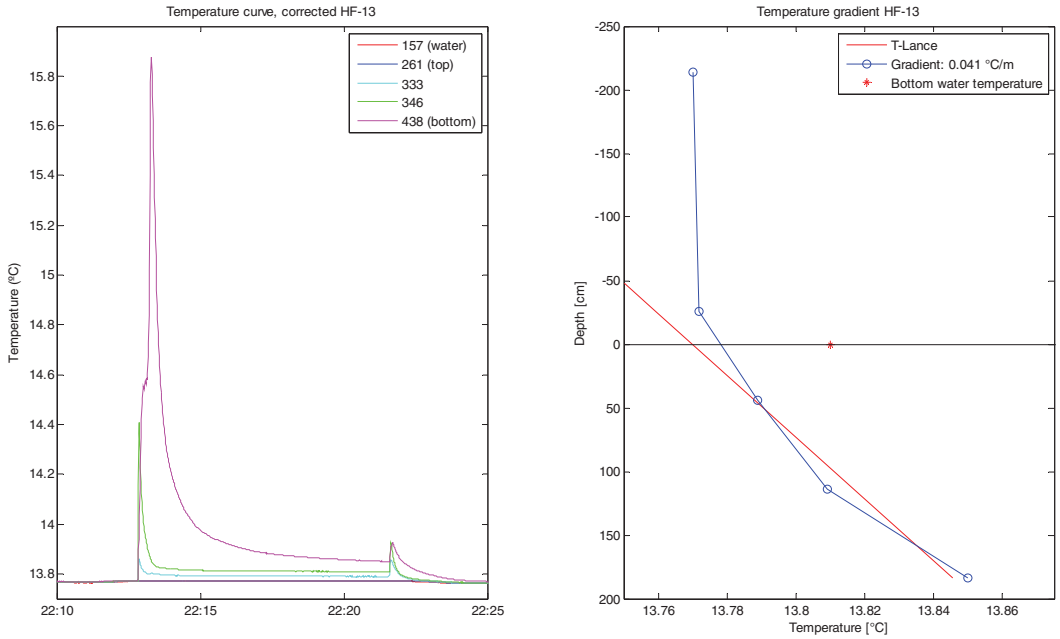

Fig. 144: Measurement HF-13. Please ignore bottom water temperature mark.

12.2 T-stick

The T-stick is a temperature measurement device built by the company RBR Ltd. (Canada). It consists basically of a short lance with temperature sensors and a data-logger (see Fig. 145). The total length and maximum penetration of the lance is 60 cm. Eight temperature probes are evenly spaced with a spacing of 8 cm. The device has a measurable temperature range of -5 – 35°C and a resolution of 0.6 mK. Intercalibration of the probes results in a precision of ± 2 mK.

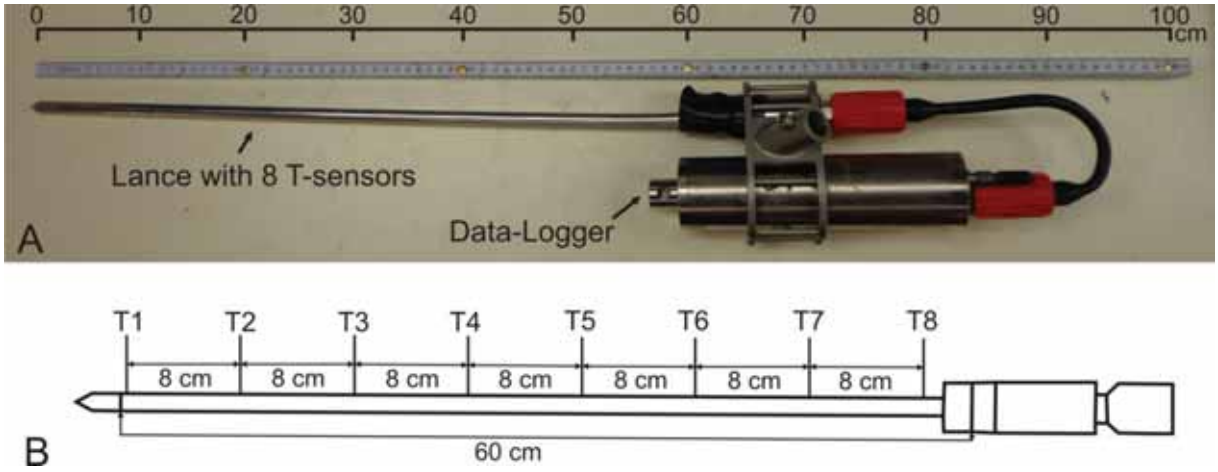

Fig. 145: A) Photograph of the T-stick consisting of lance and data-logger. B) Schematic drawing of lance showing the positions of the temperature probes (T1 – T8).

The device is operated by the ROV and measures temperatures in the uppermost sedimentary layer. The lance was bent several times during deployment which might have damaged the topmost sensor. Logger 013115 was used for all deployments except one; the 24 h long-term deployment was

conducted with the second T-stick and logger 013116. Both devices were deployed with CTD-17 (GeoB 19265-1) for later calibration. This has however not been done yet, all presented results derive only from intercalibration between the sensors.

Venere MV

On Venere MV, ROV dives were conducted to investigate all five known flare sites. The T-stick was deployed at each flare site, locations and calculated gradient are listed in Table 33.

Five measurements were conducted at Flare 1 during three ROV dives. The first gradient shows a background value of 0.010 °C/m, though it should be kept in mind that errors are higher when the gradient is lower and that the profile has a zigzag behavior. The next two measurements are located close together inside a bacterial mat with bubble streams. They show similar gradients of 0.172 and 0.194 °C/m. One profile measured in ROV Dive 341 has a very linear behavior with a gradient of 0.310 °C/m, the other one a concave shape with an average gradient of 0.060 °C/m. Except the first one, all these measurements are highly elevated up to 30 times of the background value of approximately 0.01 °C/m.

Only one T-stick deployment was conducted at Flare 2. This triggered a bubble stream which leads to zigzag temperature curves. The gradient is thus hard to estimate but was calculated to be approximately 0.182 °C/m which is similar to findings at Flare 1.

Eleven measurements exist for Flare 3 at the summit of the western cone. Here, highest gradients of up to 15 °C/m have been measured four times directly on the summit top (14.697, 15.056, 14.362 and 15.261 °C/m). Four other measurements which were also located close to the summit are less with 5 °C/m (5.003, 5.038, 4.820 and 5.453 °C/m), but still extremely elevated with respect to background value. The last three measurements are more similar to what has been observed at Flare 1 and 2, gradients are 0.104, 0.177 and 0.130 °C/m. These were located further away from the top. Almost all of these profiles show a very linear behavior.

The highest gradient of Flares 4 and 5 with 0.210 °C/m was located close to a bubble stream. Four further measurements are in a range of 0.47-0.64 °C/m all profiles show a concave shape. One deployment (ROV-343 (4)) showed temperatures in the upper sediment that are below bottom water temperature at a site of possible gas hydrate occurrence. Two attempts to insert the T-stick failed during Dive 346 due to hard sediments which led to a strong bending of the lance. The second T-stick was deployed along with the sonar ASSMO on the mound of Flare Site 5 and measured for more than 24 hours. Temperature curves show different behavior of the sensors: The four uppermost sensors are influenced by bottom water, the fifth and sixth show rather constant temperatures, and the two lowermost sensors experience small sudden changes and a general decrease of temperature.

Cetus MV

Twelve T-stick measurements were conducted during Dive 347 starting on the outer rim and moving towards the center of Cetus Mud Volcano, and from there on in smaller profiles. Gradients generally increase toward the center, values are 0.12 – 0.51 °C/m. One profile has a zigzag behavior which results in a negative gradient of -0.007 °C/m. In the center of the crater, gradients are high with

0.910 – 0.363 °C/m. Most of the profiles are highly linear, except ROV-347 (11) which has a slightly convex shape.

Nikolaus MV

One dive was conducted on Nikolaus MV during which three measurements were deployed. All of these show very low gradients and a zigzag behavior of the profiles. This zigzag shape leads in fact to negative gradients of -0.001 and -0.002 °C/m for ROV-348 (1) and (3), ROV-348 (2) is with 0.006 °C/m also less than background. These facts point towards low activity of the edifice.

Comparing gradients of all three mud volcanoes, it may be assumed that Venere MV is the most active one and Nikolaus MV rather inactive. The highest activity at Venere MV is located in the center.

It is interesting to observe that the highest gradients have the most linear shape. Also intriguing is the observation that there are in total five measurements from two different locations that have an explicitly concave shape and similar gradients of approximately 0.06 °C/m. The zigzag behavior of some profiles may result in negative or low gradients that are hard to interpret.

Table 33: List of all T-stick measurements conducted during Cruise M112.

Station	GeoB	Latitude	Longitude	Gradient	Profile	Remarks
		N	E	(°C/m)		
Venere MV (Flare 1)						
ROV-337 (1)	19202-2	38°37.084	17°11.593	0.010	zigzag	
ROV-339 (1)	19221-3	38°37.095	17°11.602	0.172		In bubble stream, lance tilted
ROV-339 (2)	19221-5	38°37.094	17°11.600	0.194		In bacterial mat without bubble stream
ROV-341 (1)	19230-3	38°37.095	17°11.609	0.310	linear	
ROV-341 (2)	19230-10	38°37.102	17°11.630	0.060	concave	T-Stick in between bacterial mat patches, soft sediment
Venere MV (Flare 2)						
ROV-350 (1)	19267-7	38°36.100	17°12.564	0.182		Near gas bubbles, insertion causes bubble stream
Venere MV (Flare 3)						
ROV-342 (1)	19232-2	38°36.433	17°11.258	0.104		Hard underneath, on a white patch
ROV-342 (2)	19232-5	38°36.433	17°11.258	0.177	linear	
ROV-344 (1)	19242-4	38°36.453	17°11.223	14.697	linear	In center of mud outflow, soft sediments
ROV-344 (2)	19242-7	38°36.453	17°11.223	15.056	linear	In curved depression
ROV-344 (3)	19242-8	38°36.456	17°11.220	5.003	linear	
ROV-344 (4)	19242-13	38°36.454	17°11.225	14.362	linear	Close to summit
ROV-344 (5)	19242-16	38°36.457	17°11.226	15.261	linear	
ROV-349 (1)	19258-2	38°36.428	17°11.287	0.130	linear	At bacterial mat on flank of Flare 3
ROV-349 (2)	19258-10	38°36.395	17°11.361	5.038	linear	On oldest flow, lance sank slightly into sediment
ROV-349 (3)	19258-13	38°36.419	17°11.328	4.820	linear	60 m up the mud flow, soft material

ROV-349 (4)	19258-16	38°36.450	17°11.283	5.453	linear	60 m up the mud flow, beginning of concave structure
Venere MV (Flare 4+5)						
ROV-343 (1)	19240-4	38°35.457	17°12.021	0.210		Close to bubble stream
ROV-343 (2)	19240-9	38°35.486	17°12.075	0.047	concave	Within bacterial mat seep, 100 m NE of Flare 5
ROV-343 (3)	19240-11	38°35.486	17°12.074	0.064	concave	1 m east of bacterial mat
ROV-343 (4)	19240-17	38°35.425	17°11.969			Central site of microbial mound, possibly gas hydrates, temperatures less than bottom water
ROV-345 (1)	19249-3	38°35.454	17°12.020			Long-term deployment on top of mound at Marker 2
ROV-345 (2)	19249-6	38°35.429	17°11.959	0.063	concave	At bubbling site
ROV-345 (3)	19249-10	38°35.428	17°11.958	0.061	concave	Background, 5 m away from Marker 3
ROV-346 (1)	19252-6	38°35.430	17°11.960			2 tries did not penetrate, lance bent afterwards
Cetus MV						
ROV-347 (1)	19253-2	37°53.117	17°27.744	0.035		Outside caldera
ROV-347 (2)	19253-3	37°53.073	17°27.745	-0.007	zigzag	On the rim
ROV-347 (3)	19253-4	37°53.017	17°27.742	0.012		At the depression
ROV-347 (4)	19253-5	37°52.961	17°27.742	0.024		On mud flow
ROV-347 (5)	19253-6	37°52.917	17°27.740	0.026		On mud flow
ROV-347 (6)	19253-7	37°52.871	17°27.738	0.051		In high backscatter
ROV-347 (7)	19253-8	37°52.832	17°27.737	0.212	linear	In direction towards center
ROV-347 (8)	19253-10	37°52.809	17°27.736	0.363	linear	End station in caldera
ROV-347 (9)	19253-13	37°52.786	17°27.735	0.201	linear	
ROV-347 (10)	19253-14	37°52.769	17°27.733	0.131	linear	
ROV-347 (11)	19253-15	37°52.754	17°27.734	0.091	convex	Southernmost station of N-S profile
ROV-347 (12)	19253-16	37°52.754	17°27.768	0.119	linear	Start of W-E profile
Nikolaus MV						
ROV-348 (1)	19255-2	37°48.996	17°58.232	-0.002	zigzag	Soft sediments
ROV-348 (2)	19255-6	37°48.896	17°58.131	0.006		On a mound structure in the center of the depression
ROV-348(3)	19255-12	37°48.814	17°58.128	-0.001	zigzag	On southern rim of crater, among pteropods

13 Biology

13.1 Biological Observations and Sampling

(H. Sahling, C. Johansen, F. Mary, L. Tamborrino)

During Leg 1 detailed seafloor observations and sampling was carried out at Venere Mud Volcano. Cold seeps have been comprehensively studied in the Mediterranean Sea as summarized in reviews by Olu et al. (2004) and Duperron et al. (2013). Therefore, it is to be expected that most of the species encountered at Venere Mud Volcano are already described. For that reason, we did not undertake any dedicated sampling program, and have a short list of samples (Table 34).

Due to methane seepage, the wide-spread occurrence (Fig. 146) of filamentous sulfur-oxidizing bacteria (cf. *Beggiatoa*) at Venere Mud Volcano is most remarkable. The mat-forming microbes indicate a geochemical habitat characterized by high sulfide flux (e.g. Sahling et al., 2002). The sulfide flux is caused by a high flux of (dissolved) methane fueling anaerobic oxidation of methane (AOM) causing sulfate to reduce to sulfide. The precipitation of sulfide minerals results in the formation of black sediments. At the seeps at Venere Mud Volcano the black sediments form circular patches of various sizes. Bacterial mats were recovered with one MIC core (Fig. 147). In association with the bacterial mats, tiny non-chemosynthetic polychaets were preserved for further taxonomic studies.

Fig. 146: Image of a black patch inhabited by filamentous bacteria taken during Quest Dive 339 (12:24:04 UTC) at Venere Mud Volcano.

At Venere Mud Volcano shells of seep-typical bivalves were ubiquitously observed at and around seeps. The majority of shells were of the vesicomyid clam genus *Isorropodon* typically 1-2 cm in length. Second most obvious were the shells of *Lucinoma kazani* that are less abundant compared to *Isorropodon* but larger in size (up to 4 cm). Other shells of the genera *Myrtea* and *Thyasira* were rarely recovered. All these clams have in common that they live in soft sediments and are partly

buried with only their posterior region protruding out of the seafloor. Therefore, living clams of these genera are difficult to observe with the ROV. We hypothesize that living clams are found in the sediments in a habitat as shown in Figure 148. Clams are mobile and may occasionally enter the black patches (Fig. 149). In the entire seep area clam shells can be observed (Fig. 150). Dead clams form a sort of halo around the seep from several to tens of meters. The widespread occurrence of shells is likely the result of several factors. For example: carbonate precipitation causes clam shells to seek out the more ideal soft sediment habitat. In addition to this, a decrease in sulfide flux may be caused by carbonate precipitation. Clams are killed by predators such as crabs and fish. Bioturbation can bring shells to the surface of the seafloor. Low sedimentation rates and insignificant carbonate dissolution preserve shells well.

Fig. 147: Image of filamentous bacteria at the surface of MIC GeoB 19208-1 at Venere Mud Volcano.

Bacterial mats and clams may characterize young seep systems or, respectively, high to moderate sulfide flux systems through soft sediments. Methane-derived carbonates may be inhabited by *Lamellibrachia anaximandri* (Vestimentifera) or bivalves of the family *Mytilidae*. Vestimentiferans are identifiable by ROV (Fig. 151) and observed at both seep sites north and south of the Venere Mud Volcano area. Bivalves of the family *Mytilidae* (such as *Idas modiolaeformis*) tend to live in porous authigenic carbonates, which was observed and collected with the suction sampler on the ROV. Physiology of *L. anaximandri* and *Idas m*. is based on mutualistic micro-macrofaunal relationship. AOM microbes provide sulfide, necessary for the microbial acitivity of the endosymbiontic sulfide-oxidizer, harboured in the tissue of *L. anaximandri* and *Idas m*.

The enclosed space under the border of the carbonate slabs clearly represent the best environment for the development of the “bush-like” colonies the *L. anaximandri* (as it was observed in the other Mediterranean seeps). In this context, tubeworms are anchored and protected by the carbonate crust, and in the meanwhile, they have the opportunity to uptake hydrogen sulfide from the close soft sediment, using their roots. In addition, the occurrence of some dead tubeworms on surface the soft sediment (ROV 341), environment can provide a better biogeochemical condition for these organisms, suggest that carbonate substrate plays a key role for the life of *L. anaximandri*.

The lifespan of *L. Anaximandri* is unknown, however, it is estimated a lifespan with the same order *L. Luymesi*, based on phylogenetic relationship (Southward et al., 2011), which is around 200 years (Cordes et al., 2005a). For this reason, only sites where methane is provided for long times, by seepage activity or gas hydrates dissociation, can host seep-tubeworms species.

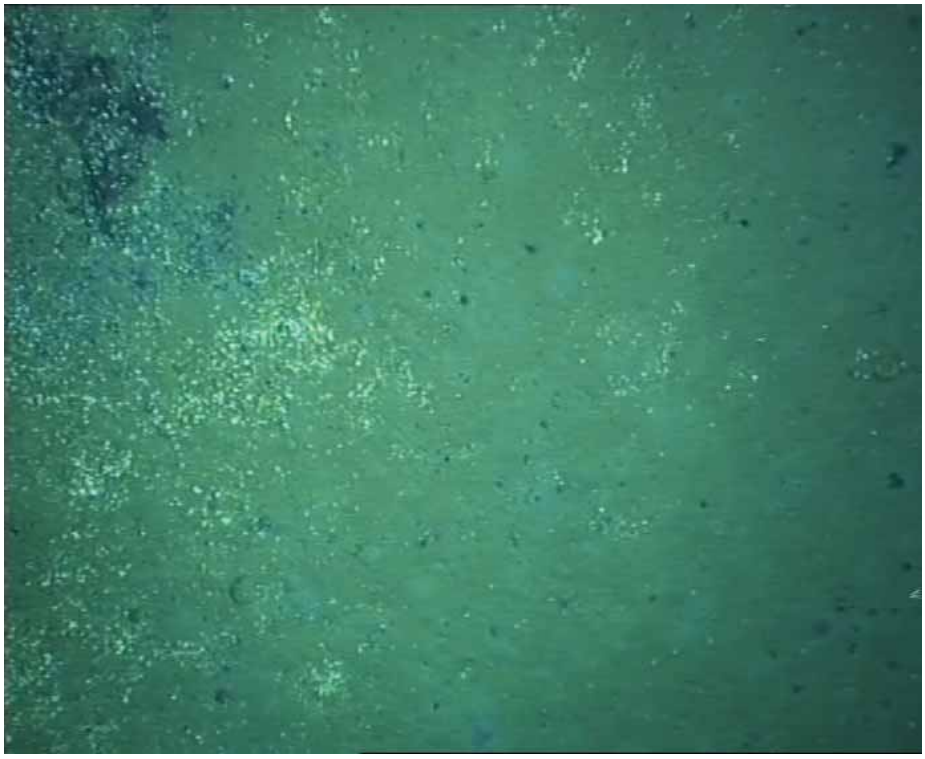

Fig. 148: Frame grab taken with the downward looking Atlas camera during Quest Dive 338 (12:45:23 UTC) at Venere Mud Volcano showing a cluster of clams.

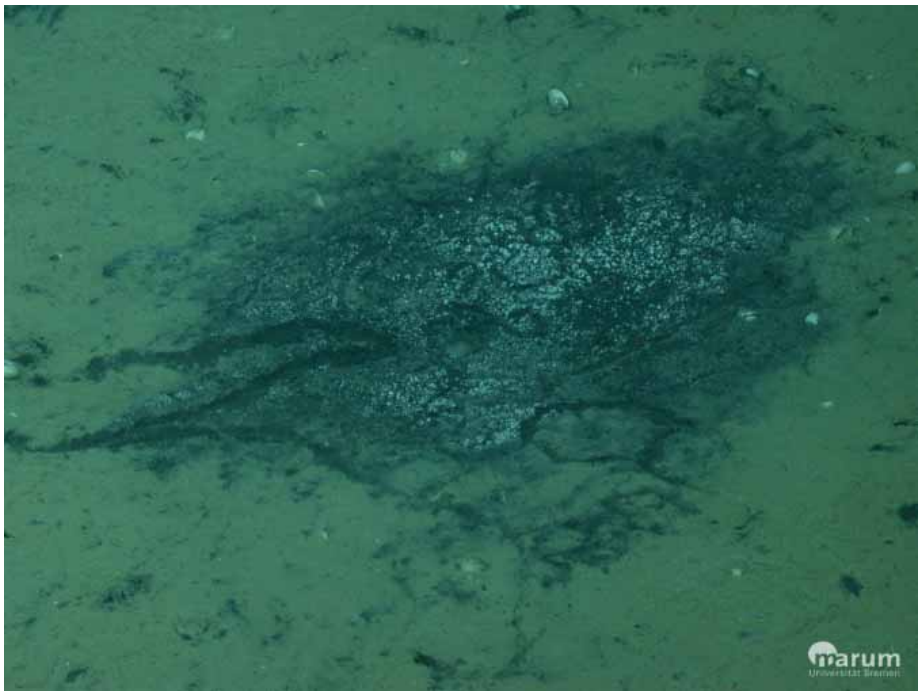

Fig. 149: Image taken during ROV dive 338 (07:58:50 UTC). Vesicomyid bivalves are mobile and leave characteristic tracks in the dark-colored sediments.

Fig. 150: Image taken during ROV Dive 338 (07:58:56 UTC). Vesicomyid bivalve shells occur ubiquitously at and around seeps.

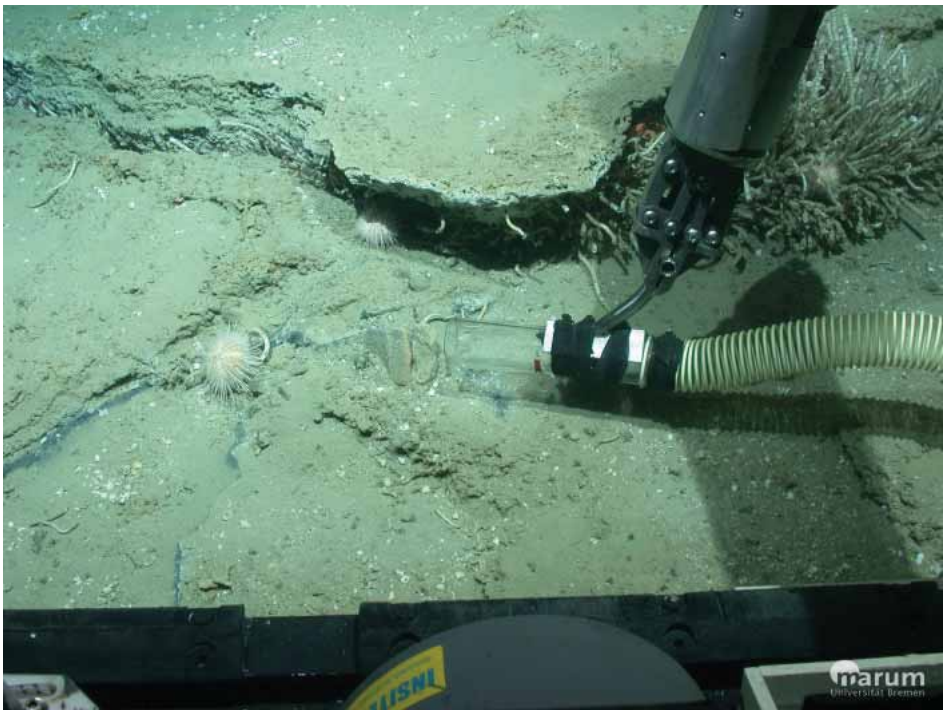

Fig. 151: Image taken during ROV dive 339 (15:11:40 UTC). Suction sampling close to a crack in methane-derived carbonates inhabited by the vestimentiferan tubeworm *Lamellibrachia anaximandri*.

Table 34: Summary of biological samples collected during Leg 1.

Station number	Tool	Sample	Preservation
GeoB19205-1	GC, In sediments attached to outside of weight	Bivalve shells, various	Dry
GeoB19205-2	MIC	Bivalve shells, various	Dry
GeoB19208-1	MIC	Vesicomyid shells	Dry
GeoB19208-1	MIC	3 Polychaeta	100 % Ethanol
GeoB19208-1	MIC	3 Polychaeta	4 % Formaldehyde

GeoB19221-11	ROV 339 Suction Sampler	2 juvenile Vesicomyids	100 % Ethanol
GeoB19221-11	ROV 339 Suction Sampler	Shells of bivalves, gastropod, tubeworm	Dry
GeoB19221-12	ROV 339 Suction Sampler	1 Mytilidae, 1 cf. Amphipoda, 1 Gastropoda	100 % Ethanol
GeoB19221-12	ROV 339 Suction Sampler	Shells of bivalves, gastropod, tubeworm	Dry
GeoB19221-	ROV 339 Rescued Pushcorer	1 Vesicomyid shell	Dry

Table 35: Summary of biological samples collected during Leg 2.

Station number	Tool	Sample	Preservation
GeoB19230-6	ROV 341 - Net	Shells of bivalves and gastropods	Dry
GeoB19230-9	ROV 341 – Rescued with ROV arm	2 tubeworms (one alive, one dead), 7 Idas M. of different size and color	Dry, together with the carbonate sample
GeoB19230-12/13/14	ROV 341 Rescued Pushcorer	Shells of vesicomyd embedded in bacterial mat sediment	Dry
GeoB19240-5	ROV 343 - Rescued with ROV arm	Tubeworms, (whitish) bacterial mats, vesicomyd (2 attached to tubeworms posterior part), small Idas m.	Dry, together with the carbonate sample

13.2 Microbiology

(M. Torres (shipboard) R. Colwell, S. Klassek (shorebased)

Anaerobic oxidation of methane (AOM) consumes about 90 % of methane produced in marine sediments before it reaches the hydrosphere (Reeburgh, 2007). This microbial methane filter is driven by methanotrophic archaea of the ANME clades, which often associate with sulfate-reducing δ-proteobacteria as consortia that couple methane oxidation with sulfate reduction at the sulfate-methane transition zone (SMTZ) (Knittel & Boetius, 2009). ANME and δ-proteobacteria have been identified as dominant clades in shallow sediments from mud volcanoes in the Mediterranean and Arctic (Pachidiaki et al., 2011; Niemann et al., 2006). However, aerobic methanotrophic bacteria dominate where high methane flux limits sulfate diffusion to shallow sediment layers (Lösekann et al., 2007) or where ample dissolved oxygen is available as a preferred electron acceptor. Assessing the distribution of methane-oxidizing microbial communities and quantifying their dynamics and activity rates in response to broad ranges of methane fluxes along mud volcano transects will improve subsurface carbon cycling models and predictions of methane release into the hydrosphere. In addition these microbiological investigations will shed light on the community development following a methane-enriched mud flow event of Venere Mud Volcano, as well as providing additional evidence for carbon cycling within the apparently dormant Cetus and Nikolaus Mud Volcanoes.

Microbial community composition above, below, and within SMTZs of mud volcano sediments corresponding to varying methane fluxes will be assessed through amplification of the 16S gene and next-generation sequencing. Fluorescent in-situ hybridization (FISH) will be used to visualize and enumerate AOM consortia. Total microbial activity will be quantified by RNA/DNA abundance ratios,

and aerobic/anaerobic methane oxidation and sulfate reduction will be measured by qPCR of *pmo*A, *mcr*A and *dsr*AB genes, respectively.

Shipboard Methods
Sediment samples were collected with push cores and gravity cores, and whole rounds for DNA and RNA extraction were processed, placed into whirlpak bags, and flash frozen in liquid nitrogen before storing at -80˚C. Before freezing, 2 ml sediment plugs were collected with sterile cutoff syringes and placed in 6 ml 2% formaldehyde in PBS buffer for fluorescent in-situ hybridization (FISH). After 8-12 hours, the samples were washed three times with PBS buffer before storing in ethanol at -80˚C. 400 ml of fresh SMTZ sediment were collected after core processing and preserved anoxically in gaspack bags at 4˚C.

Samples Collected
We collected and processed a total of 173 DNA/RNA samples (5 to 20 cc of sediment), 42 samples for FISH (2 to 5 cc of sediment) and 2 anoxic sediment samples (200 cc sediment each). See Table 31 in Chapter 11.

13.3 Dinoflagellate Sampling

(M. Torres (shipboard), C. Carbonell-Moore (shorebased)

Dinoflagellates are the second most important group of the primary producers in the oceans. They are also responsible for the majority of red tides occurring world-wide having a tremendous impact on coastal fisheries and aquaculture industries.

The earlier studies on dinoflagellates were carried by European researchers, and not surprisingly, from the Mediterranean Sea samples. Their findings are now being revised with new technologies, especially those in the molecular biology field heading towards a better understanding of dinoflagellate evolution.

The continuous filtering allows the concentration of scarce dinoflagellates in the surface, which otherwise would be missed by conventional net tows collections. This cruise provides an excellent opportunity to collect and preserve those rare Mediterranean dinoflagellates not only for morphological observations, but for DNA sequencing, which will fill the existing gaps in the current phylogenetic dinoflagellate trees.

Methods
Samples were collected by filtering seawater from the ship's pump for periods of 10 to 12 hours, using the 20 µm filters using the cod-ends of towing nets. Filters were rinsed and sample was collected in scintillation vials, and then preserved in ethanol.

Table 36: Dinoflagellate sample collection.

Sample No.	Date	Time (UTC)	Lat. (N)	Long. (E)	Comments
214	25.11.2014	08:00	37° 04.06'	15° 55.10'	collected in one filter
		19:00	37° 28.57	17° 08.63'	

215	25.11.2014	08:00	37° 04.06'	15° 55.10'	collected in one filter
		19:00	37° 28.57'	17° 08.63'	
			29		
216	26.11.2014	08:00	38° 37.03'	17° 11.57'	two filters in one vial
		20:20	38° 36.44'	17° 11.33'	
217	27.11.2014		37° 28.45'	15° 09.55'	two filters in one vial
			37° 62.57'	16° 51.2'8	
218	28.11.2014	07:01	38° 36.46'	17° 11.20'	two filters in one vial
		18:40	38° 36.44'	17° 11.31'	
219	29.11.2014	09:00	38° 37.08'	17° 11.61'	two filters in one vial
		21:13	38° 41.66'	17° 25.00'	
220	30.11.2014	06:26	38° 35.45'	17° 12.03'	two filters in one vial
		20:49	38° 36.01'	17° 12.56'	
221	1.12.2014	06:30	38° 35.45'	17° 12.04'	two filters in one vial
		20:30	38° 15.68'	17° 22.00'	
222	2.12.2014	10:20	38° 37.09'	17° 11.61'	
		20:30	38° 36.51'	17° 12.56'	
223	3.12.2014	06:46	38° 35.56'	17° 11.44'	two filters in one vial
		22:30	38° 35.45'	17° 11.94'	
224	4.12.14	07:30	38° 36.46'	17° 11.24'	Filter in co-ed looked clogged
		20:10	38° 35.45'	17° 11.94'	two filters in one vial
225	5.12.14	08:35	38° 52.62'	17° 28.90'	24 hour collection, two filters in one vial
	6.12.14	08:10	37° 49.44'	17° 59.46'	
226	6.12.14	09:10	38° 48.72'	17° 57.53'	
		21:40	37° 48.65'	17° 58.89'	
227	07.12.1	07:00	38° 48.65'	17° 58.89'	five days before adding EtOH
		20:00	38° 36.41'	17° 11.25'	

14 Weather Report

(A. Raeke, C. Rohleder)

On the 6th of November at 10:00 R/V METEOR left the harbor of Catania to expedition M112. The major focus of the expedition was to investigate the distribution, amounts and dynamics of gas hydrates associated with submarine mud volcanoes in the Ionic Sea. At the beginning of the journey the cruising area was influenced by an extensive Black Sea high and a low to the southwest of Sicily. However on the 5th of November, while still in the harbour, thunderstorms with an associated 'waterspout' developed moving close to R/V METEOR. Gusts of 38 kn were experienced. On the 6th of November a cold front crossed the area with freshening southeasterly winds. Gust of up to 10 Bft were reported, associated with heavy showers and thunderstorms. The sea increased to 4 to 5 m.

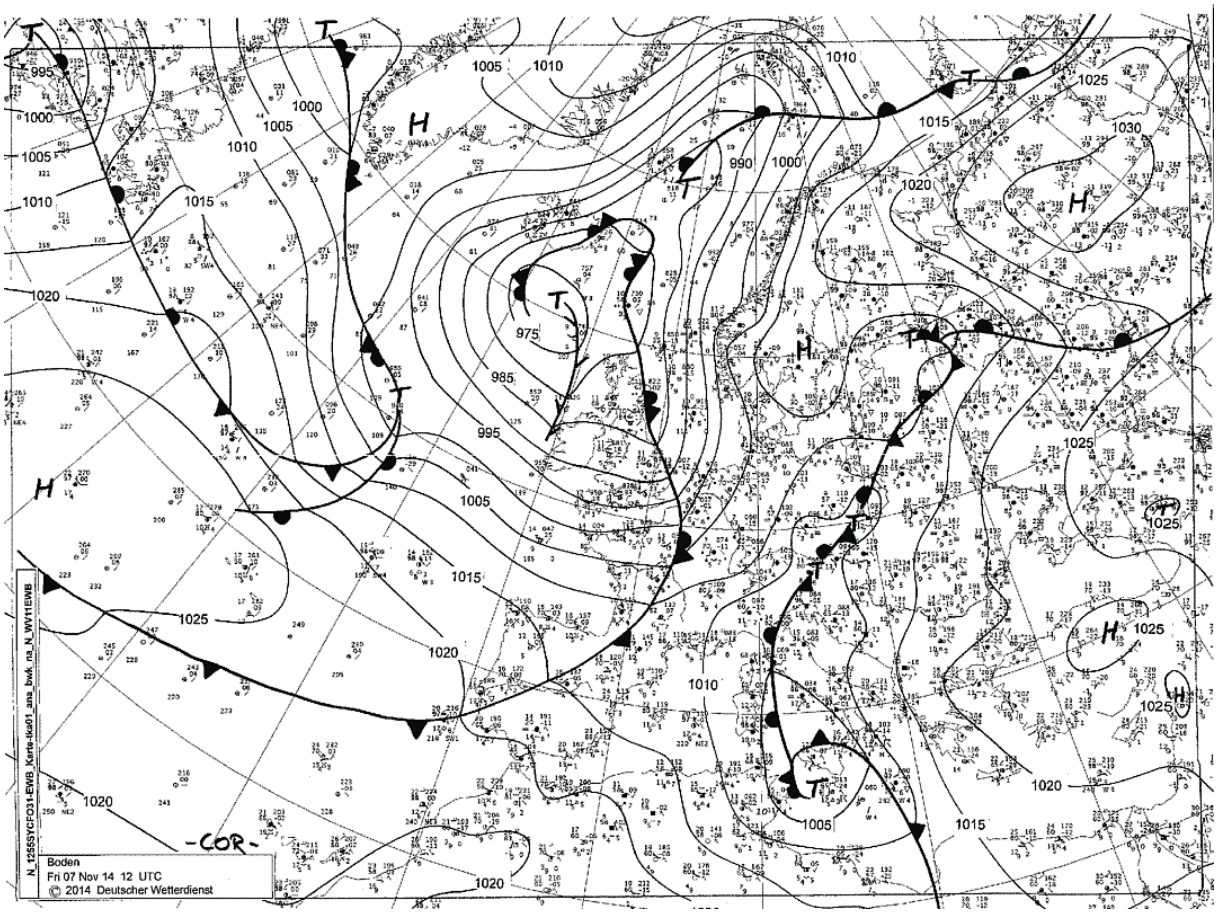

Fig. 152: Analysis 2014-11-07 12UTC.

On the afternoon of the 8th the southeast winds, close to the centre of the low, decreased to 5 Bft with the sea abating to 2 to 3 m. This calm weather conditions allowed work to map the seafloor. Later the low weakened while moving to the southeast and a ridge of a Russian high extended into the eastern Mediterranean. This allowed good working conditions with winds of 2 to 3 Bft and sea of 0.5 to 1 m. On the 11th a low moved from Tunisia into the Tyrrhenian Sea. The southeasterly winds increased to 6 to 7 Bft and the waves to 2.5 m. Local showers with lightening were experienced. From the 12th the low moved to northern Italy with a further weakening. Within a low pressure gradient the wind dropped to 4 to 5 Bft, however during sunset southeast of the Gulf of Squillace (Calabria) a dry and freshening warmer NW'ly wind with 6 Bft arose. As of the 14th a Russian high pressure ridge formed over the Ionian Sea to Libya. Sunny weather prevailed with sea conditions of

0.5 m and a wind of 3 Bft. The most sensitive devices could be used like the AUV including the Dinghy. During the night 16th/17th a trough from a low over Genoa crossed the working area. The wind increased briefly to 5 to 6 Bft and lightning was observed. Later a high over the eastern Mediterranean and a low over France caused calm conditions. However weak troughs crossed the area causing on the 19th a temporary increase of the sea to 1.5 m with winds up to 5 Bft. An extremely good visibility allowed the view to Mount Etna. Later high pressure over the central Mediterranean set in. During the night 19th/20th on the way to port of Catania the northerly wind strengthened to 5 Bft. This was due to a nozzle effect in the strait of Messina. With decreasing winds to 3 to 4 Bft R/V METEOR finally reached the harbor of Catania.

On the 22th of November R/V METEOR left Catania for the second part of the expedition M112. Stable weather conditions within an extended high pressure zone allowed a quiet return to the working area and gave good working conditions for the first days. In the next following days the high pressure zone moved to the east and from the 26th the wind shifted from easterly directions to more southerly directions with predominately winds of 2 to 4 Bft. The visibility was good, at times even very good. Later on the day some showers passed through with improving weather conditions on the next day. This allowed a short stop at the harbor of Catania for the acquisition of equipment and luggage. From the 28th the weather deteriorated with some rain developing. The sea increased to 2 m. This was due to an extensive low pressure system over the Iberian Peninsula gradually shifting further east and influencing the working area. Saturday was hazy with the sea about 2 m. Due to a strong Southerly flow dust from the desert deposited on ship and equipment.

Midweek the low was close to Sardinia and weakened further until Friday. On the night of 01th/02th of December an associated cold front crossed the area with showers and wind up to 6 Bft. A southwesterly airflow developed with thundery showers moving through. On the 5th a stronger thunderstorm reached the R/V METEOR. Despite northwest winds up to 9 Bft a radiosonde was launched. The next following weekend brought fine conditions with plenty of sunshine and a wind about 3 Bft. On the 8th of December the low over Sardinia moved to the southeast and later to Greece. A northerly airflow developed directing cold air from higher altitude over the warm waters. This caused the air mass to become unstable with scattered thunderstorms developing over Sicilia/Calabria. The week started with northerly winds with strength of 7 Bft and temperatures about 15 °C. From Tuesday the 9th with less wind the last ROV dive of the trip was conducted. Until the end of the expedition only drill cores and ship tracks were carried out as the winds were not allowing any work with the ROV. The next following weekend weather improved with a high pushing in from the west, wind and sea decreased to 0.5 m.

During the entire expedition the temperature was hovering between 13 and 21°C. The lower values within a northerly wind were measured later on the journey. The water temperature was fairly constant throughout the period with the lower values measured mainly close to the land.

Fig. 153: Funnel Cloud 2014-12-05 1140-1155UTC.

15 References

Abegg F, Hohnberg HJ, Pape T, Bohrmann G, Freitag J (2008) Development and application of pressure-core-sampling systems for the investigation of gas- and gas-hydrate-bearing sediments. Deep-Sea Research I: Oceanographic Research Papers, 55(11): 1590-1599.

Barone M, Dominici R, Muto F and Critelli S (2008) Detrital modes in a late Miocene wedge-top basin, northeastern Calabria, Italy: Compositional record of wedge-top partitioning. Journal of Sedimentary Research 78: 693-711; doi:10.2110/jsr.2008.071.

Bernard BB, Brooks JM, Sackett WM (1976) Natural gas seepage in the Gulf of Mexico. Earth and Planetary Science Letters, 31(1): 48-54.

Blechschmidt G, Cita MB, Mazzei R, Salvatorini G (1982) Stratigraphy of the Western Mediterranean Ridge and Southern Calabrian Ridge, Eastern Mediterranean. Mar. Micropaleontol. 7: 11–134.

Boetius A, Ravenschlag K, Schubert CJ, Rickert D, Widdel F, Gieseke A, Amann R, Jorgensen BB, Witte U, Pfannkuche O (2000) A marine microbial consortium apparently mediating anaerobic oxidation of methane. Nature 407: 623-626.

Bohrmann G, Pape T, and cruise participants (2007) Report and preliminary results of R/V Meteor cruise M72/3, Istanbul - Trabzon - Istanbul, 17 March - 23 April, 2007. Marine gas hydrates of the Eastern Black Sea. In: Berichte, Fachbereich Geowissenschaften, Universität Bremen, No. 261, (Ed. by G. Bohrmann, T. Pape), pp. 176, Bremen.

Borowski WS, Paull CK, Ussler III W (1999) Global and local variations of interstitial sulfate gradients in deep-water, continental margin sediments: Sensitivity to underlying methane and gas hydrates. Marine Geology 159: 131-154.

Capozzi R, Artoni A, Torelli L, Lorenzini S, Oppo D, Mussoni P, Polonia A (2012. Neogene to Quaternary tectonics and mud diapirism in the Gulf of Squillace (Crotone-Spartivento Basin, Calabrian Arc, Italy). Marine and Petroleum Geology 35(1): 219-234.

Caress DW and Chayes DN (1995) New Software for Processing Sidescan Data from Sidescan-Capable Multibeam Sonars. IEEE Oceans '95, San Diego, CA., IEEE.

Ceramicola S, Praeg D, the OGS Explora Scientific Party (2006) Mud volcanoes discovered on the Calabrian Arc: preliminary results from the HERMES-HYDRAMED IONIO 2005 campaign. CIESM Workshop Monographs 29: 35–39.

Ceramicola S, Praeg D, Cova A, Accetella D and Zecchin M (2014) Seafloor distribution and last glacial to postglacial activity of mud volcanoes on the Calabrian accretionary prism, Ionian Sea. Geo-Marine Letters 34: 111-129.

Cernobori L, Hirn A, McBride JH, Nicolich R, Petronio L, Romanelli M, STREAMERS/PROFILES working Groups (1996) Crustal image of the Ionian basin and its Calabrian margins. Tectonophysics 264: 175–189.

Chamot-Rooke N, Rangin C, Le Pichon X and DOTMED Working Group (2005b) DOTMED: A Synthesis of Deep Marine Data in the Eastern Mediterranean. Mémoires de la Société géologique de France, n.s., no. 177, 64 pp, 9 plates fl CD.

Charlou JL, Donval JP, Zitter T, Roy N, Jean-Baptiste P, Foucher JP and Woodside J (2003) Evidence of methane venting and geochemistry of brines on mud volcanoes of the eastern Mediterranean Sea. Deep Sea Research Part I: Oceanographic Research Papers, 50 (8): 941-958.

Cita MB, Ryan WBF, Paggi L (1981) Prometheus Mud Breccia. An example of shale diaprism in the western Mediterranean Ridge. Annales géologiques des Pays hélléniques 30(2): 543–570.

Cita MB, Maccagni A, Pirovano G (1982) Tsunami as triggering mechanism of homogenites recorded in areas of the eastern Mediterranean characterized by the “Cobblestone Topography”. In: S

Saxov, JK Newenhuis (eds.), Marine Slides and other Mass Movements. Plenum Press, London: 233-261.

Cita M B, Camerlenghi A, Kastens K A &McCoy F (1984) New findings of Bronze Age homogenites in the Ionian Sea: Geodynamic implications for the Mediterranean. Mar. Geol. 55: 47–62.

Cita MB and Rimoldi B (1997) Geological and geophysical evidence for the Holocene tsunami deposit in the eastern Mediterranean deep-sea record. Journal of Geodynamics 24: 293–304.

Cita MB & Rimoldi B (2005) Prehistoric mega-tsunami in the eastern Mediterranean and its sedimentary response. Rend. Fis. Acc. Lincei 9, 16: 137–157.

Cordes EE, Arthur MA, Shea K, Arvidson RS, Fisher CR (2005a) Modeling the mutualistic interactions between tubeworms and microbial consortia. PLoS Biology 3: 497–506.

de Voogd B, Truffert C, Chamot-Rooke N, Huchon P, Lallemant S, and Le Pichon X (1992, Two-ship deep seismic soundings in the basins of the eastern Mediterranean Sea (Pasiphae cruise), Geophys. J. Int., 109: 536–552, doi:10.1111/j.1365-246X.1992.tb00116.x.

Duperron S, Gaudron SM, Rodrigues CF, Cunha MR, Decker C and Olu K (2013) An overview of chemosynthetic symbioses in bivalves from the North Atlantic and Mediterranean Sea. Biogeosciences, 10(5): 3241-3267.

Faccenna C, Becker TW, Pio Lucente F, Jolivet L, Rossetti F (2001) History of subduction and back-arc extension in the Central Mediterranean. Geophysical Journal International 145: 809–820.

Faccenna C, Piromallo C, Crespo-Blanc A, Jolivet L, Rossetti F (2004) Lateral slab deformation and the origin of the western Mediterranean arcs. Tectonics 23, TC1012, doi:10.1029/2002TC001488.

Faccenna C, Molin P, Orecchio B, Olivetti V, Bellier O, Funiciello F, Minelli L, Piromallo C, Billi A (2011) Topography of the Calabria subduction zone (southern Italy): clues for the origin of Mt. Etna. Tectonics 30, TC1003. doi:10.1029/2010TC002694.

Finetti I (1982) Structure, stratigraphy and evolution of Central Mediterranean. Bollettino di Geofisica Teorica ed Applicata 24 (96): 247–312.

Finetti I (2005) The Calabrian arc and subducting Ionian slab from new CROP data. In: Finetti I (Ed.), cROP project: deep seismic exploration of the central Mediterranean and Italy. Atlases in Geoscience, vol. 1. Elsevier, Amsterdam, pp. 393–412.

Fischer J and Visbeck M (1993). Deep velocity profiling with self-contained ADCPs. Journal of Atmospheric and Oceanic Technology, 10: 764773.

Foucher M, Westbrook GK, Boetius A, Ceramicola S, Dupré S, Mascle J, Mienert J, Pfannkuche O, Pierre C and Praeg D (2009) Structure and drivers of cold ecosystems. Oceanography 22: 92-109.

Fusi N, Kenyon NH (1996) Distribution of mud diapirism and other geological structures from long-range sidescan sonar (GLORIA) data, in the Eastern Mediterranean Sea. Marine Geology 132: 21–38.

Goes S, Giardini D, Jenny S, Hollenstein C, Kahle H-G, Geiger A (2004) A recent tectonic reorganization in the south-central Mediterranean. Earth and Planetary Science Letters 226:335–345. doi:10.1016/j.epsl.2004.07.038.

Gueguen E, Doglioni C, Fernandez M (1998) On the post-25 Ma geodynamic evolution of the western Mediterranean. Tectonophysics 298: 259–269.

Guillaume B, Funiciello F, Faccenna C, Martinod J, Olivetti V (2010) Spreading pulses of the Tyrrhenian Sea during the narrowing of the Calabrian slab. Geology 38: 819–822.

Gutscher et al. (2013) Rapport de mission CIRCEE-HR, Calabrian arc Ionian Sea Research and Catastrophic Historical Earthquakes in Southern Italy: a high resolution seismic survey. N/O Le Suroit Cruise 2-24 Oct. 2013.

Heeschen KU, Hohnberg HJ, Haeckel M, Abegg F, Drews M, Bohrmann G. (2007) In situ hydrocarbon concentrations from pressurized cores in surface sediments, Northern Gulf of Mexico. Marine Chemistry, 107(4): 498-515.

Hoehler TM, Alperin MJ, Albert DB, Martens CS (1994) Field and Laboratory Studies of Methane Oxidation in an Anoxic Marine Sediment - Evidence for a Methanogen- Sulfate Reducer. Consortium. Global Biogeochemical Cycles 8: 451-463.

Joye SB, Boetius A, Orcutt BN, Montoya JP, Schulz HN, Erickson MJ, Lugo SK (2004) The anaerobic oxidation of methane and sulfate reduction in sediments from Gulf of Mexico cold seeps. Chemical Geology 205: 219-238.

Knittel K, Loesekann T, Boetius A, Kort R, Amann R (2005) Diversity and Distribution of Methanotrophic Archaea at Cold Seeps. Appl. Environ. Microbiol. 71: 467–479.

Knittel K & Boetius A (2009) Anaerobic Oxidation of Methane: Progress with an Unknown Process. Annu. Rev. Microbiol. 63: 311–334.

Kopf A (2002) Significance of mud volcanism. Reviews of Geophysics 40 (2): 1–51.

Kullenberg B (1947) The piston core sampler, Sven. Hydrogr.-Biol. Komm. Skr., Ser. 3,Hydrogr. 1 (2): 46p.

Lammers S, Suess E (1994) An improved head-space analysis method for methane in seawater. Marine Chemistry 47 (2): 115-125.

Lösekann T, Knittel K, Nadalig T, Fuchs B, Niemann H, Boetius A, Amann R (2007) Diversity and Abundance of Aerobic and Anaerobic Methane Oxidizers at the Haakon Mosby Mud Volcano, Barents Sea. Appl. Environ. Microbiol. 73, 3348–3362.

Malinverno A, Ryan WBF (1986) Extension in the Tyrrhenian Sea and shortening in the Apennines as result of arc migration driven by sinking of the lithosphere. Tectonics 5 (2): 227–245.

Mascle J, Mary F, Praeg D, Brosolo L, Camera L, Ceramicola S, Dupré S (2014) Distribution and geological control of mud volcanoes and other fluid/free gas seepage features in the Mediterranean Sea and nearby Gulf of Cadiz. Geo-Marine Letters, DOI 10.1007/s00367-014-0356-4.

Mattei M, Cifelli F, D'Agostino N (2007) The evolution of the Calabrian Arc: evidence from paleomagnetic and GPS observations. Earth and Planetary Science Letters 263: 259–274.

Minelli L, Faccenna C (2010) Evolution of the Calabrian accretionary wedge (central Mediterranean). Tectonics 29, TC4004; doi:10.1029/2009TC002562.

Minelli L, Billi A, Faccenna C, Gervasi A, Guerra I, Orecchio B, Speranza G (2013) Discovery of a gliding salt-detached megaslide, Calabria, Ionian Sea, Italy. Geophysical Research Letters 40: 4220-4224.

Morlotti E, Sartori R, Torelli L, Barbieri F, Raffi I (1982) Chaotic deposits from the external Calabrian Arc (Ionian Sea, eastern Mediterranean). Memorie della Societa` Geologica Italiana 24: 261–275.

Niemann H, Lösekann T, de Beer D, Elvert M, Nadalig T, Knittel K, Amann R, Sauter EJ, Schlüter M, Klages M, Foucher JP, Boetius A (2006) Novel microbial communities of the Haakon Mosby mud volcano and their role as a methane sink. Nature 443: 854–858.

Olu-Le Roy K, Sibuet M, Fiala-Médioni A, Gofas S, Salas C, Mariotti A, Foucher JP and Woodside J (2004) Cold seep communities in the deep eastern Mediterranean Sea: composition, symbiosis and spatial distribution on mud volcanoes. Deep-Sea Research I, 51: 1915-1936.

Orphan VJ, Ussler III W, Naehr TH, House CH, Hinrichs K-U, Paull CK (2004) Geological, geochemical, and microbiological heterogeneity of the seafloor around methane vents in the Eel River Basin, offshore California. Chemical Geology 205: 265-289.

Pachiadaki M G, Kallionaki A, Dählmann A, Lange G J D & Kormas K A (2011) Diversity and Spatial Distribution of Prokaryotic Communities Along A Sediment Vertical Profile of A Deep-Sea Mud Volcano. Microb. Ecol. 62: 655–668.

Panieri G, Polonia A, Lucchi RG, Zironi S, Capotondi L, Negri A, Torelli L (2013) Mud volcanoes along the inner deformation front of the Calabrian Arc accretionary wedge (Ionian Sea). Marine Geology 336: 84-98.

Pape T, Bahr A, Rethemeyer J, Kessler JD, Sahling H, Hinrichs KU, Klapp SA, Reeburgh WS and Bohrmann G (2010) Molecular and isotopic partitioning of low-molecular-weight hydrocarbons during migration and gas hydrate precipitation in deposits of a high-flux seepage site. Chemical Geology 269: 350-363.

Pape T, Bahr A, Klapp SA, Abegg F, Bohrmann G (2011) High-intensity gas seepage causes rafting of shallow gas hydrates in the southeastern Black Sea. Earth and Planetary Science Letters 307: 35-46.

Polonia A, Torelli L, Mussoni P, Gasperini L, Artoni A, Klaeschen D (2011) The Calabrian Arc subduction complex in the Ionian Sea: regional architecture, active deformation and seismic hazard. Tectonics 30, TC5018.

Polonia A, Bonatti E, Camerlenghi A, Lucchi RG, Gasperini L and Panieri G (2013) Mediterranean megaturbidite triggered by the ad 365 Cretan earthquake and tsunami. Nature Reports 3:1285 (DOI: 10.1038/srep01285).

Praeg D, Ceramicola S, Barbieri R, Unnithan V, Wardell N (2009) Tectonically-driven mud volcanism since the late Pliocene on the Calabrian accretionary prism, central Mediterranean Sea. Marine and Petroleum Geology 26: 1849–1865.

Praeg D, Ceramicola S, Pierre C, Mascle J, Dupré S, Andersen A, Camera L, Cova A, De Lange G, Ducassou E, Freiwald A, Harmegnies F, Hebbeln D, Loncke L, Mastalerz V, Migeon S, Taviani M (2012) Active mud volcanism and seabed seepage on the Calabrian accretionary prism, Ionian Sea [poster]. 86. Congresso Nazionale della Società Geologica Italiana (SGI), 18-20 September, Arcavacata di Rende (CS) ITALY; Rend. Online Soc. Geol. It., v. 21, pp. 973-974.

Rabaute A, Chamot-Rooke N (2007) Quantitative mapping of active mud volcanism at the western Mediterranean Ridge-backstop contact. Marine Geophysical Research 28: 271-293.

RDI (1996) Acoustic Doppler Current Profiler, Principles of Operation, A Practical Primer. RD Instruments, San Diego. Available at http://www.rdinstruments.com/rdi library. html.

Reeburgh WS (2007) Oceanic Methane Biogeochemistry. Chem. Rev. 107: 486–513.

Rehder G, Keir RS, Suess E, Rhein M (1999) Methane in the northern Atlantic controlled by microbial oxidation and atmospheric history. Geophysical Research Letters 26 (5): 587-590.

Robertson AHFand the Ocean Drilling Program Leg 160 Shipboard Scientific Party (1996) Mud volcanism on the Mediterranean Ridge; initial results of Ocean Drilling Program Leg 160. Geology 24 (3): 239–242.

Rossi S, Sartori R (1981) A seismic reflection study of the external Calabrian Arc in the northern Ionian Sea (eastern Mediterranean). Marine Geophysical Researches 4: 403–426.

Sahling H, Rickert D, Lee RW, Linke P and Suess E (2002) Macrofaunal community structure and sulfide flux at gas hydrate deposits from the Cascadia convergent margin, NE Pacific. Marine Ecology Progress Series, 231: 121-138.

Sartori R (2003) The Tyrrhenian back-arc basin and subduction of the Ionian lithosphere. Episodes 26 (3): 217–221.

Somoza L, Medialdea T, Leon R, Ercilla G, Vazquez JT, Farran M, Hernandez-Molina FJ, Gonzales J, Juan C, Fernandez-Puga MC (2012) Structure of mud volcano system and pockmarks in the region of the Ceuta Contourite Depositional System (Western Alboran Sea). Mar Geol 332-334: 4-26.

Southward EC, Andersen AC, Hourdez S (2011) Lamellibrachia anaximandri n. sp., a new vestimentiferan tubeworm (Annelida) from the Mediterranean, with notes on frenulate tubeworms from the same habitat. Zoosystema ,33 (3). Publications Scientifiques du Muséum national d'Histoire naturelle, Paris.

Suess E, Whiticar MJ (1989) Methane-derived CO2 in pore fluids expelled from the Oregon subduction zone. Palaeogeography, Palaeoclimatology, Palaeoecology 71: 119-136.

Taviani M, Angeletti L, Ceregato A, Foglini F, Froglia C and Trincardi F (2013) The Gela Basin pockmark field in the strait of Sicily (Mediterranean Sea): chemosynthetic faunal and carbonate signatures of postglacial to modern cold seepage. Biogeoscience 10: 4653-4671.

Visbeck M (2000) Deep velocity profiling using lowered acoustic Doppler current profilers: Bottom track and inverse solutions. Journal of Atmospheric and Oceanic Technology, 19: 794807.

Westaway R (1993) Quaternary uplift of southern Italy. Journal of Geophysical Research: Solid Earth, 98: 21741-21772.

Zecchin M, Caffau M, Civile D, Critelli S, Di Stefano A, Maniscalco R, Muto F, SturialeG, Roda C (2012) The Plio-Pleistocene evolution of the Crotone Basin (southern Italy): Interplay between sedimentation, tectonics and eustasy in the frame of Calabrian Arc migration. Earth-Science Reviews 115: 273-303.

16 Appendix

16.1 Appendix 1: Station List

Meteor M112

Station list

Date 2014	M112-St. No.	Instrument	GeoB St. No.	Location	Time (UTC)			Begin / on seafloor			End / off seafloor			Recovery Remarks
					Begin	on seafloor	off seafloor	Latitude N	Longitude E	Water d. (m)	Latitude N	Longitude E	Water d. (m)	
06.11.	1214-1	SVP-1	19201-1	Italy	13:36			37°29.315	16°12.446	2224				Sound velocity for multibeam calibration down to 1500 m
09.11.	1215-1	ROV-337	19202-1	Venere MV (Flare 1)	19:32	21:03	04:30	06:04	38°37.085	17°11.606	1560	38°36.604	17°11.228	1515	
09.11.	1215-1	TS	19202-2			22:13	23:14		38°37.084	17°11.593	1567				Deployment lasted 1 hour
10.11.	1216-1	AUV-62	19203-1	Venere MV	07:55			17:35	38°36.920	17°10.190	1555	38°36.442	17°11.562	1557	
10.11.	1217-1	CTD-1	19204-1	Venere MV	19:12	19:42		20:22	38°37.104	17°11.643	1554				
10.11.	1218-1	GC-1	19205-1	Venere MV (Flare 1)	20:44	21:22		22:10	38°37.102	17°11.619	1556				262 cm recovery
10.11.	1218-2	GC-2	19205-2	Venere MV (Flare 1)	22:55	23:34		00:15	38°37.103	17°11.620	1556				170 cm recovery, no storage
11.11.	1219-1	GC-3	19206-1	Venere MV	00:42	01:13		01:49	38°36.605	17°11.235	1506				227 cm recovery
12.11.	1220-1	CTD-2	19207-1	Venere MV (Flare 1)	17:25	17:28	19:10	19:12	38°37.156	17°11.603	1565	38°37.105	17°11.607	1561	No bottles closed
12.11.	1221-1	MIC-1	19208-1	Venere MV (Flare 1)	20:00	20:34		21:12	38°37.104	17°11.619	1560				3 cores succesfully filled
12.11.	1222-1	MIC-2	19209-1	Venere MV (Western peak)	21:27	22:05		22:35	38°36.607	17°11.229	1508				3 cores succesfully filled
13.11.	1223-1	CTD-3	19210-1	Venere MV (Flare 1)	05:01	05:09	06:33	06:38	38°37.165	17°11.600	1566	38°37.104	17°11.606	1560	All bottles closed
13.11.	1224-1	ROV-338	19211-1	Venere MV (Flare 1)	07:15	09:13	17:28	18:42	38°37.088	17°11.636	1556	38°37.095	17°11.611	1556	
13.11.	1224-1	Mosaik	19211-1			12:43	16:27		38°37.093	17°11.630	1565	38°37.090	17°11.625	1564	Across high backscatter area
13.11	1225-1	GC-4	19212-1	Venere MV (Flare 1)	19:32	20:04		20:38	38°37.106	17°11.623	1561				545 cm recovery, no storage. No GH.
13.11.	1226-1	GC-5	19213-1	Venere MV (in High-BS patch)	21:10	21:41		22:15	38°37.075	17°11.641	1567				232 cm recovery, no storage
14.11.	1227-1	CDT-4	19214-1	Venere MV (Flare 1)	05:01	05:07	06:01	06:05	38°37.109	17°11.622	1560				LADCP - current meter only
14.11.	1228-1	AUV-63	19215-1	Venere MV	07:28			18:01	38°36.930	17°10.207	1560	38°36.053	17°11.795	1546	Multibeam recording failed, but few files are recorded
14.11.	1229-1	CDT-5	19216-1	Venere MV (Flare 1)	18:30	18:35	20:41	20:46	38°37.037	17°11.729	1547	38°37.117	17°11.616	1561	All bottles closed. With Posidonia
15.11.	1230-1	SVP-2	19217-1	On transit to Cetus MV	17:02	17:15		17:28	37°43.570	17°53.115	2699				Sound velocity for multibeam calibration down to 400m
16.11.	1231-1	-	19218-1	Madonna (East MV)	05:00			06:43	38°11.118	16°55.932	1659				ROV dive canceled before reaching the seafloor
16.11.	1232-1	AUV-64	19219-1	Venere MV	15:10			00:38	38°37.086	17°09.877	1659	38°35.792	17°10.211	1588	
17.11.	1233-1	CTD-6	19220-1	Venere MV (Flare 2)	04:29	04:35	06:01	06:05	38°36.066	17°12.570	1587	38°36.071	17°12.559	1588	All bottles closed
17.11.	1234-1	ROV-339	19221-1	Venere MV (Flare 1)	07:00	08:24	16:16	17:31	38°37.083	17°11.606	1561	38°37.079	17°11.625	1543	
17.11.	1234-1	GBS	19221-2			09:11	09:18		38°37.095	17°11.603	1568				GBS-2 (blue), filled with gas
17.11.	1234-1	TS	19221-3			09:35	09:50		38°37.095	17°11.602	1568				In bubble stream
17.11.	1234-1	PC	19221-4			09:41	09:44		38°37.095	17°11.603	1568				R5, in bacterial mat within bubble stream
17.11.	1234-1	TS	19221-5			09:58	10:09		38°37.094	17°11.600	1567				In bacterial mat without bubble stream
17.11.	1234-1	PC	19221-6			10:03	10:03		38°37.095	17°11.602	1568				R2, in bacterial mat at rim
17.11.	1234-1	GBS	19221-7			10:25	10:26		38°37.095	17°11.602	1568				GBS-1 (yellow), filled with water
17.11.	1234-1	HD	19221-8			10:57	11:10		38°37.097	17°11.606	1569				Bubble imaging
17.11.	1234-1	HD	19221-9			11:23	11:39		38°37.096	17°11.602	1569				Bubble imaging
17.11.	1234-1	PC	19221-10			12:29	12:29		38°37.105	17°11.622	1568				R1 recovery, lost during dive 338
17.11.	1234-1	SS	19221-11			15:04	15:19		38°37.080	17°11.618	1564				Clams recovered in front of carbonates and tubes
17.11.	1234-1	SS	19221-12			15:45	15:58		38°37.080	17°11.624	1564				Recoverd a mussel and a tube worm
17.11.	1235-1	AUV-65	19222-1	Venere MV		18:25	07:11		38°36.652	17°13.279	1588	38°35.300	17°12.876	1555	
18.11.	1236-1	CTD-7	19223-1	Venere MV (Flare 1)	07:50	07:53	09:56	10:00	38°37.083	17°11.633	1549	38°37.110	38°37.111	1559	
18.11.	1237-1	ROV-340	19224-1	Venere MV (Flare 2)	10:59	12:18	15:15	16:35	38°36.049	17°12.577	1593	38°36.112	17°12.571	1593	
18.11.	1237-1	GBS	19224-2			13:20	13:38		38°36.096	17°12.571	1595				GBS-2 (blue) filled with gas in sporadic bubble stream
18.11.	1237-1	GBS	19224-3			13:56	13:57		38°36.097	17°12.571	1595				GBS-1 (yellow) filled with water close to bubble stream
18.11.	1238-1	AUV-66	19225-1	Cetus MV	21:34			08:01	37°52.589	17°28.922	2239	37°52.984	17°28.403	2239	
19.11.	1239-1	GC-6	19226-1	Cetus MV	08:32			10:00	37°52.837	17°30.375	2412				Core empty.
19.11	1240-1	GC-7	19227-1	Cetus MV	10:20			11:12	37°52.433	17°29.310	2322				165 cm recovery.
22.11.	1241-1	SVP-3	19228-1	East of Catania	12:17			12:39	37°21.533	15°48.649	2420				Down to 400 m
25.11.	1242-1	CTD-8	19229-1	Basin, SE of Sicily	05:05	05:11	07:33	07:37	37°04.003	15°55.096	3111				
25.11.	1242-2	GC-8	19229-2	Basin, SE of Sicily	08:02	09:00		10:00	37°04.006	15°55.096	3113				215 cm recovery, sediment sample taken.
25.11.	1242-3	GC-9	19229-3	Basin, SE of Sicily	10:24	11:22		12:20	37°04.010	15°55.100	3112				Core empty
26.11.	1243-1	ROV-341	19230-1	Venere MV (Flare 1)	07:02	08:26	15:25	16:49	38°37.088	17°11.604	1564	38°37.100	17°11.623	1568	
26.11.	1243-1	GBS	19230-2			08:47	08:50		38°37.095	17°11.609	1568				GBS-2 (blue) filled with water. Same position as in dive 339
26.11.	1243-1	TS	19230-3			09:04	09:14		38°37.095	17°11.609	1568				Between last T-Stick measurments, close to marker 1
26.11.	1243-1	PC	19230-4			09:27	09:29		38°37.095	17°11.608	1567				PC-10, gas hydrates came out of sediment while sampling
26.11.	1243-1	PC	19230-5			09:41	09:42		38°37.095	17°11.609	1567				PC-R1, gas hydrate chunks float up while sampling, penetration hampered, maybe gas hydrates below
26.11.	1243-1	Carbonate	19230-6			10:12	10:28		38°37.094	17°11.624	1566				Carbonate sample at northern rim of the patch in blue net

Appendix 1: Station List continued

Meteor M112

Station list

Date 2014	M112-St. No.	Instrument	GeoB St. No.	Location	Time (UTC)			Begin / on seafloor			End / off seafloor			Recovery Remarks
					Begin	on seafloor	off seafloor	End	Latitude N	Longitude E	Water d. (m)	Latitude N	Longitude E	Water d. (m)	
26.11.	1243-1	Mosaik	19230-7			11:30	12:00		38°37.082	17°11.624	1564	38°37.082	17°11.628	1563	
26.11.	1243-1	Carbonate	19230-8			13:03	13:03		38°37.081	17°11.629	1564				Large carbonate sample in sample box of yellow net
26.11.	1243-1	Carbonate	19230-9			13:10	13:10		38°37.082	17°11.629	1564				Small carbonate sample in box of yellow net
26.11.	1243-1	TS	19230-10			14:03	14:26		38°37.102	17°11.630	1567				T-Stick in between bacterial mat patches, soft sediment
26.11.	1243-1	GBS	19230-11			14:11	14:12		38°37.102	17°11.630	1568				GBS-1 (yellow) filled with water, same posizion as T-Stick
26.11.	1243-1	PC	19230-12a			14:42	14:58		38°37.102	17°11.630	1567				PC-R2 in bacterial mat, with dark patches, with PC-11
26.11.	1243-1	PC	19230-12b			14:44	14:56		38°37.101	17°11.628	1568				PC-11 with PC-R2
26.11.	1243-1	PC	19230-13a			14:46	14:55		38°37.101	17°11.628	1567				PC-R3 outside bacterial mat, with PC-12
26.11.	1243-1	PC	19230-13b			14:49	14:53		38°37.101	17°11.627	1568				PC-12 with PC-R3
26.11.	1243-1	PC	19230-14a			15:16	15:23		38°37.100	17°11.623	1567				PC-R4 inside bacterial mat, with PC-13
26.11.	1243-1	PC	19230-14b			15:21	15:21		38°37.100	17°11.623	1569				PC-13 with PC-R4
26.11.	1244-1	CTD-9	19231-1	Venere MV (Western summit)	17:48	17:52	19:12	19:17	38°36.430	17°11.282	1507				
28.11.	1245-1	ROV-342	19232-1	Venere MV (Western summit)	08:48	10:05	15:25	16:43	38°36.478	17°11.179	1499	38°36.463	17°11.292	1506	
28.11.	1245-1	TS	19232-2			13:07	13:20		38°36.433	17°11.258	1512				Hard underneath, on a white patch
28.11.	1245-1	PC	19232-3			13:12	13:13		38°36.433	17°11.258	1511				PC R1, with crystal looking pieces
28.11.	1245-1	NT	19232-4			13:28	13:31		38°36.433	17°11.258	1512				Sampled white material on yellow net
28.11.	1245-1	TS	19232-5			14:29	14:40		38°36.433	17°11.258	1512				6 images of caldera, last is 3119
28.11.	1245-1	PC	19232-6			14:33	14:36		38°36.433	17°11.258	1511				R2 inside caldera, low penetration
28.11.	1245-1	PC	19232-7			14:38	14:40		38°36.433	17°11.258	1511				R3 in much softer material, good penetration
28.11.	1245-1	GBS	19232-8			15:08	15:16		38°36.449	17°11.302	1509				GBS-2 (blue) on the rim south of WP3
28.11.	1245-1	GBS	19232-9			15:20	15:23		38°36.463	17°11.292	1506				GBS-1 (yellow) a bit north of the rim, not on flow
28.11.	1246-1	CTD-10	19233-1	Venere MV (Western summit)	18:25	18:49	21:06	21:10	38°36.447	17°11.313	1505	38°36.423	17°11.269	1500	
29.11.	1247-1	GC-10	19234-1	Venere MV (East)	07:12	07:50	07:52	08:22	38°36.663	17°11.973	1505				194 cm recovery
29.11.	1248-1	GC-11	19235-1	Venere MV (West)	08:52	09:24	09:26	09:57	38°36.457	17°11.037	1510				262 cm recovery
29.11.	1249-1	GC-12	19236-1	Venere MV (Flare 1)	10:29	11:04	11:06	11:39	38°37.094	17°11.605	1557				220 cm recovery, no storage
29.11.	1249-2	GC-13	19236-2	Venere MV (Flare 1)	11:57	12:38	12:40	13:10	38°37.095	17°11.606	1556				97 cm recovery, no storage
29.11.	1250-1	GC-14	19237-1	Venere MV (West)	13:49	14:24	14:26	15:01	38°35.930	17°11.828	1594				119 cm recovery
29.11.	1251-1	GC-15	19238-1	Venere MV (West)	15:40	16:13	16:16	16:50	38°36.757	17°11.378	1521				131 cm recovery
30.11.	1252-1	CTD-11	19239-1	Venere MV (Flare 5)	04:59	05:06	06:54	06:58	38°35.547	17°12.011	1604	38°35.453	17°12.093	1604	
30.11.	1253-1	ROV-343	19240-1	Venere MV (Flare 4+5)	07:46	09:26	17:31	19:18	38°35.425	17°11.967	1605	38°35.426	17°11.968	1606	
30.11.	1253-1	GBS	19240-2			10:37	10:56		38°35.458	17°12.022	1607				GBS-2 (blue) with gas, frequently pulsing at Flare 5
30.11.	1253-1	HD	19240-3			10:45	10:55		38°35.458	17°12.022	1607				Bubble quantification
30.11.	1253-1	TS	19240-4			11:10	11:31		38°35.457	17°12.021	1607				Third attempt close to bubble stream
30.11.	1253-1	Carbonate	19240-5			11:14	11:18		38°35.457	17°12.021	1607				2 pieces of carbonates into box of blue net
30.11.	1253-1	PC	19240-6			11:21	11:27		38°35.457	17°12.021	1607				PC-R1, first attempt failed
30.11.	1253-1	GBS	19240-7			11:45	11:46		38°35.457	17°12.021	1605				GBS-1 (yellow) with water sample in 2 m altitude
30.11.	1253-1	M	19240-8			11:50	11:50		38°35.457	17°12.021	1606				In the center of the seep structure
30.11.	1253-1	TS	19240-9			13:11	13:22		38°35.486	17°12.075	1608				Within bacterial mat seep 100 m NE of Flare 5
30.11.	1253-1	PC	19240-10			13:13	13:20		38°35.486	17°12.074	1608				PC-R2 within bacterial mat seep 100 m NE of Flare 5
30.11.	1253-1	TS	19240-11			13:23	13:35		38°35.486	17°12.074	1608				1 m East of bacterial mat
30.11.	1253-1	PC	19240-12			13:26	13:27		38°35.486	17°12.074	1608				PC-R3 next to T-Stick out of the mat
30.11.	1253-1	Mosaik	19240-13			14:49	15:24		38°35.454	17°12.023	1606	38°35.456	17°12.026	1606	Heading 303°, altitude 1.4 m
30.11.	1253-1	GBS	19240-14			15:39	15:41		38°35.458	17°12.022	1607				GBS-4 (black) with water close to bubble stream
30.11.	1253-1	PC	19240-15			16:14	16:20		38°35.425	17°11.969	1606				PC-R4 in microbial mat at edge of structure
30.11.	1253-1	PC	19240-16			16:22	16:28		38°35.425	17°11.968	1606				PC-18 close to R4
30.11.	1253-1	TS	19240-17			16:35	16:54		38°35.425	17°11.969	1606				Central site of microbial mound, with gas hydrates
30.11.	1253-1	PC	19240-18			16:41	17:07		38°35.426	17°11.969	1606				Several attempts failed
30.11.	1253-1	Shovel	19240-19			17:10	17:29		38°35.426	17°11.968	1606				Several attempts to get gas hydrate pieces
01.12.	1254-1	CTD-12	19241-1	Venere MV (Flare 5)	05:00	05:08	06:50	06:53	38°35.455	17°12.039	1598				Ship ADCP on
01.12.	1255-1	ROV-344	19242-1	Venere MV (Western summit)	07:26	08:45	16:39	18:00	38°36.453	17°11.244	1500	38°36.454	17°11.224	1497	
01.12.	1255-1	Mosaik	19242-2			08:55	09:35		38°36.456	17°11.245	1501	38°36.450	17°11.237	1501	Over mud flow from S to N
01.12.	1255-1	Mosaik	19242-3			09:54	11:09		38°36.453	17°11.218	1499	38°36.460	17°11.234	1500	Over central area of outflow
01.12.	1255-1	TS	19242-4			11:42	11:57		38°36.453	17°11.223	1499				In center of mud outflow, soft sediments
01.12.	1255-1	GBS	19242-5			11:47	11:49		38°36.453	17°11.223	1499				GBS-2 (blue) filled with water

Appendix 1: Station List continued

Meteor M112 — Station list

Date 2014	M112-St. No.	Instrument	GeoB St. No.	Location	Time (UTC)			Begin / on seafloor			End / off seafloor			Recovery Remarks
					Begin	on seafloor	off seafloor	End	Latitude N	Longitude E	Water d. (m)	Latitude N	Longitude E	Water d. (m)	
01.12.	1255-1	PC	19242-6			11:55	11:57		38°36.453	17°11.223	1499				Close to T-stick
01.12.	1255-1	TS	19242-7			12:06	12:15		38°36.453	17°11.223	1499				In the curved depression
01.12.	1255-1	TS	19242-8			12:48	13:06		38°36.456	17°11.220	1500				
01.12.	1255-1	Mosaik	19242-9			13:52	14:24		38°36.442	17°11.297	1509	38°36.441	17°11.291	1509	Transect mud flow
01.12.	1255-1	PC	19242-10			14:47	14:50		38°36.463	17°11.247	1502				PC-R6, north of fresh mud flow - hemipelagic drape
01.12.	1255-1	PC	19242-11			14:57	15:02		38°36.460	17°11.243	1502				PC-R7, with PC-15
01.12.	1255-1	PC	19242-12			15:00	15:02		38°36.460	17°11.243	1501				PC-15, with PC-R7, for volatiles
01.12.	1255-1	TS	19242-13			15:29	15:39		38°36.454	17°11.225	1499				1 Quest length from summit
01.12.	1255-1	PC	19242-14			15:30	15:34		38°36.454	17°11.225	1499				PC-R8, close to T-stick, with PC-16
01.12.	1255-1	PC	19242-15			15:33	15:36		38°36.454	17°11.225	1499				PC-16, with PC-R8
01.12.	1255-1	TS	19242-16			15:59	16:09		38°36.457	17°11.226	1500				10 m away from previous sampling area
01.12.	1255-1	PC	19242-17			16:02	16:07		38°36.456	17°11.227	1500				PC-R9, close to T-stick, sediment inside core compresses
01.12.	1255-1	PC	19242-18			16:04	16:04		38°36.456	17°11.227	1500				PC-17, with PC-R9
01.12.	1255-1	GBS	19242-19			16:23	16:25		38°36.453	17°11.223	1497				GBS-1 (yellow), 2 m above seafloor
01.12.	1255-1	GBS	19242-20			16:29	16:31		38°36.453	17°11.223	1496				GBS-4 (black), 3 m above seafloor
02.12.	1256-1	DAPC-1	19243-1	Venere MV (Flare 1)	06:58	07:51		08:30	38°37.095	17°11.604	1556				Device not released
02.12.	1256-2	DAPC-2	19243-2	Venere MV (Flare 1)	10:05	11:22		12:13	38°37.096	17°11.607	1556				Pressure and gas loss
02.12.	1257-1	GC-16	19244-1	Venere MV (East)	12:53	13:28		14:03	38°36.648	17°12.062	1518				96 cm recovery
02.12.	1258-1	GC-17	19245-1	Venere MV (Western summit)	14:34	15:06	15:08	15:35	38°36.455	17°11.223	1496				515 cm recovery, bubbles before recovery, no storage
02.12.	1258-2	GC-18	19245-2	Venere MV (Western summit)	15:59	16:34	16:37	17:45	38°36.454	17°11.222	1495				326 cm recovery
02.12.	1259-1	GC-19	19246-1	Venere MV (West)	17:34	18:07	18:11	18:57	38°36.504	17°11.615	1528				194 cm recovery, device damaged
03.12.	1260-1	CTD-13	19247-1	Venere MV (Canyon SE)	05:13	05:18	07:09	07:13	38°35.590	17°11.367	1602	38°35.560	17°11.443	1602	
03.12.	1261-1	HF-1	19248-1	Venere MV (Western summit)	11:11			11:22	38°36.450	17°11.220	1498				
03.12.	1261-2	HF-2	19248-2	Venere MV (Western summit)	11:35			11:46	38°36.452	17°11.221	1500				
03.12.	1261-3	HF-3	19248-3	Venere MV (Western summit)	11:57			12:08	38°36.452	17°11.223	1498				
03.12.	1261-4	HF-4	19248-4	Venere MV (Western summit)	12:30			12:40	38°36.454	17°11.226	1495				
03.12.	1261-5	HF-5	19248-5	Venere MV (Western summit)	12:51			13:02	38°36.455	17°11.227	1496				Came up with 1/2 - 2/3 mud
03.12.	1262-1	ROV-345	19249-1	Venere MV (Flare 4+5)	14:26	15:44	19:17	20:44	38°35.457	17°12.016	1605	38°35.427	17°11.958	1606	
03.12.	1262-1	ASSMO	19249-2			16:10	16:24		38°35.456	17°12.019	1607				Installed close to Marker 2
03.12.	1262-1	TS	19249-3			16:39	16:48		38°35.454	17°12.020	1607				Installed on top of the mound at Marker 2
03.12.	1262-1	HD	19249-4			17:16	17:37		38°35.456	17°12.021	1607				Pulsing bubble stream in front of sonar
03.12.	1262-1	GBS	19249-5			18:12	18:27		38°35.429	17°11.960	1606				GBS-1 (yellow) filled with gas, HD on, shot with lasers
03.12.	1262-1	TS	19249-6			18:33	18:42		38°35.429	17°11.959	1606				At bubbling site
03.12.	1262-1	PC	19249-7			18:37	18:40		38°35.429	17°11.959	1606				PC-R1, at bubbling site
03.12.	1262-1	PC	19249-8			18:38	18:39		38°35.429	17°11.959	1606				PC-15, at bubbling site
03.12.	1262-1	M	19249-9			18:45	18:46		38°35.428	17°11.959	1606				Marker 3, at bubbling site
03.12.	1262-1	TS	19249-10			18:56	19:15		38°35.428	17°11.958	1605				Background, 5 m away from Marker 3
03.12.	1262-1	GBS	19249-11			18:59	19:05		38°35.427	17°11.958	1606				Background, 5 m from Marker 3, GBS-2 (blue) with water
03.12.	1262-1	PC	19249-12			19:06	19:14		38°35.427	17°11.958	1606				PC-R2, not fully vertical
03.12.	1262-1	PC	19249-13			19:07	19:07		38°35.427	17°11.958	1606				PC-16, not successful
03.12.	1262-1	PC	19249-14			19:11	19:12		38°35.427	17°11.958	1606				PC-17, disturbed surface
04.12.	1263-1	CTD-14	19250-1	Venere MV (Western summit)	05:26	05:30	07:52	07:55	38°36.451	17°11.214	1495	38°36.447	17°11.236	1495	
04.12.	1264-1	DAPC-3	19251-1	Venere MV (Western summit)	08:06	09:12	09:15	09:59	38°36.452	17°11.224	1497				180 bar inside pressure chamber
04.12.	1265-1	ROV-346	19252-1	Venere MV (Flare 4+5)	11:29	12:43	19:09	20:27	38°35.448	17°12.022	1605	38°35.458	17°12.021	1607	
04.12.	1265-1	HD	19252-2			13:04	13:14		38°35.458	17°12.022	1607				At Marker 2, close to ASSMO
04.12.	1265-1	HD	19252-3			14:15	14:20		38°35.429	17°11.971	1606				Bubble stream at Waypoint2
04.12.	1265-1	Carbonate	19252-4			14:42	14:44		38°35.428	17°11.971	1606				
04.12.	1265-1	BC	19252-5			15:01	15:10		38°35.430	17°11.960	1606				At Marker 3, gas quantification
04.12.	1265-1	TS	19252-6			15:17	15:30		38°35.430	17°11.960	1607				2 tries did not penetrate, lance bent afterwards
04.12.	1265-1	PC	19252-7			15:54	15:55		38°35.445	17°11.959	1606				PC-R1, short core, hard bottom
04.12.	1265-1	GBS	19252-8			15:57	16:01		38°35.445	17° 11.959	1607				GBS-2 (blue) filled with water
04.12.	1265-1	PC	19252-9			16:19	16:21		38°35.433	17°11.944	1606				PC-R2, on top of white plates, lost upon retrieval
04.12.	1265-1	PC	19252-10			16:23	16:24		38°35.432	17°11.943	1605				PC-R3, surface with crystals
04.12.	1265-1	BC	19252-11			16:26	16:30		38°35.432	17°11.943	1605				Retrieval of crystals on top

Appendix 1: Station List continued

Meteor M112 — Station list

Date 2014	M112-St. No.	Instrument	GeoB St. No.	Location	Time (UTC)			Begin / on seafloor			End / off seafloor			Recovery Remarks
					Begin	on seafloor	off seafloor	End	Latitude N	Longitude E	Water d. (m)	Latitude N	Longitude E	Water d. (m)	
04.12.	1265-1	GBS	19252-12			17:15	17:15		38°35.428	17°11.950	1605				GBS-4 (black) with water, at collaps structure, close to gas stream
04.12.	1265-1	NT	19252-13			17:33	17:54		38°35.428	17°11.950	1606				From collaps structure
04.12.	1265-1	PC	19252-14			18:28	18:28		38°35.465	17°12.018	1607				PC-R4, at Flare 5 North of Marker 2
04.12.	1265-1	PC	19252-15			18:32	18:32		38°35.465	17°12.018	1607				PC-18, with PC-R4
05.12.	1266-1	ROV-347	19253-1	Cetus MV	09:10	10:55	17:33	19:16	37°53.121	17°27.751	2267	37°52.753	17°27.769	2233	
05.12.	1266-1	TS	19253-2			11:12	11:22		37°53.117	17°27.744	2268				Outside caldera
05.12.	1266-1	TS	19253-3			11:42	11:50		37°53.073	17°27.745	2243				On the rim
05.12.	1266-1	TS	19253-4			12:13	12:20		37°53.017	17°27.742	2250				At the depression
05.12.	1266-1	TS	19253-5			12:44	12:54		37°52.961	17°27.742	2244				On mudflow
05.12.	1266-1	TS	19253-6			13:16	13:26		37°52.917	17°27.740	2239				On mudflow
05.12.	1266-1	TS	19253-7			13:57	14:04		37°52.871	17°27.738	2236				In high backscatter
05.12.	1266-1	TS	19253-8			14:19	14:29		37°52.832	17°27.737	2232				In direction towards center
05.12.	1266-1	NT	19253-9			14:26	14:29		37°52.833	17°27.737	2231				"Grass"
05.12.	1266-1	TS	19253-10			15:06	15:17		37°52.809	17°27.736	2231				End station in caldera
05.12.	1266-1	GBS	19253-11			15:08	15:11		37°52.809	17°27.736	2232				GBS-2 (blue), end station in caldera
05.12.	1266-1	PC	19253-12			15:15	15:16		37°52.809	17°27.736	2232				PC-R7, ca. 1 m East of T-stick
05.12.	1266-1	TS	19253-13			15:30	15:42		37°52.786	17°27.735	2232				At WP 2
05.12.	1266-1	TS	19253-14			15:56	16:06		37°52.769	17°27.733	2233				
05.12.	1266-1	TS	19253-15			16:16	16:25		37°52.754	17°27.734	2235				Southermost station of this profile (N-S)
05.12.	1266-1	TS	19253-16			17:17	17:27		37°52.754	17°27.768	2234				Start W-E profile towards WP 4
05.12.	1267-1	HF-6	19254-1	Cetus MV	20:35			20:43	37°52.959	17°28.451	2258				With Posidonia
05.12.	1267-2	HF-7	19254-2	Cetus MV	21:22			21:30	37°52.806	17°28.513	2254				Posidonia not working any more
05.12.	1267-3	HF-8	19254-3	Cetus MV	21:55			22:03	37°52.754	17°28.631	2250				Came up with ca. 2/3 mud
06.12.	1268-1	ROV-348	19255-1	Nicolas MV	10:13	12:06	18:11	20:07	37°49.003	17°58.231	2676	37°48.776	17°58.110	2680	
06.12.	1268-1	TS	19255-2			12:46	12:57		37°48.996	17°58.232	2677				Close to WP 1, soft sediments
06.12.	1268-1	NT	19255-3			12:54	12:56		37°48.996	17°58.232	2677				Red net, pieces of rocks next to T-stick
06.12.	1268-1	PC	19255-4			13:03	13:05		37°48.996	17°58.232	2677				PC-R6, next to T-stick, not penetrating entirely
06.12.	1268-1	GBS	19255-5			13:11	13:11		37°48.996	17°58.232	2677				GBS-2 (blue) with water, at same location
06.12.	1268-1	TS	19255-6			15:04	15:15		37°48.896	17°58.131	2692				On a mound structure in the center of the depression
06.12.	1268-1	PC	19255-7			15:08	15:13		37°48.895	17°58.131	2692				PC-R5, close to T-stick
06.12.	1268-1	PC	19255-8			15:10	15:12		37°48.896	17°58.132	2692				PC-19, with PC-R5
06.12.	1268-1	NT	19255-9			15:35	15:39		37°48.895	17°58.126	2692				Blue net, close to WP 4 within mounds, rocks or clasts
06.12.	1268-1	GBS	19255-10			16:15	16:18		37°48.885	17°58.113	2692				GBS-1 (yellow) with water, close to pteropods, SE of WP 4
06.12.	1268-1	NT	19255-11			16:29	16:39		37°48.885	17°58.114	2692				Yellow net, sample of pteropods and small rocks
06.12.	1268-1	TS	19255-12			17:21	17:31		37°48.814	17°58.128	2683				On southern rim of crater, among pteropods
06.12.	1268-1	GBS	19255-13			17:25	17:26		37°48.814	17°58.128	2684				GBS-4 (black) with water, close to T-stick
07.12.	1269-1	CTD-15	19256-1	Venere MV (Flare 2)	05:08	05:12	07:07	07:10	38°36.115	17°12.549	1589	38°36.076	17°12.566	1588	
07.12.	1270-1	DAPC-4	19257-1	Venere MV (Flare 1)	07:43	08:31	08:33	09:15	38°37.095	17°11.604	1561				
07.12.	1271-1	ROV-349	19258-1	Venere MV (Western summit)	09:58	11:15	18:16	19:20	38°36.304	17°11.177	1523	38°36.452	17°11.217	1498	
07.12.	1271-1	TS	19258-2			12:33	12:45		38°36.428	17°11.287	1514				At bacterial mat on flank of Flare 3
07.12.	1271-1	GBS	19258-3			12:38	12:38		38°36.428	17°11.287	1515				GBS-2 (blue) with water, close to T-stick
07.12.	1271-1	PC	19258-4			12:42	12:44		38°36.428	17°11.287	1514				PC-R4, at same spot
07.12.	1271-1	Mosaik	19258-5			14:06	14:17		38°36.413	17°11.330	1518	38°36.443	17°11.357	1519	Line 1, crossing the mud flows
07.12.	1271-1	Mosaik	19258-6			14:22	14:34		38°36.437	17°11.360	1520	38°36.412	17°11.329	1518	Line 2, crossing the mu flows, SE of line 1
07.12.	1271-1	Mosaik	19258-7			14:51	15:01		38°36.382	17°11.375	1526	38°36.397	17°11.410	1527	Line 3, crossing flow to NE with 60°, ca. 80 m SW of line 2
07.12.	1271-1	Mosaik	19258-8			15:07	15:21		38°36.390	17°11.413	1528	38°36.376	17°11.363	1525	Line 4, crossing flow with 290°, 15 m SE of line 3
07.12.	1271-1	PC	19258-9			15:23	15:29		38°36.377	17°11.364	1527				PC-R7, on older mud flow, dark sediment beneath hemipelagic
07.12.	1271-1	TS	19258-10			15:55	16:03		38°36.395	17°11.361	1525				On oldest flow, sinked slightly into sediment
07.12.	1271-1	PC	19258-11			15:57	15:59		38°36.395	17°11.361	1526				PC-R8, close to T-stick, very fluid mud
07.12.	1271-1	PC	19258-12			15:59	15:59		38°36.395	17°11.361	1526				PC-3, with R8, gas bubble release
07.12.	1271-1	TS	19258-13			16:23	16:34		38°36.419	17°11.328	1519				60 m up the mud flow, soft material
07.12.	1271-1	PC	19258-14			16:26	16:29		38°36.419	17°11.328	1520				PC-R9, close to T-stick

Appendix 1: Station List continued

Meteor M112 — Station list

Date 2014	M112-St. No.	Instrument	GeoB St. No.	Location	Time (UTC) Begin	Time (UTC) on seafloor	Time (UTC) off seafloor	Time (UTC) End	Begin / on seafloor Latitude N	Begin / on seafloor Longitude E	Begin / on seafloor Water d. (m)	End / off seafloor Latitude N	End / off seafloor Longitude E	End / off seafloor Water d. (m)	Recovery Remarks
07.12.	1271-1	PC	19258-15			16:27	16:28		38°36.419	17°11.328	1520				PC-4, with PC-R9
07.12.	1271-1	TS	19258-16			17:20	17:29		38°36.450	17°11.283	1510				60 m up the mud flow, at beginning of concave structure
07.12.	1271-1	PC	19258-17			17:23	17:26		38°36.450	17°11.283	1509				PC-R10, very soft sediment
07.12.	1271-1	PC	19258-18			17:24	17:25		38°36.450	17°11.283	1509				PC-5, with PC-R10
07.12.	1271-1	GBS	19258-19			17:48	17:52		38°36.458	17°11.234	1502				GBS-1 (yellow) with water, 10 m from summit, 0.5 m altitude
07.12.	1271-1	GBS	19258-20			18:04	18:07		38°36.452	17°11.217	1499				GBS-4 (black) with water, at summit, 0.5 m altitude
07.12.	1272-1	HF-9	19259-1	Venere MV (West)	20:11			20:19	38°36.460	17°11.255	1494				On western summit
07.12.	1272-2	HF-10	19259-2	Venere MV (West)	20:38			20:46	38°36.455	17°11.286	1499				Downewards along eastern mud flow
07.12.	1272-3	HF-11	19259-3	Venere MV (West)	21:04			21:12	38°36.435	17°11.322	1505				Downewards along eastern mud flow
07.12.	1272-4	HF-12	19259-4	Venere MV (West)	21:39			21:47	38°36.401	17°11.371	1515				Downewards along eastern mud flow
07.12.	1272-5	HF-13	19259-5	Venere MV (West)	22:11			22:19	38°36.430	17°11.406	1519				Between the two cones
08.12.	1273-1	GC-20	19260-1	Venere MV (Flare 2)	06:00	06:37	06:39	07:10	38°35.802	17°11.579	1590				271 cm recovery
08.12.	1274-1	GC-21	19261-1	Venere MV (Mud flow 3)	07:31	08:04	08:07	08:41	38°35.876	17°11.714	1600				257 m recovery, no echosounder depth
08.12.	1275-1	CTD-16-1	19262-1	Venere MV	10:09	10:27	11:36	11:38	38°37.340	17°10.154	1522				
08.12.	1275-2	CTD-16-2	19262-2	Venere MV	12:12	12:16	13:26	13:29	38°36.966	17°10.522	1560				
08.12.	1276-1	GC-22	19263-1	Venere MV	13:54	14:28	14:29	15:07	38°36.448	17°11.282	1500				275 cm recovery, no storage
08.12.	1277-1	GC-23	19264-1	Venere MV (Mud flow 4)	15:24	15:54	15:56	17:00	38°36.166	17°12.041	1590				163 cm recovery
08.12.	1278-1	CTD-17	19265-1	Venere MV (SW Canyon)	16:53	16:57	18:35	18:38	38°35.697	17°11.029	1597	38°35.737	17°10.968	1594	With T-sticks for calibration
09.12.	1279-1	DAPC-5	19266-1	Venere MV	04:46	05:50		06:53	38°36.449	17°11.283	1498				Device not released
09.12.	1280-1	ROV-350	19267-1	Venere MV (Flare 2)	07:58	09:10	13:25	14:38	38°36.093	17°12.571	1593	38°36.100	17°12.563	1595	
09.12.	1280-1	GBS	19267-2			10:53	10:54		38°36.119	17°12.556	1597				GBS-4 (black), northern seep site, no bubbles, altit. 50 cm
09.12.	1280-1	Mosaik	19267-3			11:31	11:59		38°36.091	17°12.560	1595	38°36.086	17°12.566	1594	Over depression structure, 20 m lines with 1.5 m spacing
09.12.	1280-1	PC	19267-4			12:28	12:33		38°36.100	17°12.563	1596				PC-R2, area of clamshells and gas bubbles
09.12.	1280-1	PC	19267-5			12:31	12:32		38°36.100	17°12.563	1596				PC-3, with R2, gas causes loss of sediment
09.12.	1280-1	PC	19267-6			12:34	12:36		38°36.100	17°12.563	1596				PC-4, near the above, no loss due to bubbles
09.12.	1280-1	TS	19267-7			12:44	12:58		38°36.100	17°12.564	1596				Near gas bubbles, insertion causes bubble stream
09.12.	1280-1	PC	19267-8			12:46	12:47		38°36.100	17°12.564	1596				PC-R3, near T-stick, only half penetration
09.12.	1280-1	PC	19267-9			12:48	12:49		38°36.100	17°12.563	1596				PC-5, with PC-R3, only half penetration
09.12.	1280-1	PC	19267-10			12:50	12:50		38°36.100	17°12.563	1596				PC-R5, almost full penetration, brownish sediment over darker
09.12.	1280-1	GBS	19267-11			12:53	12:56		38°36.100	17°12.563	1596				GBS-2 (blue), near T-stick, bottom water sample
09.12.	1280-1	GBS	19267-12			13:06	13:07		38°36.100	17°12.563	1595				GBS-1 (yellow), with water, altitude 60 cm. few meters to left
09.12.	1280-1	M	19267-13			13:20	13:21		38°36.101	17°12.563	1595				Marker "Snowwoman", close to bacterial mat
09.12.	1281-1	DAPC-6	19268-1	Venere MV	15:00	16:05	16:07	17:07	38°36.450	17°11.282	1500				Ca. 180 bar pressure inside
09.12.	1282-1	GC-24	19269-1	Venere MV (Mud flow 1)	17:44	18:19	18:21	19:05	38°36.105	17°11.915	1590				300 cm recovery
09.12.	1283-1	GC-25	19270-1	Venere MV (Mud flow 1)	19:21	20:03	20:06	20:46	38°36.176	17°11.129	1534				255 cm recovery
09.12.	1284-1	CTD-18	19271-1	Venere MV (South)	21:17	21:23	22:56	23:02	38°35.853	17°12.060	1594	38°35.870	17°12.027	1594	Posidonia at 23 m instead of 10 m
09.12.	1285-1	CTD-19	19272-1	Venere MV (Southern flank)	23:44	23:47	00:50	00:52	38°36.081	17°11.682	1566				Technical problems with winch
10.12.	1286-1	CTD-20	19273-1	Venere MV (Western summit)	01:22	01:27	03:07	03:12	38°36.426	17°11.260	1505	38°36.493	17°11.187	1497	
10.12.	1287-1	CTD-21	19274-1	Venere MV (Northern flank)	03:43	03:47	04:45	04:46	38°36.700	17°10.942	1532				
10.12.	1288-1	CTD-22	-	Venere MV	05:12			05:17	38°35.470	17°12.650	1613				CTD not working, not deployed
10.12.	1289-1	GC-26	19275-1	Venere MV (Flank)	07:05	07:44	07:46	08:18	38°36.022	17°11.865	1587				93 cm recovery
10.12.	1290-1	GC-27	19276-1	Venere MV	08:40	09:27	09:29	10:00	38°36.393	17°11.348	1516				195 m recovery, no storage
10.12.	1291-1	GC-28	19277-1	Venere MV (Western flow)	10:32	11:07	11:09	11:43	38°36.167	17°10.873	1543				38 cm recovery, hit carbonates on seafloor
10.12.	1292-1	GC-29	19278-1	Venere MV (NW flow)	12:07	12:47	12:49	13:24	38°36.338	17°10.850	1535				293 cm recovery, posidonia failed while in water
10.12.	1293-1	GC-30	19279-1	Venere MV	14:12	14:42	14:44	15:20	38°34.784	17°12.881	1560				404 cm recovery
10.12.	1293-2	-	19279-2	Venere MV	16:00			16:10	38°34.790	17°12.880	1560				Winch failure, not deployed
10.12.	1293-3	MIC-3	19279-3	Venere MV	16:24	17:03	17:05	17:50	38°34.783	17°12.883	1560				3 cores succesfully filled
10.12.	1294-1	GC-31	19280-1	Venere MV	18:05	18:35	18:37	19:07	38°36.851	17°12.048	1513				286 cm recovery
10.12.	1295-1	CTD-23	19281-1	Venere MV (NW channel)	19:34	19:39	21:27	21:32	38°36.149	17°09.983	1555	38°36.142	17°09.871	1555	
11.12.	1296-1	GC-32	19282-1	Cetus MV	07:00	07:44	07:47	08:34	37°52.275	17°28.362	2287				Serious overpenetration
11.12.	1297-1	GC-33	19283-1	Cetus MV	09:22	10:03	10:06	11:00	37°52.807	17°27.736	2216				293 cm recovery, serious overpenetration, no storage

Appendix 1: Station List continued

Meteor M112 Station list

					Time (UTC)				Begin / on seafloor			End / off seafloor			
Date 2014	M112-St. No.	Instrument	GeoB St. No.	Location	Begin	on seafloor	off seafloor	End	Latitude N	Longitude E	Water d. (m)	Latitude N	Longitude E	Water d. (m)	Recovery Remarks
11.12.	1298-1	GC-34	19284-1	Cetus MV	11:28	12:13		13:10	37°51.789	17°30.230	2432				Overpenetration
11.12.	1299-1	GC-35	19285-1	Cetus MV	13:45	14:30		15:13	37°52.067	17°29.900	2378				Overpenetration ca. half of weight part
11.12.	1300-1	GC-36	19286-1	Cetus MV	15:47	16:31		17:20	37°52.140	17°30.436	2438				
12.12.	1301-1	DAPC-7	19287-1	Venere MV (West)	05:57	06:55	06:58	07:59	38°36.394	17°11.361	1516				Ca. 200 bar pressure
12.12.	1302-1	CTD-24	19288-1	Venere MV (SE basin)	08:35	08:39	10:01	10:03	38°35.462	17°12.637	1622	38°35.454	17°12.615	1615	
12.12.	1303-1	GC-37	19289-1	Sartori MV	13:15	13:50	13:51	14:40	38°12.200	17°35.712	1960				Ca. 3 m recovery, in low backscatter area, posidonia failed
12.12.	1304-1	GC-38	19290-1	Sartori MV	15:01	15:39	15:41	16:20	38°11.732	17°36.241	1958				Ca. 5 m recovery

Instruments

AUV: SEAL 5000
ROV: QUEST 4000
DAPC: Autoclave piston corer
GC: Gravity corer
GC-T: GC with MTLs
MIC: Minicorer

SVP: Sound velocity profiler
CTD: CTD with hydro casts + LADCP

ROV payload

TS: T-Stick
GBS: Gas bubble sampler
BC: Bubble catcher
PC: Push corer
NT: Net
ASSMO: Autonomous scanning sonar
M: Marker
SS: Suction sampler
HD: Zeus record
NS: Niskin bottle

16.2 Appendix 2: Core Descriptions DAPC

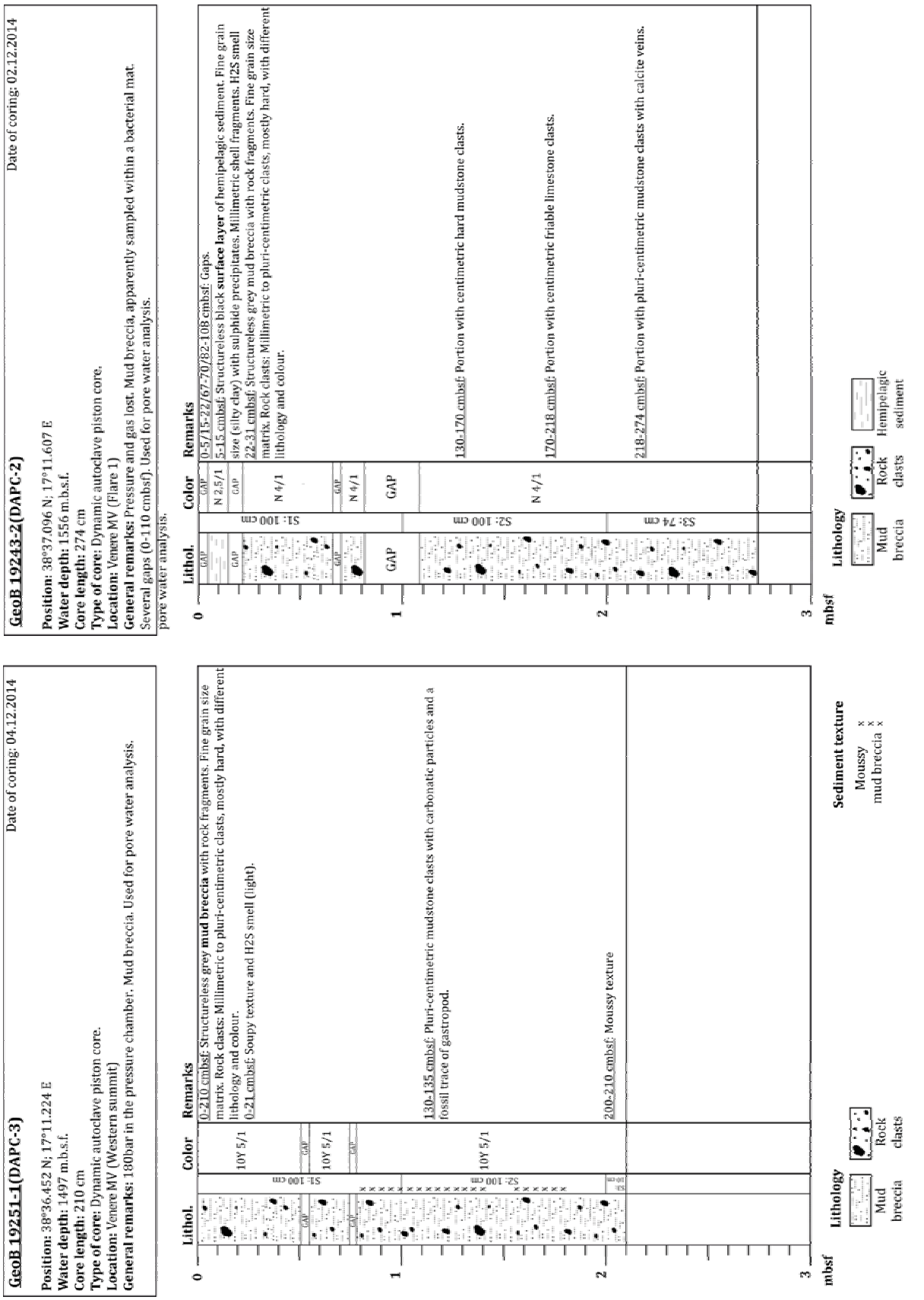

Appendix 2: Core Descriptions DAPC continued

GeoB 19257-1(DAPC-4) Date of coring: 07.12.2014

Position: 38°37.095 N; 17°11.604 E
Water depth: 1561 m.b.s.f.
Core length: 182 cm
Type of core: Dynamic autoclave piston core.
Location: Venere MV (Flare 1)
General remarks: Used for pore water analysis. Clasts in the core catcher: pluri-centimetric mudstone with calcitic veins.

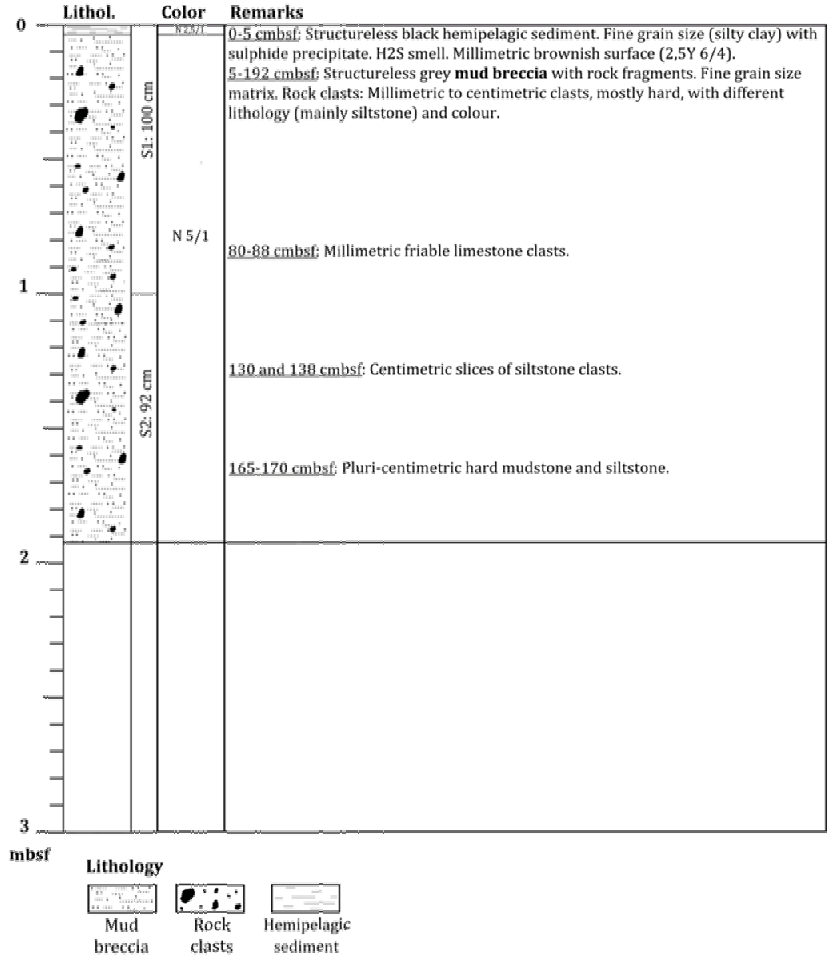

GeoB 19268-1(DAPC-6) Date of coring: 09.12.2014

Position: 38°36.450 N; 17°11.282 E
Water depth: 1500 m.b.s.f.
Core length: 253 cm
Type of core: Dynamic autoclave piston core.
Location: Venere MV
General remarks: Ca. 180bar of pressure inside. Used for pore water analysis.

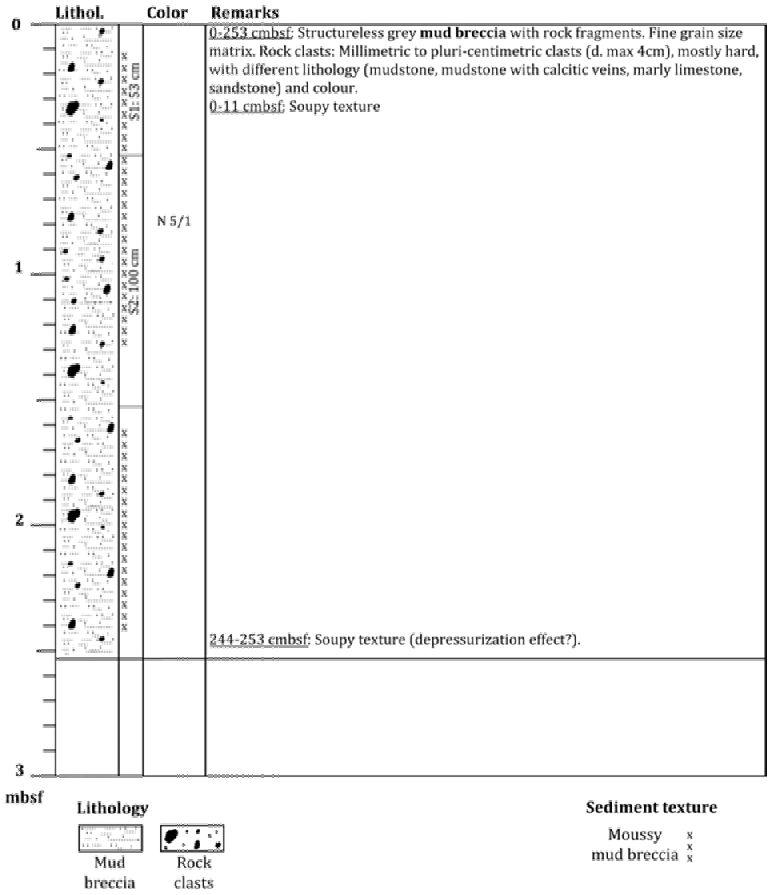

Appendix 2: Core Descriptions MIC

GeoB 19208-1_MIC-1 Date of coring: 12.11.2014

Position: 38°37.156 N; 17°11.621 E
Water depth: 1560 m.b.s.f.
Core length: 26 cm
Type of core: Mini core
Location: Venere MV (Flare site)
General remarks: The black moussy layer was keeped in sample (15.5 cm to 21 cm).

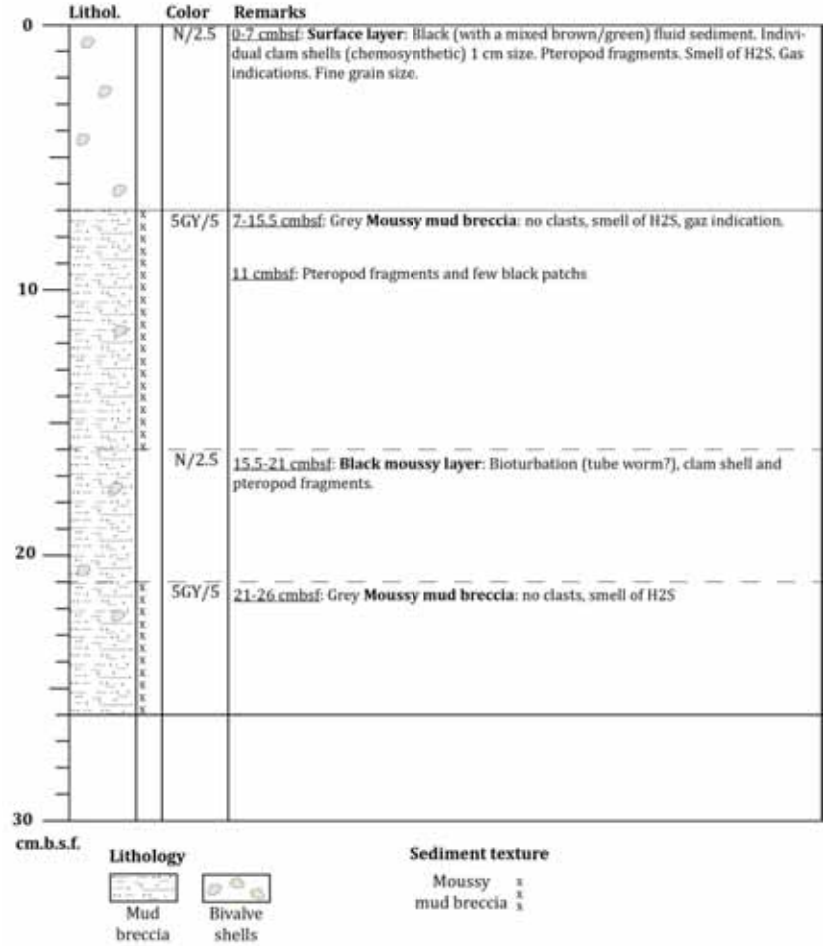

GeoB 19208-1_MIC-2 Date of coring: 12.11.2014

Position: 38°37.156 N; 17°11.621 E
Water depth: 1560 m.b.s.f.
Core length: 26 cm
Type of core: Mini core
Location: Venere MV (Flare site)
General remarks: This MIC was keeped in sample.

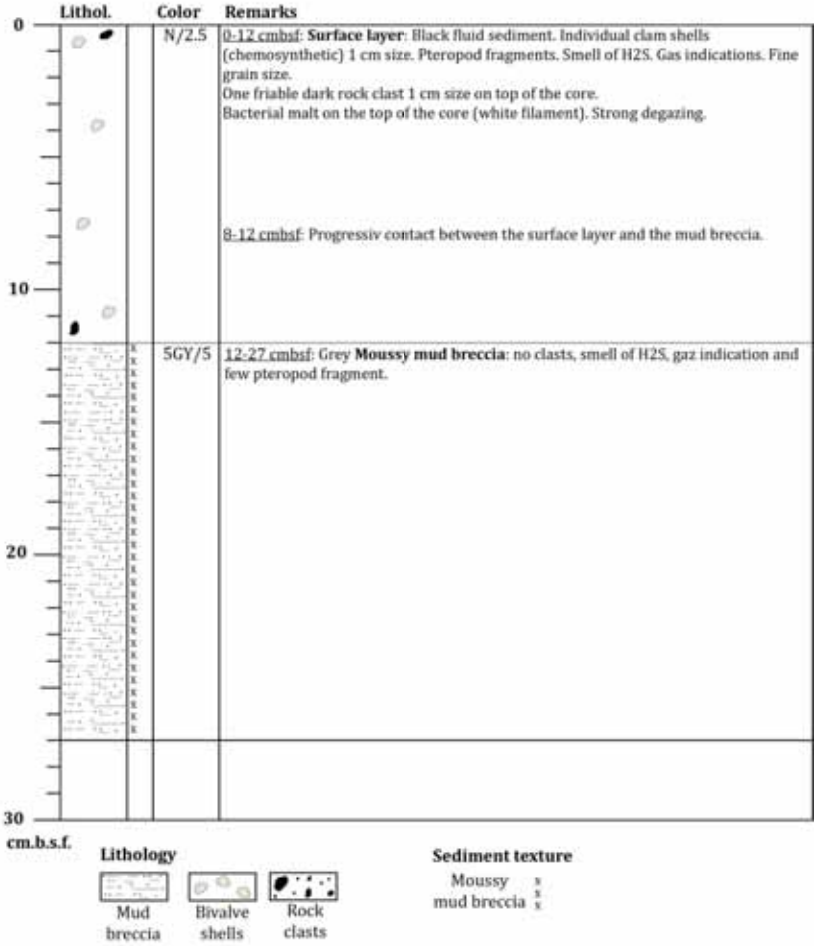

Appendix 2: Core Descriptions MIC continued

GeoB 19209-1 Date of coring: 12.11.2014

Position: 38°36.607 N; 17°11.229 E
Water depth: 1508 m.b.s.f.
Core length: 27 cm
Type of core: Mini core
Location: Venere MV (Western peak, upper flank)
General remarks: This MIC was keep in sample. 3 bags: One fore the top (0-7cm), the seconde for the mixe (8-12cm), the third for the mud breccia (13-27cm)

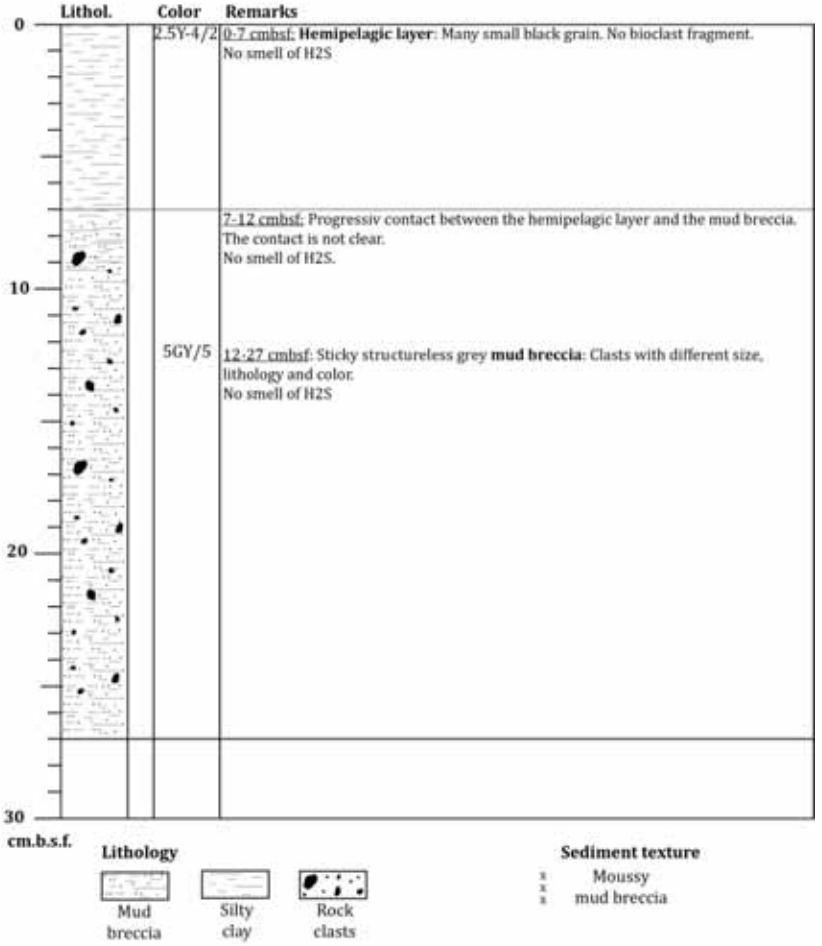

GeoB 19279-3 Date of coring: 26.11.2014

Position: 38°34.783 N; 17°12.883 E
Water depth: 1560 m.b.s.f.
Core length: 14 cm
Type of core: Mini core
Location: Venere MV
General remarks: This MiC is used only for sedimentological description, as a reference for the others.

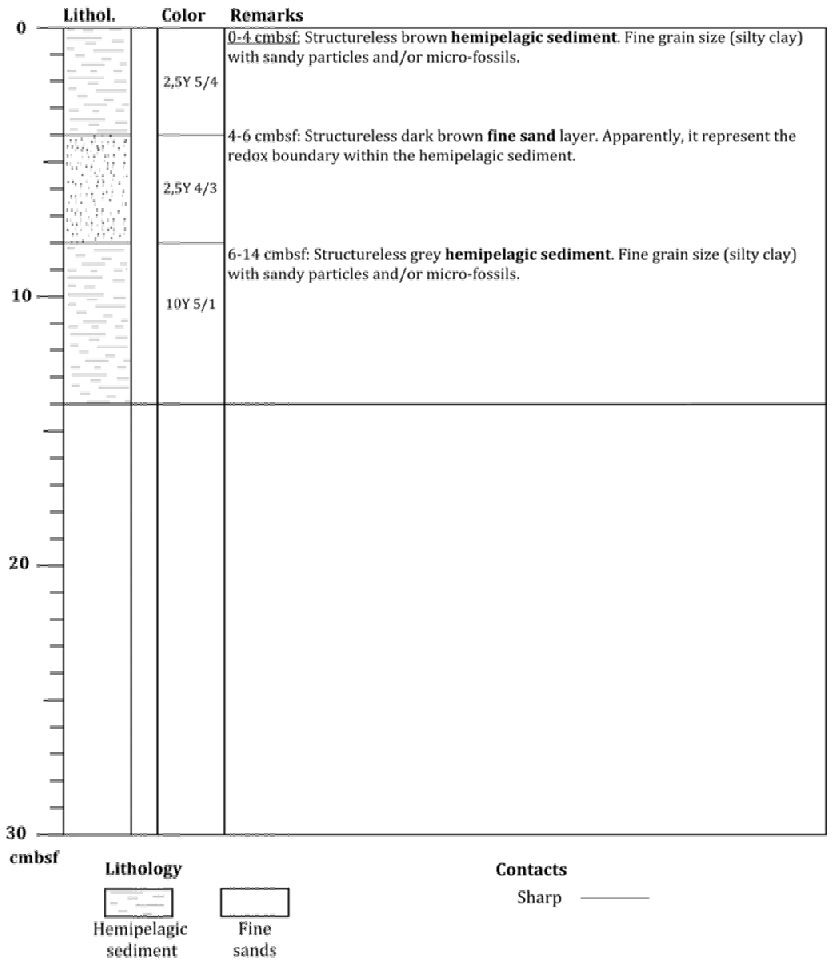

Appendix 2: Core Descriptions GC

GeoB 19205-1(GC-1) Date of coring: 10.11.2014

Position: 38°37.101 N; 17°11.619 E
Water depth: 1556 m.b.s.f.
Core length: 262 cm
Type of core: Gravity core. Liner: PVC
Location: Venere MV (Flare site)
General remarks:

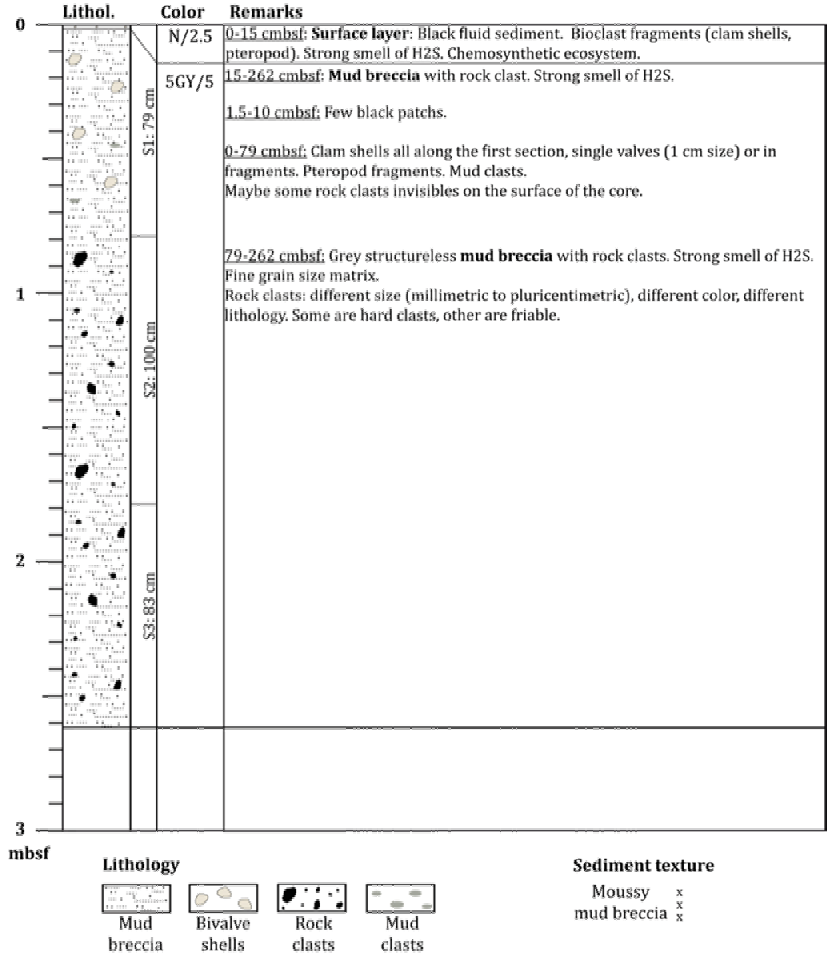

GeoB 19205-2(GC-2) Date of coring: 10.11.2014

Position: 38°37.103 N; 17°11.621 E
Water depth: 1556 m.b.s.f.
Core length: 176 cm
Type of core: Gravity core. Liner: Plastic bag
Location: Venere MV (Flare site)
General remarks: Pore water analysis. This core was keep as sample.

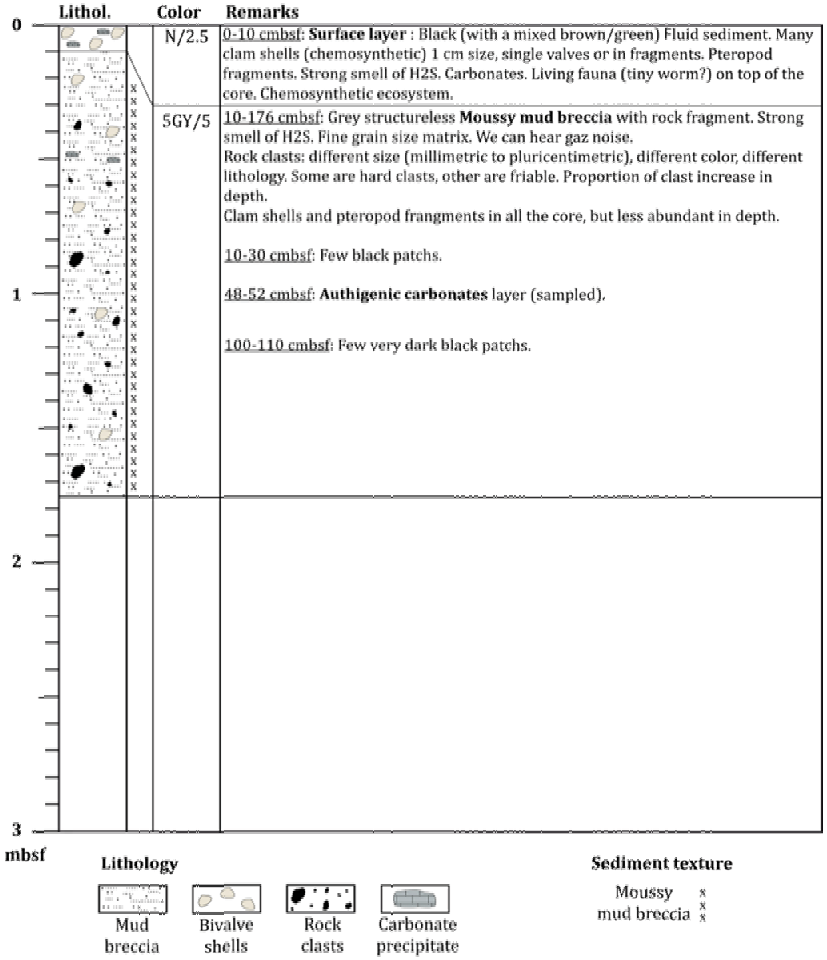

Appendix 2: Core Descriptions GC continued

GeoB 19206-1(GC-3) Date of coring: 11.11.2014

Position: 38°36.605 N; 17°11.235 E
Water depth: 1506 m.b.s.f.
Core length: 227 cm
Type of core: Gravity core. Liner: PVC
Location: Venere MV
General remarks:

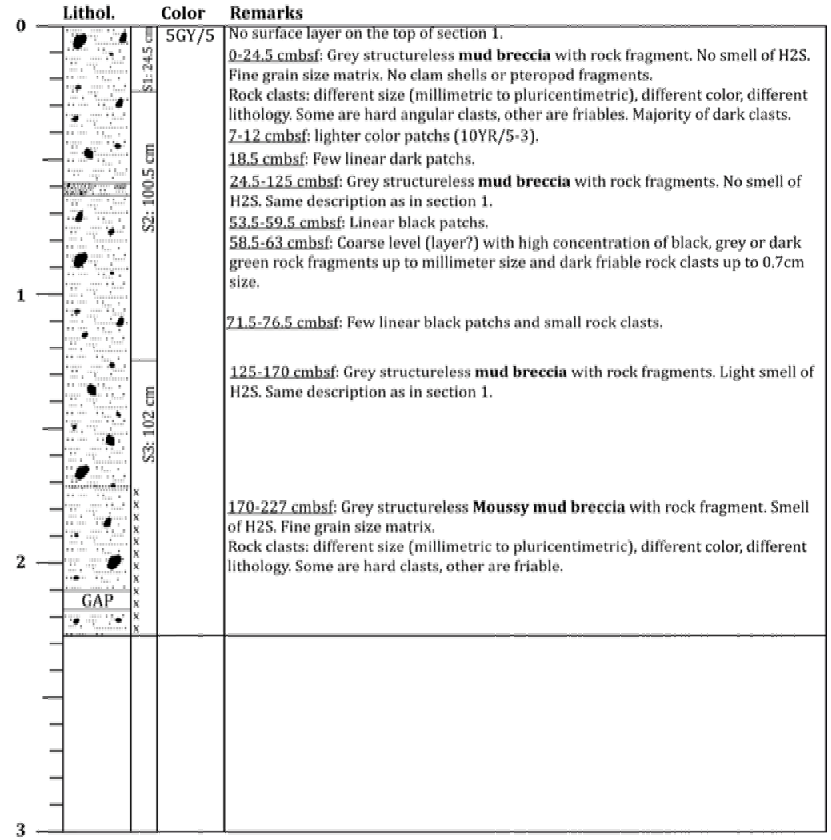

GeoB 19213-1 Date of coring: 13.11.2014

Position: 38°37.075 N; 17°11.641 E
Water depth: 1567 m.b.s.f.
Core length: 232 cm
Type of core: Gravity core. Liner: Plastic bag
Location: Venere MV (in high-BS patch)
General remarks:

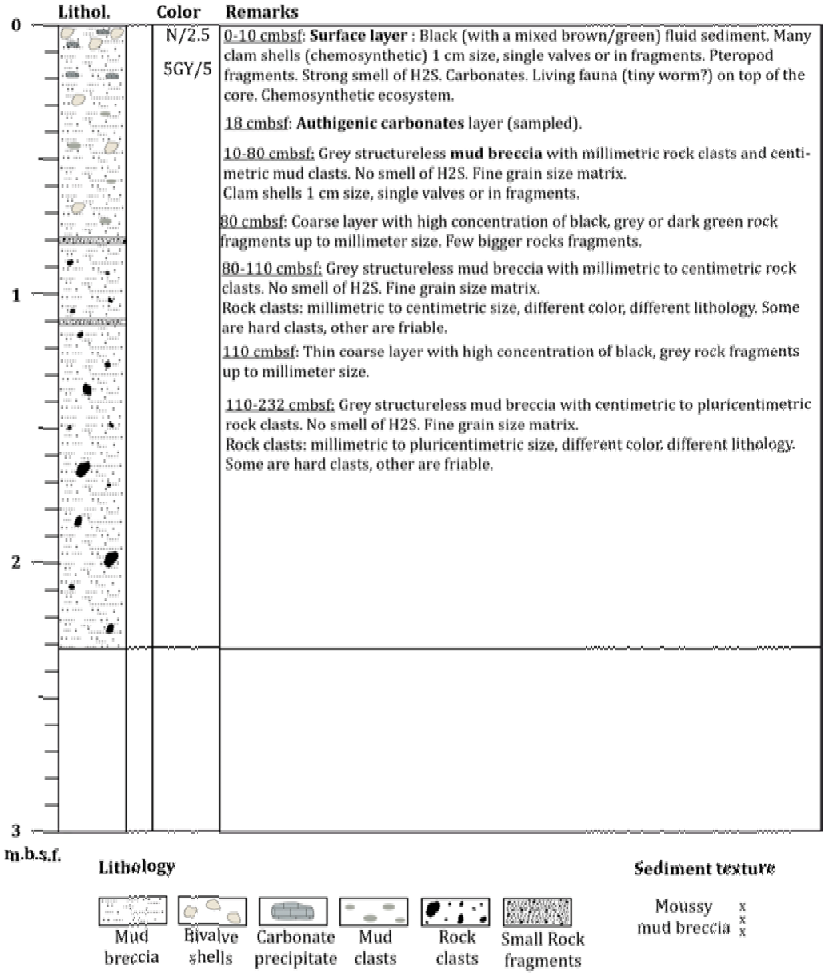

Appendix 2: Core Descriptions GC continued

GeoB 19227-1(GC-7) Date of coring: 19.11.2014

Position: 37°52.433 N; 17°29.210 E
Water depth: 2322 m.b.s.f.
Core length: 165 cm
Type of core: Gravity core. Liner: PVC
Location: Cetus MV
General remarks: Porosity sampling

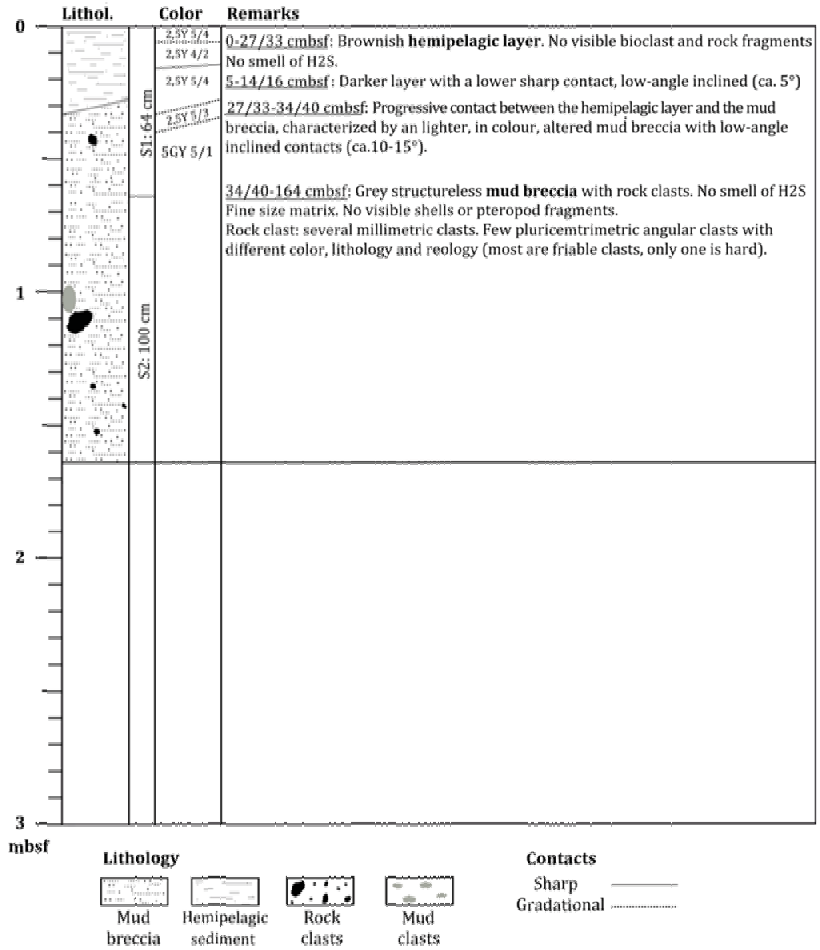

GeoB 19229-2(GC-8) Date of coring: 26.11.2014

Position: 37°04.006 N; 15°55.096 E
Water depth: 3113 m.b.s.f.
Core length: 215 cm
Type of core: Gravity core. Liner: PVC
Location: Deep-sea basin, SE of Sicily
General remarks:

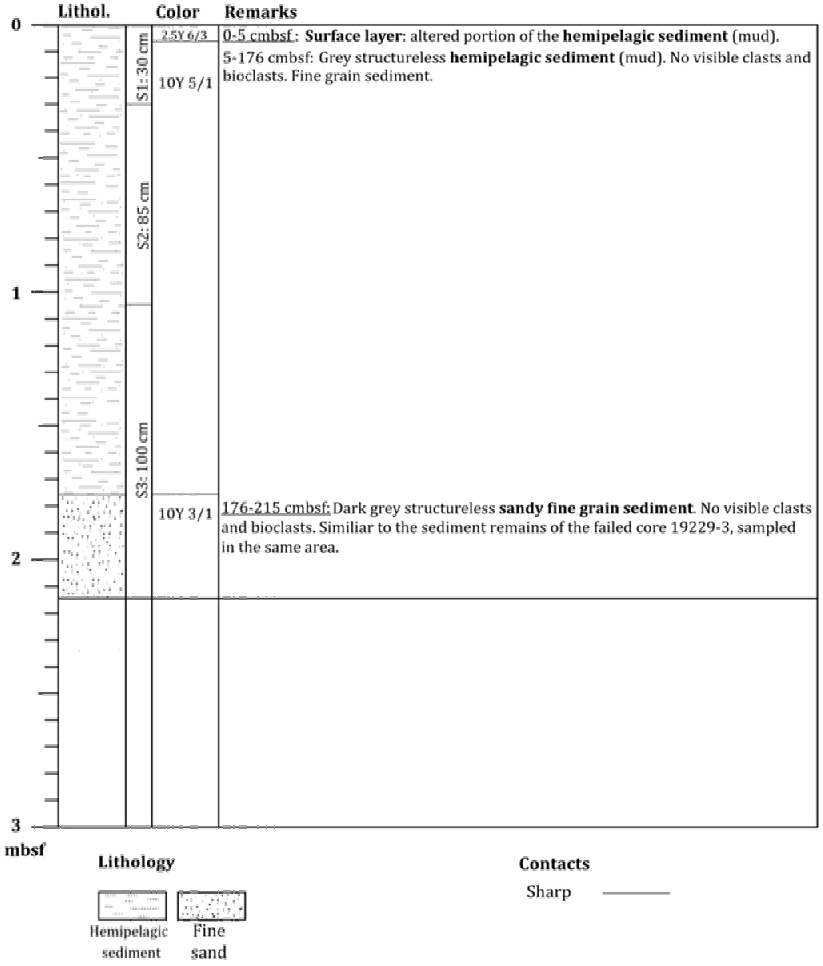

Appendix 2: Core Descriptions GC continued

GeoB 19234-1(GC-10) Date of coring: 29.11.2014

Position: 38°36.663 N; 17°11.973 E
Water depth: 1505 m.b.s.f.
Core length: 194 cm
Type of core: Gravity core. Liner: PVC
Location: Venere MV (Eastern summit)
General remarks: Mud breccia covered by a 50-cm layer of hemipelagic sediment of different lithologies. No shells and bioclasts observed.

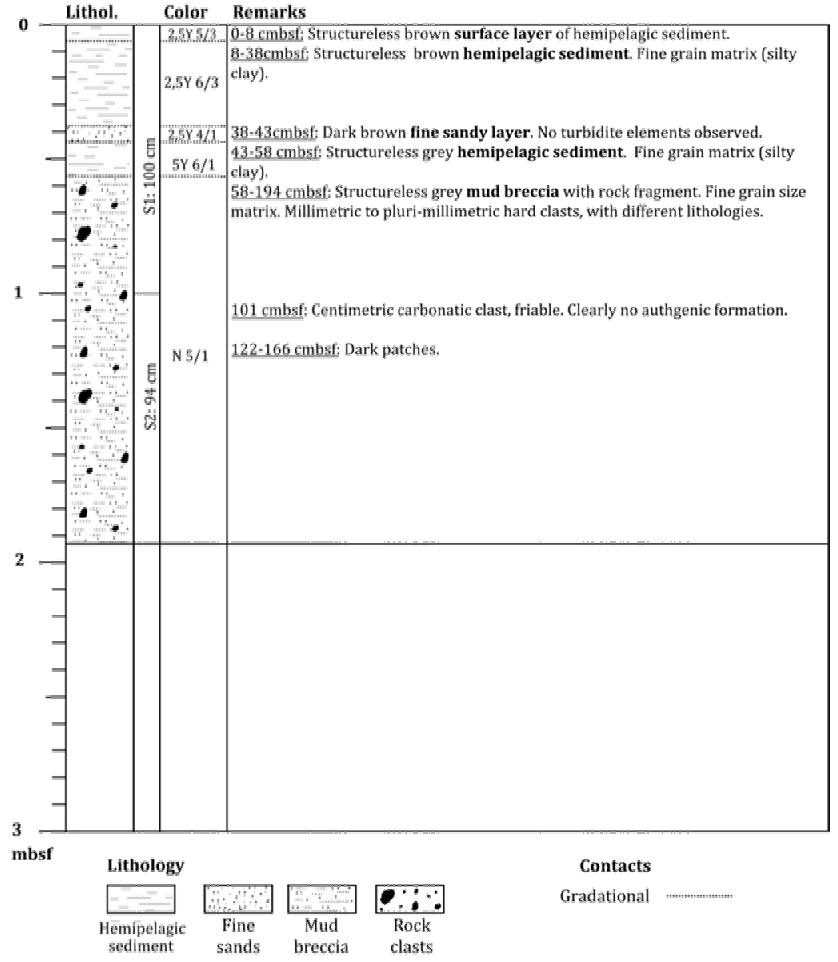

GeoB 19235-1(GC-11) Date of coring: 29.11.2014

Position: 38°36.457 N; 17°11.037 E
Water depth: 1510 m.b.s.f.
Core length: 262 cm
Type of core: Gravity core. Liner: PVC
Location: Venere MV (West)
General remarks:

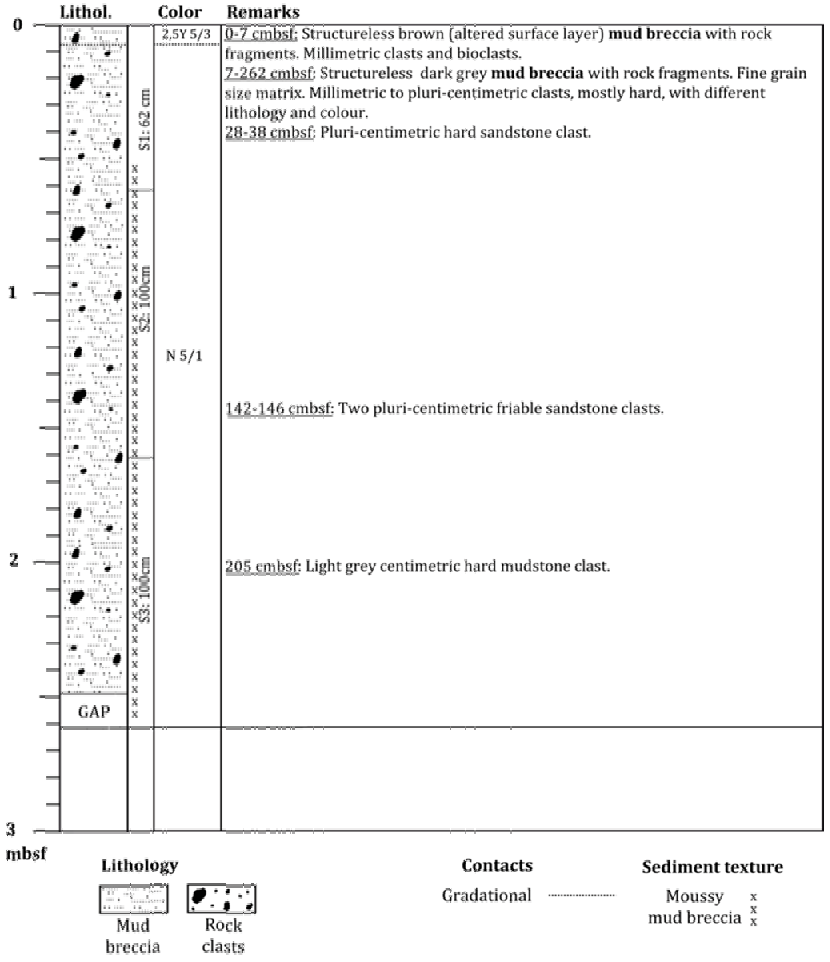

Appendix 2: Core Descriptions GC continued

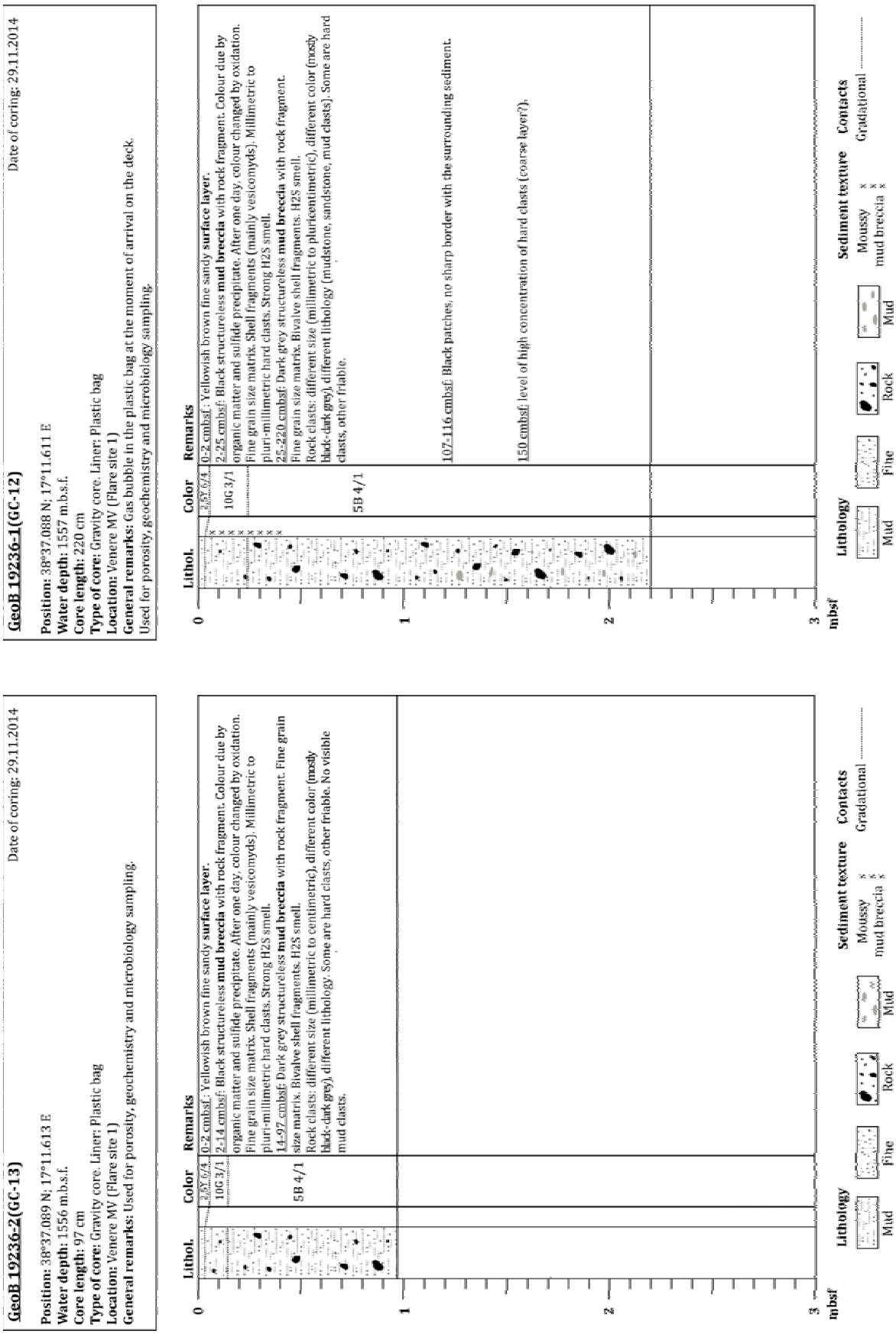

Appendix 2: Core Descriptions GC continued

GeoB 19237-1(GC-14) Date of coring: 29.11.2014

Position: 38°35.930 N; 17°11.828 E
Water depth: 1594 m.b.s.f.
Core length: 119 cm
Type of core: Gravity core. Liner: PVC
Location: Venere MV (West)
General remarks:

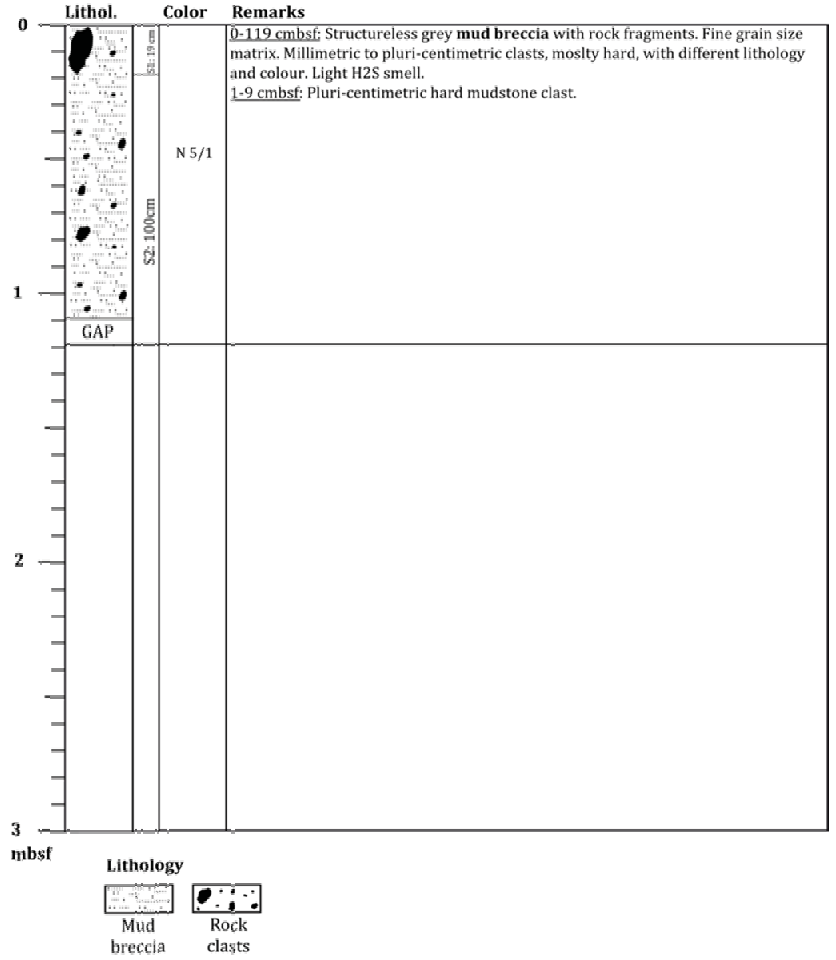

GeoB 19238-1(GC-15) Date of coring: 29.11.2014

Position: 38°35.757 N; 17°11.378 E
Water depth: 1521 m.b.s.f.
Core length: 131 cm
Type of core: Gravity core. Liner: PVC
Location: Venere MV (West)
General remarks:

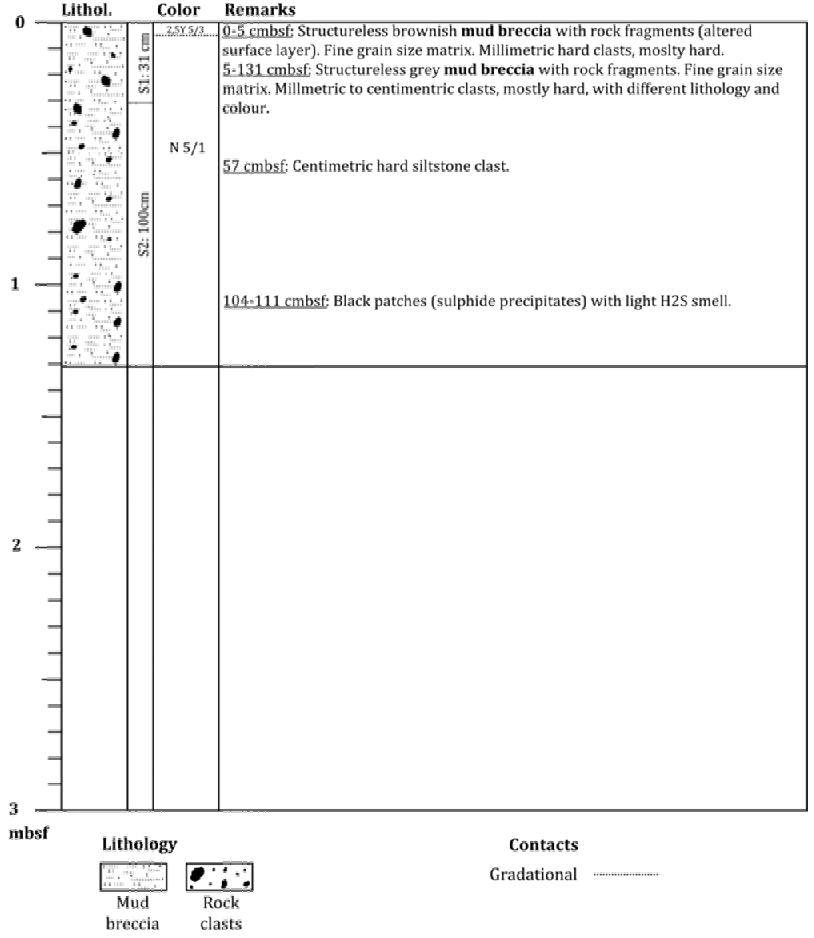

Appendix 2: Core Descriptions GC continued

GeoB 19244-1(GC-16) Date of coring: 02.12.2014

Position: 38°36.648 N; 17°12.062 E
Water depth: 1518 m.b.s.f.
Core length: 96 cm
Type of core: Gravity core. Liner: PVC
Location: Venere MV (East)
General remarks:

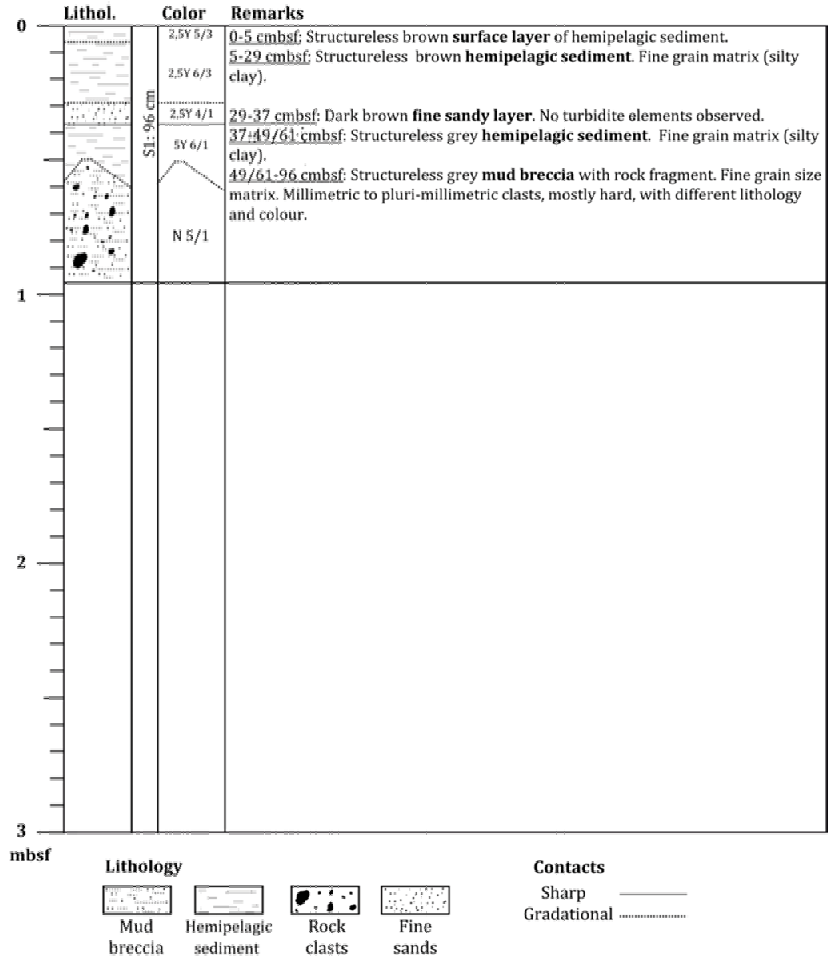

GeoB 19245-1(GC-17) Date of coring: 02.12.2014

Position: 38°36.455 N; 17°11.223 E
Water depth: 1496 m.b.s.f.
Core length: 515 cm
Type of core: Gravity core. Liner: Foil
Location: Venere MV (Western summit)
General remarks: Used for porosity, methane, microbiology sampling. Pluri-centimetric clasts sampled every meter.

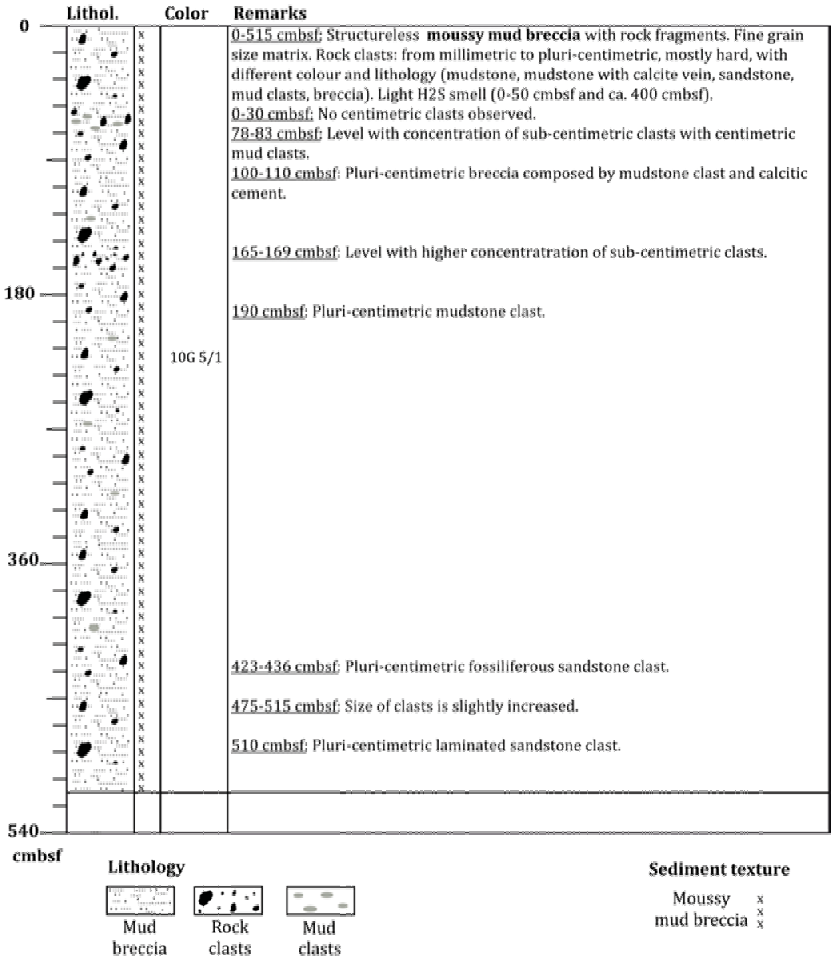

Appendix 2: Core Descriptions GC continued

GeoB 19245-2(GC-18) Date of coring: 02.12.2014

Position: 38°36.454 N; 17°11.222 E
Water depth: 1495 m.b.s.f.
Core length: 326 cm
Type of core: Gravity core. Liner: PVC
Location: Venere MV (Western summit)
General remarks:

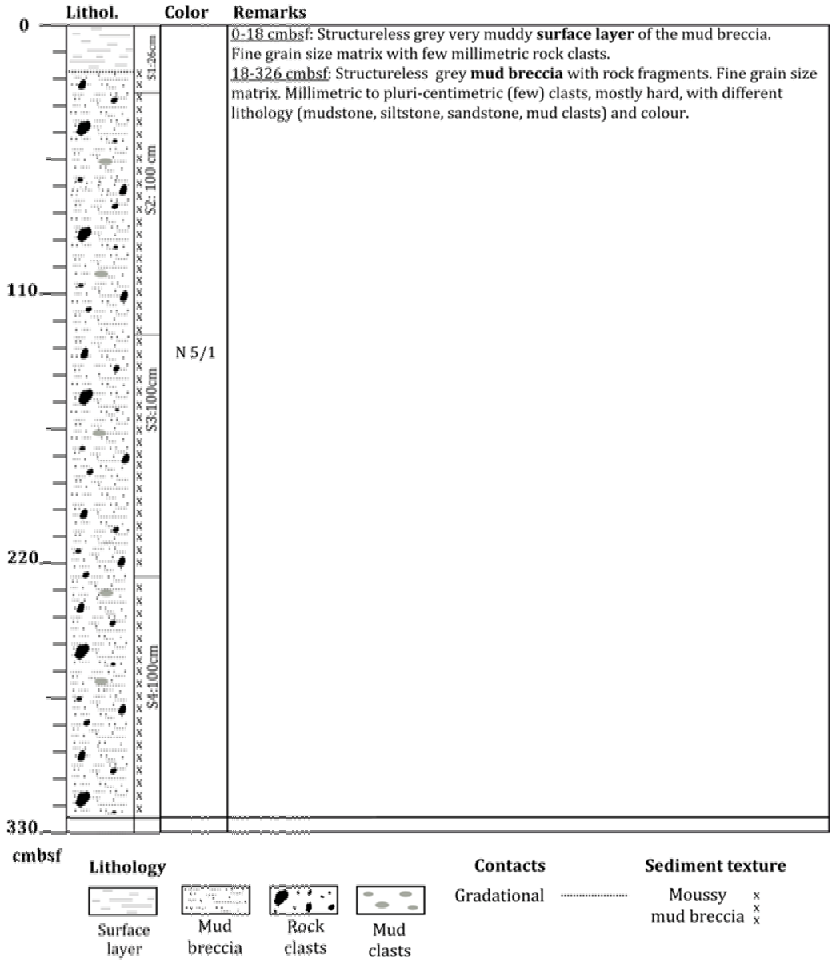

GeoB 19246-1(GC-19) Date of coring: 02.12.2014

Position: 38°36.504 N; 17°11.615 E
Water depth: 1528 m.b.s.f.
Core length: 194 cm
Type of core: Gravity core. Liner: PVC
Location: Venere MV (West)
General remarks: Mud breccia covered by ca. 20-cm layer of hemipelagic sediment. Higher density of the mud breccia compared to other sampled during the M112 cruise. Device damaged during sampling acitivity.

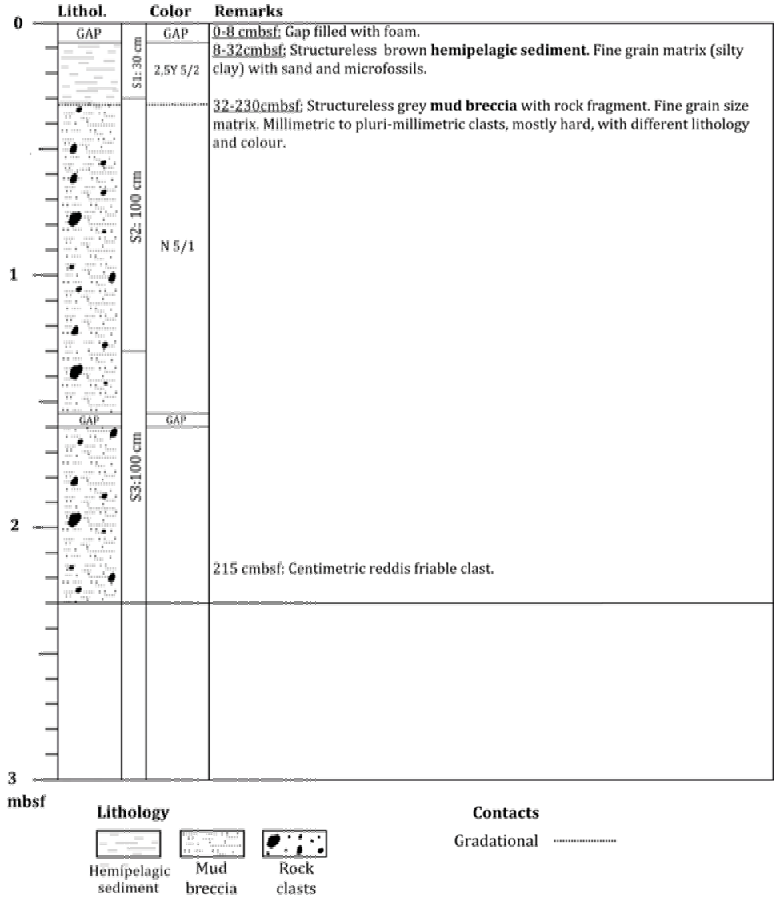

Appendix 2: Core Descriptions GC continued

GeoB 19263-1(GC-22) Date of coring: 08.12.2014

Position: 38°36.448 N; 17°11.282 E
Water depth: 1500 m.b.s.f.
Core length: 275 cm
Type of core: Gravity core. Liner: Foil
Location: Venere MV
General remarks: Moussy mud breccia. Used for porosity, methane and micrbiology analysis.

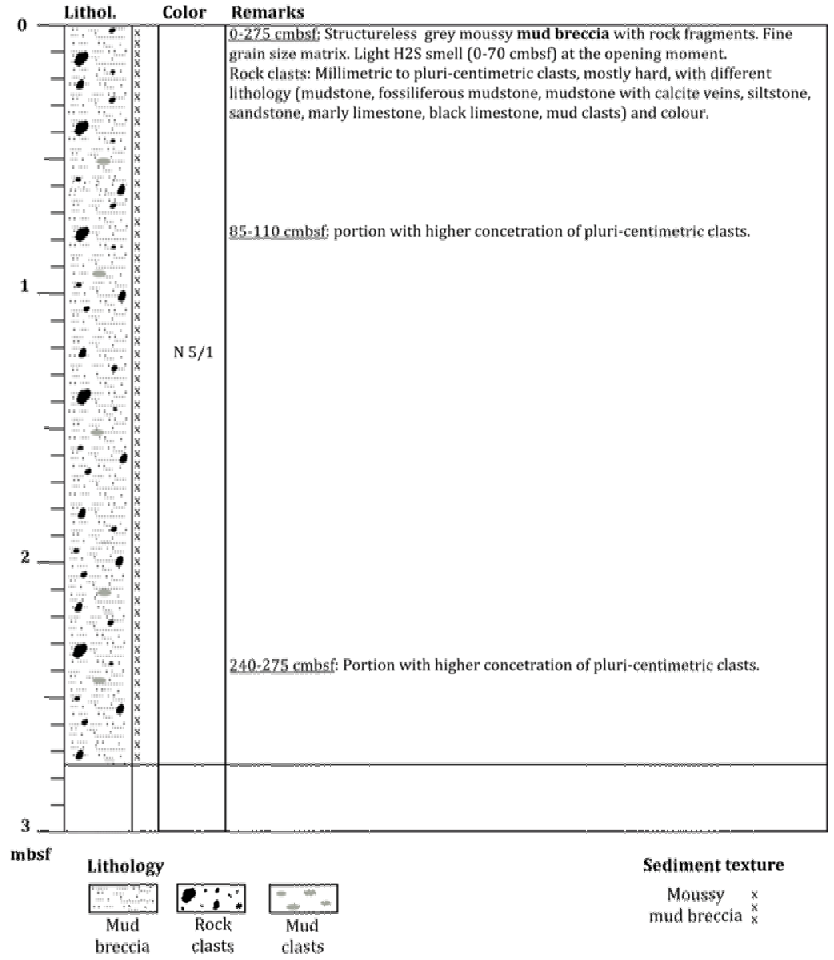

GeoB 19276-1(GC-27) Date of coring: 10.12.2014

Position: 38°36.393 N; 17°11.348 E
Water depth: 1516 m.b.s.f.
Core length: 195 cm
Type of core: Gravity core. Liner: Foil
Location: Venere MV
General remarks: Moussy mud breccia. Used for porosity, methane and microbiology analysis.

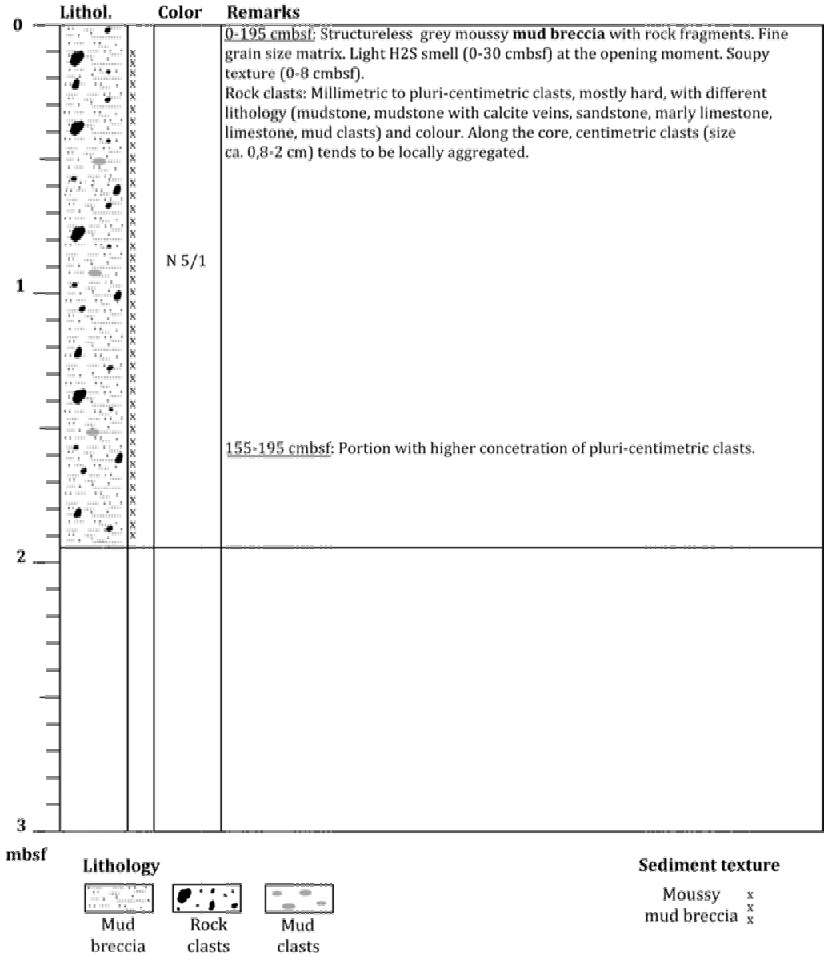

Appendix 2: Core Descriptions GC continued

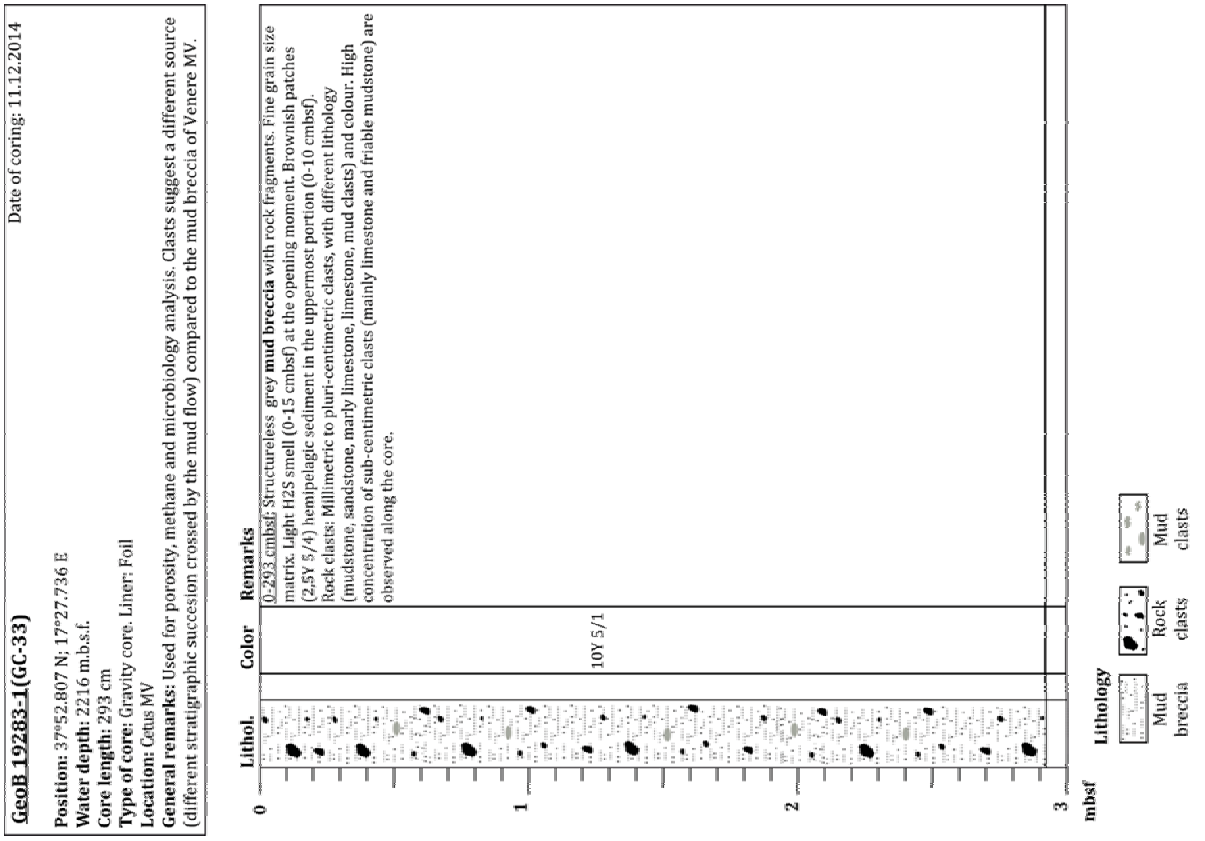

Appendix 2: Core Descriptions GC continued (plastic bag)

GeoB 19212-1 Date of coring: 13.11.2014

Position: 38°37.103 N; 17°11.621 E
Water depth: 1561 m.b.s.f.
Core length: 545 cm
Type of core: Gravity core. Liner: Plastic bag
Location: Venere MV (Flare site)
General remarks: Clasts samples

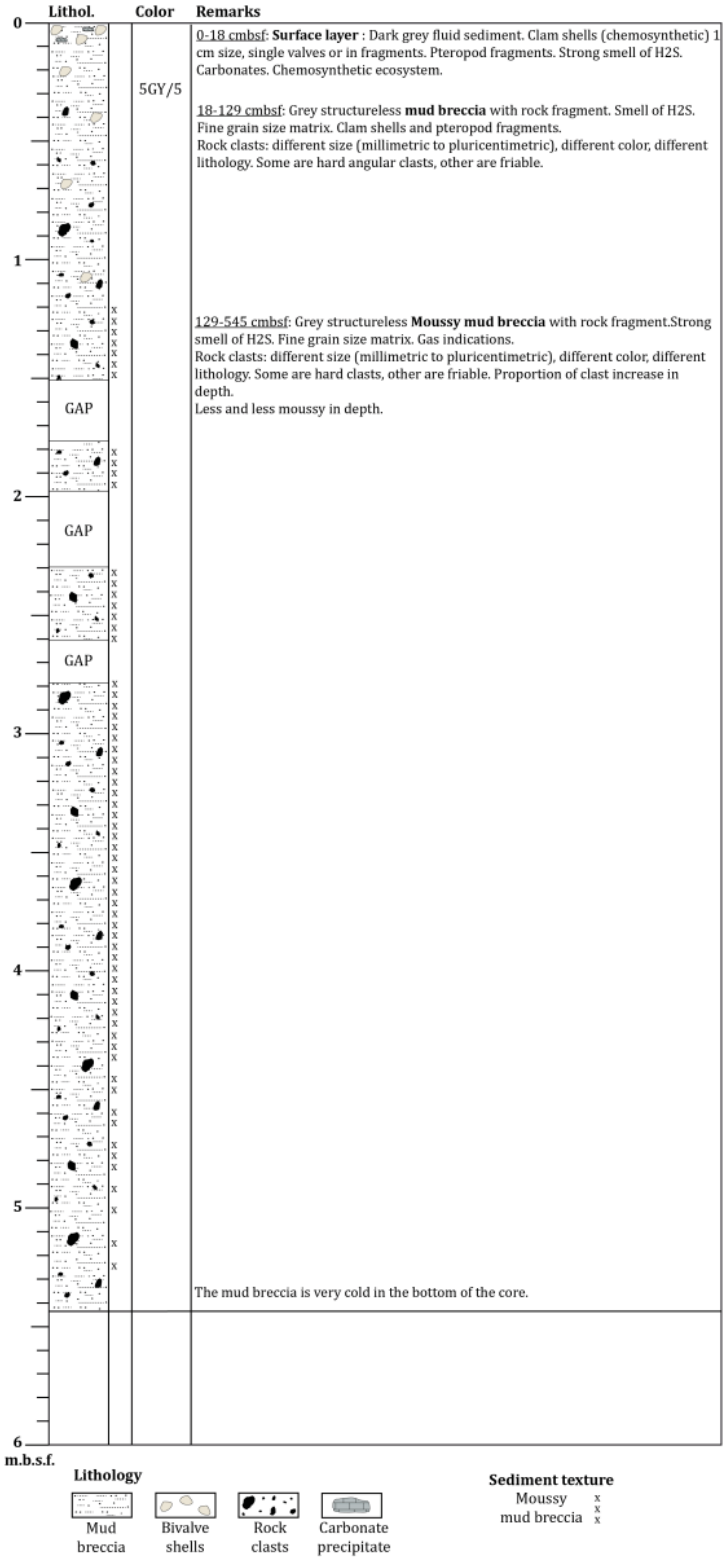

16.3 Appendix 3: CTD Profiles

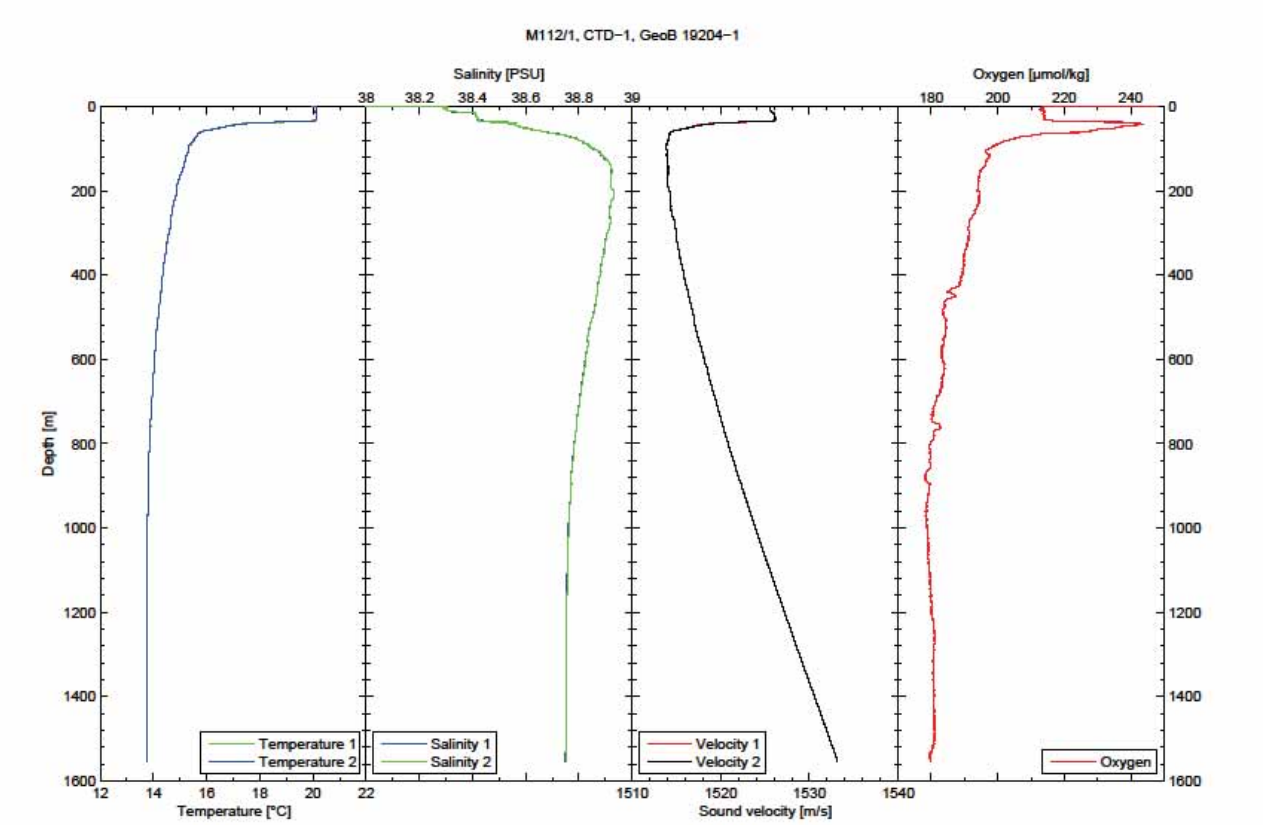

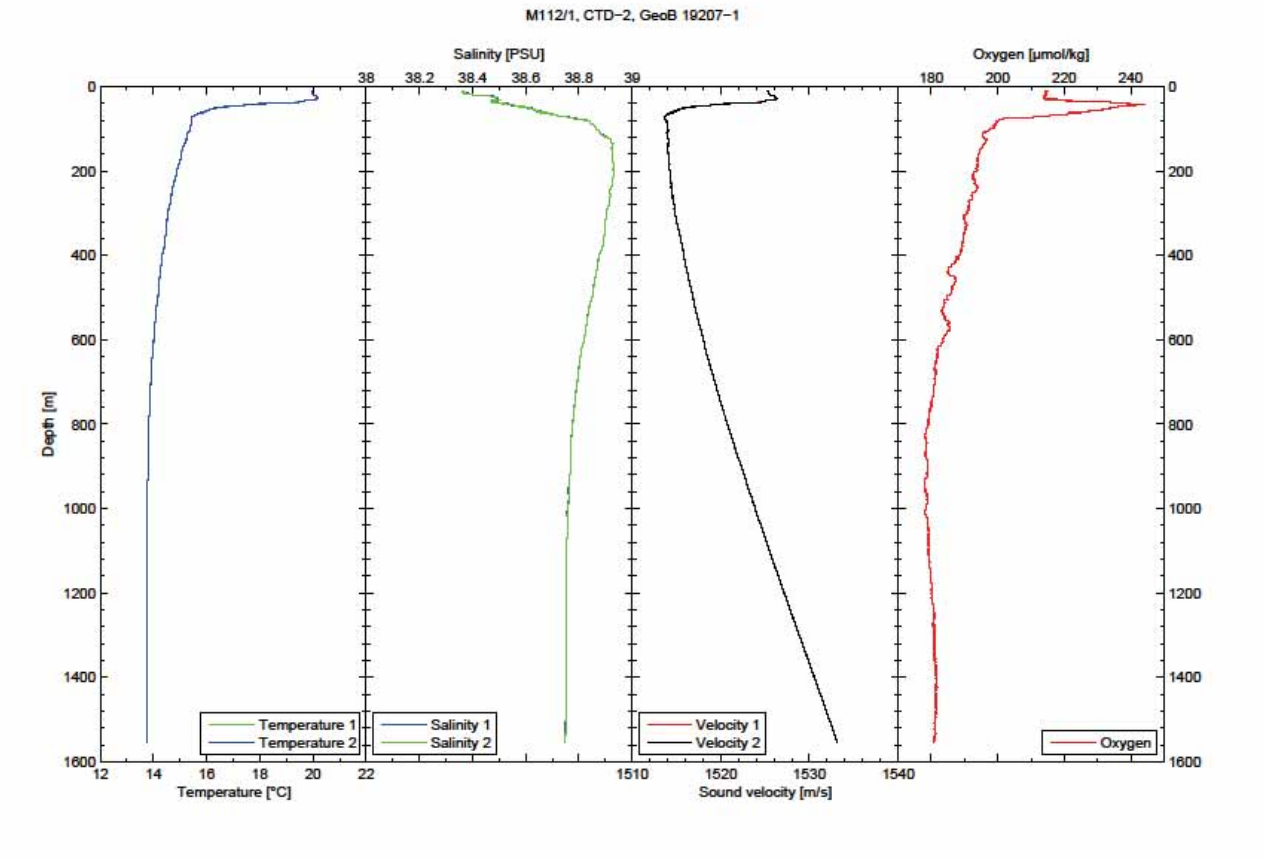

Appendix 3: CTD Profiles continued

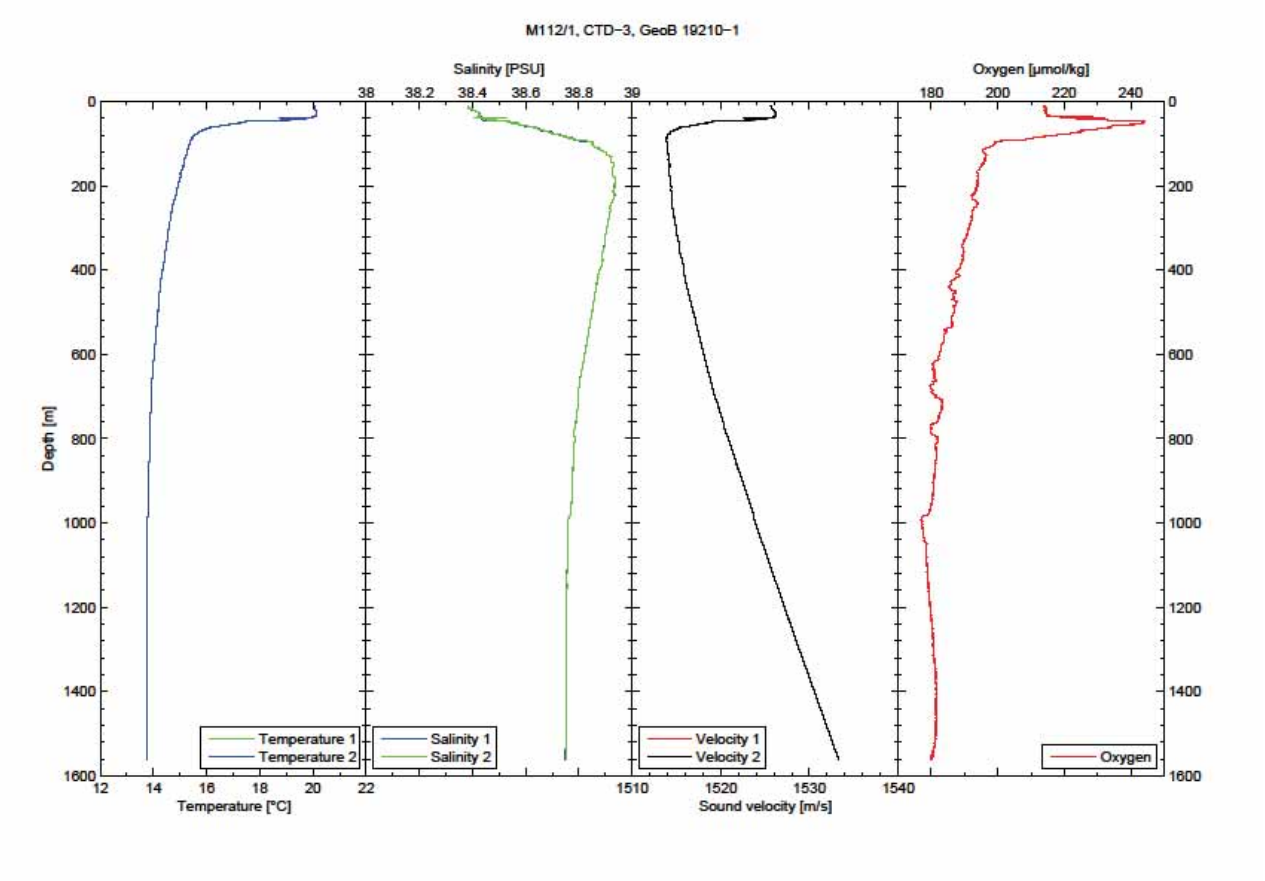

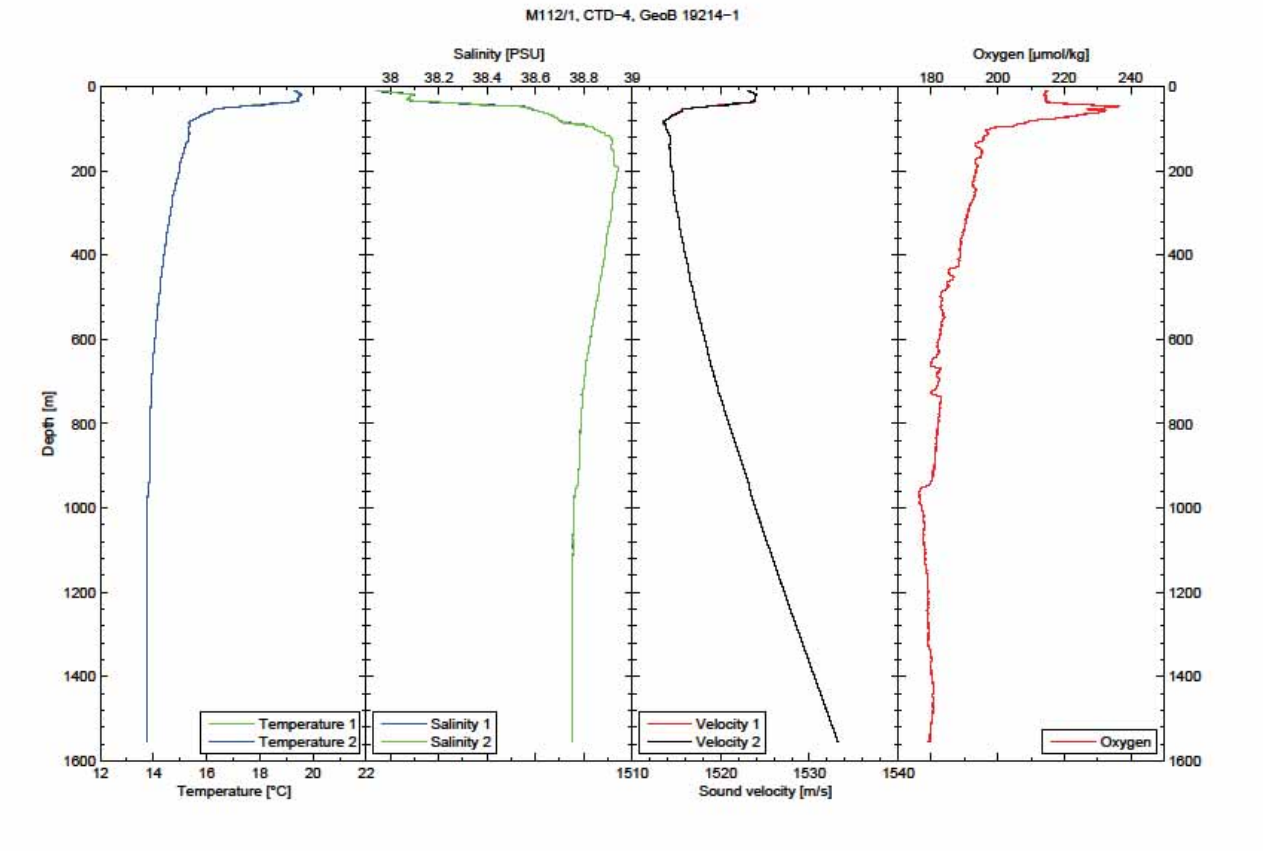

Appendix 3: CTD Profiles continued

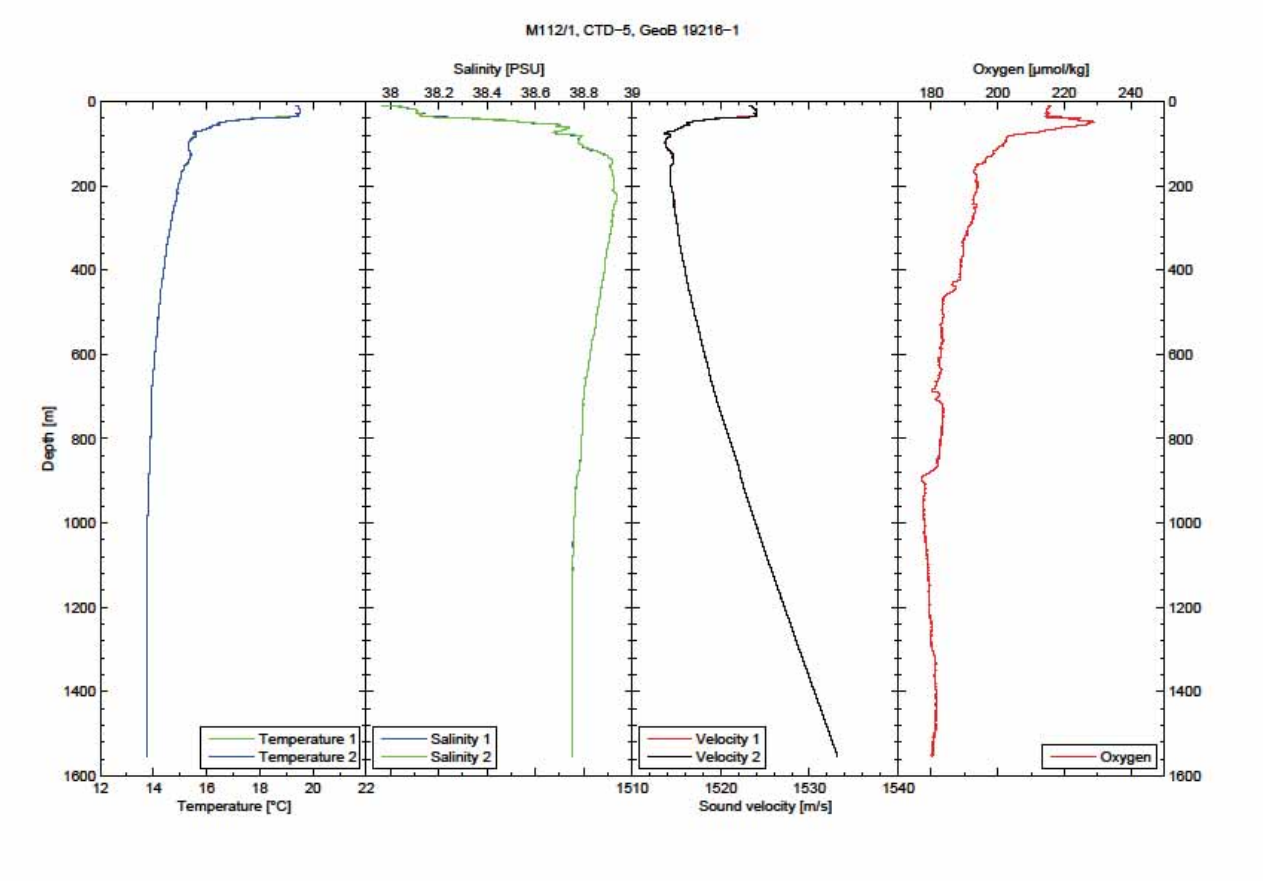

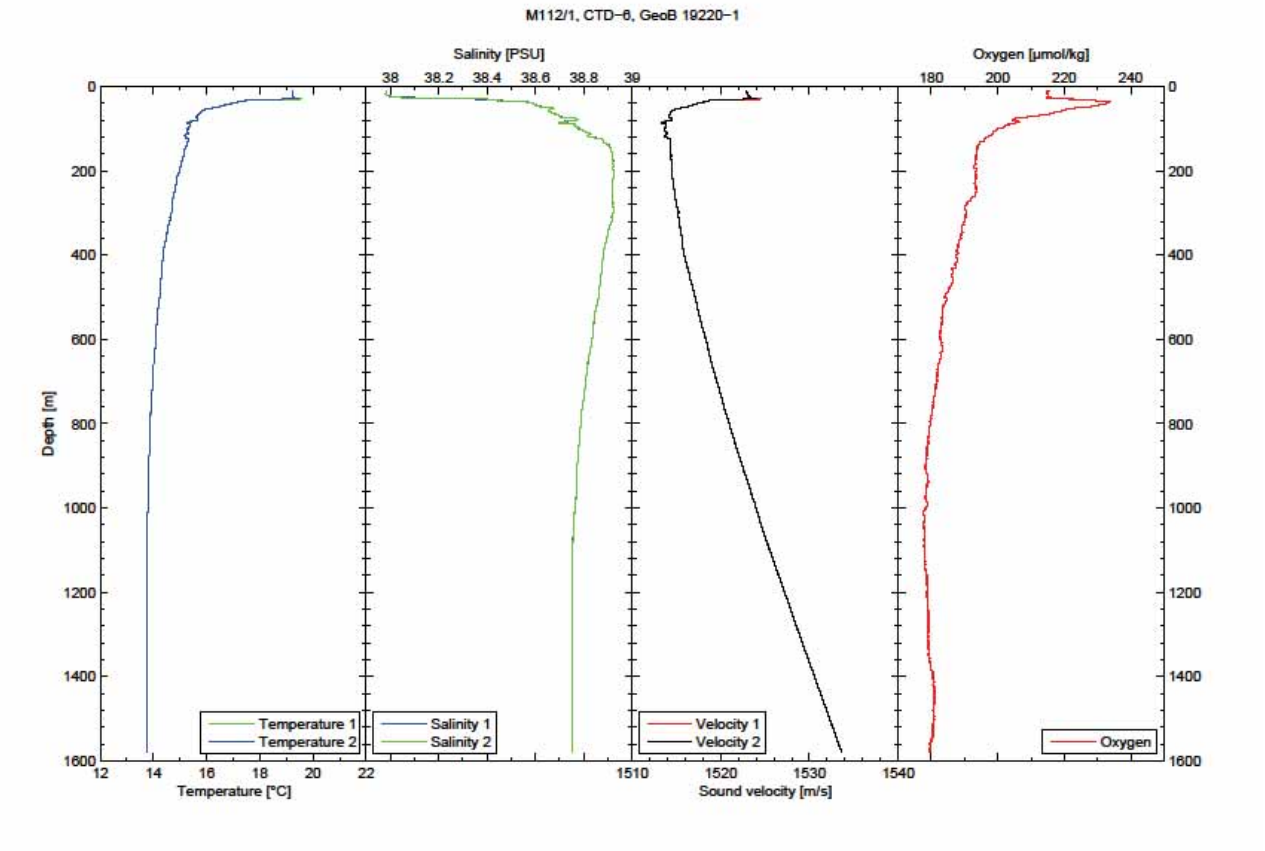

Appendix 3: CTD Profiles continued

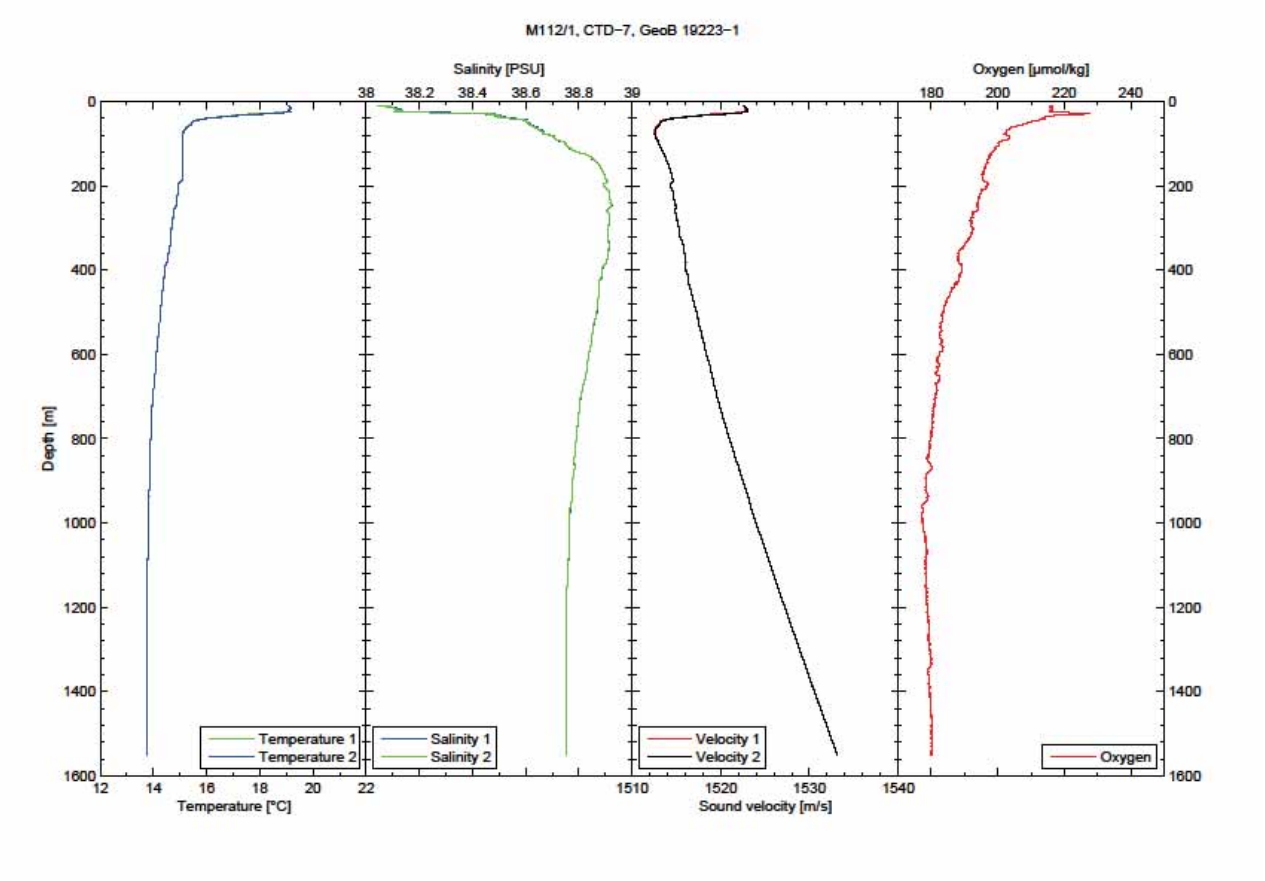

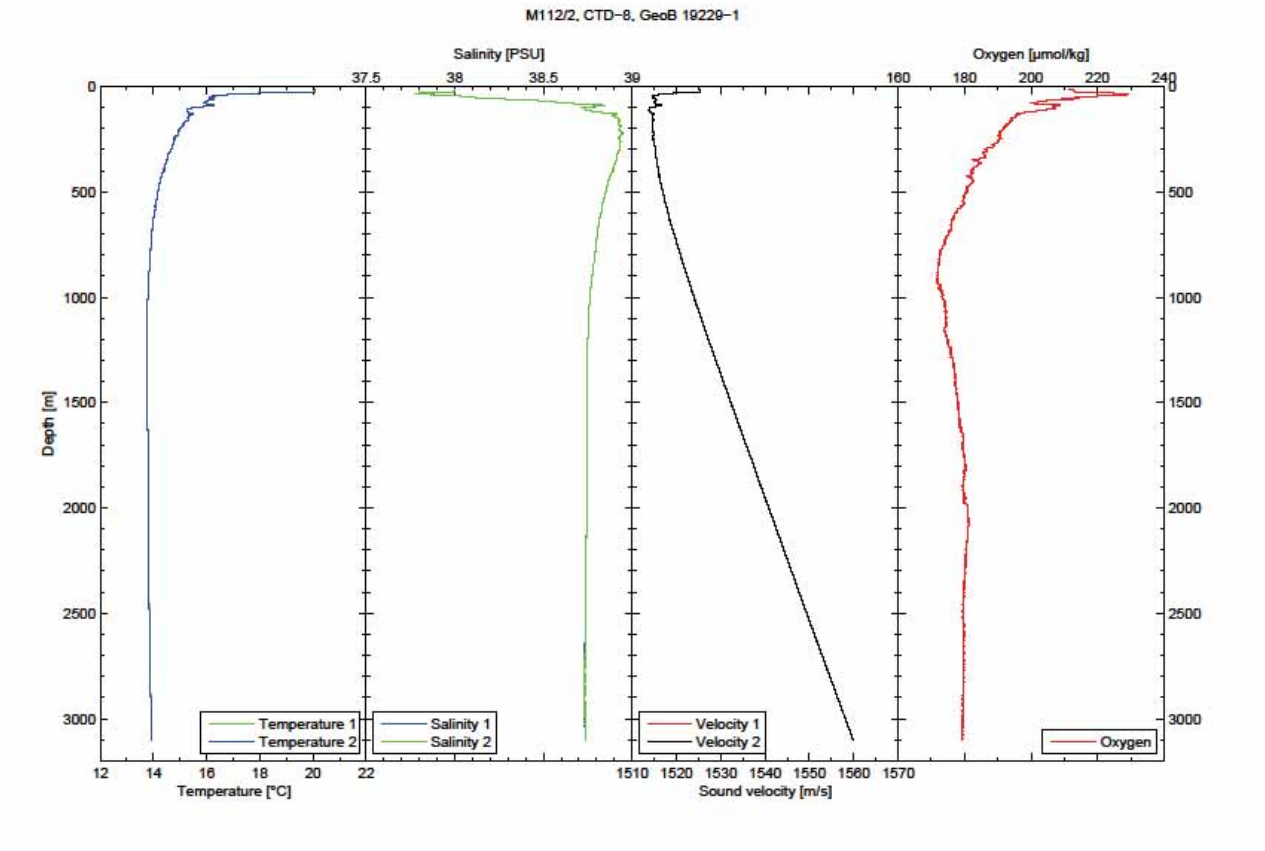

Appendix 3: CTD Profiles continued

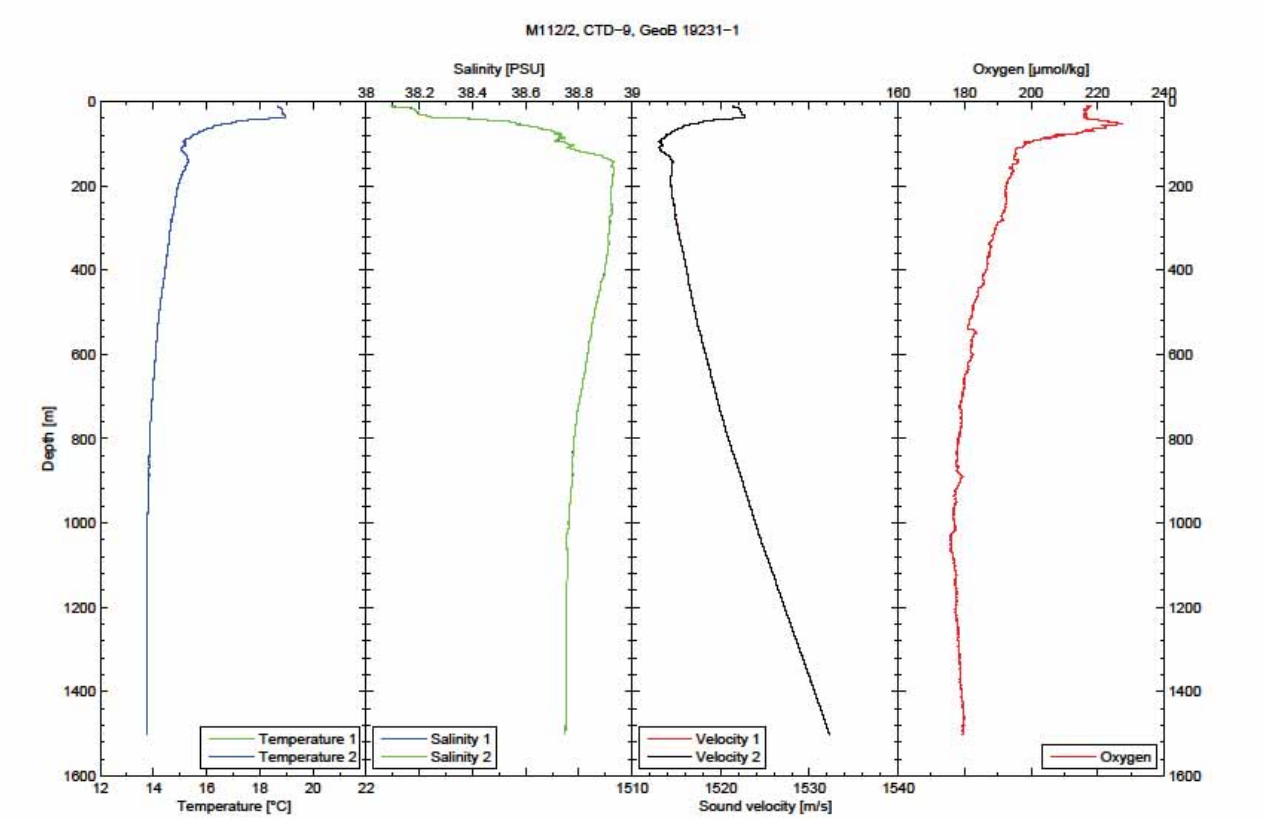

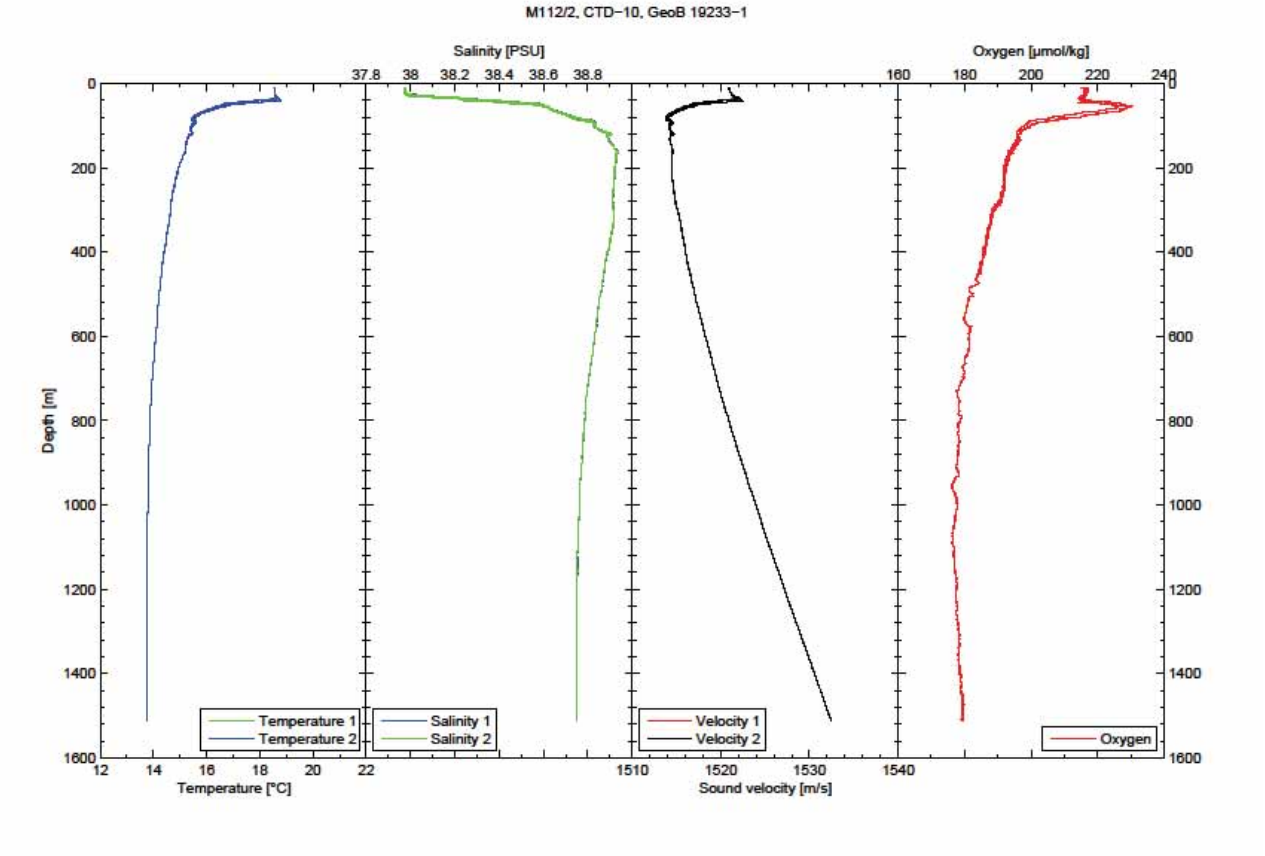

Appendix 3: CTD Profiles continued

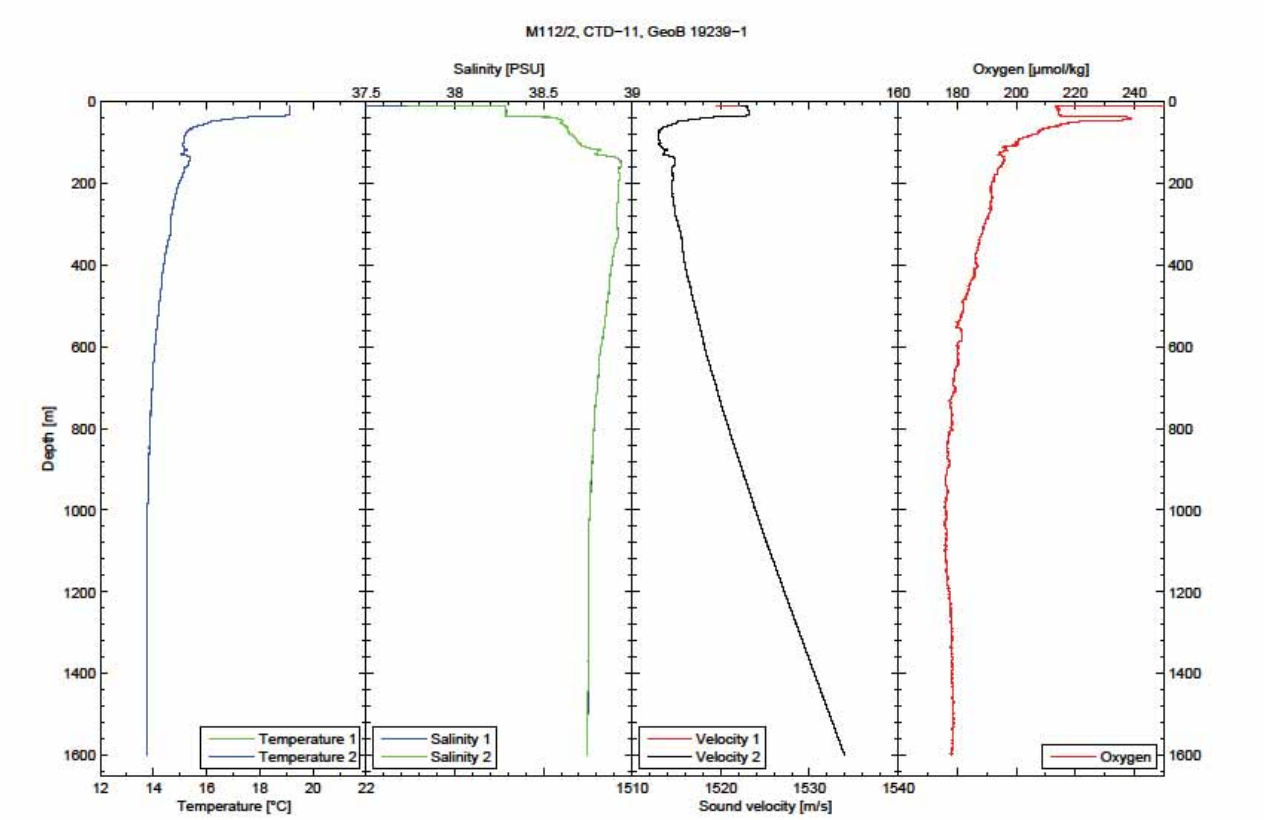

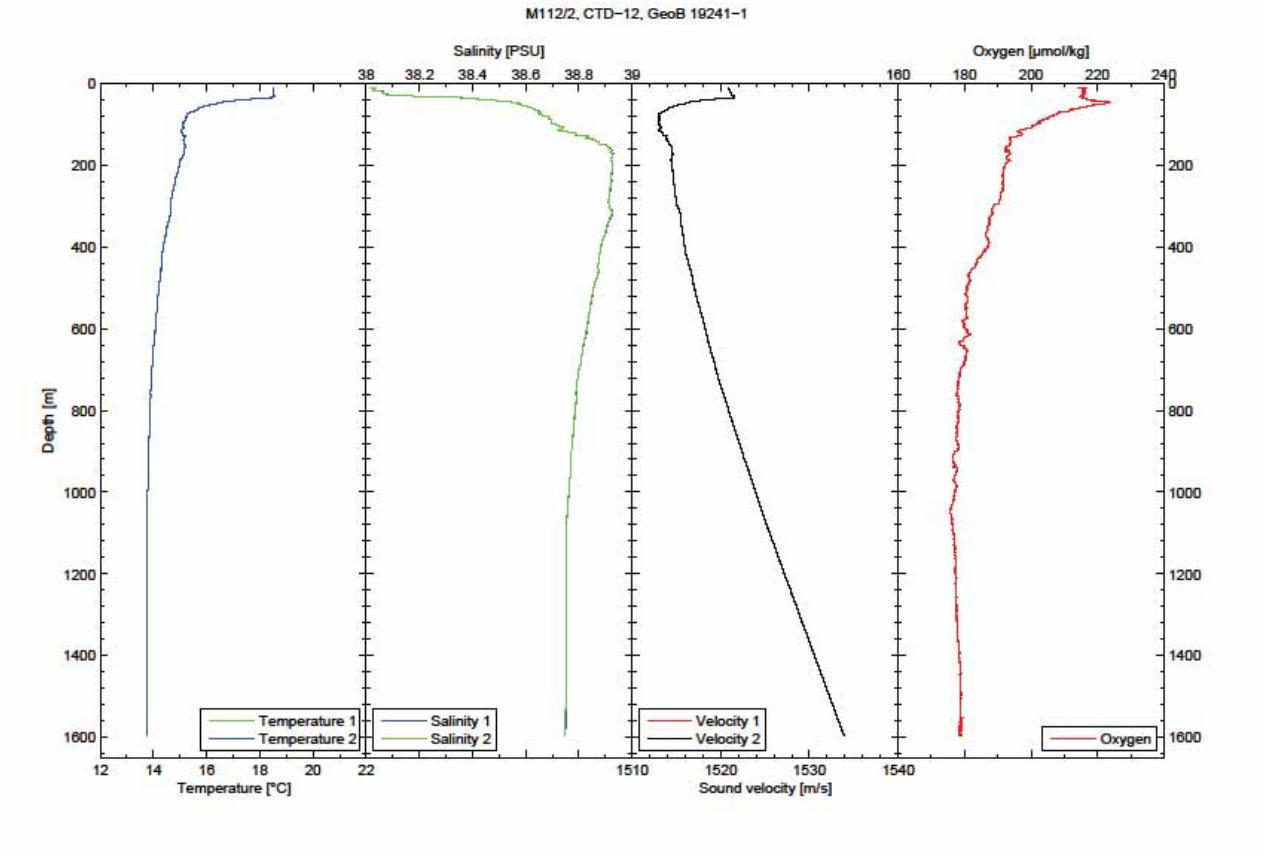

Appendix 3: CTD Profiles continued

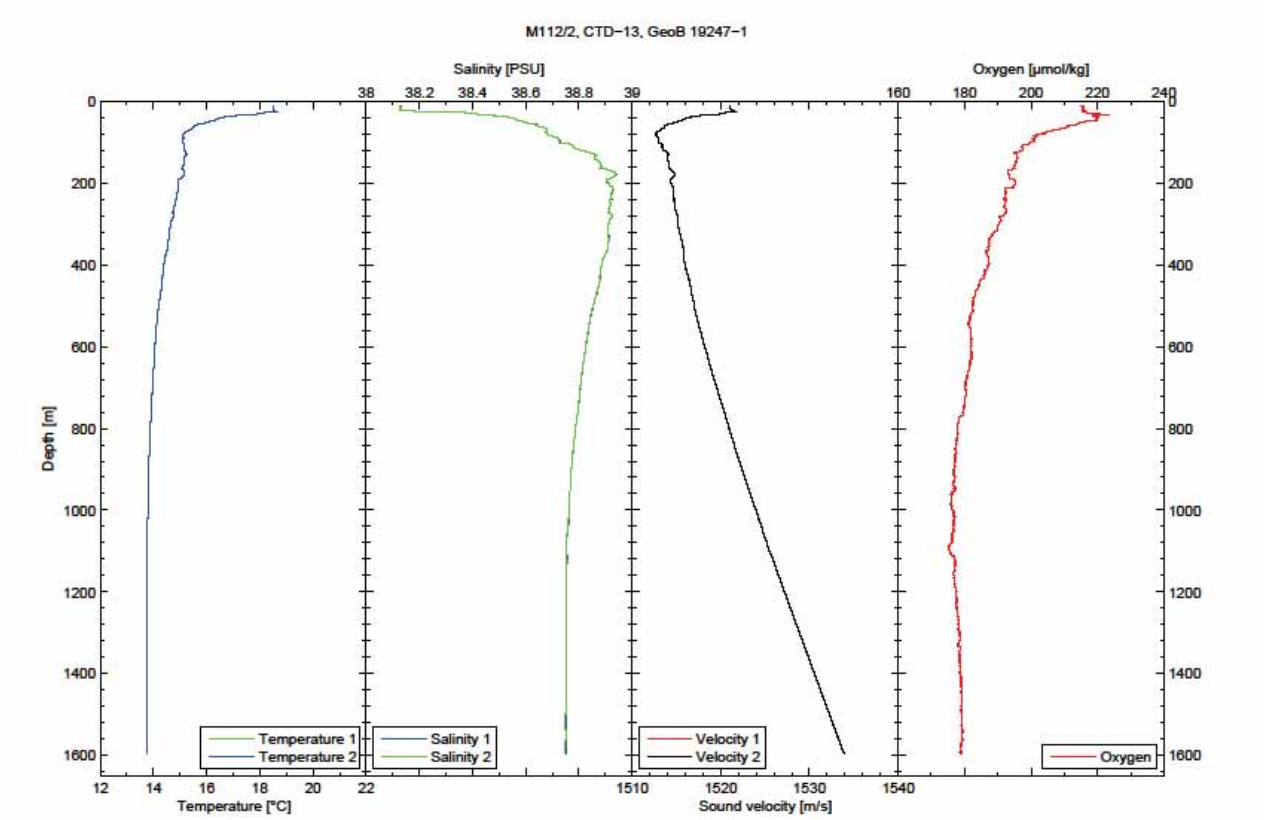

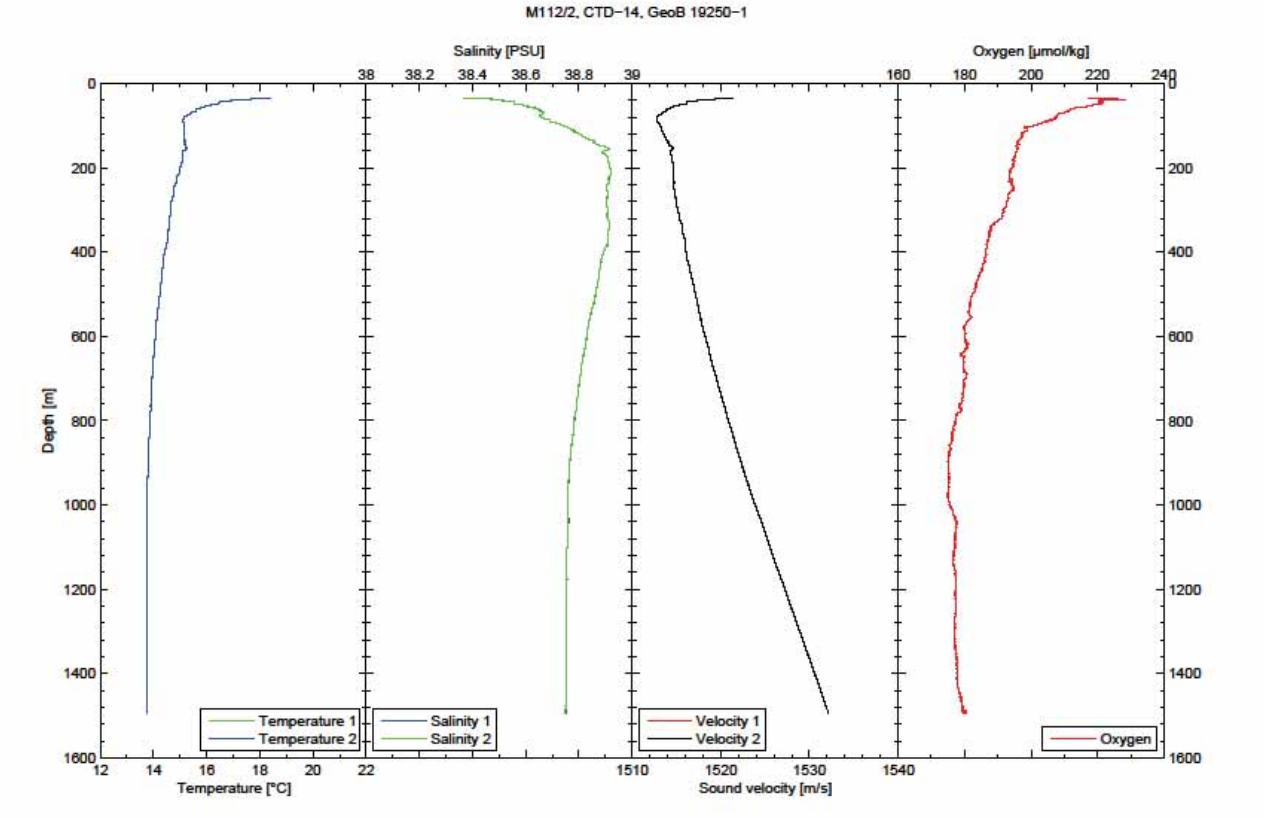

Appendix 3: CTD Profiles continued

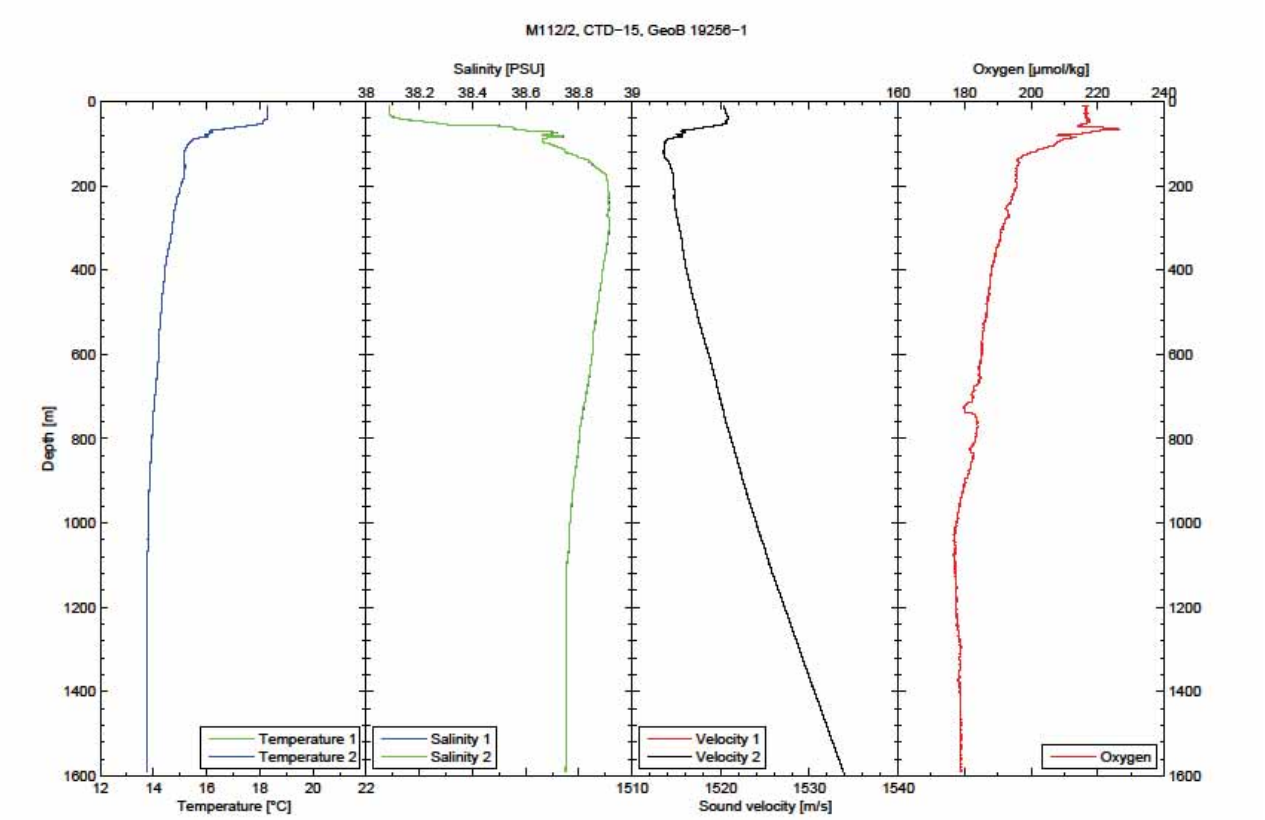

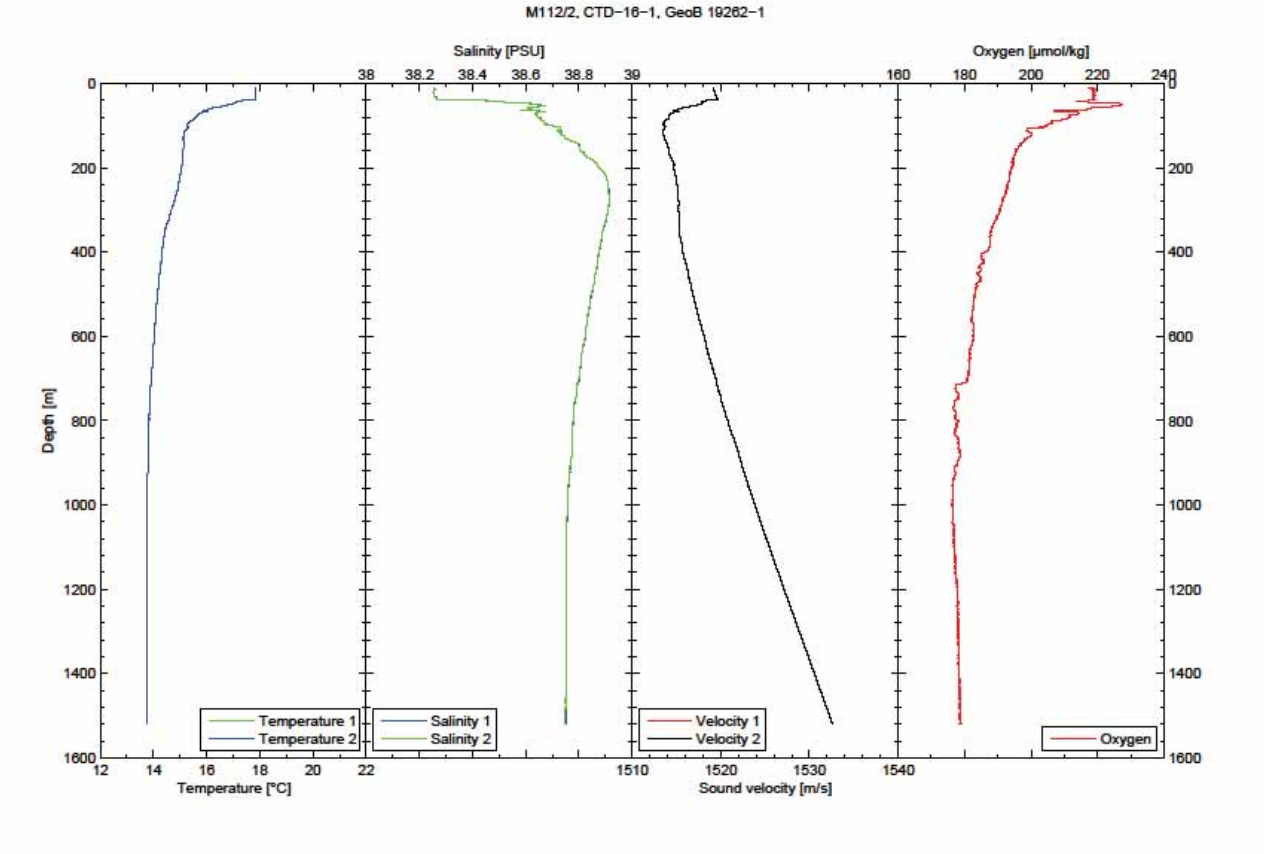

Appendix 3: CTD Profiles continued

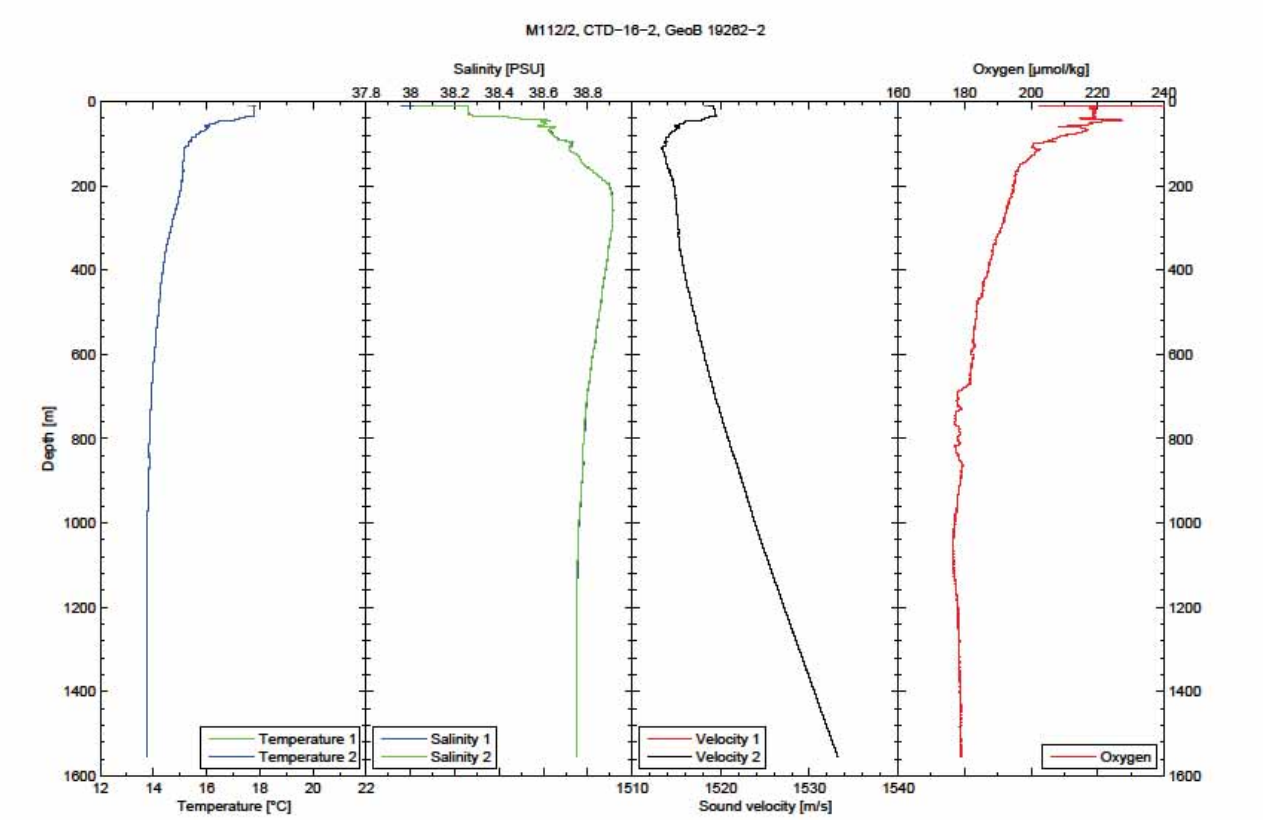

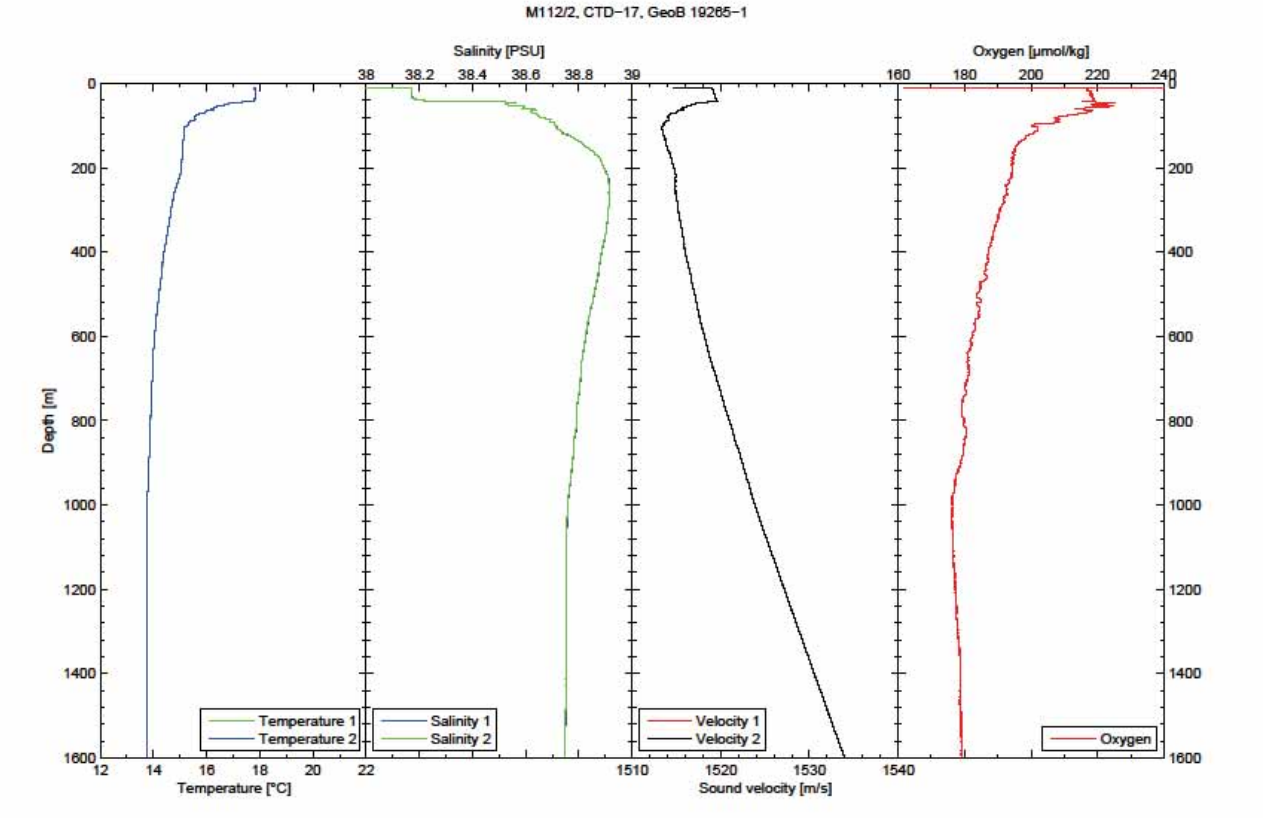

Appendix 3: CTD Profiles continued

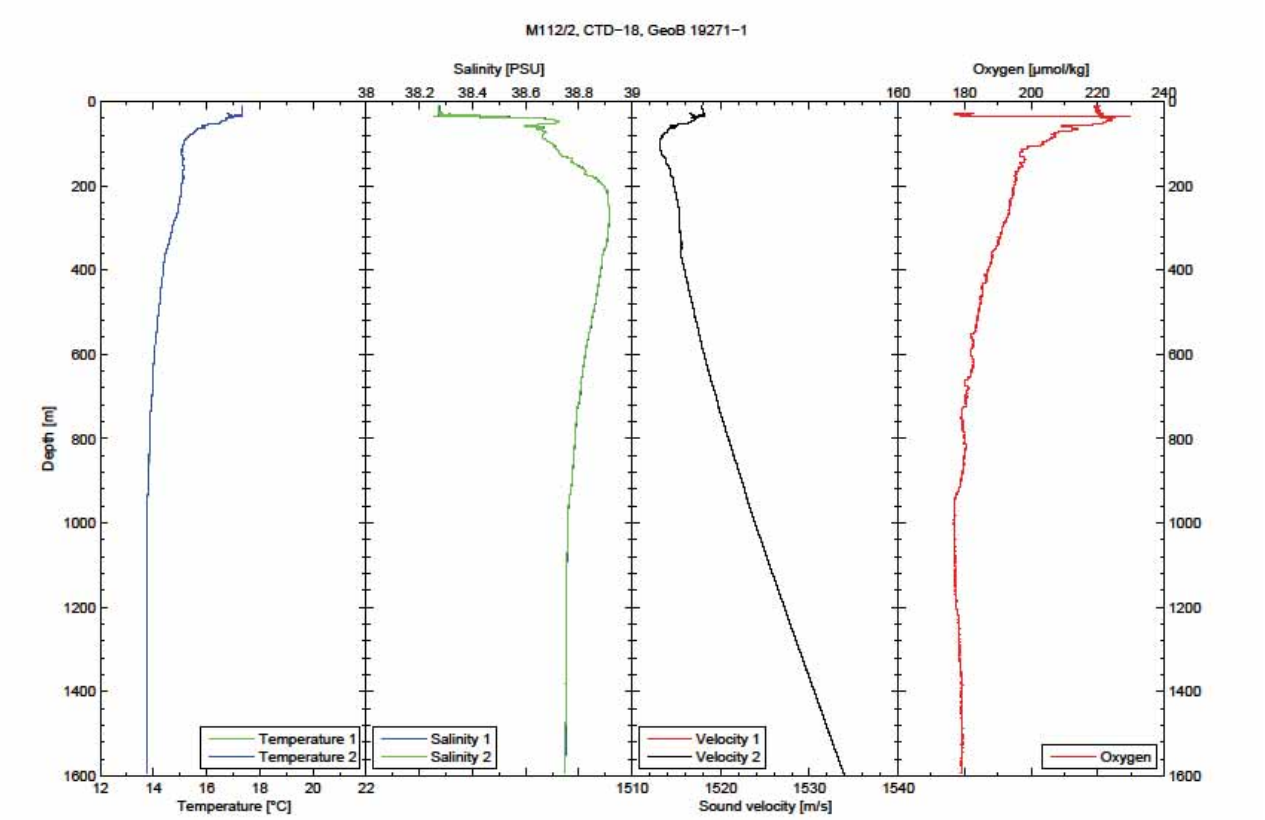

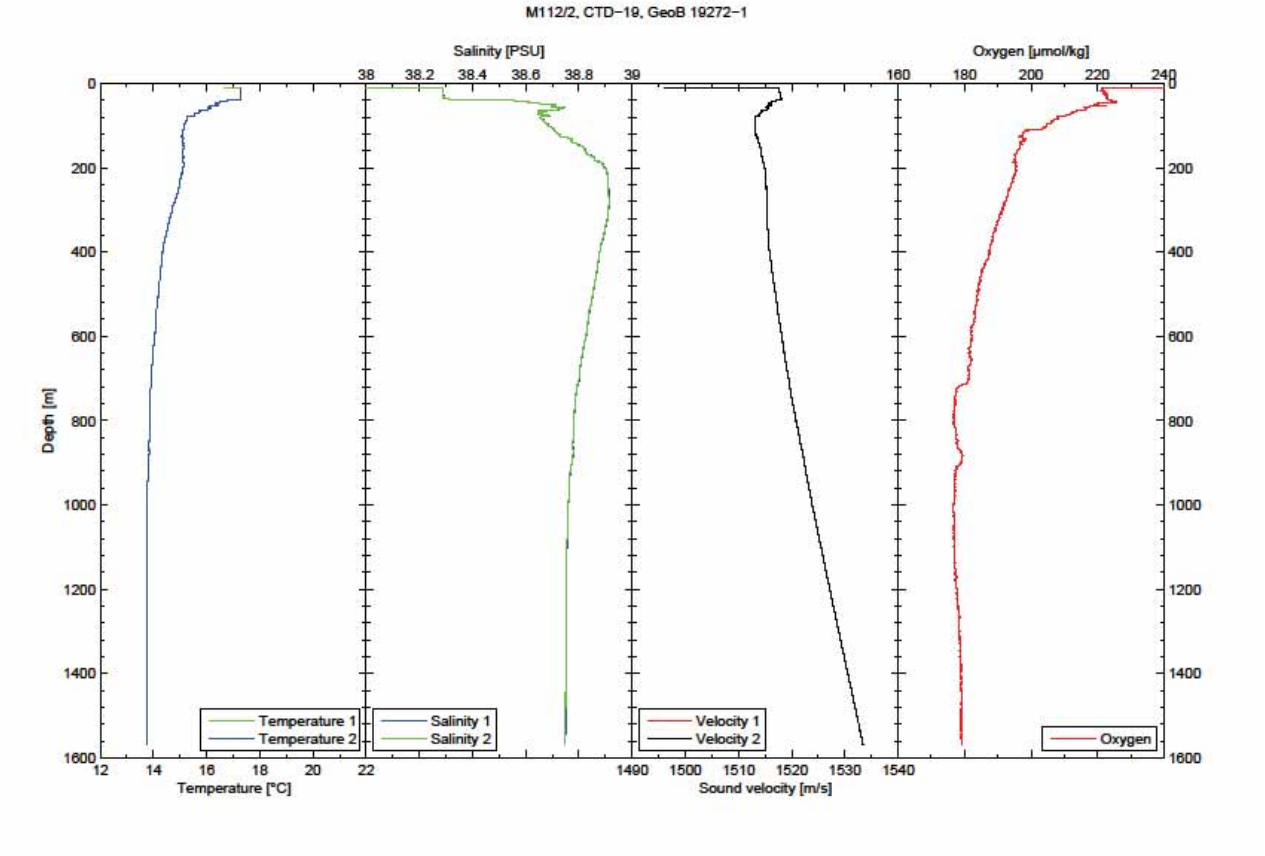

Appendix 3: CTD Profiles continued

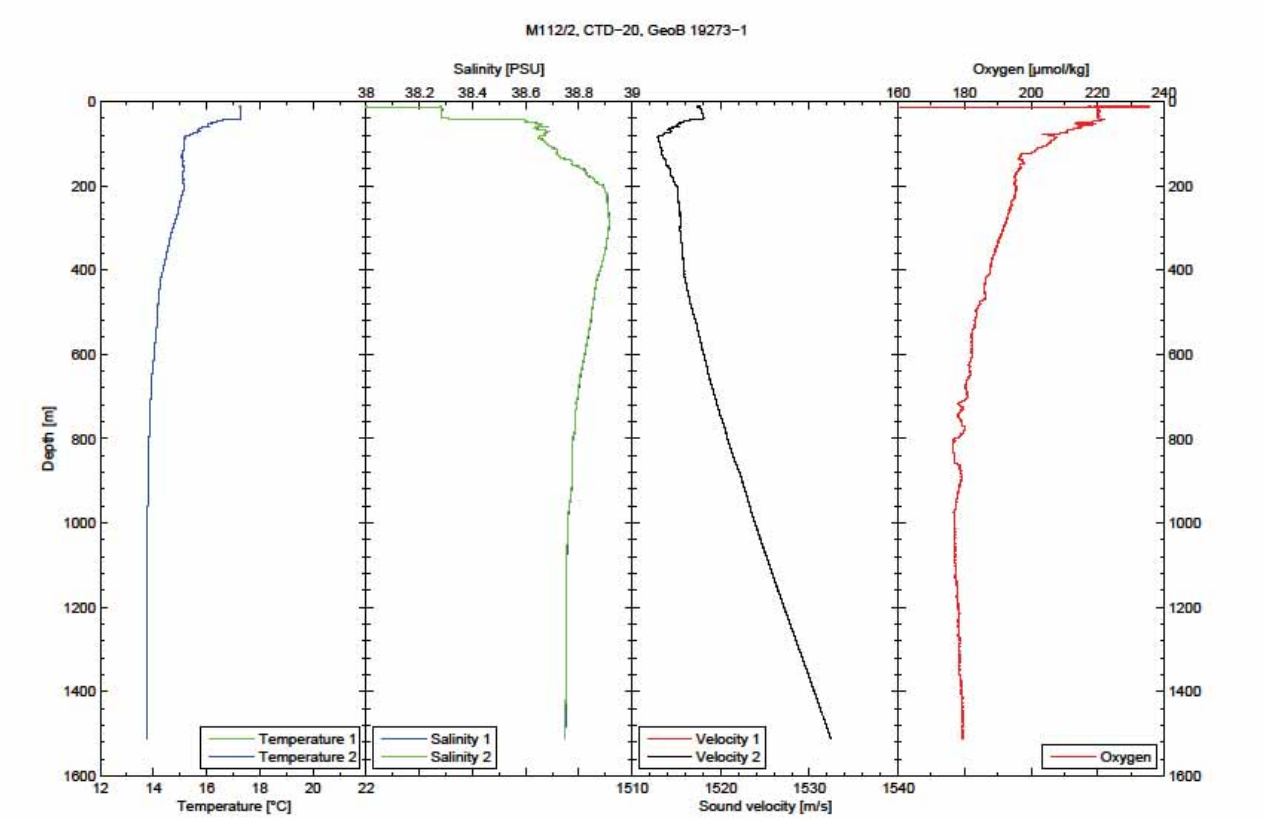

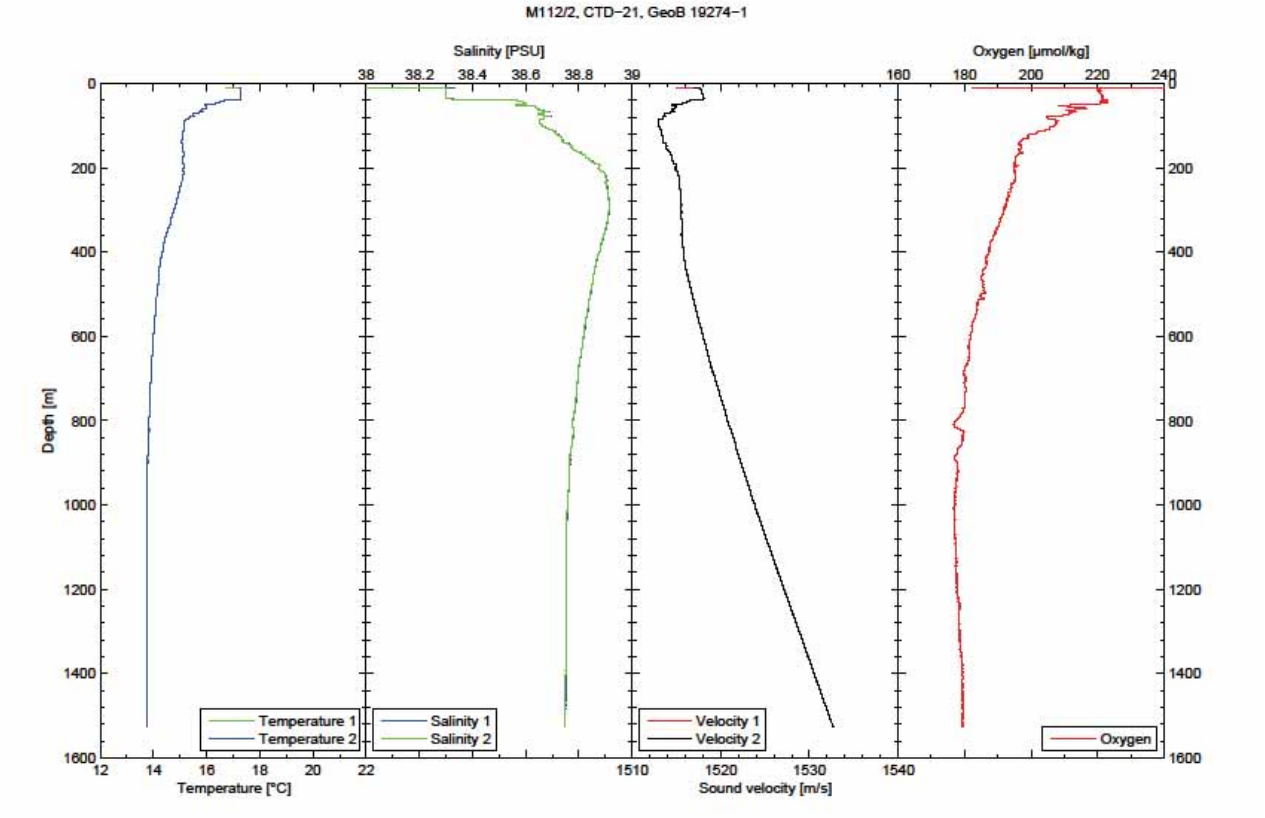

Appendix 3: CTD Profiles continued

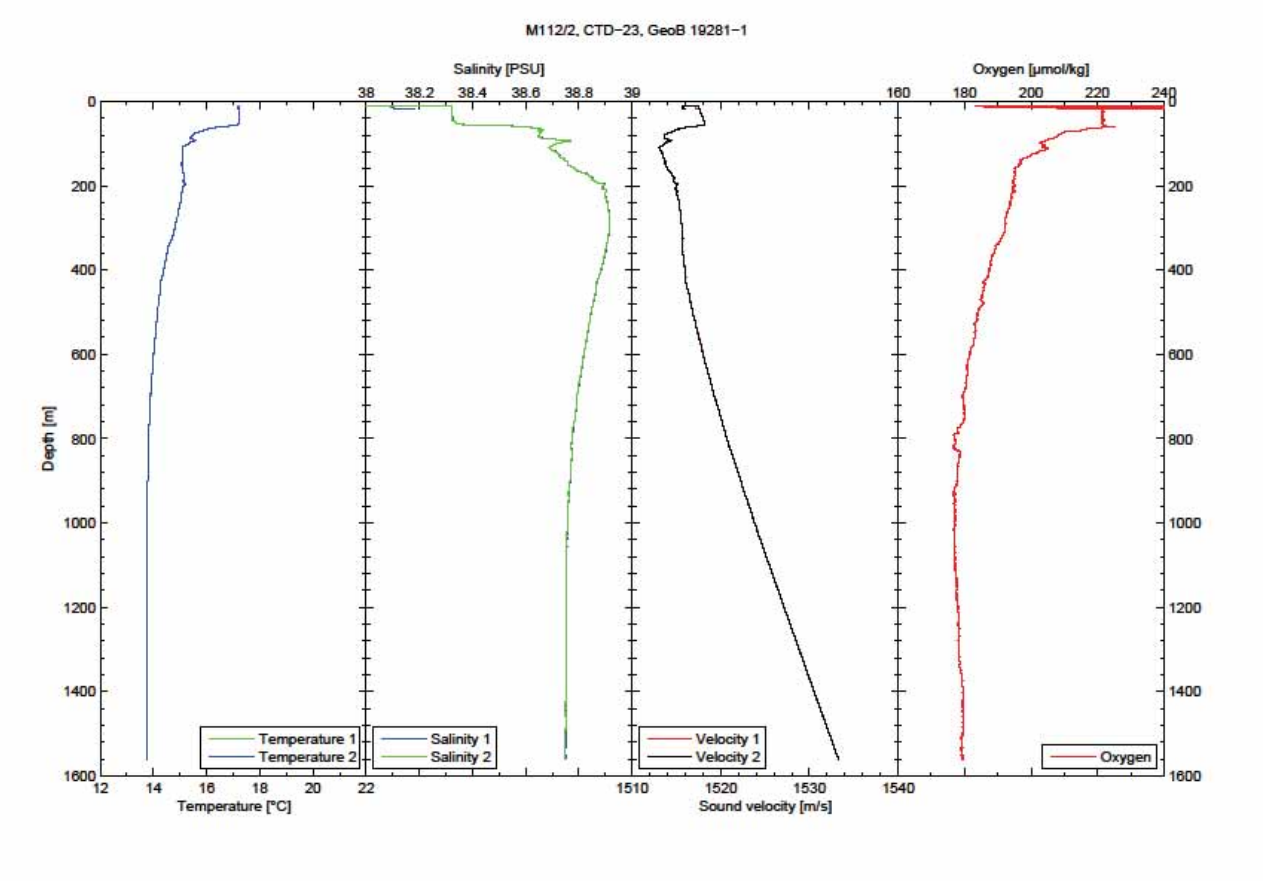

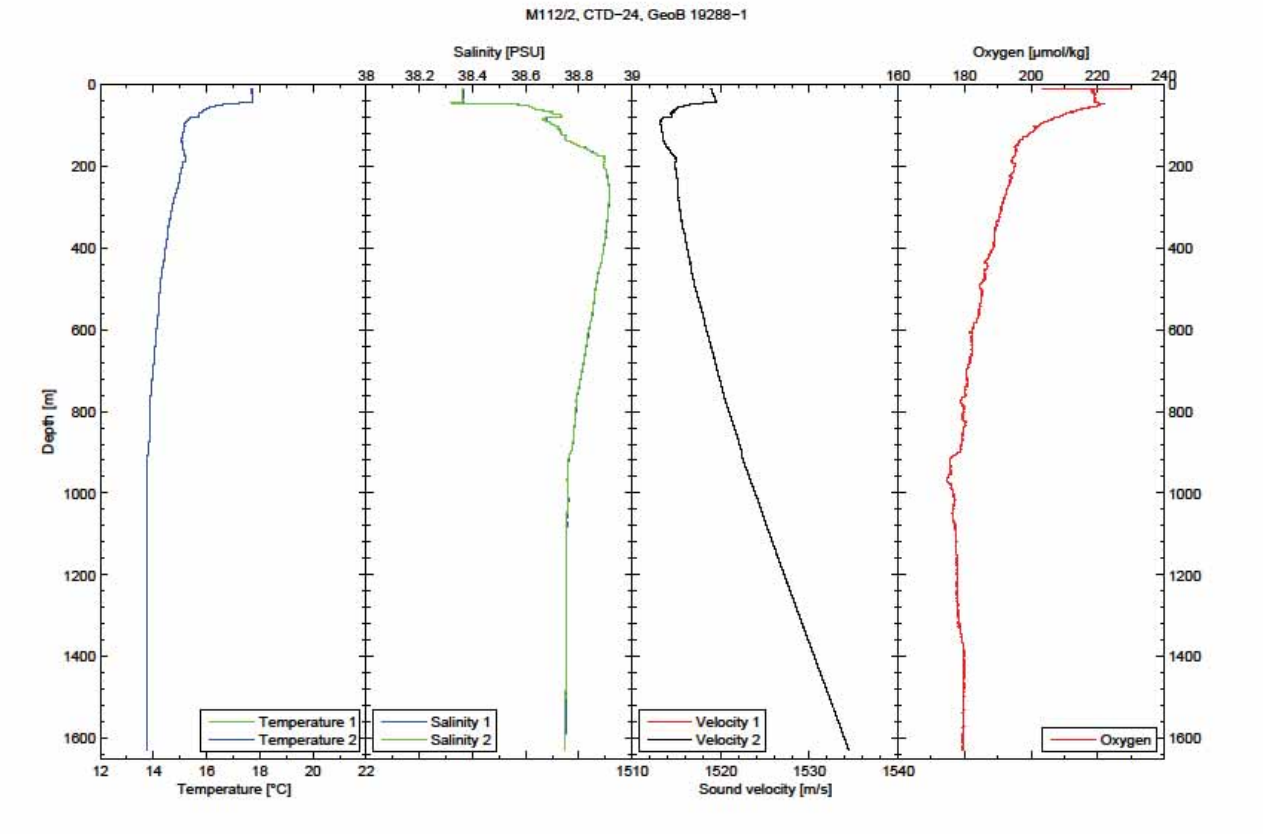

16.4 Appendix 4: Article in Corriere della Sera

Stampa | Stampa senza immagine | Chiudi

DAL 6 NOVEMBRE AL 15 DICEMBRE UNA CAMPAGNA NEI MARI DELL'ITALIA MERIDIONALE

Al largo della Calabria alla ricerca di gas idrati, possibile fonte di metano

Trovato un sito favorevole nello Ionio in corrispondenza del vulcano di fango denominato Venere a 1.500 metri di profondità

Simona Regina

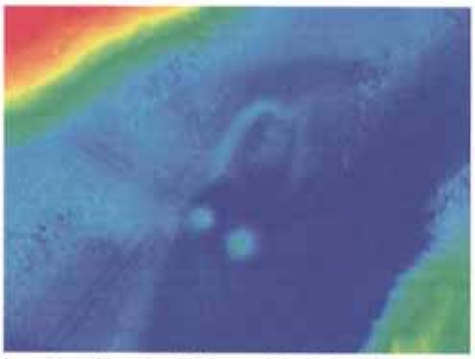

Immagine chiamata «Madonna dello Ionio» del fondale al largo della Calabria che mostra fattezze assomiglianti a quelle di una donna distesa. È uno dei vulcani di fango scoperti sull'arco calabro durante la campagna mediterranea del 2005. L'immagine ha vinto il primo premio del concorso BP-Kongsberg Underwater Images Competition 2006 (da Ogs Trieste)

Vulcani attivi che non eruttano lava. Presenti sia sulla terra emersa sia sui fondali marini, sono i cosiddetti vulcanelli di fango. Colline alte da pochi decimetri a centinaia di metri da cui ciclicamente fuoriescono fluidi freddi e gassosi: *mud flows*, cioè colate di argilla, metano e altri idrocarburi. Nel 2005, durante la campagna mediterranea a bordo della nave di ricerca Ogs-Explora, nell'ambito di due progetti europei (Hermes e Hydramed) i ricercatori dell'Istituto nazionale di oceanografia e geofisica sperimentale (Ogs) di Trieste ne hanno identificati alcuni nel mar Ionio, a sud della Calabria, che sono poi stati oggetto di studio di diverse campagne di ricerca europee. L'ultima, in ordine di tempo, è la campagna M112, coordinata dal Center for Marine Environmental Sciences dell'Università di Brema, che si conclude il 15 dicembre.

Appendix 4: Article in Corriere della Sera continued

LA CAMPAGNA M112 La nave tedesca Meteor è salpata il 6 novembre da Catania per una campagna oceanografica di cinque settimane con l'obiettivo di studiare i vulcani di fango al largo delle coste meridionali dell'Italia. In particolare, l'intento è cercare fuoriuscite di bolle di gas e analizzare gli ecosistemi sulle pendici dei vulcani, con lo scopo di verificare l'eventuale presenza nel sottosuolo di gas idrati. Apparentemente simili al ghiaccio secco, i gas idrati sono composti solidi formati da acqua e gas, che si formano in condizioni di basse temperature e pressione altissima nei sedimenti del fondo del mare e rappresentano una riserva concentrata di metano. Proprio per la fuoriuscita di fluidi gassosi, i vulcani di fango marini possono essere caratterizzati dalla presenza di idrati: in Antartide, per esempio, ne sono stati individuati alcuni associati ai gas idrati, «ma finora un solo sito con presenza di gas idrati è stato identificato nel Mediterraneo: al largo della Turchia», spiega Silvia Ceramicola, ricercatrice dell'Ogs. Ora l'equipaggio di Meteor sta cercando di fare chiarezza su eventuali concentrazioni di gas idrati in corrispondenza dei vulcani al largo della Calabria.

LA NAVE DI RICERCA METEOR Meteor, su cui lavorano a bordo 60 persone di diverse nazionalità, è attrezzata con tecnologie all'avanguardia per studiare le fuoriuscite di fluidi a fondo mare. In particolare un veicolo sottomarino autonomo che consente di acquisire dati micro-batimetrici; un veicolo sottomarino remoto, pilotato cioè dalla nave, che dispone di videocamere, braccia robotiche e strumenti per osservare e campionare sedimenti del fondale, e diversi sistemi di carotaggio, incluso uno che permette di acquisire e conservare campioni di gas idrati a pressioni ambientale. Ed è così che il team internazionale di ricercatori ha registrato, nelle scorse settimane, la fuoriuscita di bolle di gas da un sito conosciuto come vulcani di fango Venere, formato da due coni di circa 100 metri di altezza che si trovano sul fondale dello Ionio, a una profondità di 1.500 metri, a 30 chilometri al sud della costa calabrese.

Appendix 4: Article in Corriere della Sera continued

IL CENSIMENTO DEI VULCANI DI FANGO «La presenza di vulcani di fango nel Mediterraneo è stata scoperta oltre 35 anni fa, ma è solo negli ultimi quindici che è stata individuata la vera estensione del fenomeno, grazie all'uso di strumenti sempre più avanzati, come il *multibeam*, un sonar speciale che consente di rilevare le caratteristiche morfologiche del fondo marino», spiega Daniel Praeg, ricercatore a bordo di Meteor, che insieme alla collega Ceramicola ha scoperto i vulcani di fango al largo della Calabria. «Una volta indentificati», prosegue la ricercatrice, «indagini sismiche a riflessione permettono di investigare la geometria e l'architettura dei vulcani di fango, le cui strutture si possono estendere anche a profondità di diversi chilometri».

DOVE LE PLACCHE SI INCONTRANO «Il mar Ionio», continua Ceramicola, «è un'area dove la placca africana incontra, o meglio, si immerge sotto la placca europea, ed è sede di grandi processi geologici dinamici. Le placche infatti si muovono e la compressione può causare un aumento di pressione, capace di provocare la risalita di fluidi. Del resto», spiega, «in tutte le zone di subduzione ci sono vulcani di fango, perché i fluidi - che favoriscono lo scorrimento delle placche l'una sull'altra - quando raggiungono pressioni altissime salgono verso l'alto portandosi dietro sedimenti compatti che trovano lungo il percorso». Questi fenomeni eruttivi sul fondo mare e distanti dalla costa costituiscono potenziali pericolosità se vi passano sopra cavi sottomarini. Diversa è invece la situazione se sono prossimi alla linea di costa - come nei pressi di Catanzaro, dove un vulcanello attivo si trova sulle pendici di un canyon sottomarino, e la fuoriuscita di materiale ne favorisce l'instabilità con la progressiva erosione del fondale vicino al litorale - o se si trovano sulla terra emersa. L'eruzione di gas e fango, il 27 settembre, nella riserva naturale di Macalube, in provincia di Agrigento, ha causato la morte di due bambini.

15 dicembre 2014 | 09:39

From report No. 289 onwards this series is published under the new title:
Berichte aus dem MARUM und dem Fachbereich Geowissenschaften der Universität Bremen
A complete list of all publications of this series from no. 1 to 292 (1986 – 2012) was printed at last in issue no. 292.

No. 289 – Mohtadi, M. and cruise participants (2012). Report and preliminary results of RV SONNE Cruise SO 223T. TransGeoBiOc. Pusan – Suva, 09.09.2012 – 08.10.2012. 47 pages.
No. 290 – Hebbeln, D., Wienberg, C. and cruise participants (2012). Report and preliminary results of R/V Maria S. Merian cruise MSM20-4. WACOM – West-Atlantic Cold-water Corals Ecosystems: The West Side Story. Bridgetown – Freeport, 14 March – 7 April 2012. 120 pages.
No. 291 – Sahling, H. and cruise participants (2012). R/V Heincke Cruise Report HE-387. Gas emissions at the Svalbard continental margin. Longyearbyen – Bremerhaven, 20 August – 16 September 2012. 170 pages.
No. 292 – Pichler, T., Häusler, S. and Tsuonis, G. (2013). Abstracts of the 3rd International Workshop "Research in Shallow Marine and Fresh Water Systems". 134 pages.
No. 293 – Kucera, M. and cruise participants (2013). Cruise report of RV Sonne Cruise SO-226-3. Dip-FIP - The extent and structure of cryptic diversity in morphospecies of planktonic Foraminifera of the Indopacific Warm Pool. Wellington – Kaohsiung, 04.03.2013 - 28.03.2013. 39 pages.
No. 294 – Wienberg, C. and cruise participants (2013). Report and preliminary results of R/V Poseidon cruise P451-2. Practical training cruise onboard R/V Poseidon - From cruise organisation to marine geological sampling: Shipboard training for PhD students on R/V Poseidon in the Gulf of Cádiz, Spain. Portimao – Lisbon, 24 April – 1 May 2013. 65 pages.
No. 295 – Mohtadi, M. and cruise participants (2013). Report and preliminary results of R/V SONNE cruise SO-228, Kaohsiung-Townsville, 04.05.2013-23.06.2013, EISPAC-WESTWIND-SIODP. 107 pages.
No. 296 – Zonneveld, K. and cruise participants (2013). Report and preliminary results of R/V POSEIDON cruise POS448. CAPRICCIO – Calabrian and Adriatic Past River Input and Carbon ConversIOn In the Eastern Mediterranean. Messina – Messina, 6 – 23 March 2013. 47 pages.
No. 297 – Kopf, A. and cruise participants (2013). Report and preliminary results of R/V SONNE cruise SO222. MEMO: MeBo drilling and in situ Long-term Monitoring in the Nankai Trough accretionary complex, Japan. Leg A: Hong Kong, PR China, 09.06.2012 – Nagoya, Japan, 30.06.2012. Leg B: Nagoya, Japan, 04.07.2012 – Pusan, Korea, 18.07.2012. 121 pages.
No. 298 – Fischer, G. and cruise participants (2013). Report and preliminary results of R/V POSEIDON cruise POS445. Las Palmas – Las Palmas, 19.01.2013 – 01.02.2013. 30 pages.
No. 299 – Hanebuth, T.J.J. and cruise participants (2013). CORIBAR – Ice dynamics and meltwater deposits: coring in the Kveithola Trough, NW Barents Sea. Cruise MSM30. 16.07. – 15.08.2013, Tromsø (Norway) – Tromsø (Norway). 74 pages.
No. 300 – Bohrmann, G. and cruise participants (2014). Report and Preliminary Results of R/V POSEIDON Cruise P462, Izmir – Izmir, 28 October – 21 November, 2013. Gas Hydrate Dynamics of Mud Volcanoes in the Submarine Anaximander Mountains (Eastern Mediterranean). 51 pages.
No. 301 – Wefer, G. and cruise participants (2014). Report and preliminary results of R/V SONNE Cruise SO219A, Tohoku-Oki Earthquake – Japan Trench, Yokohama – Yokohama, 08.03.2012 – 06.04.2012. 83 pages.
No. 302 – Meinecke, G. (2014). HROV: Entwicklung und Bau eines hybriden Unterwasserfahrzeugs – Schlussbericht. 10 pages.
No. 303 – Meinecke, G. (2014). Inverse hydroakustische USBL-Navigation mit integrierter Kommunikation – Schlussbericht. 10 pages.
No. 304 – Fischer, G. and cruise participants (2014). Report and preliminary results of R/V POSEIDON cruise POS464, Las Palmas (Canary Islands) – Las Palmas (Canary Islands), 03.02.2014 – 18.02.2014. 29 pages.
No. 305 – Heuer, V.B. and cruise participants (2014). Report and preliminary results of R/V POSEIDON cruise POS450, DARCSEAS II – Deep subseafloor Archaea in the Western Mediterranean Sea: Carbon Cycle, Life Strategies, and Role in Sedimentary Ecosystems, Barcelona (Spain) – Malaga (Spain), April 2 – 13, 2013. 42 pages.
No. 306 – Bohrmann, G. and cruise participants (2015). Report and preliminary results of R/V METEOR cruise M112, Dynamic of Mud Volcanoes and Seeps in the Calabrian Accretionary Prism, Ionian Sea, Catania (Italy) – Catania (Italy), November 6 – December 15, 2014. 217 pages.